



# Durham E-Theses

---

## *Commentaries on Instantons*

ROBSON, CALUM,JOSHUA

### How to cite:

---

ROBSON, CALUM,JOSHUA (2020) *Commentaries on Instantons*, Durham theses, Durham University. Available at Durham E-Theses Online: <http://etheses.dur.ac.uk/13472/>

### Use policy

---

The full-text may be used and/or reproduced, and given to third parties in any format or medium, without prior permission or charge, for personal research or study, educational, or not-for-profit purposes provided that:

- a full bibliographic reference is made to the original source
- a [link](#) is made to the metadata record in Durham E-Theses
- the full-text is not changed in any way

The full-text must not be sold in any format or medium without the formal permission of the copyright holders.

Please consult the [full Durham E-Theses policy](#) for further details.

# Commentaries on Instanton Dynamics

Calum Robson

A Thesis presented for the degree of  
Doctor of Philosophy



Centre for Particle Theory  
Department of Mathematical Sciences  
Durham University  
United Kingdom

February 2020



# Commentaries on Instanton Dynamics

Calum Robson

Submitted for the degree of Doctor of Philosophy

February 2020

**Abstract:** I examine the dynamics of noncommutative instantons of instanton number 2 and commutative instantons of instanton number 3 in 5d Yang Mills theory. I begin by detailing the construction of the instanton solutions, their moduli space, and the moduli space potential using an explicit parametrisation of the moduli space coordinates in terms of the biquaternions. I then go on to numerically analyse the dynamics on the moduli spaces I have constructed.



# Declaration

The work in this thesis is based on research carried out in the Department of Mathematical Sciences at Durham University. No part of this thesis has been submitted elsewhere for any degree or qualification.

**Copyright © 2020 Calum Robson.**

“The copyright of this thesis rests with the author. No quotation from it should be published without the author’s prior written consent and information derived from it should be acknowledged.”



# Acknowledgements

I would like to begin by thanking my family- my parents and my brother and sister; Kezia and Joel. Without their support this PhD would neither have been begun nor finished. Next, I'd like to thank my supervisor Prof. Douglas Smith for his guidance and patience through the course of a PhD which at times has not been straightforward. The number of other people who have helped and encouraged me over the past few years is too great to mention in full, so I will settle for some specific examples. I am extremely grateful for the support of the chaplain at University College Durham, Ric Whaite; and for his advice in matters both pastoral and academic. I am especially grateful for his confidence in me which was very welcome at those times when my confidence in myself was somewhat lacking. I would also like to thank Lindsey Goodhew and Tim Ferguson for providing a listening ear and helpful advice at some crucial times. Moving on, the considerable amount of programming the PhD ended up involving would have been impossible without the assistance of Joe Farrow, who also provided his own code for finding geodesics which was essential for some of the more complicated simulations. More than this, I am thankful for his friendship over the years we've shared an office. This brings me on to the many friends who have shared the past few years with me. There are far too many to recall, so I will restrict myself to two categories. First I am deeply thankful for Will and Sarah Clarke and for Edward Hardyman, whose friendship has supported me from my undergraduate days and has been vital over the past few years. Finally all my friends at St. Nics Church Durham- Ben, the Prices, the Hulberts, Diego, Rachel, Mary, Andrew, Zoe, Tom, Lizelke, David,



Paul, Jack, Abi, Vicky, the Sleece, and many others. I don't know how I would have managed to get through the last year – or even more so the last six months – without you.

The PhD was fully funded by a grant from the Science and Technology Facilities Council (STFC).

*God hath created nothing simply for itself: but each thing in all things, and of every thing each part in other hath such interest, that in the whole world nothing is found whereunto any thing created can say, "I need thee not."*

— from *A Learned Sermon on the Nature of Pride* by Richard Hooker, c. 1585



*Dedicated to*

My Parents

*and*

to Kezia and Joel



# Contents

<b>Abstract</b>	<b>iii</b>
<b>List of Figures</b>	<b>xvii</b>
<b>1 Introduction</b>	<b>1</b>
1.1 Topological Solitons . . . . .	1
1.2 Outline of Thesis . . . . .	2
<b>I Background Material</b>	<b>5</b>
<b>2 Fibre Bundles</b>	<b>7</b>
2.1 Fibre Bundles . . . . .	7
2.1.1 Examples of Bundles . . . . .	8
2.1.2 Sections and Triviality . . . . .	11
2.2 Connection . . . . .	12
2.2.1 Preliminaries . . . . .	13
2.2.2 The Connection . . . . .	15
2.2.3 The Connection One form . . . . .	17
2.2.4 Field Strength . . . . .	20
2.3 Some Algebraic Topology . . . . .	21

2.3.1	Homotopy Theory . . . . .	21
2.3.2	Chern Classes . . . . .	24
2.3.3	Examples . . . . .	28
<b>3</b>	<b>Instantons</b>	<b>31</b>
3.1	Instantons . . . . .	31
3.2	Noncommutativity . . . . .	34
3.2.1	Quaternions and Biquaternions . . . . .	36
3.3	ADHM . . . . .	39
3.3.1	Motivating the Constuction . . . . .	42
3.3.2	Solving the ADHM equations . . . . .	46
3.4	Dyonic Instantons . . . . .	51
3.4.1	Solving the Scalar Field . . . . .	53
<b>4</b>	<b>The Moduli Space</b>	<b>57</b>
4.1	The Moduli Space . . . . .	57
4.2	Moduli Space of Dyonic Instantons . . . . .	61
4.2.1	The Complex Subspace . . . . .	65
4.3	Constructing the Moduli Space Metric . . . . .	66
4.4	Constructing the Potential . . . . .	72
<b>II</b>	<b>Particular Solutions</b>	<b>75</b>
<b>5</b>	<b>One and Two Instantons</b>	<b>77</b>
5.1	The Single $U(2)$ Instanton . . . . .	78
5.1.1	The Potential . . . . .	79

---

5.1.2	The Metric . . . . .	81
5.2	Two U(2) Instantons . . . . .	82
5.3	ADHM Constraints . . . . .	82
5.3.1	Finding biquaternion solutions . . . . .	85
5.3.2	Using the Symmetries . . . . .	87
5.4	The Noncommutative solution . . . . .	96
5.4.1	Checking the previous solution . . . . .	97
5.4.2	The Noncommutative Case . . . . .	102
5.5	The Scalar Field . . . . .	106
5.6	The Potential . . . . .	108
5.6.1	The Large $\tau$ limit . . . . .	110
5.7	The Metric . . . . .	110
5.7.1	The metric itself . . . . .	112
5.7.2	Checking the Solution . . . . .	112
5.8	Conclusion . . . . .	113
<b>6</b>	<b>Two Instanton Dynamics</b>	<b>115</b>
6.1	The Setup . . . . .	115
6.1.1	Numerical Checks . . . . .	118
6.2	Pure Instantons . . . . .	120
6.3	Dyonic Instantons . . . . .	136
6.3.1	Orbiting Behaviour . . . . .	149
6.4	The Six Parameter Space . . . . .	152
6.5	Conclusions . . . . .	155



---

<b>7</b>	<b>Three Instantons</b>	<b>161</b>
7.1	Solving the $O(3)$ equations . . . . .	162
7.2	The Scalar Field . . . . .	163
7.3	The Potential . . . . .	164
7.4	$O(3)$ Metric . . . . .	165
7.5	3 Instanton Dynamics . . . . .	167
<b>8</b>	<b>Conclusion</b>	<b>173</b>
8.0.1	Further work . . . . .	176
<b>A</b>	<b>The Two- Instanton Scalar Field</b>	<b>179</b>
A.0.2	Solving the equations . . . . .	180
<b>B</b>	<b>The Two Instanton Potential</b>	<b>183</b>
<b>C</b>	<b>The Two Instanton Metric</b>	<b>187</b>
<b>D</b>	<b>The Three Instaton Scalar Field</b>	<b>193</b>
<b>E</b>	<b>The Three Instanton Potential</b>	<b>197</b>
<b>F</b>	<b>The Three Instanton Metric</b>	<b>201</b>

# List of Figures

- 6.1 The setup of the Instantons. The instantons are located at  $\pm(x, b) = (\omega \cos(\chi), \omega \sin(\chi))$ . They have size  $\tilde{\rho}_i = \sqrt{\rho_i^2 + \frac{4\zeta^2}{\rho_i^2}}$  . . . . . 116
- 6.2 Scattering of Dyononic instantons with  $b = 0.5$  and  $\zeta = 1.15$ . The upper plot shows the  $|\tau|$  parametrisation, the lower shows  $\sqrt{|\tau|^2 + |\sigma|^2}$ . The radii of the instantons are not shown. In this case the  $\sigma$  behaviour dominates and after the interaction the position of the instantons goes as  $\frac{1}{|\tau|^2}$  – the  $\tau$  case had to be run for many more time steps (50000 as opposed to 2400). This is presumably because the size of the instantons becomes very large and so  $\sigma$  continues to dominate  $\tau$  in the definition of the instanton position . . . . . 119
- 6.3 The scalar field profile for the Commutative instantons. The left graph is when they are nearly coincident, the right when they are separated. The solid line shows the profile along the imaginary direction of the complex subspace; the dotted line shows the profile off the complex subspace we are elsewhere considering. . . . . 121
- 6.4 The scalar field profile for the Noncommutative instantons with  $\zeta=0.025$ . The left graph is when they are nearly coincident, the right when they are separated. The solid line shows the profile along the imaginary direction of the complex subspace; the dotted line shows the profile off the complex subspace we are elsewhere considering. . . . . 121

6.5 The scalar field profiles for coincident (left) and seperated (right) Instantons with  $\zeta = 0.1$ . The dotted and solid lines have the same meaning as before. As discussed in the main text these graphs are probably not reliable due to being calculated only to first order in the Moyal product . . . . . 121

6.6 A top down 2D contour plot of the noncommutative part of figure 6.5. The brighter circles in the dark spots show that the splitting of the two peaks really does indicate a ring structure . . . . . 122

6.7 The scalar field profiles in 1D and 2D for the case in figure 6.5, but with  $\zeta=0.15$ . Note that increasing  $\zeta$  has increased the size of the rings.122

6.8 Change of scattering angle (left) with noncommutative parameter  $\zeta$  for  $b = 0.5$ , with the other parameters as discussed in the main body of the text. On the right is the commutative case, with  $\zeta = 0$ . Increasing either  $b$  or the parameter  $\rho$  moves the peak to higher values of  $\zeta$ . In the case of  $b$  this is because we need a larger size, and hence larger  $\zeta$  to compensate for the same seperation. It is less clear what the explanation is in the case of  $\rho$ , though the nonlinear dependence of the instanton size on both  $\rho$  and  $\zeta$  almost certainly plays a role. 125

6.9 Zooming in on the discontinuity in figure 6.8. Individual scattering examples from this graph are shown in figure 6.11 . . . . . 125

6.10 Scattering for two instantons with  $b = 0.5$ , and, moving in each row from left to right,  $\zeta = \{0.1, 0.86, 0.87, 0.88\}$ ; This corresponds to the region to the left of and around the peak in figure 6.8. Where the sizes are not shown this is in order to make the trajectories clearer. Note that the instantons go from glancing off one another, to moving parallel, to crossing over, and then deflecting . . . . . 126

- 
- 6.11 Graphs of the interaction around the peak, zoomed in at the center, with  $\zeta = \{0.8187, 0.882, 0.89, 0.9\}$ . The vertical lines on the graph are the results of confusion about which parts of the trajectory belong to which instanton, and can be ignored. More detailed interpretation of the graphs is given in the main text, however I think that the description of the position is breaking down somewhat, and this explains the discontinuities in the scattering angle graph. I conclude that the correct behaviour is the looping behaviour in the first and last graphs, which rotates in a clockwise direction, and that the connection of the two loops is an error in the plotting. . . . . 127
- 6.12 Scattering for two instantons with  $b = 0.5$ , and  $\zeta = 0.9, 1, 1.15, 2$ . This corresponds to the right side of the peak. Note that the Instanton angle begins to turn back on itself, until the scattering becomes a direct repulsion  $\zeta = 1.15$ , then opens to about  $\pi/4$  . . . . . 128
- 6.13 Plot of scattering angle vs. noncommutative parameter  $\zeta$  for the initial parallel scattering, shown for particular cases in figure 6.15. The jump at  $\zeta = 6$  is a discontinuity similar to those analysed in figure 6.9, and is shown in more detail in figure 6.14 . . . . . 129
- 6.14 Plot of scattering angle vs. noncommutative parameter  $\zeta$  for the initial parallel scattering, zooming in on the discontinuity. Note the splitting on the left hand side- this is analysed in figure 6.16 . . . . 130

- 6.15 Scattering behaviour for the setup in 6.18, for  $\zeta = \{0, 5.5, 8.85, 9.5, 8.85\}$ .  
 The Instantons begin by not interacting in the commutative case, then begin to interact as the noncommutative parameter is increased. At the peak at  $\zeta = 5.85$ , the interaction is complicated and even the  $\sqrt{\sigma^2 + \tau^2}$  description seems to break down. As in the original case, figure 6.12, the instantons then completely reflect off one another. The explanation for this behaviour seems to be that increasing  $\zeta$  increases the size of the instantons, so that they are no longer separated and begin to interact . . . . . 131
- 6.16 Zoomed in graphs showing rapid oscillatory behaviour of in the splitting on the left of figure 6.14. We have  $\zeta = \{5.7757, 5.78, 5.8, 5.9\}$ . The instanton trajectories rotate a full circle over a very small parameter range. This seems to correspond to the removal of a second set of loops from the centre of the interaction. As before, the vertical lines are due to errors in constantly identifying the instanton positions 132
- 6.17 Plot of scattering angle vs. impact parameter for different values of  $\zeta$ . From left to right we have  $\zeta = \{0.65, 1.5, 3\}$  . . . . . 133
- 6.18 Plot of scattering angle vs. noncommutative parameter  $\zeta$  for the near orthogonal scattering, with  $b = 0.1$  . . . . . 134
- 6.19 Plot of scattering angle vs. noncommutative parameter  $\zeta$  for the nearly orthogonal scattering with  $\rho = 2$  and  $b = 0.1$ , note that the plateau at the start is wider than figure 6.18, where  $\rho = 1$  . . . . . 134
- 6.20 Examples of scattering behaviour for the orthogonal scattering with  $b = 0$  for  $\zeta = \{0, 2\}$ . . . . . 135
- 6.21 Examples of scattering behaviour for the near orthogonal scattering with  $b = \{0.1, 0.01\}$ . Note that the scattering becomes almost completely repulsive for the smaller values of  $b$  . . . . . 135

- 6.22 Graphs of scattering angle vs. initial Instanton size for  $\zeta = 0$  (above), and  $\zeta = 0.3$  (below). As the distance between the Instantons is 1, this represents the case where  $\zeta$  is small compared to the separation. The true size of the Instanton is within 12% of the  $\rho$  after  $\rho = 0.6$ , which is about the top of the peak in the below graph. I therefore assume the graph is reliable after this point. . . . . 137
- 6.23 Graphs of scattering angle vs. initial Instanton size for  $\zeta = 0.3$ , and  $b = 0.05$ . This represents the cases where  $\zeta$  is greater than the separation. This is shown specifically in figure 6.24. Again, after the initial peak. After the peak, the true size is within 17% of the parameter  $\rho$ , and so the graph is a good description. Hence the qualitative behaviour is the same as in the noncommutative case in figure 6.22 . . . . . 138
- 6.24 This is the evolution of the  $\zeta = 0.3$  system introduced in figure 6.23, for  $\rho = \{0.8, 1.2, 4\}$ . As seen in that figure, the scattering angle decreases slightly to begin with, then increases with the parameter  $\rho$  139
- 6.25 Graph showing variation of scattering angle vs. gauge angle  $\theta$  for  $b = 0.5$  and  $\zeta = 2$ . As can be seen, there is very little change in the angle for different  $\theta$  – the overall change is of the order of 0.0001. This is almost certainly just numerical noise, and the true scattering angle remains effectively constant . . . . . 139
- 6.26 Graph showing variation of scattering angle vs. gauge angle  $\theta$  for  $b = 0.5$  and  $\zeta = 1$ . As show in figure 6.29 the jump at the origin is real, and involves a switch in the chirality of the scattering . . . . 140
- 6.27 Graph showing variation of scattering angle vs. gauge angle  $\theta$  for  $b = 4$  and  $\zeta = 1$ . Note that here there is no jump in the chirality. I have checked this explicitly . . . . . 140

- 
- 6.28 Graph showing variation of scattering angle vs. gauge angle  $\theta$  for  $b = 0.5$  and  $\zeta = .1$ . Note that here there is no jump in the chirality, unlike in the case of  $\dot{\theta}$  . . . . . 141
- 6.29 Graph showing examples of scattering for cases from figure 6.26. Here,  $\dot{\theta} = -0.2$  on the left, and  $0.2$  on the right. Note the chirality of the scattering has reversed, confirming the discontinuity shown in figure 6.26 is physical . . . . . 141
- 6.30 Plot of dyonic instanton scattering for  $b = 0.5$ ,  $|q| = 0.1$ ,  $\zeta = 0$  (above),  $\zeta = 0.5$  (below) . . . . . 142
- 6.31 Plot of dyonic instanton scattering for  $b = -1$ ,  $|q| = 0.1$ ,  $\zeta = 0$  (above),  $\zeta = 1$  (below). Note the visible oscillations on the right hand graph. . . . . 143
- 6.32 Plot of dyonic instanton scattering for  $b = 2.9$ ,  $|q| = 0.1$ ,  $\zeta = 0$  (above),  $\zeta = 1$  (below). . . . . 144
- 6.33 Graph of scattering angle vs. noncommutative parameter  $\zeta$  for  $b = 0.5$ . Particular scattering examples from this graph are discussed in figure 6.34 . . . . . 145
- 6.34 Scattering behaviour for the system presented in figure 6.33, for  $\zeta = \{1, 2, 4, 5\}$ . At  $\zeta = 1$ , corresponding to the flat part of that graph, the particles are almost completely reflected. Once the behaviour becomes more chaotic, there is a variety of behaviour with no clear pattern. Examples include deflection at  $\zeta = 2$ , some kind of orbiting at  $\zeta = 4$ , and repulsion at  $\zeta = 5$  . . . . . 146
- 6.35 Graph showing scattering angle vs. magnitude of potential,  $q$ , in the commutative case ( $\zeta = 0$ ). The graphs for small  $\zeta$  (below 0.3 at most), and large  $\zeta$  (at least above 2) show the same behaviour. Note that these bounds are not the cut-off points, merely the lowest and highest points I have observed this behaviour. . . . . 147

6.36	Graph showing scattering angle vs. $q$ for $\zeta = 0.5$ . . . . .	147
6.37	Graph showing scattering angle at very low values of $q$ for $\zeta = 0.5$ . . . . .	148
6.38	Graph of scattering with orbiting behaviour, with $\zeta = 0.5$ , $b = 0.5$ , $q = 0.00438$ . . . . .	148
6.39	Scattering angle vs. parameter $\rho$ for $\zeta = q = 0.1$ . As in figures 6.22 and 6.23 I expect $\rho$ to be a good approximation to the true initial size after the peak . . . . .	149
6.40	Scattering angle vs. Impact parameter for $\zeta = q = 0.5$ . . . . .	150
6.41	The behaviour as described in the text, varying around the first of these graphs. In that graph, $\zeta = 4$ , $q = 0.1$ , $b = 0.5$ . The second shows the complicated repulsion behaviour for $\rho = 0.005$ , and the third shows the orbit at $\zeta = 0.4003$ . . . . .	151
6.42	Graph of scattering with orbiting behaviour, for the case $\zeta = 0.5$ , $b = 0.2.9$ , $q = 0.00438$ . . . . .	152
6.43	Graph showing variation of scattering angle $\phi$ with $\zeta = 0$ , $\rho_1 = \rho_2 = 1$ and $b = 0.5$ . . . . .	154
6.44	Graph showing variation of scattering angle $\phi$ with $\zeta = 0$ , $\rho_1 = \rho_2 = 1$ and $b = 0.1$ . . . . .	154
6.45	Graph showing scattering examples from figure 6.47, with $\phi = \pi$ above and $\phi = 3\pi/2$ below. Note that the scales are different on the two graphs, and that the behaviour is extremely different. . . . .	155
6.46	Graph showing variation of scattering with gauge angle $\phi$ , where $\zeta = 0$ and $b = 0.5$ . In both graphs $\rho_1 = 1$ . In the top graph, $\rho_2 = 5$ , and in the bottom graph $\rho_2 = 0.1$ . Note that the scattering angle is much smaller in this case. . . . .	156



- 
- 6.47 Graph showing variation of scattering angle  $\phi$  with  $\zeta = 1$ ,  $\rho_1 = \rho_2 = 1$  and  $b = 0.5$ . The true instanton size is therefore  $\sqrt{2}$ , and so is roughly comparable to the separation. The splitting of the left peak appears to be a numerical error. . . . . 157
- 6.48 Graph showing variation of scattering angle  $\phi$  with  $\zeta = 1$ ,  $\rho_1 = \rho_2 = 1$  and  $b = 4$ . The true instanton size is therefore  $\sqrt{2}$ , and so is much smaller than the separation. Note that the sinusoidal form is much more preserved, but now oscillates around zero rather than away from it 157
- 6.49 Graph showing scattering examples from figure 6.47, with  $\phi = \pi$  above and  $\phi = 3\pi/2$  below. Note that there is very little difference. 158
- 6.50 Graph showing scattering examples from figure 6.48, with  $\phi = \pi$  above and  $\phi = 3\pi/2$  below . . . . . 158
- 6.51 Graph showing variation of gauge angle  $\phi$  with  $\zeta = 1$ ,  $\rho_1 = 1$ ;  $\rho_2 = 5$  and  $b = 0.5$ . The true instanton sizes are  $\sqrt{2}$  and just over 25 respectively. . . . . 159
- 7.1 Plot of the scalar field profile for three separated instantons . . . . 168
- 7.2 Plot of the scalar field profile for two instantons, with the third far separated off to the right . . . . . 168
- 7.3 Plot of the topological charge density with one instanton at the origin and the other two at decreasing values of  $\tau_i$ . Note the apparent right angled scattering . . . . . 169

- 7.4 Comparison of scattering in three instanton case with one instanton far away from the other two (top), with the 4 parameter (orthogonal) case for two instantons. This is with  $b = 0.1$ . Note the orthogonal scattering in both cases. Here the three instanton initial parameters are  $\{\tau_{1R}, \tau_{1I}, \tau_{1R}, \tau_{1I}, u_R, u_I, v_R, v_I, w_R, w_I\}$  are  $\{10, -0.01, 20, 0.01, 1, 0, 0, 1, 1, 1\}$ , and their initial velocities are  $\{0.03, 0, -0.03, 0, 0, 0, 0, 0, 0, 0\}$ . This means that the two instantons which are interacting are orthogonal in the gauge group, and the third is at  $(-30,0)$ , which is sufficiently separated not to qualitatively affect the interaction . . . . . 170
- 7.5 Comparison of scattering in three instanton case with one instanton far away from the other two (top), with the 4 parameter (orthogonal) case for two instantons. This is with  $b = 0.5$ .  $\{10, -0.5, 20, 0.5, 1, 0, 0, 1, 1, 1\}$ , and their initial velocities are  $\{0.03, 0, -0.03, 0, 0, 0, 0, 0, 0, 0\}$ . This means that the two instantons which are interacting are orthogonal in the gauge group, and the third is at  $(-30,0)$ , which is sufficiently separated not to qualitatively affect the interaction . . . . . 171
- 7.6 Three Instantons scattering. One begins stationary at the origin, whilst the other two move in with equal and opposite positions.  $\{\tau_{1R}, \tau_{1I}, \tau_{1R}, \tau_{1I}, u_R, u_I, v_R, v_I, w_R, w_I\}$  are  $\{10, 0.01, -10, -0.01, 1, 0, 0, 1, 1, 1\}$ , and their initial velocities are  $\{0.05, 0, -0.05, 0, 0, 0, 0, 0, 0, 0\}$ . The two instantons that come in from the sides are orthogonal in the gauge group to each other, but not to the stationary one at the origin 172



# Chapter 1

## Introduction

### 1.1 Topological Solitons

The aim of this thesis is to present new solutions for the moduli space dynamics of certain Instanton solutions. Instantons are a specific example of Topological Solitons, which are nonlinear solutions to certain PDEs. Because the properties of these solutions are tied to topological invariants of the spaces they are defined upon, they are very stable- no continuous transformation (including time evolution) of the solutions can cause these properties to change.

Solitons were first observed in nature by John Scott Russel in 1834, however they first began to play a role in particle physics in Yukawa theory, where they are known as Skyrmions [61]. Shortly afterwards, Coleman and Mandelstam discovered the existence of solitons in Sine-Gordon Theory [14][47]. Since then, solitonic solutions have been discovered in many theories. Perhaps the most prominent are Kinks in one spatial dimension, Vortices in two spatial dimensions, and monopoles in three spatial dimensions. [52].

In this thesis, we are interested in Instanton solutions. These are four dimensional solitonic solutions, found in Yang Mills theory. Originally discovered in [6], their applicability was massively increased by the discovery of the ADHM method for constructing them [2]. They have many applications, from deriving semiclassical

corrections to the Yang Mills path integral [21], to the fact that they appear as the low energy limits of certain brane configurations in String Theory [58].

## 1.2 Outline of Thesis

The thesis is divided into two parts. In the first, I present an overview of the theory which I use in the second part to calculate the particular instanton solutions.

In the first chapter, I give an overview of the theory of Fibre bundles, which provides the mathematical underpinning to the study of Instantons. This largely follows the presentation in [53] and [16]. I begin by defining a bundle itself, then move on to considering the notions of Connections and Curvature on a bundle. Next, I briefly discuss Characteristic classes and the Topological Degree of a map, and show how these objects are connected.

In the second chapter, I introduce Instantons themselves. In the remainder of the thesis we will be studying instantons defined upon both commutative and non-commutative spacetimes. Therefore the next thing to describe is the nature of noncommutative spacetime. This includes a brief discussion of the biquaternions – the algebra  $\mathbb{C} \times \mathbb{H}$ . I then look at how to calculate instantons in practice- this uses the ADHM construction first developed in [2]. I conclude the chapter by showing how the construction can be extended to include Dyonic Instantons, where there is a scalar field upon the instanton background, following the method first outlined in [21].

In the third chapter I introduce the Instanton Moduli space [48]. Once again, I illustrate how this construction can be extended to dyonic instantons via introducing a potential on the Moduli space, following the presentation in [22]. After explaining the theoretical basis, I present a practical method for calculating the moduli space metric and potential for noncommutative  $U(N)$  instantons, which generalises that presented for  $SU(2)$  commutative instantons in [1]. This concludes the first section

of the thesis.

In the second part of the thesis I use the results in the first part to calculate some particular solutions. First (in the fourth chapter), I rederive the single noncommutative  $U(2)$  instanton presented in [3]. I then move to the case of two  $U(2)$  instantons. First, I rederive the commutative solution in [1], but starting from biquaternion rather than quaternion parameters. Then I look for a solution to the noncommutative two instanton case. I show that the solution presented in [37] does not satisfy the full ADHM equations, however I was unable to find a full solution myself. I was, however, able to find a solution defined on a subspace of the full moduli space spanned by the  $\mathbb{C} \times \mathbb{C}$  subgroup of  $\mathbb{C} \times \mathbb{H}$ . This is a geodesic submanifold of the full moduli space. After finding this solution, I use it to derive the metric and potential on this subspace. I check the answers correspond to the commutative solution and the one-instanton solution in the appropriate limits. In the fifth chapter, I use these results to numerically evaluate scattering in this subspace. I compare these results to the results for the commutative two-instanton in [1].

Finally, in the sixth chapter I look at the commutative three Instanton case. Again, I was unable to find a solution to the ADHM equations for the full moduli space, however I was again able to find one for the complex subspace spanned by the  $\mathbb{C}$  subgroup of  $\mathbb{H}$  (In this chapter I was working with the quaternions, and not the biquaternions). I used this solution to calculate the moduli space metric and potential for that subspace. Numerical scattering calculations proved to be very computationally expensive, however I was able to plot scalar field and topological charge density profiles, and to get a some examples of the instanton scattering, which allowed me to make some comparison to the two instanton case in the appropriate limits.



# Part I

## Background Material





# Chapter 2

## Fibre Bundles

In this chapter, I introduce some ideas from differential topology which are essential for understanding Instantons. I begin by defining the notion of a Fibre Bundle, then I introduce the idea of a *Connection* on the bundle. This leads into a discussion of Curvature. After defining these things, I briefly discuss Homotopy Theory, and then Characteristic classes. After explaining the relation between these concepts, I am then ready to introduce Instantons themselves, which will be done in the next chapter. This section mainly follows [16], with additions from [53] and [59].

### 2.1 Fibre Bundles

Now we introduce the notion fundamental to this section: The Fibre Bundle itself. First, we will give the definition, then build up from the most familiar example – the tangent bundle – to Principle bundles; and finally to associated vector bundles. We conclude by defining sections of bundles.

A Fibre Bundle is a Manifold  $E$ , and triple  $\{F, M, G\}$ , where  $E$  is equipped with an surjective map  $\pi : E \rightarrow M$ . We call  $F$  the Fibre,  $M$  the base space, and  $G$  the structure group, which has a left action on  $F$ . We require that the following conditions are satisfied

- 1. We require that  $\pi^{-1}(x) \cong F \quad \forall x \in M$

- 2. We require an open covering  $\{U_i\}$  of  $M$ , an associated set of maps  $\phi_i : U_i \times F \rightarrow \pi^{-1}(U_i)$  satisfying  $\pi \circ \phi_i(x, f) = x$  for  $x \in U_i$  and  $f \in F$ . This is not necessarily the same covering which is used to make  $M$  into a Manifold [59]. These maps are called local trivialisations.
- 3. At each point  $x \in M$ , we have that the map  $\phi_i(x, f)$  is a diffeomorphism mapping  $F \rightarrow F_x$ .
- 4. On the intersections  $U_i \cap U_j$ , we define  $g_{ij} \equiv \phi_{i,x}^{-1} \phi_{j,x}$ . We require  $g_{ij}$  to be an element of  $G$

The maps  $g_{ij}$  have a couple of properties worth noting. First,  $g_{ij}^{-1} = g_{ji}$ . Second, on triple intersections  $U_i \cap U_j \cap U_k$  we have  $g_{ij}g_{jk} = g_{ik}$ . By the definition of the local trivialisations  $\phi_i$  we have that  $E$  is locally a direct product  $U_i \times F$ . If we can make all the transition functions identity maps, then it will also be true globally that  $E = M \times F$ . In this case, we call  $E$  a *Trivial Bundle* (hence the name, ‘local trivialisaton’ for the  $\phi_i$ ).

Now, the  $\phi_i$  can be seen as providing local coordinates for the bundle. The question as to whether or not a bundle is trivial becomes the question of whether we can assign coordinates consistently across the whole bundle. This problem is familiar from general relativity, and it is also the root of gauge theory – we will later see that the choice of transition functions  $g_{ij}$  is linked to our choice of a gauge.

As well as changing coordinates between patches, we can also change coordinates within patches. This corresponds to using a different trivialisation  $\tilde{\phi}_i$ . We can define a coordinate changing map  $f_i = \phi_{i,x}^{-1} \circ \tilde{\phi}_{i,x}$ , and it follows that  $\tilde{g}_{ij} = f_i^{-1}g_{ij}f_j$ .

### 2.1.1 Examples of Bundles

We now move into some examples

**Example 2.1.1.** The Mobius Strip and the Cylinder. A nice way to see how this works is to consider these two spaces, as used in [53]. As manifolds  $E$ , the cylinder

is definable as  $[0, 1] \times S^1$  and the Mobius strip is given via the quotient construction  $[0, 1] \times [0, 1] / \sim$ ; where  $\sim$  is defined by  $[0, t] \equiv [1, 1 - t]$ . Both spaces have base space  $M = S^1$  and fibre  $F = [-1, 1]$ , with a projection  $\pi$  from the total space  $E$  to the central  $S^1$  of each space given by  $(x, y) \rightarrow x$ . We will see that we end up with  $G = \mathbb{Z}_2$  (A rare example where the structure group is not also a Lie group). We now check the conditions

- 1. It is clear that  $\pi^{-1}(x) \cong [-1, 1]$
- 2. For both the mobius strip and the cylinder, we can cover the  $S^1$  via two open sets,  $U_1 = (0, 2\pi)$ ;  $U_2 = (-\pi, \pi)$ . For  $u_i \in U_i$  the corresponding local trivialisations are given by  $\phi_1^{-1}(u_1) = (\theta_1, t)$ ;  $\phi_2^{-1}(u_2) = (\theta_2, t)$  where  $\theta_1 \in (0, 2\pi)$ ,  $\theta_2 \in (-\pi, \pi)$  and  $t \in [-1, 1]$
- 3. This is clearly satisfied
- 4. The intersection  $U_1 \cap U_2$  has two components;  $I_A = (0, \pi)$  and  $I_B = (\pi, 2\pi)$ . As for the transition functions,  $t_A$  defined on  $I_A$  is the identity map, whereas there are two choices for  $t_B$ , the map on  $I_B$ . For  $\theta_B \in I_B$ , either  $\phi_1^{-1} = \phi_2^{-1} = (\theta_B, t)$  or  $\phi_1^{-1} = (\theta_B, t)$ ;  $\phi_2^{-1} = (\theta_B, -t)$

In the first case,  $t_B$  is also the identity map, and we have the Cylinder, which is a trivial bundle over  $S^1$ . In the second case, we have  $t_B : (\theta_B, t) \rightarrow (\theta_B, -t)$ . Since  $t_B^2$  is the identity,  $t_B \in \mathbb{Z}_2$ , and so this is the structure group of the Mobius strip considered as a bundle over  $S^1$ .

**Example 2.1.2.** Tangent Bundle. Probably the most well known example of a Fibre Bundle is the Tangent Bundle. This is the collection of all the tangent spaces of a manifold  $M$ .

$$TM \equiv \cup_{p \in M} T_p M \quad (2.1.1)$$

The base space here is the manifold  $M$ , the fibres are the tangent bundles at each point, and we can choose the structure group  $G$  to be  $GL(N)$ , where  $N$  is the dimension of the tangent space. The projection  $\pi$  maps from  $T_p M$  to the point

$p \in M$ . Note that if we have coordinates  $x_i$  on the manifold, then our tangent space can be parameterised by  $\left\{ \frac{\partial}{\partial x_i} \right\}$ . Then

- 1. This is by definition
- 2. We can use the open sets  $U_m$  used to define  $M$  as a manifold. Then we can parameterise  $U_m \times F$  by  $\left\{ x_i, \frac{\partial}{\partial x_i} \right\}$ , since the coordinates  $x_i$  are defined on each set  $U_m$ . It is then clear that we can define  $\phi : (U_m \times T_p M) \rightarrow \text{Span} \left\{ \frac{\partial}{\partial x} \right\} \sim T_p M$
- 3. This also follows by definition
- 4. Coordinates on different tangent spaces  $\left\{ \frac{\partial}{\partial x_i} \right\}, \left\{ \frac{\partial}{\partial x_j} \right\}$  are related by  $g_{ij} = \frac{\partial x_j}{\partial x_i}$ . Hence the structure group is  $GL(n, \mathbb{R})$

**Example 2.1.3.** Vector Bundle. This is a simple generalisation of the Tangent Bundle, in which the fibre is a  $k$ -dimensional vector space  $V$  rather than the tangent plane. The structure group is  $GL(k)$ .

**Example 2.1.4.** Principle Bundle. A principle bundle  $P$  has a fibre equal to the structure group  $G$ . These are sometimes called  $G$ -bundles. The action of the structure group on the bundle becomes left multiplication of  $G$  on itself. If we define the projection and local trivialisations by

$$\phi_i(p) = (x, g^{-1}p) ; \pi(p) = x \quad (2.1.2)$$

then we can also define a right multiplication of  $p \in P$  by  $a \in G$  by

$$pa = \phi(x, ga) \quad (2.1.3)$$

Because multiplication in  $G$  is associative, the operations of left and right multiplication commute. In addition, the operation of right multiplication is independent of the local coordinates, since

$$pa = \phi_j(x, g_j a) = \phi_j(x, g_{ij}(x)g_i) = \phi_i(x, g_i) \quad (2.1.4)$$

so we can simply write the right action as  $P \times G \rightarrow P : p \times a \rightarrow pa$ . It can be shown [53] that this action is free and transitive on each fibre.

**Example 2.1.5.** Associated Bundles. The final example to discuss is the building block for gauge theories, Associated Bundles. These combine the ideas of Vector bundles and Principle bundles. We start with a principle bundle  $P$  whose structure group  $G$  has a faithful representation  $\rho(g)$ , which acts on the left of an  $n$  dimensional vector space  $V$ . We take the product  $P \times E$ , and then define the Associated Bundle  $E_\rho$  as

$$P \times_\rho V \equiv P \times V / \sim ; \sim : (p, v) \cong (g^{-1}p, \rho(g)v) \quad (2.1.5)$$

To understand what this means, consider that we can get every element of  $g$  from  $e$  by multiplication with elements in  $G$ , with  $e$  the identity in  $G$ . If we rewrite the equivalence relationship as  $(pg, v) \sim (p, \rho(g)v)$ , we can see that this makes every element  $g$  in the fibre  $G$  at  $x$  congruent to its orbit in space  $V$ , via  $(pg, V) \sim (p, \rho(g)V)$ . This effectively replaces  $G$  by  $V$  as the fibre over  $M$ .

We can define new projections and local trivialisations on the equivalence classes. First we define  $\pi_E([p, v]) = \pi(p)$ . This is well defined since  $\pi(pg) = \pi(p)$  under the equivalence relation above. The new trivialisations are

$$\phi_E^{-1} : E_\rho \rightarrow P \times V : [p, v] \rightarrow (\pi(p), \rho(g)v) \quad (2.1.6)$$

It can be shown (see [53]) that this definition is independent of the choice of representative of the equivalence classes, and that the transition functions are changed, as we might expect, from  $g_{ij}$  to  $\rho(g_{ij})$

## 2.1.2 Sections and Triviality

A local section is a smooth map  $U_i \rightarrow E$ , satisfying  $\pi \circ s(x) = x$ . The most common example of a section is that of vector fields on the tangent bundle, which are maps  $U_i \rightarrow T_p M$ . If we can extend the local section to a smooth map  $M \rightarrow E$ , we call it a Global Section. For vector fields, we have the following theorem

**Theorem 2.1.1.** *A vector bundle of rank  $n$  is trivial iff it admits  $n$  linearly independent sections*

Even nontrivial vector bundles have a trivial global section, which maps each point to the origin in the fibre. For principle bundles, this is not possible, as we have to have a well defined coordinate system on  $G$  to define what the zero element actually is. This allows us to prove the following strong result (see [53])

**Theorem 2.1.2.** *A Principle Bundle is Trivial iff it allows a global section*

These two results together make Associated Bundles very useful, via

**Theorem 2.1.3.** *A Vector Bundle is trivial iff its Associated Principle Bundle is trivial*

This means that we can use either of the two above theorems to verify the Triviality of both a Vector bundle and its associated Principle bundle, as the triviality of one implies the triviality of the other.

## 2.2 Connection

In this section, the structure group  $G$  will always be a Lie group. In the previous section we defined a fibre bundle in terms of a large number of coordinate patches, ‘stitched together’ by the transition functions  $g_{ij}$ . If we begin in one coordinate patch, we want to know how to cross over to another. To do this, we need a curve, which is defined [53] by it’s initial point and starting tangent vector. What does it mean to stay on, ‘the same curve’ as we move between patches? This is one way to see what is meant by the idea of ‘Connection’. Another is to ask how, if we move on a curve  $\gamma$  in the base space, we move, if at all, in the fibre  $F$ . There turn out to be four notions of connection, which are all equivalent and all of which are necessary for a full geometric picture of what is going on. I will present them in a particular order, following [16], but this fact should be born in mind.

We will start by wanting some notion of *Parallel Transport*, that is to say, given a vector  $v \in T_p E$ , can I define a unique vector in  $T_q E$  which corresponds to  $v$  in the sense that it is the tangent vector to a curve  $\gamma$  beginning at  $p$  with tangent  $v$ . The answer turns out to be, ‘Yes’, but to see this we need to construct some more machinery.

We begin by looking at the action of Lie groups on themselves, in particular discussing the Lie Algebra and its associated Maurer-Cartan forms. This allows us to define the Horizontal and Vertical subspaces of a Principle bundle  $P$ , and in turn to define the horizontal lift of a curve in the base space  $M$ . Finally, we combine these notions to define the *connection one form*, or *gauge field* in physics language. This sets up a discussion of the curvature in the next section.

### 2.2.1 Preliminaries

A Lie group has two actions on itself, a left and a right action, which I will denote, as is standard, by

$$L(g)h = gh; \quad R(g)h = hg \quad (2.2.1)$$

respectively. These actions induce corresponding differentials on the tangent space of the group, denoted by

$$L_{g*} : T_h G \rightarrow T_{gh} G; \quad R_{g*} : T_h G \rightarrow T_{hg} G \quad (2.2.2)$$

We say that a vector field  $X$  is *left invariant* if  $L_{g*}(X_h) = X_{gh}$ . The space of all left invariant vector fields on a Lie Group is called the *Lie Algebra* of  $G$ , and is denoted  $\mathfrak{g}$ . A consequence of this definition is that the vector field at every point is defined by its value  $A \in T_e G$ . It is therefore common to identify  $\mathfrak{g}$  with  $T_e G$  and define the Lie algebra to be the tangent space at the origin. Another well known property of Lie Algebras is that their generators  $T_a$  satisfy

$$[T_a, T_b] = f_{ab}^c T_c \quad (2.2.3)$$



Where the  $f_{ab}^c$  are called the *Structure Constants* of the algebra. If we choose an  $A \in \mathfrak{g}$ , this generates a one parameter subgroup of  $G$  via exponentiation- in geometric terms, it gives a curve in  $G$  defined by

$$\sigma_t(g) \equiv g \exp(tA) = R_{\exp(tA)}g \quad (2.2.4)$$

Using the fact that the vector field generated by  $A$  is left invariant, we can calculate the tangent vector to the curve to be

$$\frac{d\sigma_t(g)}{dt} = gA = L_{g*}A = X_{A|_G} \quad (2.2.5)$$

This shows that, as we expect, the tangent vector at each point is the vector field generated by  $A$  at that point. From here we can define a map from  $T_gG$  to  $\mathfrak{g} = T_eG$  by pulling the vector back along the curve. If we have the basis  $T_a$  in  $T_eG$ , so that  $A = A^a T_a$ , and a basis  $X_a \in T_gG$ , so that  $X_A = A^b X_b$ , then we can define the *Maurer – Cartan form*

$$\Theta \equiv T_a \otimes \eta^a \quad (2.2.6)$$

where  $\eta^a$  is the dual basis to  $X_a$ , i.e.  $\eta^a X_b = \delta_b^a$ . To see that this has the desired property, we calculate

$$\Theta(X_A)|_g = T_a \otimes \eta^a (A^b X_b) = T_a \delta_b^a A^b = T_a A^a = A \quad (2.2.7)$$

as required. Note that the Maurer – Cartan form is not unique, and depends upon our choice of  $A$ .

The final ingredient we need is the notion of the adjoint action

$$ad_G : G \rightarrow G : h \rightarrow ghg^{-1} \quad (2.2.8)$$

This induces a corresponding differential

$$ad_{g*} : T_hG \rightarrow T_{ghg^{-1}}G \quad (2.2.9)$$

Which, when applied to  $T_e G$  gives the adjoint representation of  $\mathfrak{g}$

$$Ad_g : \mathfrak{g} \rightarrow \mathfrak{g} : V \rightarrow gVg^{-1} \quad (2.2.10)$$

### 2.2.2 The Connection

As it turns out, the specification of a Maurer-Cartan form is both necessary and sufficient to define a connection on a principle bundle. However, it is easiest to understand the meaning of a connection via the idea of horizontal and vertical subspaces.

At every point in the principle bundle  $P$ , we can decompose  $T_p P$  into two subspaces, which we call the horizontal and vertical subspaces

$$T_p P \sim H_p P \times V_p P \quad (2.2.11)$$

These are defined by specifying  $T_p V$  as those vectors tangent to  $G$ , and  $T_p H$  as their complement. We require this choice to satisfy the, ‘equivariance condition’

$$H_{pg} P = R_{g*} H_g P \quad \forall g \in G \quad (2.2.12)$$

This means that the choice of the horizontal subspace at  $p$  determines all the choices in the sum of the orbit of the elements of the group  $g$ . Since we saw that we associated a principle bundle to a vector bundle by using these orbits, this condition essentially guarantees that the transformation applies consistently to that construction.

We can use this to define a *Horizontal lift*

**Definition 2.2.1.** Let  $P$  be a principle bundle over  $M$ , and let  $\gamma$  be a curve in  $M$ .

We define the *horizontal lift* of  $\gamma$  to be  $\gamma_p$ , where

- $\pi(\gamma_p) = \gamma$
- All tangent vectors to  $\gamma_p$  are horizontal; i.e. if  $X_p$  is a tangent vector then  $X_p \in H_p$ .

Further, we have

**Theorem 2.2.1.** *Suppose we have a curve  $\gamma \in M$  with  $p \in \pi^{-1}(\gamma(0))$ . There is a unique horizontal lift such that  $\gamma_p(0) = p$*

Note that, whilst we have here defined the Horizontal subspaces first, then required the horizontal lifts to lie in them, we could have defined the lifts first and defined the subspaces to be the span of their tangent vectors at every point.

The above definition and theorem give us what we want— given a point  $p \in P$  we can define uniquely a parallel transport along the curves  $\gamma_p$ . We can extend this definition from a principle bundle to its associated vector bundle. Suppose  $E_\rho$  is the vector bundle associated to  $P$  via the representation  $\rho$ . Given a horizontal lift  $\gamma_p(t)$  on  $P$ , we define the horizontal lift in  $E$  as

$$\gamma_E(t) = [(\gamma_p(t), v)] \quad (2.2.13)$$

i.e., the elements of the equivalence class

$$(\gamma_p(t), v) \sim (g^{-1}\gamma_p(t), \rho(g)v) \quad (2.2.14)$$

for  $g \in G$ . If we choose a different lift in  $P$ , this definition will still work, we will just get a different lift in  $E_\rho$ . Because of the equivalence condition, any other lift in  $P$  would be written as  $\gamma'_p(t) = \gamma_p(t)a$  for some  $a \in G$ . Then

$$\gamma'_E(t) = [(\gamma'_p(t), v)] = [(\gamma_p(t), \rho^{-1}(a)v)] \quad (2.2.15)$$

If we choose a local trivialisation  $\phi_P^{-1}$  for  $P$ , we can write  $\gamma_P(t) = \phi_P(t)(\gamma_t, g(t))$ . This induces a local trivialisation  $\phi_E^{-1}$  on  $E$ , in which  $\gamma_P(t) = \phi_E(t)(\gamma_t, \rho(g(t)))$ . We see that if the parallel transport in  $P$  is determined by  $g(t)$ , the transport in  $E_\rho$  is determined by  $\rho(g(t))$ .

### 2.2.3 The Connection One form

So far we have encountered three of the four definitions of connection. These are Parallel Transport, division into Horizontal and Vertical subspaces and Horizontal lifts. The fourth, and final is the *connection one form*, which is the definition that matches up most easily to the standard presentation of gauge theories. Once again we will begin by working in a principle bundle  $P$ .

Previously we have dealt mainly with the horizontal subspace – now we consider the vertical subspace. We saw in (2.2.4) that an element  $A \in \mathfrak{g}$  generates a one parameter subgroup (i.e. a curve) in  $G$ . We can modify this construction to generate a one parameter subgroup in  $P$ , which will lie in the fibre at each point of the base space  $M$  – recall that this fibre is isomorphic to  $G$

$$\sigma_t(p) = R_{\exp(tA)}p = p \exp(tA) \quad (2.2.16)$$

Under this definition,  $\pi(p) = \pi(\sigma_t)$ , since elements of  $\pi(\sigma_t)$  arise from the right action of  $G$  on  $p$ . This means that the tangent vectors to  $\sigma_t(p)$  are elements of the vertical subspace  $V_pP$ . This allows us to define a map  $\mathfrak{g} \rightarrow V_pP$  by mapping  $A \in \mathfrak{g}$  to  $\frac{d}{dt}\sigma_t(p)|_{t=0}$ . In terms of the action of the tangent vector on an arbitrary function  $f$ , we can write

$$X_A(f(p)) \equiv \pi(\sigma_t) \quad (2.2.17)$$

where we call  $X_A$  the *fundamental vector field* associated with  $A$ . If we take the set  $\{T^a\}$  of basis elements of  $\mathfrak{g}$ , these generate a basis  $\{X_{T^a}\}$  for  $V_pP$ . We can now define the *connection one form* a projection from  $T_pP$  to  $V_pP$ :

**Definition 2.2.2.** Let  $\omega$  be a Lie algebra valued one form– that is,  $\omega \in \Lambda^1P \otimes \mathfrak{g}$ . Then  $\omega$  is a connection if it satisfies

- $\omega(X_A) = A, \forall A \in \mathfrak{g}$
- $R_g^*\omega = Ad_{g^{-1}}\omega$

The first condition makes  $\omega$  into a Maurer–Cartan form, whereas the second ensures the horizontal subspaces are equivariant. We can define the horizontal subspaces as

$$H_p P = \{X \in T_p P \mid \omega(X) = 0\} \quad (2.2.18)$$

Suppose  $X \in H_p P$ . Equivariance requires  $R_{g^*} X \in H_{pg} P$ . But by the second condition above, we have

$$\omega(R_{G^*} X) = R_g^* \omega(X) = g^{-1} \omega(X) g = 0 \quad (2.2.19)$$

Therefore  $R_{g^*} X$  is horizontal, and by the action of  $g$  on  $p$  must lie in  $H_{pg}$  as required. This shows that the connection one form, which first determines the vertical subspaces, is equivalent to the horizontal lift construction, which begins by determining the horizontal ones. This is clearly also equivalent to choosing the horizontal and vertical subspaces at each point, and we have seen that the Horizontal lift construction gives a notion of parallel transport. Therefore the four definitions of connection are equivalent.

To make the connection to physics, we note that most of the time in physical applications we are working over a manifold. Therefore we can define a *local connection one form*  $A_i$  as

**Definition 2.2.3.**  $A_i \equiv s_i^* \in \Lambda U_i \otimes \mathfrak{g}$

where  $s_i$  is a section. This differs from the above in that it is only defined on a particular  $U_i$ , not on the whole of  $P$ . We have

**Theorem 2.2.2.** *If  $A_i$  is a local connection one form, and  $s_i$  is a local section defined on the same open set  $U_i$ , there is a unique connection one form  $\omega \in \pi^{-1}(U_i)$  so that  $A_i = s_i^* \omega$*

How does it transform if we choose a different section  $s_j$ ? To see this we will need to sketch a proof of the above theorem, following [16]

*Proof.* Given a section  $s_i$  on  $U_i$ , and a point  $p$  in the fibre  $\pi^{-1}(U_i)$ , we can always

find a  $g_i \in G$  so  $p = s_i(x)g_i$ , for  $x \in \pi(p)$ . We can then define a local trivialisation

$$\phi^{-1} : \pi^{-1}(U_i) \rightarrow U_i \times G : p \rightarrow (x, g_i) \quad (2.2.20)$$

With this definition, the section itself is written as  $s_i(x) = (x, e)$ . On an overlap  $U_i \cap U_j$ , the sections transform as

$$s_i(x) = \phi_i(x, e) = \phi(x, g_{ji}(x)e) = \phi_j(x, g_{ji}(x)) = \phi_j(x, e)g_{ij} = s_j(x)g_{ji}(x) \quad (2.2.21)$$

With these preparations, we can prove the theorem. This requires both proving that  $\omega$  exists, and that it is unique. I will give the outlines, and point the reader to [16] or [53] for more details. First we must prove existence. To do this, one proposes the definition

$$\omega|_{U_i} = g_i^{-1}\pi^*A_i g_i + g_i^{-1}d_P g_i \quad (2.2.22)$$

and shows that it satisfies two sets of conditions. First, it must actually satisfy the condition  $s_i^*\omega|_{U_i}(X) = A_i(X)$  from the theorem. Second, it must satisfy the conditions 2.2.2 to actually be a connection one form. The details are straightforward but not particularly illuminating and are given in the references above.

The second thing we need to check is the uniqueness of this definition. If we have  $\omega|_{U_i}$  and  $\omega|_{U_j}$  then do these definitions agree on the intersection  $U_i \cap U_j$ . Using our proposed definition for  $\omega$  we would require.

$$g_i^{-1}\pi^*A_i g_i + g_i^{-1}d_P g_i = g_j^{-1}\pi^*A_j g_j + g_j^{-1}d_P g_j \quad (2.2.23)$$

On the intersection we have  $g_j = g_{ij}g_i$  and  $s_j = s_i g_{ij}$ . We can therefore start by calculating

$$\pi^*A_j = g_{ij}^{-1}\pi^*A_i g_{ij} + g_{ij}^{-1}d_P g_{ij} \quad (2.2.24)$$

Noting that  $s_i^*\pi^* = \text{Id}_M$  and that  $s_i^*$  commutes with  $d_P$ , we can pull this back using either one of the sections to give

$$A_j = g_{ij}^{-1}A_i g_{ij} + g_{ij}^{-1}d_P g_{ij} \quad (2.2.25)$$

This establishes the equivalence (2.2.23) that we were looking for.  $\square$

This result

$$A_j = g_{ij}^{-1} A_i g_{ij} + g_{ij}^{-1} d_P g_{ij} \quad (2.2.26)$$

is actually a very interesting one from the point of view of theoretical physics. We can write it in the form,

$$A'(x) = g(x)^{-1} A(x) g(x) + g(x)^{-1} dg(x) \quad (2.2.27)$$

Then this should be very familiar as the expression for the gauge transformation of the gauge potential from particle physics!

A final interesting consequence of the above theorem is that, if the same information is contained in the globally defined  $\omega$  as in the locally defined  $A_i$ , this means that the global information about  $P$  is contained in the gauge transformations  $g_{ij}$  – gauge freedom plays a vital role in the integrity of the construction.

## 2.2.4 Field Strength

We now move to talking about the Curvature of the bundle. To do this we define the curvature 2-form. In physics terms, this is the *Field Strength* tensor, the object which actually appears in the Yang Mills action (see below).

The first step is to define an *exterior covariant derivative*, in terms of the usual exterior derivative, as

**Definition 2.2.4.**  $D\alpha(X_1, \dots, X_{p+1}) = d_P(X_1^H, \dots, X_{p+1}^H)$

where  $X_i^H \in H_p P$  is the horizontal part of  $X_i$ , and  $d_P \alpha \equiv (d_p \alpha^a) \otimes T_a$ . Note that because of the equivalence of the differing notions of connection, this construction is equivalent to the usual definition of the covariant derivative in terms of  $A_i$ ,  $D_i(X) = dX + i[A_i, X]$ .

Now we can define the *Curvature 2-form*  $\Omega$  of  $\omega$  on  $P$  as

**Definition 2.2.5.**  $\Omega = D\omega \in \Lambda^2 P \otimes \mathfrak{g}$

We now list, without proof, some properties of this object

**Theorem 2.2.3.** *The following are true:*

- $D\Omega = 0$  (*Bianchi's Identity*)
- $R_g^* = Ad_{g^{-1}}\Omega = g^{-1}\Omega g$
- $\Omega = d_P\omega + \omega \wedge \omega = d_P + \frac{1}{2}[\omega, \omega]$  (*Cartan Structure Equations*)

**Definition 2.2.6.** As before, we define the object more familiar from particle physics as the local pullback using a section  $s_i$

$$F_i = s_i^*\Omega \in \Omega^2 U_i \otimes \mathfrak{g} \quad (2.2.28)$$

We have the well known formula

$$F_i = s_i^* d_P\omega + s_i^*(\omega \wedge \omega) = d(s_i^*) + s_i^*\omega \wedge s_i^*\omega \quad (2.2.29)$$

$$= dA_i + A_i \wedge A_i \quad (2.2.30)$$

and, induced by the second of (2.2.3), if two sections are related as  $s'(x) = s(x)g(x)$ ,

$$F'(x) = g(x)^{-1}F(x)g(x) \quad (2.2.31)$$

## 2.3 Some Algebraic Topology

We continue building up to the definition of an Instanton. First I will briefly overview homotopy theory. This is essential for geometrically understanding how Instantons work. I will then show the derivation of the Chern classes via De Rham Cohomology along with certain results from the Theory of Invariant Polynomials. Finally I will show how these notions coincide for the cases we are interested in.

### 2.3.1 Homotopy Theory

Homotopy is a useful topological invariant [33]. We will start by defining homotopies of based loops, and use these to define the first homotopy group. We will state the



definition of the higher homotopy groups, then move on to defining the Brouwer map, or topological degree, which gives equivalent information for the spaces we are interested in. Finally we will look at homotopy groups arising from the specific examples of  $U(1)$  and  $SU(2)$  – the latter is the one we are interested in from the point of view of Instantons.

**Definition 2.3.1.** Suppose  $\alpha$  and  $\beta$  are both based loops on  $M$  – i.e.  $\alpha : [0, 1] \rightarrow M$ , with  $\alpha(0) = \alpha(1) = x \in M$ . Then we say they are *homotopic* to one another if there is a continuous map

$$H : I \times I \rightarrow M : (s, t) \rightarrow H(s, t) \quad (2.3.1)$$

with the properties

$$H(s, 0) = \alpha(s); \quad H(s, 1) = \beta(s), \quad \forall s \in I \quad (2.3.2)$$

and

$$H(0, t) = H(1, t) = x \quad (2.3.3)$$

We can show that this is an equivalence relation, and denote the equivalence class of  $\alpha$  as  $[\alpha]$ . If we define the product  $\alpha \circ \beta$  of two loops to be tracing out first  $\alpha$  then  $\beta$ , and  $\alpha^{-1}$  to be tracing out  $\alpha$  in reverse order, then we can define a group whose elements are the homotopy classes  $[\alpha]$ . The homotopy classes are necessary as whilst  $\alpha \circ \alpha^{-1}$  is clearly not the same as the constant loop  $\alpha(t) = x$ , they are homotopic to it. With this in mind we have

**Definition 2.3.2.** The *Fundamental group* or *First Homotopy group*,  $\Pi_1(M, x)$  is the group formed by the homotopy classes of loops based at  $x$ . If  $M$  is path connected, then this definition is independent of the point chosen, and so we denote it  $\Pi_1(M)$ .

We can define higher homotopy groups  $\Pi_n$  in an analogous manner, by looking at maps  $\alpha : I^n \rightarrow M$ , with the based condition that  $\delta M$ , the boundary of the manifold,

maps to a single point  $X$ . In general calculating these groups is highly non-trivial; however if the maps we are considering are between spaces of the same dimensions (which is true in our case), we can get the same information by considering the *Brouwer degree* of the map.

**Definition 2.3.3.** Let  $M$  and  $N$  be manifolds of dimension  $n$ , and let  $\Omega$  be a normalised volume form on  $N$ , so that  $\int_N \Omega = 1$ . Then the *Brouwer degree*, or *topological degree* of a map  $\phi : M \rightarrow N$  is defined as

$$\deg(\phi) = \int_M \phi^* \Omega \quad (2.3.4)$$

This definition is independent of our choice of volume form  $\Omega$ , and we can prove that  $\deg(\phi)$  is both an integer and a topological invariant. To see how this works in practice, we will look at  $\Pi_1(U(1))$ , which arises from considering  $U(1)$  bundles over  $S^2$ , in the context of Dirac Monopoles [16].

First, note that  $\Pi_1(U(1)) \cong \Pi_1(S^1)$ , which is therefore composed of maps from a circle to itself. These are given by

$$g_{n,a} : t \rightarrow \exp(i(nt + a)) \quad (2.3.5)$$

Two maps  $g_{n,a}$  and  $g_{n,b}$  are homotopic, but  $g_{n,a}$  and  $g_{m,a}$  are not. So we need only consider maps of the form

$$g_n = \exp(int) \quad (2.3.6)$$

Therefore our homotopy classes are  $[g_n]$ , meaning that

$$\Pi_1(U(1)) \cong \mathbb{Z} \quad (2.3.7)$$

We call  $n$  the *winding number* of the map. We can take the volume form

$$\Omega = \frac{1}{2\pi i} g^{-1} dg, \quad g \in U(1) \quad (2.3.8)$$

which gives

$$\deg(\phi) = \int_M \phi^* \Omega = \frac{1}{2\pi i} \int_M g_n(t)^{-1} \frac{dg_n(t)}{dt} dt = n \quad (2.3.9)$$

The topological degree is the winding number; and as expected it is an integer.

We now move on to the group we will be using throughout this document,  $\Pi_3(SU(2))$ . Rather than calculating the group explicitly, we will use the fact that classes in the group are classified by their Brouwer degree. We can take the following volume form on  $SU(2)$

$$\Omega = \frac{1}{24\pi^2} \text{Tr}(g^{-1}dg \wedge g^{-1}dg \wedge g^{-1}dg) \quad (2.3.10)$$

where

$$g = c_0 \mathbb{1}_2 + c_i \tau_i; \quad c_0^2 + c_i^2 = 1 \quad (2.3.11)$$

where the  $\tau_i$  are the Pauli matrices. If we define  $g : S^3 \rightarrow SU(2) : x \rightarrow g(x)$  we can define the topological degree as

$$\int_{S^3} g^* \Omega = \frac{1}{24\pi^2} \int_{S^3} \text{Tr}(g'^{-1}dg' \wedge g'^{-1}dg' \wedge g'^{-1}dg') = n \quad (2.3.12)$$

Where  $dg = \partial_i g dx^i$ . This tells us that  $\Pi_3(SU(2)) = \mathbb{Z}$ .

### 2.3.2 Chern Classes

Let  $\mathfrak{g}$  be a Lie Algebra and  $X_i \in \mathfrak{g}; i \in 1, \dots, n$ . A Polynomial  $P(X_1, \dots, X_n)$  is called *symmetric* if

$$P(X_1, \dots, X_i, \dots, X_j, \dots, X_n) = P(X_1, \dots, X_j, \dots, X_i, \dots, X_n); \quad \forall i, j \quad (2.3.13)$$

It is further called a *symmetric invariant polynomial* if

$$P(g^{-1}X_1g, \dots, g^{-1}X_ng) = P(X_1, \dots, X_n) \quad (2.3.14)$$

where  $g \in G$ , the Lie group corresponding to  $\mathfrak{g}$ . Finally, we can take the, ‘diagonal’ of a symmetric invariant polynomial by taking all the  $X_i$  to be equal. This is simply called an *invariant polynomial (of degree  $n$ )*

$$P_n(X) \equiv P(X, \dots, X) \quad (2.3.15)$$

where it is understood that  $P$  has  $n$  arguments – this is what is meant by the polynomial being of degree  $n$ .

We will want to extend this definition from polynomials in  $\mathfrak{g}$  to polynomials in  $\mathfrak{g}$ -valued differential forms. We can write a  $\mathfrak{g}$  valued  $p$ -form as

$$\alpha_i = \eta_i X_i \tag{2.3.16}$$

where no sum over  $i$  is implied,  $\eta_i$  is a standard  $p$ -form (valued in  $\mathbb{R}$ ) and  $X_i \in \mathfrak{g}$  as before. Then we get an object with analogous properties to the above by defining an invariant polynomial of  $\mathfrak{g}$ -forms as

$$P(\alpha_1, \dots, \alpha_n) = P(X_1, \dots, X_n) \eta_1 \wedge \dots \wedge \eta_n \tag{2.3.17}$$

We can then define an Invariant polynomial of degree  $n$  analogously as

$$P_n(\alpha_n) \equiv P(\alpha^n) = P(X^n) \eta \wedge \dots \wedge \eta \tag{2.3.18}$$

We will be interested in polynomials in  $F$ , the field strength 2-form. These have the following important properties. A proof can be found in [16].

**Theorem 2.3.1.** *Let  $P_n(F)$  be a an Invariant Polynomial in the Field Strength  $F$ .*

*Then:*

- $P_n(F)$  is closed; i.e.  $dP_n(F) = 0$
- If  $F$  and  $F'$  are two curvature 2-forms corresponding to different connections on the same bundle, then the difference  $P_n(F) - P_n(F')$  is exact, i.e.  $P_n(F) - P_n(F') = dQ_{2n-1}(A', A)$ , for some  $dQ$ , where  $A'$  and  $A$  are the connection one-forms corresponding to  $F', F$ .
- Given  $A$  and  $A'$  as above, we can define a homotopy between them,  $A_t = A + t\theta$ ;  $\theta = A' - A$ . This induces a field strength homotopy

$$F_t = dA_t + A_t \wedge A_t = F + tD\theta + t^2\theta \wedge \theta \tag{2.3.19}$$

In terms of these, we can find an explicit expression for  $Q$

$$Q_{2n-1}(A, A') = n \int_0^1 dt P(A' - A, F_t^{n-1}) \quad (2.3.20)$$

The third condition allows us to define the *Chern-Simons Form*. Suppose we are working on one of the patches  $U_i$  of the bundle. Then we can always define a trivial connection  $A'$ . Using the third part of the above theorem we can define the Chern-Simons form as

$$Q_{2n-1}(A) \equiv Q_{2n-1}(A, 0) = n \int_0^1 dt P(A, F_t^{n-1}) \quad (2.3.21)$$

where

$$A_t = tA, \quad F_t = t dA + t^2 A \wedge A = tF + (t^2 - t)A \wedge A \quad (2.3.22)$$

Given a one-form connection we can always construct an associated Chern-Simons Form using (2.3.21).

Invariant Polynomials are closed and non-trivial, therefore they represent a non-trivial de Rham cohomology class  $[P_n(F)] \in H^{2n}(M, \mathbb{R})$ . We call this the *characteristic class*. Since the difference of two polynomials from two connections is exact, this does not depend upon the choice of connection.

**Definition 2.3.4.** The *Total Chern class* of a principle bundle  $P$  with  $G$  a lie group is

$$\det\left(1 + \frac{i}{2\pi}F\right) \quad (2.3.23)$$

where  $F$  is the field strength defined above. This is an invariant polynomial in  $F$ .

**Definition 2.3.5.** Since  $F$  is a two form,  $c(F)$  is a sum of forms of degree  $2n$

$$c(F) = 1 + c_1(F) + c_2(F) + \dots \quad (2.3.24)$$

We call  $c_n(F) \in \Lambda^{2n}M$  the *nth Chern class*

It is important to note that chern classes of higher dimension than the base space  $M$  vanish – i.e. if  $M$  has dimension  $m$  then  $c_n = 0 \forall 2n > m$ .

In order to calculate this, it is usual to use a gauge transformation – in mathematical terms a choice of section – to diagonalise  $F$  to a matrix with 2-forms  $x_i$  on the diagonal. Then

$$\begin{aligned} \det(1 + \tilde{F}) &= \det \left[ \text{diag}(1 + x_1, \dots, 1 + x_k) \right] = \prod_{i=1}^k (1 + x_i) & (2.3.25) \\ &= 1 + (x_1 + \dots + x_k) + (x_1 x_2 + \dots + x_{k-1} x_k) + \dots + (x_1 x_2 \dots x_k) \\ &= 1 + \text{Tr} \tilde{F} + \frac{1}{2} \left[ (\text{Tr} \tilde{F})^2 - \text{Tr} \tilde{F}^2 \right] + \dots + \det \tilde{F} \end{aligned}$$

where  $\tilde{F} = \frac{i}{2\pi} F$ . From this we can read off

$$c_1 = \text{Tr} \tilde{F} = \frac{i}{2\pi} \text{Tr} F \quad (2.3.26)$$

$$c_2 = \frac{1}{2} \left[ (\text{Tr} \tilde{F})^2 - \text{Tr} \tilde{F}^2 \right] = \frac{1}{8\pi^2} \left[ \text{Tr}(F \wedge F) - \text{Tr} F \wedge \text{Tr} F \right] \quad (2.3.27)$$

⋮

$$c_k = \det \tilde{F} = \left( \frac{i}{2\pi} \right)^k \det F \quad (2.3.28)$$

We can use the fact that the Chern classes are independent of the connection to define

**Definition 2.3.6.** The *Chern numbers* are defined by

$$c_n \equiv \left( [c_n(F)], M \right) = \int_M c_n(F) \quad (2.3.29)$$

It can be shown that on a complex manifold, these are always integers [16]

We can further define

**Definition 2.3.7.** For a Lie group  $G$ , the *Total Chern Character* is defined as

$$ch(F) = \text{Tr} \exp \left( \frac{i}{2\pi} F \right) = \sum_n \frac{1}{n!} \text{Tr} \left( \frac{i}{2\pi} F \right)^n \quad (2.3.30)$$

Analogous to the case of the Chern classes, we can define

**Definition 2.3.8.** The *Chern characters* are defined as

$$ch_n(F) = \frac{1}{n!} \text{Tr} \left( \frac{i}{2\pi} F \right)^n \quad (2.3.31)$$

We can relate them to the Chern classes as

$$ch_0(F) = k \quad (2.3.32)$$

$$ch_1(F) = c_1(F) \quad (2.3.33)$$

$$ch_2(F) = -c_2(F) + \frac{1}{2}c_1(F) \wedge c_1(F) \quad (2.3.34)$$

We now move on to some examples. Once more, we will start by looking at  $U(1)$  as a test case, before moving to the  $SU(2)$  instantons we are interested in in the rest of the thesis.

### 2.3.3 Examples

For a  $U(1)$  bundle over a two dimensional manifold, the only nonzero Chern class is  $c_1(F)$ . Locally,  $F = dA$  and so we have

$$c_1(F) = d\left(\frac{i}{2\pi}A\right) \quad (2.3.35)$$

This implies that

$$Q_1(A) = \frac{i}{2\pi}A \quad (2.3.36)$$

Alternatively we could have calculated

$$Q_1(A) = \int_0^1 dt P(A) = \int_0^1 dt c_1(A) = \int_0^1 dt \frac{i}{2\pi}A = \frac{i}{2\pi}A \quad (2.3.37)$$

Now we move on to look at  $SU(2)$ . Because, for  $SU(2)$ , the trace vanishes,  $c_1(F) = 0$ .

This means that  $ch_2(F) = -c_2(F)$ , so it is usual to use, ‘Chern class’ to refer to both.

Instantons are usually defined in 4 dimensional Euclidean Space. We are interested in solutions with finite Action. For this to be the case, we need the solution to become pure gauge at infinity, which means

$$A|_{S_\infty^3} = g^{-1}dg \rightarrow F|_{S_\infty^3} = 0 \quad (2.3.38)$$

Where  $S_\infty^3$  is the 3-sphere at infinity in  $\mathbb{R}^4$ . Therefore these solutions are classified by maps  $g : S_\infty^3 \rightarrow SU(2)$ . We saw the topological degree of this map in (2.3.12). We now show that this is linked to the Chern classes of this set-up.

As stated above  $c_1 = 0$ , and so we need only look at  $c_2$ . To calculate this, we use the fact that  $c_2(F) = dQ_3(A)$ . This can be calculated from the definition (2.3.21) as

$$\begin{aligned} Q_3 &= 3 \int_0^1 dt P(A, F_t) = \frac{1}{4\pi^2} \int_0^1 dt \text{Tr}(A \wedge F_t) \\ &= \frac{1}{4\pi^2} \int_0^1 dt \text{Tr}(tA \wedge dA + t^2 A \wedge A \wedge A) \\ &= \frac{1}{8\pi^2} \text{Tr}\left(A \wedge dA + \frac{2}{3} A \wedge A \wedge A\right) \end{aligned} \quad (2.3.39)$$

Incidentally, this is the well known Chern Simons form. We can now use this to calculate  $c_2$  via

$$\begin{aligned} c_2 &= \int_{S^4} c_2(F) = \int_{S_\infty^3} Q_3(A) = \frac{1}{8\pi^2} \int_{S_\infty^3} \text{Tr}\left(A \wedge dA + \frac{2}{3} A \wedge A \wedge A\right) \\ &= \frac{1}{8\pi^2} \int_{S_\infty^3} \text{Tr}\left(F \wedge A - \frac{1}{3} A \wedge A \wedge A\right) = -\frac{1}{24\pi^2} \int_{S_\infty^3} \text{Tr}\left(A \wedge A \wedge A\right) \\ &= -\frac{1}{24\pi^2} \int_{S_\infty^3} \text{Tr}\left(g^{-1} dg \wedge g^{-1} dg \wedge g^{-1} dg\right) \end{aligned} \quad (2.3.40)$$

Up to a sign this is identical to the topological degree of the map, linking the homotopy with the Chern classes. It is often convenient to add a point at infinity to  $\mathbb{R}^4$  – though in fact to do this consistently we need to define instantons via the bundle construction. In this case, we have two open sets covering the sphere; the north and south hemispheres,  $U_N$  and  $U_S$ . On these sets we have

$$F^N = dA^N + A^N \wedge A^N, \quad F^S = dA^S + A^S \wedge A^S \quad (2.3.41)$$

where

$$A^N = g^{-1} A^S g + g^{-1} dg; \quad \text{which implies } F^N = g^{-1} F^S g \quad (2.3.42)$$

as we would expect for the transformations of these objects. Here the computation of  $c_2$  splits into a sum of contributions for each  $U_i$ , but we eventually get

$$c_2 = \frac{1}{24\pi^2} \int_{S_\infty^3} \text{Tr}\left(g^{-1} dg \wedge g^{-1} dg \wedge g^{-1} dg\right) \quad (2.3.43)$$



This is precisely the degree of the map  $g$ , which is always an integer  $k$ . Therefore the classification in terms of  $c_2$  is equivalent to the homotopy group  $\Pi_3(SU(2))$ . The reason we need to see both these formulations is that the Lagrangian of the relevant gauge theory is based around  $c_2$ , but the geometric interpretation of instantons in terms of transition functions between  $U_N$  and  $U_S$  is a much easier thing to visualise. We now have all the machinery we need to define instantons, which we will do in the next chapter.

# Chapter 3

## Instantons

In this chapter we define what instantons are, and discuss their construction via the ADHM method. Many of the instantons we discuss in this thesis are defined over noncommutative space, so we must first introduce this concept. We also look at the notation I will be using to describe the quaternions, and introduce their complexification, the biquaternions.

### 3.1 Instantons

We can now finally define what an instanton is. Let  $F$  be the field strength of an  $SU(2)$  bundle over  $R^4$ . Writing  $F = \frac{1}{2}F_{ij} dx^i \wedge dx^j$ , with the further understanding that  $F_{ij} = F_{ij}^a T_a$ , we have the following *Yang Mills* Lagrangian:

$$S_{YM} = \frac{1}{4} d^4x F_{ij}^a F_a^{ij} = -\frac{1}{2} \int d^4x \text{Tr}(F_{ij} F^{ij}) = - \int d^4x \text{Tr}(F \wedge \star F) \quad (3.1.1)$$

Here  $\star F$  is the Hodge dual of  $F$ , which is defined in flat space as

$$\star F_{ij} = \frac{1}{2} \epsilon_{ijkl} F^{kl} \quad (3.1.2)$$

Noting that we can write

$$\frac{1}{4} \int (F_{ij}^a \pm \star F_{ij}^a)(F_a^{ij} \pm \star F_a^{ij}) = - \int \text{Tr}(F \pm \star F) \wedge \star(F \pm \star F) \quad (3.1.3)$$

$$= -2 \int \text{Tr}(F \wedge \star F) \mp 2 \int \text{Tr}(F \wedge F)$$

We can get a lower bound on the action as

$$S_{YM} = -\frac{1}{2} \int \text{Tr}(F \pm \star F) \wedge \star(F \pm \star F) \pm \int \text{Tr}(F \wedge F) \geq 8\pi^2 |k|^2 \quad (3.1.4)$$

where in this context, we call  $k$  the *Instanton number* and define it as

$$k = -c_2(F) = ch_2(F) \quad (3.1.5)$$

We can see that this is achieved when  $F = \pm \star F$ . We call such solutions selfdual (SD) and anti selfdual (ASD) instantons respectively. In this thesis, we will be calculating anti selfdual instantons, which correspond to positive  $k$ . Since instantons are minima of the action, they are a solution of the equations of motion. This is a specific example of a Bogomolny bound. These are named for the paper [8] for Monopoles, but actually were first shown for instantons in [6]. Bogomolny bounds are arguments, like the one above, which involve showing (usually by some kind of completing the square) that the energy of a system is bounded from below. This can also be understood in supersymmetric terms [60]. Supersymmetry considerations imply that the Hamiltonian  $\mathcal{H}$  acting on the supersymmetric vacuum  $|0\rangle$  must be zero, however it is sometimes possible to add an integer to the Hamiltonian to get the equation. This integer comes from the central charge of the supersymmetric algebra, and is a topological invariant.

$$(\mathcal{H} \pm \mathbb{Z}) |0\rangle = 0 \quad (3.1.6)$$

This then allows solutions where  $\mathcal{H} = \mp \mathbb{Z}$ . Such solutions are called BPS states. Instantons are a particular example of these states, where the central charge  $\mathbb{Z}$  is the Instanton number  $k$ . They break some amount of the supersymmetries of the underlying theory. In particular, pure instantons break half, and so are known as  $\frac{1}{2}$ -BPS states, whereas dyonic instantons break another half, preserving only a quarter of the original supersymmetries, and so are known as  $\frac{1}{4}$ -BPS states. The

final thing to consider is Derrick's Theorem [20]. This is a non – existence theory which gives a straightforward condition to check if solitons exist in a particular theory [52]. Derrick's theorem is valid for finite energy solutions in flat space. The general idea is that a soliton solution, being a local minima of the energy, must be invariant under any variation of the energy – this includes spatial rescalings. If there are no fixed points of the transformation of the energy under spatial rescaling, then there can be no stationary points of the energy as a whole, and therefore no solitons. More specifically, if  $\mathbf{x} \in \mathbb{R}^d$ , then a spatial rescaling is a map  $\mathbf{x} \rightarrow \mu\mathbf{x}$ , where  $\mu \in \mathbb{R}_{>0}$ . The energy of the system will be a function of the fields in the system,  $E(\psi_i)$ . Under the spatial rescaling, there will be a one parameter family of these fields under that rescaling. We label these  $\Psi_i^{(\mu)}$ . We can define the variation of the energy under these rescalings as

$$e(\mu) = E(\psi^{(\mu)}) \quad (3.1.7)$$

Derrick's theorem then states

**Theorem 3.1.1.** *If, for a set of finite energy fields  $\Psi_i(\mathbf{x})$ , the function  $e(\mu)$  has no stationary point (excluding the vacuum), then the theory has no static, finite energy solutions (other than the vacuum)*

It is necessary to explain what is meant by a static field. We can always make a gauge choice so that  $A_0 = 0$ . In this case, static means that there is no electric field  $F_{i0}$ . Now, applied to Yang Mills theory in  $d + 1$  dimensions (where  $d \geq 4$ ), the general form of the energy functional will be

$$E = \int \left( |F|^2 + |D\Phi|^2 + U(\phi) \right) d^d x \equiv E_4 + E_2 + E_0 \quad (3.1.8)$$

Where  $\phi$  is a scalar field, and  $U$  is a gauge potential. Looking at the mass dimensions of the constituent parts under the rescaling we get

$$e(\mu) = \mu^{4-d} E_4 + \mu^{2-d} E_2 + \mu^{-d} E_0 \quad (3.1.9)$$

If  $d = 4$ , then this becomes

$$E_4 + \frac{1}{\mu^2}E_2 + \frac{1}{\mu^4}E_0 \quad (3.1.10)$$

This has no stationary point apart from the vacuum  $E_4 = E_2 = E_0 = 0$ , and therefore there are no static solutions in 4d Yang Mills with a scalar field. However in pure Yang Mills, we only have  $e(\mu) = E_4$ . This is completely independent of the scale, and therefore solitonic solutions are possible – i.e. Instantons as described above. This limits Instantons to appear in pure Yang Mills in 4d, however the presence of an additional length scale in noncommutative theories means that they are not defined in flat Euclidean space, and therefore they are not subject to these constraints.

In dimensions greater than 4 we can find a solution as follows. First, we multiply both sides by  $\mu^4$  to get

$$\mu^4 E_4 + \mu^2 E_2 + E_0 = 0 \quad (3.1.11)$$

This is a quadratic equation in  $\mu^2$ , and so we can solve for it as

$$\mu^2 = \frac{-(2-d)E_2 \pm \sqrt{(2-d)^2 E_2^2 - 4(4-d)E_4 E_0}}{2(4-d)} \quad (3.1.12)$$

Therefore we can have Solitonic solutions in Yang Mills with  $d \geq 5$

## 3.2 Noncommutativity

It is convenient to introduce the study of noncommutative spacetimes into the study of Instantons. It is convenient because it allows us to resolve singularities on the Instanton moduli space (see the next chapter). It was first show in [54] that this was possible, and since then many examples have been constructed (see [12] for a selection).

To construct a noncommutative version of  $\mathbb{R}^4$ , we simply impose an anti-commutation relation on the spacetime coordinates

$$[x^n, x^m] = \theta^{mn} \quad (3.2.1)$$

Here  $m, n$  are the Euclidean Lorentz indices, and  $\theta^{mn}$  is a real, antisymmetric, constant matrix. We can always rotate it into the form

$$\theta^{mn} = \begin{bmatrix} 0 & \theta^{12} & 0 & 0 \\ -\theta^{12} & 0 & 0 & 0 \\ 0 & 0 & 0 & \theta^{34} \\ 0 & 0 & -\theta^{34} & 0 \end{bmatrix} \quad (3.2.2)$$

There are several interesting subcases of this matrix [12]; but for the purposes of this Thesis, I will consider the so called selfdual (SD) case, where  $\theta^{12} = \theta^{34} = 2\zeta$ . This does not involve any loss of generality however. This is because when one follows the ADHM construction of Instantons (see section 3.3) however it turns out both that anti selfdual (ASD) instantons on anti selfdual noncommutative  $\mathbb{R}^4$  are equivalent to commutative instantons (as are selfdual instantons on selfdual spacetime) and that ASD instantons on SD spacetime are equivalent to SD instantons on ASD spacetime. It turns out the noncommutativity of the spacetime coordinates forces us to modify our notion of the multiplication of functions. Rather than the usual multiplication, we use the *Moyal Star Product*. This was developed in 1947, long before the idea of noncommutative spacetimes were thought up, to give a well defined notion of phase space measure for noncommuting positions and momenta [49]. This is defined as

$$f(x) \star g(x) = \exp\left(\frac{i}{2}\theta^{ij}\partial_i\partial'_j\right)f(x)g(x')|_{x=x'} \quad (3.2.3)$$

This gives the following expansion on powers of  $\theta^{ij}$

$$f(x) \star g(x) = f(x)g(x) + \frac{i}{2}\theta^{ij}\partial_i f(x)\partial_j g(x) + \mathcal{O}(\theta^2) \quad (3.2.4)$$

This becomes important when calculating the gauge potential and field strength to be

$$A_i \rightarrow g^{-1} \star A_i \star g + g^{-1} \star \partial_i g \quad (3.2.5)$$

This modifies the definition of the Field Strength to be

$$F_{ij} = \partial_{[i}A_{j]} - i[A_i, A_j]_{\star} \quad (3.2.6)$$

Where

$$[A_i, A_j]_{\star} = A_i \star A_j - A_j \star A_i \quad (3.2.7)$$

as one might expect. This has two effects on our Instanton solutions. First of all, it allows us to find solutions with no commutative equivalent, since the additional length scale  $[\zeta] = [length]^2$  and the fact we are not in Euclidean flat space means Derrick's theorem does not apply.

Secondly, and less positively, in theory it implies we have an infinite number of terms to calculate. However we can avoid this thanks to an isomorphism between the algebra of functions with the  $\star$ - product, and certain operators over Hilbert space. This is more fully discussed in [25], however I will give a brief overview of the argument here.

For simplicity, following [37] we consider the case where only  $x_1$  and  $x_2$  have a nonzero commutation relation. Given a function  $f(x_1, x_2)$  defined on these variables, we have an associated operator on the Hilbert Space of  $\hat{x}_1, \hat{x}_2$ , where these are the quantised variables associated with  $x_1$  and  $x_2$ . This operator is given by

$$\hat{O}_f(\hat{x}_1, \hat{x}_2) = \frac{1}{4\pi^2} \int d^2\alpha \exp\left(-i(\alpha_1\hat{x}_1 + \alpha_2\hat{x}_2)\right) \tilde{f}(\alpha_1, \alpha_2) \quad (3.2.8)$$

Where  $\tilde{f}(\alpha_1, \alpha_2)$  is the Fourier transform of  $f(x_1, x_2)$ . Given two such functions,  $f, g$ , changing variables, and using the Baker- Campbell- Hausdorff formula, we can now calculate

$$\hat{O}_f \hat{O}_g = \frac{1}{4\pi^2} \int d^2\gamma \exp\left(-i(\gamma_1\hat{x}_1 + \gamma_2\hat{x}_2)\right) \widetilde{f \star g}(\alpha_1, \alpha_2) \quad (3.2.9)$$

This shows the algebra of functions on noncommutative space spanned by  $(x_1, x_2)$  is isomorphic to the algebra of operators on the Hilbert space spanned by  $\hat{x}_1$  and  $\hat{x}_2$ .

### 3.2.1 Quaternions and Biquaternions

There is one final ingredient we must look at before moving on to defining the ADHM construction. This construction turns out to be describable in terms of either the Quaternions, or their complexification, the biquaternions, and therefore I discuss these

groups and the conventions which I am using here.

The group  $\mathbb{C} \times \mathbb{H}$ , known as Complex Quaternions, Biquaternions and even Tessarions has a long history [35]. To avoid confusion I will refer to the group as Biquaternions in the rest of the thesis. As discussed in [51], the algebra is equipped with three notions of conjugation. We write a general element of the group as

$$q = q_R + iq_I = q_{R0} + \mathbf{q}_R + i(q_{I0} + i\mathbf{q}_I) \quad (3.2.10)$$

Where  $q_R, q_I \in \mathbb{H}$ , and correspondingly  $q_{R0}, q_{I0} \in \mathbb{R}$  and  $\mathbf{q}_R, \mathbf{q}_I \in SU(2)$  considered as the quaternion imaginary part of  $\mathbb{H}$ . Then we have a Complex conjugation  $q^*$ , which takes

$$q_R + iq_I \rightarrow q_R - iq_I \quad (3.2.11)$$

We also have a quaternion conjugation  $\bar{q}$

$$q_R + iq_I \rightarrow q_R^\dagger + (iq_I)^\dagger \rightarrow \bar{q}_R + i\bar{q}_I = q_{R0} - \mathbf{q}_R + i(q_{I0} - \mathbf{q}_I) \quad (3.2.12)$$

Finally we have a total conjugation  $q^\dagger$  which applies both these operations simultaneously

$$q_R + iq_I \rightarrow \bar{q}_R - i\bar{q}_I = q_{R0} - \mathbf{q}_R - i(q_{I0} - \mathbf{q}_I) \quad (3.2.13)$$

This group has several very interesting properties, which are sadly beyond the scope of this thesis. First of all, they are isomorphic to  $Cl(3)$  [51], which itself is a representation of the Dirac algebra [26]. Second, we can describe Lorentz Transformations in terms of the actions of biquaternions on themselves (these facts seem to be re-discovered every few decades. A particularly interesting comparison can be drawn between [42] and the line of thought reviewed in [34], which both use biquaternions to rederive Dirac Theory, independently and via different methods). Finally, it has been shown in [24] that the biquaternions contain all the representations of the Lorentz group in the form of algebraic ideals.

These are indications that the Biquaternions have a more fundamental role in physics than is usually recognised. Another argument for this is provided in [9]. In this



book, Bohm argues that the most appropriate mathematical object to describe reality is the Algebra. This is because Algebras have both a notion of the action of one part of reality on another, via their multiplication, and a notion of relative proportion, via their addition. Bohm additionally argues that we should not want nilpotent elements in the algebra we choose, since interactions corresponding to these elements would not be observable on a macro level. Such algebras are called division algebras, and over the real numbers, the only such algebras are  $\mathbb{R}$ ,  $\mathbb{C}$ , and  $\mathbb{H}$ , whereas over  $\mathbb{C}$  the only division algebra is  $\mathbb{C}$  itself. So the group  $\mathbb{C} \times \mathbb{H} \cong \mathbb{C} \times \mathbb{C}_{\mathbb{C}}$  is a very natural object under this line of reasoning.

We conclude this section with some comments on notation. We use the basis  $\sigma_n$  for the quaternions, with  $\sigma_n = (\mathbb{1}_2, i\tau_i)$ , where the  $\tau_i$  are the standard Pauli matrices. We also define  $\bar{\sigma}_n = (\mathbb{1}_2, -i\tau_i)$ . Further, we define the selfdual object

$$\sigma_{mn} = \frac{1}{4} \left( \sigma_m \bar{\sigma}_n - \sigma_n \bar{\sigma}_m \right) \quad (3.2.14)$$

and the anti-selfdual

$$\bar{\sigma}_{mn} = \frac{1}{4} \left( \bar{\sigma}_m \sigma_n - \bar{\sigma}_n \sigma_m \right) \quad (3.2.15)$$

With these definitions, we have

$$\sigma_0 = \begin{bmatrix} 1 & 0 \\ 0 & 1 \end{bmatrix}, \quad \sigma_1 = \begin{bmatrix} 0 & -1 \\ 1 & 0 \end{bmatrix}, \quad \sigma_2 = \begin{bmatrix} 0 & i \\ i & 0 \end{bmatrix}, \quad \sigma_3 = \begin{bmatrix} i & 0 \\ 0 & -i \end{bmatrix} \quad (3.2.16)$$

Finally, the fact that the biquaternions have multiple notions of conjugation means that there are multiple notions of the imaginary part. I will use  $\text{Im}_{\mathbb{H}}$  to denote the quaternion imaginary part, defined for  $q = q_0 + \mathbf{q} \in \mathbb{H}$ , with  $q_0 \in \mathbb{R}$  and  $\mathbf{q} \in SU(2)$  as

$$\text{Im}_{\mathbb{H}}(q) = \mathbf{q} \quad (3.2.17)$$

We also have the complex imaginary part, defined for  $z \in \mathbb{C}$ ,  $z = x + iy$  as

$$\text{Im}_{\mathbb{C}}(z) = y \quad (3.2.18)$$

Note that  $\text{Im}_{\mathbb{C}}$  doesn't include the factor  $i$  which we must add in by hand where it is required- this is done to match with the usual definition of  $\text{Im}$  in the complex case, however it does mean some care has to be taken when restricting from  $\mathbb{H}$  to  $\mathbb{C}$ , as  $i$  then corresponds to the imaginary quaternion basis vector, which is included in  $\text{Im}_{\mathbb{H}}$  but not in  $\text{Im}_{\mathbb{C}}$ .

In the case of a biquaternion  $q = q_R + iq_I$  we have

$$\text{Im}_{\mathbb{C}}(q) = q_I ; \text{Im}_{\mathbb{H}}(q) = \mathbf{q}_R + i\mathbf{q}_I \quad (3.2.19)$$

where  $\mathbf{q}_R$  and  $\mathbf{q}_I$  are the quaternion imaginary parts of  $q_R$  and  $q_I$  respectively. We similarly define  $\text{Re}_{\mathbb{H}}$  and  $\text{Re}_{\mathbb{C}}$ .

### 3.3 ADHM

To actually calculate an Instanton solution, we can use the ADHM construction. This was first developed in [2] following a suggestion in [46]. There is a strong link between the ADHM construction and Twistors, and this is discussed in [59]. The Twistor implications of noncommutative instantons are discussed in [39]. Another mathematical motivation comes via the topic of Hyper- Kahler quotients, and this is the approach taken by [22]. These treatments are beyond the scope of this thesis. Instead I will first of all give a simple outline of the ADHM construction. I will then go into more detail, presenting the ADHM solution as an Ansatz for the self dual field strength, and showing how this motivates the construction, following the presentation in [21]. I will finish by explaining in detail how to carry out the construction in both the commutative and noncommutative cases, following [12].

The main ingredient in the ADHM construction is the ADHM Data  $\Delta$ . This is an  $(N + 2k) \times 2k$  matrix, where  $N$  is the degree of the gauge group  $SU(N)$  or  $U(N)$ , and  $k$  is the Instanton number, or topological degree. In the commutative case the entries are usually taken to be real, whereas in the noncommutative case they are taken as being complex. However, as I will show we can take them to be complex

in the commutative case too, and use the additional symmetry this gives to recover the usual real solution. Therefore I will treat the entries as being complex in the remainder of this thesis unless otherwise stated. With this in mind, we have

$$\Delta = \begin{bmatrix} \Lambda \\ \Omega \end{bmatrix} \quad (3.3.1)$$

where  $\Lambda$  is an  $N \times 2k$  complex matrix and  $\Omega$  is a  $2k \times 2k$  complex matrix. It is often useful for the purpose of performing calculations to treat these as being instead biquaternion-valued matrices (or quaternion-valued, for real matrices). The matrix  $\Omega$  can always be treated as a  $k \times k$  matrix of biquaternions.  $\Lambda$  is a bit trickier. For some values of  $N$  and  $k$  there is a straightforward identification – for example, for the  $U(2)$  instantons we will be considering in this Thesis, we can always write  $\Lambda$  as a row of  $N$  quaternions. In general this might not be so obvious, however we will always end up considering  $\Delta^\dagger \Delta$  in any practical calculation, and as we shall see below, this can always be written in quaternion form. The reason we consider this is that the commutative ADHM method involves solving the equation

$$\Delta^\dagger \Delta = \mathbb{1}_2 \otimes f^{-1} \quad (3.3.2)$$

where  $f$  is an invertible  $k \times k$  matrix, and we can think of  $\mathbb{1}_2$  as the quaternion identity. This also means we can look at the ADHM equation above as

$$\text{Im}_{\mathbb{H}}(\Delta^\dagger \Delta)_{ij} = 0 \quad (3.3.3)$$

where  $\text{Im}_{\mathbb{H}}$  takes the quaternion imaginary part. In terms of  $\Lambda$  and  $\Omega$ , the matrix  $\Delta^\dagger \Delta$  will look like

$$\Delta^\dagger \Delta = \Lambda^\dagger \Lambda + \Omega^\dagger \Omega \quad (3.3.4)$$

This is always a  $2k \times 2k$  complex valued matrix, so we can always think of it as a  $k \times k$  biquaternion matrix.

To calculate instantons over noncommutative space, we again use (3.3.2); however the presence of the noncommutativity must be taken into account. Here I give the

form we will be using in the rest of the paper, where the nonzero elements of  $\theta_{mn}$  are all chosen to be  $2\zeta$ . I will discuss the case of a more general  $\theta_{mn}$  in a later section. I will sketch the derivation of the noncommutative ADHM equation here, and comment upon it more fully in the more detailed derivation in section 3.3.2.

To start with, we can always write the matrix  $\Delta$  as  $a + bx$ , where  $a$  and  $b$  are matrices of the same dimension as  $\Delta$  and  $x$  are the space-time coordinates. This means that the matrix  $\Delta^\dagger \Delta$  can be written as

$$a^\dagger a + x(b + b^\dagger) + x^2 b^\dagger b \quad (3.3.5)$$

The linear part can be shown to be proportional to the identity and hence can be neglected. In the commutative case this is also true for the quadratic part. However in the noncommutative case there is an ambiguity in the definition of  $x^2$  because the spacetime coordinates do not commute. This turns out to mean that this term contributes a factor of  $4i\zeta\sigma_3$  to each of the diagonal components of  $\Delta^\dagger \Delta$ . This means we must modify the ADHM equation (3.3.2) to be

$$(\Delta^\dagger \Delta)_{ij} = \mathbb{1}_2 \otimes f_{ij}^{-1} - 4\zeta\sigma_3\delta_{ij} \quad (3.3.6)$$

Once we have solved equation (3.3.2), or its noncommutative analogue, we can use it to calculate the gauge potential and field strength in the following way.

We need to find zero eigenvectors  $U$  of  $\Delta^\dagger$ , normalised so that  $U^\dagger U = 1$ , satisfying

$$U^\dagger \Delta = \Delta^\dagger U = 0 \quad (3.3.7)$$

This implies that  $U$  has dimension  $N + 2k$  as a complex vector. Once we have this  $U$  we can use it to define the gauge potential as

$$A_\mu = U^\dagger \delta_\mu U \quad (3.3.8)$$

and the field strength as

$$F_{\mu\nu} = -4U^\dagger b f \sigma_{mn} b^\dagger U \quad (3.3.9)$$

where  $b$  is a  $(N + 2k) \times 2k$  matrix whose top  $N \times 2k$  part is 0 and whose bottom  $2k \times 2k$  part is the identity, and  $\sigma_{\mu\nu}$  is as given in (3.2.15). This procedure works for both the commutative and the noncommutative cases. We might worry whether the presence of the Moyal product (see section 3.2) might make the above procedure invalid for the noncommutative case, since the Field Strength is defined in terms of the Moyal product rather than the usual wedge product (see equation (3.2.6)). However, in that section we argued that the algebra of functions on noncommutative space (including  $A_\mu$  and  $F_{\mu\nu}$ ) was isomorphic to the algebra of operators on the Hilbert Space generated by the noncommutative position operations  $\hat{x}_i$ . If we think of  $A$  and  $F$  as operators on this space in the non commutative case then, provided there are no terms in  $[\hat{x}_i, \hat{x}_j]$  appearing, they will have the same structure as in the commutative case, where we have the commutative versions of the operators  $A$  and  $F$  on the Hilbert Space spanned by the commutative position operators. As mentioned, the only changes would be if we had terms in  $[\hat{x}_i, \hat{x}_j]$  appearing in the definition of  $A$  or  $F$ . However, it will be seen in the more detailed derivation that we do not, and therefore can use the same definitions.

### 3.3.1 Motivating the Constuction

Now we have the outline of the construction, it makes sense to try and give an idea where it comes from. To do this we will follow the presentation given in [21], to motivate it as an ansatz. As in that paper, we will not consider the general  $U(N)$  case, but will look at the  $SU(2)$  case where the motivation for the construction is easier to see. After doing this, we will derive the construction rigorously using a general  $U(N)$  gauge group.

In this section, the the index  $n$  refers to the spacetime coordinate (which can also be thought of as labelling the  $SO(3,1)$  representation), whilst the indices  $\alpha, \beta$  and  $\dot{\alpha}, \dot{\beta}$  are the usual dotted and undotted indices for representations of  $SU(2)$  or  $U(2)$ . The index corresponding to the instanton number  $k$  is given by the roman letters  $i, j, k$  or  $l$ . The greek index  $\lambda$  or  $\kappa$  indicates the, 'ADHM index', which goes in general from

which here goes from 0 to  $k$ . This notation is possible because, as discussed above, for  $N = 2$ , we can write all the tensors involved as quaternion valued matrices. This is not possible for general  $U(N)$ , so we will have to modify our notation for that case; however initially looking at the  $U(2)$  case makes the principles involved much clearer.

We start with a zero instanton solution of Yang Mills theory, which is pure gauge by definition

$$A_{n\dot{\beta}}^{\dot{\alpha}} = \bar{U}^{\dot{\alpha}\alpha} \partial_n U_{\alpha\dot{\beta}}; \quad \bar{U}^{\dot{\alpha}\alpha} U_{\alpha\dot{\beta}} = \delta_{\dot{\beta}}^{\dot{\alpha}} \quad (3.3.10)$$

In the usual commutative presentation,  $U \in SU(n)$  – we can take  $U \in U(n)$ , however the additional  $U(1)$  turns out to decouple. In the noncommutative case, however, we must consider the  $U(n)$  case, since  $SU(n)$  is not closed under the Moyal product [32].

The motivation for the ADHM construction comes from spotting that the single instanton solution also has the very similar form

$$A_{n\dot{\beta}}^{\dot{\alpha}} = \bar{U}_{\lambda}^{\dot{\alpha}\alpha} \partial_n U_{\lambda\alpha\dot{\beta}}; \quad \bar{U}_{\lambda}^{\dot{\alpha}\alpha} U_{\lambda\alpha\dot{\beta}} = \delta_{\dot{\beta}}^{\dot{\alpha}} \quad (3.3.11)$$

where  $\lambda$  is summed over 0 and 1, and, for the gauge choice called, ‘singular gauge’ (because it leads to a coordinate singularity at the centre of the Instanton [63])

$$U_{0\alpha\dot{\beta}} = \sqrt{\frac{x^2}{x^2 + \rho^2}} \cdot \sigma_{0\alpha\dot{\beta}}, \quad U_{1\alpha\dot{\beta}} = -\frac{\rho}{x^2} \sqrt{\frac{x^2}{x^2 + \rho^2}} x_{\alpha\dot{\alpha}} \bar{u}^{\dot{\alpha}\beta} \sigma_{0\beta\dot{\beta}} \quad (3.3.12)$$

It is natural therefore to assume an ansatz for the  $n$  instanton solution to be

$$A_{n\dot{\beta}}^{\dot{\alpha}} = \bar{U}_{\lambda}^{\dot{\alpha}\alpha} \partial_n U_{\lambda\alpha\dot{\beta}}; \quad \bar{U}_{\lambda}^{\dot{\alpha}\alpha} U_{\lambda\alpha\dot{\beta}} = \delta_{\dot{\beta}}^{\dot{\alpha}} \quad (3.3.13)$$

where  $\lambda$  is now summed from 0 to  $n$ . In this notation, the Field strength is defined as

$$F_{mn}^{\dot{\alpha}}{}_{\dot{\beta}} \equiv \partial_{[m} A_{n]}^{\dot{\alpha}}{}_{\dot{\beta}} + A_{[m}^{\dot{\alpha}}{}_{\dot{\beta}} A_{n]}^{\dot{\gamma}}{}_{\dot{\beta}} = \partial_{[m} \bar{U}_{\lambda}^{\dot{\alpha}\alpha} (\delta_{\lambda\kappa} \delta_{\alpha}^{\beta} - \mathcal{P}_{\lambda\kappa\alpha}^{\beta}) \partial_{n]} U_{\kappa\beta\dot{\beta}} \quad (3.3.14)$$

with

$$\mathcal{P}_{\lambda\kappa\alpha}^{\beta} = U_{\lambda\alpha\dot{\alpha}} \bar{U}_{\kappa}^{\dot{\alpha}\beta} \quad (3.3.15)$$

with this definition,  $\mathcal{P}$  (and therefore  $1 - \mathcal{P}$ ) is a projection operator, and satisfies

$$0 = (1 - \mathcal{P})U = \bar{U}(1 - \mathcal{P}), \quad \mathcal{P} = \bar{\mathcal{P}} \quad (3.3.16)$$

The second part of the ADHM ansatz is to assume that we can factorize

$$1 - \mathcal{P} \equiv \delta_{\lambda\kappa} \delta_{\alpha}^{\beta} - \mathcal{P}_{\lambda\kappa\alpha}^{\beta} = \Delta_{\lambda\alpha\dot{\alpha}} f_{lk}^{\dot{\alpha}} \bar{\Delta}_{k\kappa}^{\dot{\beta}\beta} \quad (3.3.17)$$

For some matrices  $\Delta$  and  $f$ , this second condition is called the, 'Completeness relation'. It is trivial in the commutative case, however there are some complications in the noncommutative case. The issue is that, whereas the normalisation of  $U(x)$  is trivial in the commutative case, there is an ambiguity in the case where  $x$  is itself an operator. We must therefore be careful to pick a good definition for this normalisation. These issues were first discussed in [12]. They begin with the fact that in the noncommutative case,  $1 - \mathcal{P} \equiv \mathcal{P}' = \delta f \delta^\dagger$ , a Hermitian projection operator, is a  $[N + 2k] \times [N + 2k]$  dimensional matrix of operators on some Fock space  $\mathcal{H}$  – that is

$$\mathcal{P}' : \mathcal{H}^{N+2k} \rightarrow \mathcal{P}'\mathcal{H}^{N+2k} \subset \mathcal{H}^{N+2k} \quad (3.3.18)$$

They then consider the eigenvalues of this operator. Because it is a projection operator, its eigenvalues are either 0 or 1. Following [12], we denote the zero-mode eigenstates by  $|\psi^p\rangle$  and the non zero-mode eigenstates as  $|\phi^p\rangle^r$ . This means we have

$$\mathcal{P}' |\psi^p\rangle, \quad |\psi^p\rangle \in \mathcal{H}^{N+2k}, \quad \langle \psi^p | \psi^q \rangle = \delta^{pq} \quad (3.3.19)$$

and

$$\mathcal{P}' |\phi^p\rangle, \quad |\phi^p\rangle \in \mathcal{H}^{N+2k}, \quad \langle \phi^p | \phi^q \rangle = \delta^{pq} \quad (3.3.20)$$

The set of the eigenstates of a Hermitian operator is automatically complete – i.e. we have

$$1_{[N+2k] \times [N+2k]} = \sum_p |\psi^p\rangle \langle \psi^p| + \sum_r |\phi^p\rangle \langle \phi^p| \quad (3.3.21)$$

Since the eigenvalues associated to the  $|\phi^r\rangle$  are all 1 we have

$$\sum_p |\psi^p\rangle \langle \psi^p| + \Delta_{[N+2k] \times [k] \times [2]} f_{[k] \times [k]} \Delta_{[2] \times [k] \times [N+2k]} = 1_{[N+2k] \times [N+2k]} \quad (3.3.22)$$

Therefore the ADHM completeness relation (3.3.17) will hold iff

$$\sum_p |\psi^p\rangle \langle \psi^p| = UU^\dagger \quad (3.3.23)$$

This requires

$$\left\{ |\psi^p\rangle \right\} = \left\{ U_{[N+2k] \times [N]} |s_{[N]}\rangle \right\} \quad (3.3.24)$$

where the  $|s_u\rangle$  are some arbitrary normalised states in  $\mathcal{H}$

This condition is not automatic, however. Any state of the form  $U|s\rangle$  is automatically a zero mode eigenstate of  $\mathcal{P}'$ , however in general it is not true that all zero mode eigenstates have this form. In fact, we must carefully determine the precise form of  $U$  in each case that will make the completeness relation true. This is rather non trivial, however as it only affects the value of  $U$ , and not the validity of the remainder of the solution, it is only necessary if one is constructing an explicit expression for the gauge potential, which we are not. The only point we use  $U$  is in section 4.4, and here we take it in a limit in which any noncommutative effects (which must be proportional to  $\zeta$ ) are automatically neglected. Having taken note of this, we also solve the conditions in (3.3.16) by assuming

$$0 = \bar{\Delta}_{k\kappa}^{\dot{\beta}\beta} U_{\kappa\beta\dot{\alpha}} = \bar{U}_\lambda^{\dot{\beta}\alpha} \Delta_{\lambda\alpha\dot{\alpha}}, \quad \bar{f} = f \quad (3.3.25)$$

In terms of these new variables, and following an integration by parts, the field strength becomes

$$F_{mn}^{\dot{\alpha}\dot{\beta}} = \bar{U}_\lambda^{\alpha\dot{\alpha}} \partial_{[m} \Delta_{\lambda\alpha\dot{\gamma}} f_{lk}^{\dot{\gamma}} \partial_{n]} \bar{\Delta}_{k\kappa}^{\dot{\delta}\dot{\beta}} U_{\kappa\beta\dot{\beta}} \quad (3.3.26)$$

Now we can see from this that if  $\partial\Delta$  is proportional to  $\sigma_m$ , and if  $\sigma_m$  commutes with  $f$ , then the RHS of (3.3.26) is proportional to  $\sigma_{mn}$ , and therefore is automatically self- dual, just as we want. Therefore we have the third and final part of the ADHM



ansatz, which assumes first that  $\Delta$  is linear in  $x$

$$\Delta_{\lambda\alpha\dot{\alpha}} = a_{\lambda\alpha\dot{\alpha}} + b_{\lambda\alpha}{}^{\beta} x_{\beta\dot{\alpha}} \quad (3.3.27)$$

where  $a$  and  $b$  are constant complex- quaternion valued matrices. Second, we assume

$$f_{lk}{}^{\dot{\alpha}}{}_{\dot{\beta}} = f_{lk} \delta^{\dot{\alpha}}{}_{\dot{\beta}} \quad (3.3.28)$$

This gives us the following self- dual expression for the field strength

$$F_{mn}{}^{\dot{\alpha}}{}_{\dot{\beta}} = 4\bar{U}_{\lambda}{}^{\dot{\alpha}\alpha} b_{\lambda\alpha}{}^{\beta} \sigma_{mn\beta}{}^{\gamma} f_{lk} \bar{b}_{k\kappa\gamma}{}^{\delta} U_{\kappa\delta\dot{\beta}} \quad (3.3.29)$$

Comparing the dimensions of the null spaces of  $U\bar{U}$  and  $1 - \Delta f \bar{\Delta}$ , we find that  $\Delta$ , and hence  $a$  and  $b$ , are matrixes of dimension  $(N + 2k) \times 2k$  as complex matrices. If  $N$  is divisible by two, then we can think of these as are matrices of dimension  $(N/2 + k) \times k$  biquaternion matrices. However even if  $N$  is not divisible by two, the matrix  $\Delta^{\dagger}\Delta$  is always a  $2k \times 2k$  complex matrix, and so can always be thought of as a  $k \times k$  biquaternion matrix. This will be important in the next section. Having determined the form of the Ansatz, we must now look to solving it.

### 3.3.2 Solving the ADHM equations

In this section I will give the details of the method to solve the ADHM equations. In this section I shall largely follow [12]. Here we move from the specific case of  $U(2)$  instantons in the previous paper, to general  $U(N)$  instantons – this requires a slight change in notation. Following [12], our indices are given by

Instanton number indices $i, j$	$1 \leq i, j \leq k$
Colour Indices $u, v$	$1 \leq u, v, \leq N$
ADHM indices $\lambda, \mu$	$1 \leq \lambda, \mu \leq N + 2k$
Weyl/ Quaterionic indices	$\alpha, \beta, \dot{\alpha}, \dot{\beta} = 1, 2$
Lorentz indices	$m, n, = 0, 1, 2, 3$

In the commutative case the three parts of the Ansatz considered above are equivalent to solving the equation. In the noncommutative case, as discussed above, there are subtleties with the completeness relation. Checking the completeness relation is rather non-trivial, so I will assume that the completeness relation holds in what follows.

$$\bar{\Delta}_i^{\beta\lambda} \Delta_{\lambda j\dot{\alpha}} = \delta^{\beta\dot{\alpha}} (f^{-1})_{ij} \quad (3.3.30)$$

Essentially this constraint means that the part of  $\Delta^\dagger \Delta$  proportional to the identity is allowed to be arbitrary – the constraints only affect the imaginary quaternion parts, which end up forced to be zero in the commutative case, and proportional to some noncommutative deformation otherwise.

The matrix  $\Delta$  has dimension  $(N + 2k) \times 2k$ , where  $N$  is the order of the gauge group  $U(N)$ , and  $k$  is the instanton number. We assume it has the form  $a + bx$ , for the spacetime parameter  $x$ , with  $a$  and  $b$  matrices of the same dimensions as  $\Delta$ . We can see (following [21]) that we can multiply  $\Delta$  on the right by a unitary matrix without changing the value of  $\Delta^\dagger \Delta$ , and hence without changing the solutions to the ADHM equation (3.3.2). This corresponds to the transformation

$$\Delta_{\lambda j\dot{\alpha}} \mapsto \Lambda_{\lambda\kappa} \Delta_{\kappa j\dot{\alpha}}, \quad f \mapsto f, \quad U_{\lambda j} \mapsto \Lambda_{\lambda\kappa}^\alpha U_{\kappa j}, \quad \Lambda^{-1} \Lambda = 1$$

Since the matrix  $f$  is arbitrary, we can conjugate both sides of the equation by an arbitrary matrix in  $GL(k)$  to get a physically equivalent set of solutions. This corresponds to the transformation

$$\Delta_{\lambda j\dot{\alpha}} \mapsto \Delta_{\lambda k\dot{\alpha}} \Upsilon_{kl}, \quad f \mapsto \Upsilon^{-1} \cdot f \cdot (\Upsilon^{-1})^\dagger, \quad U \mapsto U$$

There is also an  $SU(N)$  gauge transformation we can apply to the vector  $U$ , but this will be dealt with at a later stage in the proceedings. At this stage we use the above transformations to put  $a$  and  $b$  into the following canonical forms:

$$a = \begin{bmatrix} \mathbf{v}_{N \times 2k} \\ \Omega_{2k \times 2k} \end{bmatrix} \quad b = \begin{bmatrix} \mathbf{0}_{N \times 2k} \\ \mathbb{1}_{2k \times 2k} \end{bmatrix}$$

where the subscripts are dimensions of the submatrices over the real numbers. Using the indices given above in (3.3.2), we write this as

$$\Delta_{\lambda j \dot{\alpha}} = a_{\lambda j \dot{\alpha}} + b^{\alpha \lambda j} \bar{x}_{\alpha \dot{\alpha}} \quad (3.3.31)$$

Where  $\bar{x}_{\alpha \dot{\alpha}} = x_n \bar{\sigma}_{\alpha \dot{\alpha}}^n$ . We can see how much of the symmetries represented by  $\Upsilon$  and  $\Lambda$  are left by looking at which matrices preserve the canonical forms of  $a$  and  $b$  given above. Noting that we apply both these transformations simultaneously, as

$$\rightarrow \Lambda_{\lambda \kappa \beta}{}^{\alpha} \Delta_{\kappa k \alpha \dot{\beta}} \Upsilon_{kl} \quad (3.3.32)$$

it isn't too hard to see that preserving the form of  $b$  requires that this transformation takes the following form

$$\begin{bmatrix} q & \vec{0} \\ \vec{0} & R^T \end{bmatrix} \cdot \Delta \cdot R \quad (3.3.33)$$

Here,  $R$  belongs to  $SU(k)$  if we allow complex parameters, or  $SO(k)$  if we restrict to real ones. The element  $q$  belongs to  $U(1)$  and so the whole thing represents an action of  $U(k)$  on the matrix  $\Delta$ . This fits with derivations from string theory (see [63] and [39]). Defining

$$Q \equiv \begin{bmatrix} q & \vec{0} \\ \vec{0} & R^T \end{bmatrix} \quad (3.3.34)$$

and looking at the total transformations given above, we can see that the residual symmetry we need to mod out is given by

$$\Delta \mapsto \begin{bmatrix} q & \vec{0} \\ \vec{0} & R^T \end{bmatrix} \cdot \Delta \cdot R, \quad f \mapsto R^T \cdot f \cdot R, \quad U \mapsto RU$$

Following [12] once more, we can further decompose  $a + bx$  as

$$a_{\lambda j \dot{\alpha}} = a_{(u+i\alpha)j \dot{\alpha}} = \begin{bmatrix} \omega_{uj \dot{\alpha}} \\ (a'_{\alpha \dot{\alpha}})_{ji} \end{bmatrix} \quad (3.3.35)$$

$$\bar{a}_j^{\lambda \dot{\alpha}} = \bar{a}_j^{(u+i\alpha) \dot{\alpha}} = \begin{bmatrix} \bar{\omega}_{uj}^{\dot{\alpha}} & (\bar{a}'^{\alpha \dot{\alpha}})_{ji} \end{bmatrix} \quad (3.3.36)$$

$$b_{\lambda j}^{\beta} = b_{(u+i\alpha)j}^{\beta} = \begin{bmatrix} 0 \\ \delta_{\alpha}^{\beta} \delta_{ij} \end{bmatrix} \quad (3.3.37)$$

$$\bar{b}_{\beta j}^{\lambda} = \bar{b}_{\beta j}^{u+i\alpha} = \begin{bmatrix} 0 & \delta_{\beta}^{\alpha} \delta_{ij} \end{bmatrix} \quad (3.3.38)$$

Using these we can write  $\bar{\Delta}\Delta = \delta_{\dot{\alpha}}^{\dot{\beta}}(f^{-1})_{ij}$  as

$$\bar{a}_i^{\dot{\beta}\lambda} a_{\lambda j \dot{\alpha}} + x^{\dot{\beta}\beta} \bar{b}_{\beta i}^{\lambda} a_{\lambda j \dot{\alpha}} + \bar{a}_i^{\dot{\beta}\lambda} b_{\lambda j}^{\alpha} \bar{x}_{\alpha \dot{\alpha}} + x^{\dot{\beta}\beta} \bar{b}_{\beta i}^{\lambda} b_{\lambda j}^{\alpha} \bar{x}_{\alpha \dot{\alpha}} \quad (3.3.39)$$

We can now solve the constraints. To do this, we split this expression into three parts, the first term not containing  $x$ , the next two terms linear in  $x$  and the third term quadratic in  $x$ .

With the first term, following [12] we simply write this as

$$(\bar{a}^{\dot{\beta}} a_{\dot{\alpha}})_{ij} \quad (3.3.40)$$

Next, the linear part. This is best dealt with by using the definition  $x^{\dot{\beta}\beta} = x_m \sigma^{m\dot{\beta}\beta}$ , where the  $\sigma^{m\dot{\beta}\beta}$  are the quaternion basis for  $SU(2)$ . Then we can factorise the terms as

$$x_m \left( \sigma^{m\dot{\beta}\beta} (a'_{\beta\dot{\alpha}})_{ij} + (\bar{a}'^{\dot{\beta}\alpha})_{ij} \bar{\sigma}_{\alpha\dot{\alpha}}^m \right) \quad (3.3.41)$$

The ADHM constraints force the imaginary part of this expression to vanish. This can only occur if we set  $a'_{ij} = \bar{a}'_{ji}$ . Then the linear part becomes

$$x_m \left( \sigma^{m\dot{\beta}\beta} (a'_{\beta\dot{\alpha}})_{ij} + \text{hermitian conjugate} \right) \quad (3.3.42)$$

Which is proportional to  $\delta_{\dot{\alpha}}^{\dot{\beta}}$ , and so is proportional to the quaternion identity, and does not enter into the constraints.

We now come to the third term,  $x^{\dot{\beta}\beta} \bar{b}_{\beta i}^{\lambda} b_{\lambda j}^{\alpha} \bar{x}_{\alpha \dot{\alpha}}$ . Using the splitting of  $b_{\lambda j}^{\alpha}$  given above, this becomes

$$x^{\dot{\beta}\beta} \bar{x}_{\beta\dot{\alpha}} \delta_{ji} \equiv x_m x_n \left( \sigma_m^{\dot{\beta}\beta} \bar{\sigma}_{n\beta\dot{\alpha}} \right) \delta_{ij} \quad (3.3.43)$$

We can expand the term in the brackets as

$$\frac{1}{2} \left( \sigma_m^{\dot{\beta}\beta} \bar{\sigma}_{n\beta\dot{\alpha}} + \sigma_m^{\dot{\alpha}\beta} \bar{\sigma}_{n\beta\dot{\beta}} + \sigma_m^{\dot{\beta}\beta} \bar{\sigma}_{n\beta\dot{\alpha}} - \sigma_m^{\dot{\alpha}\beta} \bar{\sigma}_{n\beta\dot{\beta}} \right) \quad (3.3.44)$$

The first two terms are proportional to the quaternion identity and so can be disregarded. The second two terms are equal by definition to  $i\eta_{mn}^a \tau^a$ , where the  $\eta$  are the 't Hooft symbols introduced in [62]

$$\eta_{1\mu\nu} = \begin{bmatrix} 0 & 0 & 0 & 1 \\ 0 & 0 & 1 & 0 \\ 0 & -1 & 0 & 0 \\ -1 & 0 & 0 & 0 \end{bmatrix}, \quad \eta_{2\mu\nu} = \begin{bmatrix} 0 & 0 & -1 & 0 \\ 0 & 0 & 0 & 1 \\ 1 & 0 & 0 & 0 \\ 0 & -1 & 0 & 0 \end{bmatrix}, \quad \eta_{3\mu\nu} = \begin{bmatrix} 0 & 1 & 0 & 0 \\ -1 & 0 & 0 & 0 \\ 0 & 0 & 0 & 1 \\ 0 & 0 & -1 & 0 \end{bmatrix} \quad (3.3.45)$$

and the  $\tau^a$  are the Pauli matrices  $\tau_i = i\sigma_i, i = 1, 2, 3$ . The  $\eta_{mn}^a$  are antisymmetric in  $m$  and  $n$  so we can replace  $x_m x_n$  by  $\frac{1}{2}[x_m, x_n]$ . In the commutative case this vanishes; here it is equal to half the matrix  $i\theta_{mn}$  defined above. Therefore the third term is equal to

$$-\frac{1}{2}\theta_{mn}\eta_{mn}^a \tau^{a\ \alpha\dot{\beta}} \delta_{ij} \quad (3.3.46)$$

Putting this all together we find that the ADHM constraints are given by

$$\left(\bar{a}^{\dot{\beta}} a_{\dot{\alpha}}\right)_{ij} = f_{ij} \mathbb{1}_{\dot{\alpha}}^{\dot{\beta}} + \frac{1}{2}\theta_{mn}\eta_{mn}^a \tau_{\dot{\alpha}}^{a\dot{\beta}} \delta_{ij} \quad (3.3.47)$$

and

$$a'_{ij} = \bar{a}'_{ji} \quad (3.3.48)$$

Equation (3.3.47) is in fact three equations, one for each of the imaginary quaternion generators (we do not care about the arbitrary fourth component, proportional to the identity). We can rewrite it by contracting with each of these generators. The contraction with the identity element by definition gives the term proportional to  $\delta_{\dot{\beta}}^{\dot{\alpha}}$ , and the three imaginary generators give

$$\tau_{\dot{\beta}}^{a\dot{\alpha}} \left(\bar{a}^{\dot{\beta}} a_{\dot{\alpha}}\right)_{ij} = \theta_{mn}\eta_{mn}^a \delta_{ij} \quad (3.3.49)$$

Going back to our choice of  $\theta_{mn}$ , with the nonzero entries equal to  $2\zeta$  (in fact, we have  $\theta_{mn} = 2\zeta\eta_{mn}$ ) this equation becomes

$$\tau_{\dot{\beta}}^{a\dot{\alpha}} \left(\bar{a}^{\dot{\beta}} a_{\dot{\alpha}}\right)_{ij} = -8\zeta\delta_{a3}\delta_{ij} \quad (3.3.50)$$

It is convenient to re-express this in terms of the quaternion basis we are using. It is also clearer to drop the explicit dotted quaternion indices.

$$\sigma_a \cdot (\bar{a}^{\dot{\beta}} a_{\dot{\alpha}})_{ij} = -8i\zeta \delta_{a3} \delta_{ij} \quad (3.3.51)$$

i.e., the component of  $\Delta^\dagger \Delta$  proportional to the quaternion identity is arbitrary, whilst the components proportional to the imaginary quaternions are equal to the corresponding component of the non commutative deformation, and the only component which is there in our case is the  $\sigma_3$  component. We can finally rewrite this as

$$\text{Im}((a^\dagger a)_{ij}) = -4i\zeta \sigma_3 \delta_{ij} \quad (3.3.52)$$

Note that here we have used biquaternion components for both the commutative and the noncommutative cases. Using these in principle adds three extra degrees of freedom to each of the components of the matrix  $\Delta^\dagger \Delta$  (we don't care about the component proportional to the complex unit). However the symmetric nature of the matrix means that in fact there are only  $\frac{1}{2}n(n+1)$  additional degree of freedom. This is counterbalanced by the fact that the matrix  $R$  in (3.3.2) is promoted from  $SO(n)$  in the real quaternion case to  $SU(n)$  in the biquaternion case. Now,  $SU(n)$  has  $n^2 - 1$  components, whereas  $SO(n)$  has  $\frac{1}{2}n(n-1)$  components. This means that there are an additional  $\frac{1}{2}n(n+1)$  components in the symmetry group which cancel out the apparent additional degrees of freedom in the constraints.

## 3.4 Dyonic Instantons

In this Thesis we will be looking not only at pure Instantons but at Dyonic instantons. Here, following the presentation in [1] we modify the action introduced in (3.1.1) by introducing a scalar field, so that it becomes

$$S_{YM} = \int d^5x \frac{1}{4} F_{ij}^a F_a^{ij} + \frac{1}{2} D_u \phi D^u \phi \quad (3.4.1)$$

This solution has Energy, Topological Charge, and Electrical Charge given respectively by

$$\begin{aligned} E &= \int d^4x \text{Tr} \left( \frac{1}{2} F_{i0} F_{i0} + \frac{1}{4} F_{ij} F_{ij} + \frac{1}{2} D_0 \phi D_0 \phi + \frac{1}{2} D_i \phi D_i \phi \right), \\ k &= -\frac{1}{16\pi^2} \int d^4x \epsilon_{ijkl} \text{Tr} (F_{ij} F_{kl}), \\ Q_E &= \int d^4x \text{Tr} (D_i \phi F_{i0}) = \int d^4x \text{Tr} (D_i \phi)^2 \end{aligned} \quad (3.4.2)$$

We use a Bogomolyni argument of the type discussed in section 3.1 to give us a bound on the energy.

$$E = \int d^4x \text{Tr} \left( \frac{1}{2} F_{i0} F_{i0} + \frac{1}{4} F_{ij} F_{ij} + \frac{1}{2} D_0 \phi D_0 \phi + \frac{1}{2} D_i \phi D_i \phi \right) \quad (3.4.3)$$

Completing the square gives us

$$\begin{aligned} E &= \int d^4x \text{Tr} \left( \frac{1}{8} \left( F_{ij} \pm \frac{1}{2} \epsilon_{ijkl} F_{kl} \right)^2 + \frac{1}{2} \left( F_{i0} \pm D_i \phi \right)^2 + \frac{1}{2} D_i \phi D_i \phi \right. \\ &\quad \left. + \frac{1}{8} \epsilon_{ijkl} F_{ij} F_{kl} \mp F_{i0} D_i \phi \right) \end{aligned} \quad (3.4.4)$$

So we get

$$E \geq 2\pi^2 |k| + |Q_E| \quad (3.4.5)$$

where

$$\begin{aligned} k &= -\frac{1}{16\pi^2} \int d^4x \epsilon_{ijkl} \text{Tr} (F_{ij} F_{kl}), \\ Q_E &= \int d^4x \text{Tr} (D_i \phi F_{i0}) = \int d^4x \text{Tr} (D_i \phi)^2 \end{aligned} \quad (3.4.6)$$

The conditions for this bound to be satisfied are

$$\begin{aligned} F_{ij} &= \frac{1}{2} \epsilon_{ijkl} F_{kl} \\ F_{i0} &= D_i \phi \\ D_0 \phi &= 0 \end{aligned} \quad (3.4.7)$$

With the boundary condition on  $\phi$  that it goes to the vev  $\phi_0 = iq$  at infinity [43]. The second and third of these are satisfied provided the fields are static and  $A_0 = \phi$ . This means that when  $\phi = 0$ , the solution reduces to precisely that of a

pure instanton, and such solutions are in one-to-one correspondence with the pure instanton solutions discussed above. Therefore, we can use the ADHM method just as before, and additionally try and solve the equation

$$D^2\phi = 0 \tag{3.4.8}$$

We might wonder why this does not fall foul of Derrick's Theorem, which we stated forbade stable static solutions to the Yang Mills equations with a scalar field. The answer is that this solution is only valid as the approximation to a non-static solution, which would not fall under the conditions for Derrick's theorem. As explained in, e.g. [57], these are not exact solutions but are approximate solutions valid for small values of the scalar field vev. The full equations of motion are

$$D_i F^{ij} = [\Phi, D^j \Phi] \tag{3.4.9}$$

$$D^2\phi = 0 \tag{3.4.10}$$

The first of which is not the equation of motion for an Instanton. However to first order in the vev, that equation becomes

$$D_i F^{ij} = 0 \tag{3.4.11}$$

which is the Instanton equation of motion. The solutions to these non-static equations to first order in the vev are the same as the above, except with  $A_0 = 0$  (this will be essentially true anyway if the vev is small). Clearly these are in one-to-one correspondence with the static solutions. We can therefore use these stable non-static solutions to approximate the static solutions provided the vev is small. This will be discussed further in section 4.2.

### 3.4.1 Solving the Scalar Field

The method outlined here is mainly based on Appendix 1 in [1], generalised to the case of arbitrary non commutative instantons. The method used is based on that in



[21]. It begins with the Ansatz

$$\phi = iU^\dagger \mathcal{A}U; \quad \mathcal{A} = \begin{bmatrix} q & 0 \\ 0 & P \end{bmatrix} \quad (3.4.12)$$

where  $\phi$  is the scalar field we are trying to calculate and  $U$  is an element of the null space of the ADHM Matrix  $\Delta$ . Further,  $q \in u(N)$ , where  $N$  is the degree of the instanton gauge group, and  $P \in u(k)$ , where  $k$  is the Chern- Simons number/ number of instantons we are considering. In fact,  $iq$  is the vev of the scalar field. For the real ADHM construction, we can use  $o(k)$  rather than  $u(k)$ . In the biquaternion case in theory there is an additional  $u(1)$ , promoting the symmetry group to  $u(2)$ , however as we can choose the vev we will always choose this to lie in  $su(2)$  so this additional  $u(1)$  will not in fact contribute.

Note that the equation for  $\phi$  has the form of a rotation of  $\mathcal{A}$  by  $U$ . We can think of this as follows. The matrix  $\mathcal{A}$  belongs in  $u(n) \times u(k)$ . We can imagine it being defined on a  $u(n) \times u(k)$  bundle over  $\mathbb{R}^4$ . However we know the ADHM construction breaks the ‘gauge group’  $u(n) \times u(k)$  down to  $u(n)$ . We can therefore see the rotation as rotating  $\mathcal{A}$  into the  $u(n)$  subspace picked out by the ADHM constraints. This interpretation can be confirmed by the straightforward observation that  $U^\dagger(\mathbb{1} - UU^\dagger)\mathcal{A}U = 0$ . A long and algebraic justification for the ansatz is given in [21]. Regardless of the justification for the Ansatz, once we have it, the problem of solving for  $\phi$  becomes the problem of solving for  $P$  above. It is shown in [21] that the equation of motion for  $\phi$

$$D^2\phi = 0 \quad (3.4.13)$$

expands as

$$D^2\phi = -4iU^\dagger\{fbf^\dagger, \mathcal{A}\}U + 4iU^\dagger bf \text{Tr}_2(\Delta^\dagger \mathcal{A} \Delta) f b^\dagger U = 0 \quad (3.4.14)$$

Here,  $\text{Tr}_2$  refers to the quaternion trace on each element of a matrix, not to the trace of the matrix itself, which is written  $\text{Tr}$ . Hence, applied to a (complex/ real) quaternion valued matrix,  $\text{Tr}_2$  will give a complex/ real valued matrix, whereas  $\text{Tr}$

will give a (complex/real) quaternion.

With  $\mathcal{A}$  written as above, the first term is  $-4iU^\dagger\{f, p\}U$ . For the second term, we recall that  $\Delta$  can be written as

$$\Delta = \begin{bmatrix} \Lambda \\ \Omega - \mathbb{1}x \end{bmatrix} \quad (3.4.15)$$

Writing  $\Omega' = \Omega - \mathbb{1}x$ , and using the ADHM constraint  $\Delta^\dagger\Delta = \Lambda^\dagger\Lambda + \Omega'^\dagger\Omega' = f^{-1}$  we can see

$$\begin{aligned} \text{Tr}_2(\Delta^\dagger\mathcal{A}\Delta) &= \text{Tr}_2(\Lambda^\dagger q\Lambda) + \text{Tr}_2(\Omega'^\dagger\mathcal{A}\Omega') \\ &= \text{Tr}_2(\Lambda^\dagger q\Lambda) + \frac{1}{2}\text{Tr}_2([\Omega'^\dagger, P]\Omega' - \omega'^\dagger[\Omega', P] + \{P, \Omega'^\dagger\Omega'\}) \\ &= \text{Tr}_2(\Lambda^\dagger q\Lambda) + \frac{1}{2}([\Omega'^\dagger, P]\Omega' - \Omega'^\dagger[\Omega', P] + \{P, f^{-1}\} - \{P, \Lambda^\dagger\Lambda\}) \\ &= \text{Tr}_2(\Lambda^\dagger q\Lambda) + \frac{1}{2}(2\Omega'^\dagger P\Omega' - \{\Omega'^\dagger\Omega', P\} + \{P, f^{-1}\} - \{P, \Lambda^\dagger\Lambda\}) \end{aligned} \quad (3.4.16)$$

Now, note that  $x$  in the above expression is always the coefficient of  $\mathbb{1}$ . Therefore the terms involving  $x$  in the above expression cancel, and we can everywhere replace  $\Omega'$  by  $\Omega$  (this is most easily seen from the third line above).

We can use these to rewrite (3.4.14) as

$$D^2\phi = -4i\left(U^\dagger\{f, P - \frac{1}{2}\text{Tr}_2(P)\}U + U^\dagger b f \left(\text{Tr}_2(\Lambda^\dagger q\Lambda) + \frac{1}{2}(2\Omega'^\dagger P\Omega' - \{\Omega'^\dagger\Omega', P\} - \{P, \Lambda^\dagger\Lambda\})\right)\right) \quad (3.4.17)$$

Since  $P$  has complex components, not quaternion-valued ones,  $\text{Tr}_2(P) = P$  and the first term vanishes. Hence the e.o.m.  $D^2\phi = 0$  is equivalent to

$$\text{Tr}_2(\Lambda^\dagger q\Lambda) + \frac{1}{2}(2\Omega'^\dagger P\Omega' - \{\Omega'^\dagger\Omega', P\} - \{P, \Lambda^\dagger\Lambda\}) = 0 \quad (3.4.18)$$

This gives one equation for each component of  $P$ , allowing us to solve for  $P$  and hence, by extension, for  $\phi$ .



# Chapter 4

## The Moduli Space

### 4.1 The Moduli Space

This section follows [22] and [1]. Essentially, the *Moduli Space* of instanton solutions is the space of inequivalent solutions to the self dual Yang Mills equations, (3.3.2). Here, equivalent solutions mean those which differ by local gauge transformations – solutions which can be transformed into each other by global gauge transformations are considered inequivalent – the reasoning behind this is discussed in [15]. The general idea is that we want to consider as equivalent any solutions which differ only by a local gauge transformation, since we usually think of local gauge transformations as describing mathematical redundancies rather than physically distinct solutions. However fixing the local gauge so as to determine a specific form of the potential  $A$  or the Field Strength  $F$  doesn't fix any of the global symmetries, and so solutions differing by a global gauge symmetry are seen as being inequivalent. The principle of the construction turns out to be the same for commutative and noncommutative instantons, however the explicit construction of the moduli space and potential requires modification in the noncommutative case, which will be discussed at the appropriate points.

There are two particular properties these spaces have. The first comes from the fact that Instanton solutions are classified by the instanton number  $k$ . This is a

topological invariant and therefore the moduli space  $\mathfrak{M}$  splits into disconnected components describing the solutions of charge  $k$ ,  $\mathfrak{M}_k$ . The second property, which is less obvious, is that  $\mathfrak{M}$  is in fact a manifold. Though here there is the subtlety that  $\mathfrak{M}$  has conical singularities in the commutative case, formed when the instantons shrink to zero size. In the noncommutative case the fact of noncommutativity means that the instantons cannot shrink to zero size, and so the singularities are resolved to 2-spheres. This is in fact a major motivation for studying noncommutative instantons.

The moduli space is actually a special class of manifold called a *HyperKähler Manifold*, and the proof that it is a manifold involves showing it satisfies these more special conditions. This is beyond the scope of the thesis, however details are given in [22]

Since the moduli space is a manifold, we can give it coordinates. These are called *Collective Coordinates*. They have a complicated relationship to the symmetries of the theory, which are discussed in [22]. In particular, there are 4 coordinates denoting the position of the centre of mass of the instanton solution which arise out of the fact that the instanton breaks the translational invariance of the theory. This means that the moduli space is a direct product

$$\mathfrak{M}_k = \mathbb{R}^4 \times \hat{\mathfrak{M}}_k \tag{4.1.1}$$

where  $\hat{\mathfrak{M}}_k$  is the moduli space with the centre of mass component factored out, known as the *centred moduli space*. We usually ignore the centre of mass part, and work directly with  $\hat{\mathfrak{M}}_k$ . The remaining coordinates on the moduli space can be taken to be the ADHM parameters. There are  $4kN - 4$  of these, where  $k$  is the instanton number and  $N$  is the dimension of the gauge group (the full moduli space with the centre of mass left in has  $4kN$  coordinates). In the noncommutative case there is an extra parameter, the noncommutative parameter  $\zeta$ , however we do not treat this as a collective coordinate.

As first described in [48], we can introduce a time dependence into the collective

coordinates on the moduli space. If we label these coordinates as  $z_r$ , then we can write any instanton solution as  $A_i(\mathbf{z}, x)$ , where  $\mathbf{z}$  is the vector of the moduli space coordinates, and  $x$  is the usual spacetime coordinate. We can then introduce dynamics by introducing a time dependence  $\mathbf{z}(t)$ . The instanton solutions then become  $A_i(\mathbf{z}(t), x)$ . This allows us to approximate individual solutions involving small velocities as slow motion between different instanton solutions on the moduli space. For sufficiently small velocities, these dynamics can be described by geodesic motion on the moduli space. This procedure was first developed for monopoles – a review of which is given in [64]. To fully describe it we first have to develop the idea of zero modes.

Each point on the moduli space is a solution to the self dual Yang Mills equations,  $A_i(x)$ . Now consider a fluctuation  $A_i(x) + \delta A_i(x)$ . If it is also to be a solution to the equations (and hence lie in the moduli space), it must satisfy the linearised self duality equation

$$\mathcal{D}_m \delta A_n - \mathcal{D}_n \delta A_m = \epsilon_{mnkl} \mathcal{D}_k \delta A_l \quad (4.1.2)$$

As well as this, we also want it not to be related to  $A_n(x)$  by a local gauge transformation. We do this by requiring them to be orthogonal to gauge transformations. We use the natural metric on the space of all solutions

$$g(\delta A_i(x), \delta A'_i(x)) = \int d^4x \text{Tr}(\delta A_i(x) \delta A'_i(x)) \quad (4.1.3)$$

and then use this to induce a metric on the moduli space after quotienting out the gauge-equivalent solutions. We then require that under this metric, zero modes  $\delta A_i(x)$  are orthogonal to all gauge transformations  $D_i \Lambda$

$$g(\delta A_i(x), D_i \Lambda(x)) = - \int d^4x \text{Tr}(D_i(\delta A_i) \Lambda) \quad (4.1.4)$$

This is equivalent to satisfying

$$D_i \delta A_i = 0 \quad (4.1.5)$$

We get an interesting result if we write each of these conditions in a quaternion basis. Firstly, (4.1.2), like the ADHM equations, is really three equations

$$\bar{\tau}_{\dot{\beta}}^{\dot{\alpha}} \bar{\mathcal{D}}^{\dot{\beta}\alpha} \delta A_{\alpha\dot{\alpha}} = 0 \quad (4.1.6)$$

Where the  $\bar{\tau}_{\dot{\beta}}^{\dot{\alpha}}$  are the usual Pauli matrices (the dotted indices are the usual Weyl  $SU(2)$  indices, as discussed in section 3.2.1 and we have

$$\mathcal{D} \equiv \sigma_n \mathcal{D}_n; \quad \bar{\mathcal{D}} \equiv \bar{\sigma}_n \mathcal{D}_n; \quad (4.1.7)$$

The gauge orthogonality condition, equation (4.1.4), can also be written as

$$\bar{\mathcal{D}}^{\dot{\alpha}\alpha} \delta A_{\alpha\dot{\alpha}} = 0 \quad (4.1.8)$$

we can then combine these equations to get

$$\bar{\mathcal{D}}^{\dot{\alpha}\alpha} \delta A_{\alpha\dot{\beta}} = 0 \quad (4.1.9)$$

This is the Dirac equation in the instanton background, for a spinor  $\psi_{\alpha} = \delta A_{\alpha\dot{\beta}}$ . Note that because of the free  $\dot{\beta}$  index, this equation gives two Weyl spinors, or a single Dirac spinor.

Now we have introduced the zero modes, we can go on to discuss the dynamics on the moduli space, following [1]. Because our fields now have a time dependence, they will no longer automatically satisfy the Yang Mills equations. In particular, Gauss' law is modified to

$$D_i F_{i0} = D_i (D_i A_0 - \dot{z}^r \delta_r A_i) = 0 \quad (4.1.10)$$

where  $i$  is a spacetime index, and  $r$  labels the moduli space coordinates. Therefore  $\delta_r A_i$  refers to a zero mode on the quotient moduli space in the  $r$  direction. This is distinct from  $\partial_r A_i$ . Following [1] this refers to the tangent vector in the  $r$  direction on the unquotiented moduli space.

With this in mind, equation (4.1.10) is now solved by

$$A_0 = \dot{z}^r \epsilon_r \quad (4.1.11)$$

for a small perturbation  $\epsilon_r$  satisfying

$$D_i(D_i\epsilon_r - \partial_r A_i) = 0 \quad (4.1.12)$$

This implies that, for the electrical components of the field strength

$$F_{i0} = z^r \delta_r A_i \quad (4.1.13)$$

In terms of the zero modes

$$\delta_r A_i = \partial_r A_i - D_i \epsilon_r \quad (4.1.14)$$

For slow moving instantons, this will be the only part of the Field Strength which contributes. Substituting this into the Yang Mills action, we get the following effective action on the moduli space

$$S = \frac{1}{2} \int d^5x \text{Tr}(F_{i0} F_{i0}) = \frac{1}{2} \int dt g_{rs} \dot{z}^r \dot{z}^s \quad (4.1.15)$$

where

$$g_{rs} = \int d^4x \text{Tr}(\delta_r A_i \delta_s A_i) \quad (4.1.16)$$

is the induced metric on the (quotiented) moduli space. We will discuss below how to calculate this using the ADHM solution.

## 4.2 Moduli Space of Dyonic Instantons

We now move on to discussing the moduli space of dyonic instantons. This section follows the relevant section in [1] very closely, as well as the discussion in [57]. As discussed in section 3.4, each dyonic instanton has a unique underlying pure instanton. We can therefore identify the moduli spaces pointwise. However, the fact that dyonic instantons have an electric charge means that the moduli space structure is modified, and the dynamics are altered by the addition of a potential. This method was first used for monopoles in [4] and [5], and was extended to Instantons in [43].



To recap: The action for dyonic instantons is

$$S = - \int d^5x \left( \frac{1}{4} \text{Tr}(F_{\mu\nu}F^{\mu\nu}) + \frac{1}{2} \text{Tr}(D_\mu\phi D^\mu\phi) \right) \quad (4.2.1)$$

This leads to the equations of motion

$$\begin{aligned} D_j F^{ji} + [A_0, D^i A_0] - [\phi, D^i \phi] &= 0 \\ D_j F^{j0} - [\phi, D^0 \phi] &= 0 \\ D_i D^i \phi &= 0 \end{aligned} \quad (4.2.2)$$

These are solved by taking  $F_{ij}$  to be self dual, with  $A_0 = \phi$ ; where  $\phi$  is solved for using it's eom. In principle, to analyse their dynamics, we could explicitly construct the moduli space and it dynamics. This would be rather difficult, so it is usual to take advantage of the fact that these solutions, with non- zero  $\phi$  are in one- to- one correspondence to pure instanton solutions, where  $\phi=0$ . This link allows us to use the moduli space techniques developed for pure instantons and apply them to the dyonic cases. We start with the equations of motion for 4d instantons with a scalar field

$$D_i F^{ij} = [\phi, D^j \phi] \quad (4.2.3)$$

$$D^2 \phi = 0 \quad (4.2.4)$$

with  $\phi$  going to the vev on the boundary. As discussed in section 3.4, Derrick's theorem means that there are no actual instanton solutions to these equations. However, to first order, we can solve these equations in the same way as 4.2.2, just with  $A_0 = 0$ . These approximate solutions are instantons, and lift in a one- to-one correspondence to solutions of 4.2.2. We call these, 'constrained instanton solutions'. As in the pure instanton case, we are interested in solutions modulo gauge invariance. Because of the one to one correspondence between the two sets of solutions, the cosets also lift to the dyonic case.

We now need to consider to consider how the zero modes are affected by this process. Just as in the pure instanton case, we can introduce time dependence to the Instanton

solutions via the collective coordinates. The same trick also works for the scalar field, which we label as  $\phi(\mathbf{z}(t); \mathbf{x})$ , corresponding to the gauge potential  $A_i(\mathbf{z}(t); \mathbf{x})$ , where  $\mathbf{z}(t)$  are the time-dependent moduli space coordinates, and  $\mathbf{x}$  are the spacetime coordinates. The presence of the scalar field modifies Gauss' law to

$$D_{i0}F_{i0} + [D_0\phi, \phi] = 0 \quad (4.2.5)$$

which is no longer solved on the moduli space. However, we can approximately solve it. This allows us to use the same methods as in the pure Instanton case to analyse the moduli space motion. However because our solution is only approximate, there is a restricted regime in which this analysis is valid. The approximate solution, as before, is constructed by taking the static solution and perturbing it by some  $\epsilon_r$

$$A_0 = \phi + \dot{z}^r \epsilon_r \quad (4.2.6)$$

This gives us

$$F_{i0} = -(\dot{z}^r \delta_r A_i - D_i \phi) \quad (4.2.7)$$

Why is this solution only an approximation? The first part of Gauss' law poses no problem, since the fact that  $D^2 = 0$  means that  $D_i F_{i0} = 0$ . However the second term in Gauss' law,  $[D_0\phi, \phi]$ , is not zero, and hence the law is not satisfied. However, this second term is of order  $\dot{z}^r |q|^2$ , where  $q$  is the VEV of  $\phi$ . This implies that there might be some limit of small  $|q|$  and  $\dot{z}^r$  in which this approximation is valid.

To confirm this, recalling that the zero modes  $\delta_r A_i$  form a basis of the space of all zero modes, we note that  $D_i \phi$  satisfies the linear self-duality equations (4.1.2) and is also orthogonal to gauge elements, since  $D^2 \phi = 0$ . This means that it is a zero mode, and therefore we can write

$$D_i \phi = |q| K^r \delta_r A_i \quad (4.2.8)$$

for some vectors  $K_r$ .

It turns out that these vectors are not arbitrary, but are Killing vectors of the metric. This is because, at infinity,  $D_i \phi$  must be pure gauge – it is a global  $U(N)$

transformation by  $q$ . Because this is a symmetry of the full Yang-Mills solution, it induces a symmetry on the moduli space, and the associated vectors  $K^r$  are therefore Killing vectors. In this notation, the electric component of the field strength becomes

$$F_{i0} = -(\dot{z}^r - |q|K^r)\delta_r A_i = -\dot{y}^r \delta_r A_i \quad (4.2.9)$$

for

$$y^r = z^r - |q|K^r t \quad (4.2.10)$$

The effective action on the moduli space is now

$$S = \frac{1}{2} \int d^5x \text{Tr}(F_{i0}F_{i0} - D_i\phi D_i\phi + D_0\phi D_0\phi) \quad (4.2.11)$$

If we neglect terms of order  $\dot{z}^2|q|^2$ , we get the rather nice form

$$S = \frac{1}{2} \int dt \left( g_{rs} \dot{y}^r \dot{y}^s - |q|^2 g_{rs} K^r K^s \right) \quad (4.2.12)$$

This is the same as the pure instanton equation (4.1.15) but with the addition of a potential

$$V = \frac{1}{2} \int d^5x \text{Tr}(D_i\phi D_i\phi) = \frac{|q|^2}{2} \int dt g_{rs} K^r K^s \quad (4.2.13)$$

As stated above, this analysis is only valid in certain limits, in fact in the limit

$$\dot{z}^2, |q| \leq 1; \quad (4.2.14)$$

where we can ignore terms of order  $\dot{z}^2|q|^2$  and higher. The geometric interpretation of this is both that the kinetic energy of the Instanton solution is sufficiently small, and that the potential evaluated on the Instanton solutions, which lie on the moduli space, is shallow compared to the potential on non-Instanton solutions evaluated off the moduli space. This allows us to imagine our approximate solution as lying in a steep valley given by the locally small potential around the moduli space solutions, where the small kinetic energy prevents our dynamics from, ‘climbing away’ from the moduli space.

### 4.2.1 The Complex Subspace

There is one final technical point to discuss. The Moduli space has several subspaces, which are preserved under the geodesic motion – i.e. a geodesic beginning in one of these subspaces will remain in it throughout its motion.

The subspace we are interested in is as follows. The moduli space is a manifold over the collective coordinates  $\mathbf{z}$ . However, as we saw in section 3.3 these collective coordinates are parametrised by the (bi)quaternions. That algebra can be thought of as  $\mathbb{C} \times \mathbb{C} \times \mathbb{H} = \mathbb{C} \times \mathbb{C}_{\mathbb{C}}$ , where the last expression is to be understood via the Cayley- Hamilton construction of the quaternions. The quaternions therefore contain a complex subspace  $\mathbb{C}$ , preserved under the action of the other  $\mathbb{C}$  making up the quaternions. Correspondingly the biquaternions have the subspace  $\mathbb{C} \times \mathbb{C}$ . We can therefore restrict from the full moduli space where the collective coordinates are biquaternions, to a submanifold where they lie in  $\mathbb{C} \times \mathbb{C}$ .

This corresponds to conjugating all the moduli space coordinates by a unit quaternion  $q$ , e.g.  $\tau \rightarrow q\tau\bar{q}$ . This corresponds geometrically to a rotation about some axis represented by  $q$ , and therefore imposing invariance under such rotations corresponds to choosing a two dimensional plane within the four dimensional quaternions. Because  $\bar{q}q = 1$ , if we multiply two (bi)quaternions together and apply this rotation to each of them then the result is that the entire product is rotated- e.g.

$$\Delta^\dagger \Delta \rightarrow q\Delta^\dagger \bar{q}q\Delta\bar{q} = q\Delta^\dagger \Delta\bar{q} \quad (4.2.15)$$

We can therefore think of all our equations and objects (for example the scalar field and potential) as being rotated in the same overall way. In the commutative space, for pure instantons we can see the invariance of this subspace automatically, since the elements of  $\mathbb{C} \in \mathbb{H}$  automatically commute with all other elements, meaning that they form an ideal within that group [24]. For Dyonic Instantons, we must choose the imaginary direction to be the same as the vev in  $SU(2)$ . In the noncommutative case, the presence of the noncommutative parameter means that the spacetime coordinates do not automatically commute. The only complex subspace which is

preserved in this case is the complex subspace spanned by  $\{\mathbb{1}, \sigma_3\}$ , as, since  $\sigma_3$  is the direction associated with the non commutativity, it is preserved under rotations of the space, and  $\mathbb{1}$  commutes with everything. We must then align the plane within  $\mathbb{H}$  that we are preserving with this direction. Hence we see, as would be expected, the presence of a noncommutative parameter reduces the symmetries of the theory. It is necessary to define what is meant by a geodesic submanifold, particularly in the presence of a potential. A geodesic submanifold is a submanifold which has the property that any geodesic beginning in that submanifold, with motion tangent to the submanifold, will remain in it. If there is a potential present then we require that this potential is invariant under the symmetries defining the submanifold. We then require that this submanifold has the property defined by the solutions of the equations of motion with the potential which begin in the submanifold, with tangent parallel to it, remain in that submanifold; in an analogous way to the concept of a geodesic submanifold above.

Calculations on the full quaternionic moduli space are very computationally expensive, and this subspace is often much easier to run simulations on. In addition, the commutativity of this subspace makes solving the ADHM equations on this restricted part of the theory much easier.

### 4.3 Constructing the Moduli Space Metric

Now we have outlined the theory behind the moduli space, we move on to practical calculations. We start with the metric on the space. This section is based on appendix 2 in [1], which is itself based on the method of [56] for calculating the metric determinant. This technique was adapted in [57] for the moduli space metric of two instantons, which they calculated to order  $|\tau|^{-2}$ . In [1] this is extended to the full metric for 2 commutative  $U(2)$  instantons. I present the argument for arbitrary gauge group and topological charge.

As above, the metric on the moduli space is defined as

$$g_{rs} = \int d^4x \operatorname{Tr}^*(\delta_r A_i \delta_s A_i) \quad (4.3.1)$$

where

$$\delta_r A_i = \partial_r A_i - D_i \epsilon_r \quad (4.3.2)$$

and

$$\operatorname{Tr}^*(q) = \operatorname{Tr}_2(\operatorname{Tr}(q)) \quad (4.3.3)$$

There is one mode for each of the  $8k$  moduli space coordinates, labelled here by the indices  $r$  and  $s$ . The index  $i$  refers to spacetime coordinates. Recall these zero modes are orthogonal to gauge transformations by definition

$$D_i(\delta_r A_i) = 0 \quad (4.3.4)$$

We can use this fact to find an explicit expression for the metric. First, we need an expression for  $\partial_r A_i|_{z=z_0}$  in terms of the ADHM data. To do this, we recall that  $A_i = U^\dagger \partial_i U$ , and use the identity  $U = PU$  with  $U$  the projection operator  $\mathbb{1} - \Delta f \Delta^\dagger$  to derive

$$\partial_r U = -\Delta f \partial_r \Delta^\dagger U + P \partial_r U \quad (4.3.5)$$

This allows us to get the necessary result

$$\partial_r A_i|_{z=z_0} = -iU^\dagger \partial_r \Delta f \bar{e}_i b^\dagger U + iU^\dagger b e_i f \partial_r \Delta^\dagger U + D_i(iU^\dagger \partial_r U) \quad (4.3.6)$$

around an arbitrary point of the moduli space  $z_0$ . The zero mode is then this expression with the gauge dependent part removed. The third term above is explicitly a gauge transformation, however we also need to ensure that there is no gauge part implicit in the first two terms. To do this, we use the residual transformations described in equation (3.3.2) to transform the ADHM data as

$$\Delta \rightarrow q \Delta R, \quad U \rightarrow QU, \quad Q(z_0) = \mathbb{1}, \quad R(z_0) = \mathbb{1} \quad (4.3.7)$$

It can be seen that this transformation leaves  $A_i$  invariant, and that

$$\partial_r A_i|_{z=z_0} = -iU^\dagger C_r f \bar{e}_i b^\dagger U + iU^\dagger b e_i f C_r^\dagger U + D(iU^\dagger \partial_r(Q^\dagger U)) \quad (4.3.8)$$

with

$$C_r = \partial_r \Delta + \partial_r Q \Delta + \Delta \partial_r R \quad (4.3.9)$$

It turns out we can choose  $C_r$  so that the first two terms of  $\delta_r A_i$  have no gauge part – i.e. they are a zero mode. To do so we must prove the following

**Lemma 4.3.1.** If we choose  $C_r$  to be independent of  $x$  with

$$\Delta^\dagger C_r = (\Delta^\dagger C_r)^{T^*} \quad (4.3.10)$$

the expression

$$\partial_r A_i = -iU^\dagger C_r f \bar{e}_i b^\dagger U + iU^\dagger b e_i f C_r^\dagger U \quad (4.3.11)$$

will be a zero mode

To do this, we first note that this condition is equivalent to the two conditions

$$a^\dagger C_r = (a^\dagger C_r)^{T^*}; \quad b^\dagger C_r = (b^\dagger C_r)^{T^*} \quad (4.3.12)$$

and then consider the expression (forming part of  $\delta_r A_i$  above)

$$a_i := U^\dagger b f e_i \quad (4.3.13)$$

We can then calculate

$$D_i a_j = \partial_i a_j - i A_i a_j = U^\dagger e_i b f \Delta^\dagger b f e_j + U^\dagger b f (\bar{e}_i b^\dagger \Delta + \Delta^\dagger b e_i) \quad (4.3.14)$$

We then write  $\Delta^\dagger b$  in terms of its quaternion components as  $c_k \bar{e}_k$ , where the  $c_k$  are complex valued matrices. It is important to note that since  $\Delta^\dagger b = \Omega$ , the bottom  $2k \times 2k$  part of the ADHM data, the  $c_k$  are hermitian, since  $\Omega$  is hermitian by construction. Keeping this fact in mind, we can write (4.3.14) as

$$D_i a_j = U^\dagger b f c_k f (e_i \bar{e}_k e_j + \bar{e}_i e_k e_j + \bar{e}_k e_i e_j) \quad (4.3.15)$$

Now, we use the identity  $\bar{e}_i e_j = -\bar{e}_j e_i + 2\delta_{ij}$  to get

$$D_i a_j = -U^\dagger b f c_k (e_i \bar{e}_j e_k - 2\delta_{jk} e_i - 2\delta_{ik} e_j) \quad (4.3.16)$$

Then we can see  $a_j$  satisfies both the linear self- dual field equation

$$D_{[i} a_{j]} = \frac{1}{2} \epsilon_{ijkl} \quad (4.3.17)$$

and the zero mode condition  $D_i a_i = 0$ . What does this say about the full mode  $\delta_r A_i$ ? We calculate

$$\begin{aligned} D_i(\delta_r A_i) &= -i D_i U^\dagger C_r D_i a_j^\dagger + i a_j C_r^\dagger D_i U - i U^\dagger C_r (D_i a_j)^\dagger + i D_i a_j C_r^\dagger U \\ &= -i U^\dagger b f (e_i \Delta^\dagger C_r \bar{e}_j - e_j C_r^\dagger \Delta \bar{e}_i) f b^\dagger U - i U^\dagger C_r D_i a_j^\dagger + i D_i a_j C_r^\dagger U \\ &\quad - i U^\dagger C_r D_i a_j^\dagger + i D_i a_j C_r^\dagger U \end{aligned} \quad (4.3.18)$$

Here we have used the fact that

$$D_i U^\dagger - i A_i U^\dagger = U^\dagger e_i b f \Delta^\dagger \quad (4.3.19)$$

The discussion above of  $D_i a_j$  shows that the last two terms of (4.3.18) are a zero-mode. We must therefore check the first two terms. The only parts of these which depend on the moduli space coordinates are

$$e_i \Delta^\dagger C_r \bar{e}_j - e_j C_r^\dagger \Delta \bar{e}_i \equiv K_{ij} \quad (4.3.20)$$

So the first two terms being a zero mode are equivalent to

$$K_{[ij]} = \frac{1}{2} \epsilon_{ijkl} K_{ij} ; K_{ii} = 0 \quad (4.3.21)$$

and these are satisfied iff  $\Delta^\dagger C_r = (\Delta^\dagger C_r)^{T^*}$ . This proves the above lemma. To use this result, we must see what this condition says about the form of  $C_r$ . First we recall the definitions

$$C_r = \partial_r \Delta + \partial_r Q \Delta + \Delta \partial_r R \quad (4.3.22)$$



$$Q = \begin{bmatrix} q & 0 \\ 0 & R^{-1} \end{bmatrix} \quad (4.3.23)$$

Note that we can write  $C_r$  as

$$\partial_r a + \partial_r Q a + a \partial_r R + \left( \partial_r b + \partial_r Q b + b \partial_r R \right) x \quad (4.3.24)$$

Next we set  $q = 1$ . This means it does not contribute to the variation of  $Q$ , which means

$$\partial_r Q = -b \partial_r R b^\dagger \quad (4.3.25)$$

Then we see that the part of  $C_r$  proportional to  $x$  is zero, since  $\partial_r b$  is zero as  $b$  is a constant matrix and the other two terms cancel. This leaves us with

$$C_r = \partial_r a + \partial_r Q a + a \partial_r R \quad (4.3.26)$$

With this form, and the fact that  $R^{T^*} = -R$ , since  $R$  is unitary, it is straightforward that  $b^\dagger C_r = (b^\dagger C_r)^{T^*}$ . The second condition,  $a^\dagger C_r = (a^\dagger C_r)^{T^*}$ , is satisfied iff

$$a^\dagger \partial_r a - (a^\dagger \partial_r a)^{T^*} - a^\dagger b \partial_r R b^\dagger a - (a^\dagger b \partial_r R b^\dagger a)^{T^*} + a^\dagger a \partial_r R - (a^\dagger b \partial_r R b^\dagger a)^{T^*} = 0 \quad (4.3.27)$$

We have therefore reduced the problem of finding the zero modes to solving the above equation.

The metric is then derived from the inner product of two zero modes. To find this, we use the following result from ([56])

$$\text{Tr}^*(\delta_r A_i \delta_s A_i) = -\frac{1}{2} \partial^2 \text{Tr}^*(C_r^\dagger P C_s f + f C_r^\dagger C_s) \quad (4.3.28)$$

Where  $P = \mathbb{1} - \Delta f \Delta^\dagger$ . We can then use Stoke's Theorem to find the metric

$$\begin{aligned} g_{rs} &= -\frac{1}{2} \int d^4 x \partial^2 \text{Tr}^*(C_r^\dagger P C_s f + f C_r^\dagger C_s) \\ &= \int d^4 x \text{Tr}^*(C_r^\dagger P_\infty C_s + C_r^\dagger C_s)_{ij} \\ &= 2\pi^2 \text{Tr}^*(C_r^\dagger P_\infty C_s + C_r^\dagger C_s)_{ij} \\ &= 2\pi^2 \text{Tr}^*\left(\partial_r a^\dagger (1 + P_\infty) \partial_s a - \left(a^\dagger \partial_r a - (a^\dagger \partial_r a)^T\right)_{ij} \partial_s R\right) \end{aligned} \quad (4.3.29)$$

Here

$$\begin{aligned} P_\infty &= \lim_{x \rightarrow \infty} P = \mathbb{1}_{n+2k \times n+2k} - bb^\dagger \\ &= \begin{bmatrix} \mathbb{1}_{n/2 \times n/2} & 0 \\ 0 & 0_{k \times k} \end{bmatrix} \end{aligned} \quad (4.3.30)$$

Remembering

$$\Delta(x) = \begin{bmatrix} \Lambda \\ \Omega + \tilde{\rho} \mathbb{1}_{k \times k} \end{bmatrix} - x \begin{bmatrix} 0 \\ \mathbb{1}_{k \times k} \end{bmatrix} \quad (4.3.31)$$

(Note – the term in  $\tilde{\rho}$  gives the center of mass, and is usually absorbed into the  $x$  component by a suitable choice of coordinates, but it is there, and therefore we consider it here – albeit briefly). The first term above then gives

$$2\pi^2 \text{Tr}^*(da^\dagger(1 + P_\infty)da) = 2\pi^2 \text{Tr}^*(2\Lambda^\dagger\Lambda + \Omega^\dagger\Omega + 2d\tilde{\rho}^\dagger d\tilde{\rho}) \quad (4.3.32)$$

The  $d\tilde{\rho}^\dagger d\tilde{\rho}$  directions are flat (by which I mean isomorphic to  $\mathbb{R}_4$ ) and so we ignore them. This gives the first part of the metric

$$ds_1^2 = 2\pi^2 \text{Tr}^*(da^\dagger(1 + P_\infty)da) = 2\pi^2 \text{Tr}^*(2\Lambda^\dagger\Lambda + \Omega^\dagger\Omega) \quad (4.3.33)$$

Now for the second part of the metric

$$ds_2^2 = 2\pi^2 \text{Tr}^*\left(\left(a^\dagger da - (a^\dagger da)^{T*}\right)dR\right) \quad (4.3.34)$$

To find an explicit expression here, we write  $dR$  in terms of its components considered as a  $U(k)$  matrix, and solve for them using (4.3.27). We get one equation for each component, and solving them gives  $dR$  in terms of the ADHM parameters in  $a$ . We will see this explicitly in the specific cases below. Once we have done this, we can put all these parts together to get the full metric

$$\begin{aligned} ds^2 &= ds_1^2 + ds_2^2 = 2\pi^2 \left( \text{Tr}^*(da^\dagger(1 + P_\infty)da) \right. \\ &\quad \left. + \text{Tr}^*\left(\left(a^\dagger da - (a^\dagger da)^{T*}\right)dR\right) \right) \\ &= 2\pi^2 \left( \text{Tr}^*(2d\Lambda^\dagger d\Lambda + d\Omega^\dagger d\Omega) + \text{Tr}^*\left(\left(a^\dagger da - (a^\dagger da)^{T*}\right)dR\right) \right) \end{aligned} \quad (4.3.35)$$

## 4.4 Constructing the Potential

Now we have the metric, we look at how to calculate the potential for the dyonic instanton moduli space. This makes use of the solution for the scalar field in section 3.4.1. Recall the definition of the potential

$$\mathcal{V} = \int d^4x \operatorname{Tr}(D_i\phi D_i\phi) \quad (4.4.1)$$

Integrating by parts and using the fact that  $D^2\phi = 0$  via its equation of motion we get

$$\mathcal{V} = \lim_{R \rightarrow \infty} \int_{|x|=R} dS^3 \hat{x}_i \operatorname{Tr}(\phi D_i\phi) \quad (4.4.2)$$

Using the facts that  $\phi = U^\dagger \mathcal{A}U$ ,  $D_i = \partial_i - iA_i$  and  $A_i = U^\dagger \partial_i U$ , a moderately long calculation gives

$$D_i\phi = iU^\dagger e_i b f \Delta^\dagger \mathcal{A}U + iU^\dagger \mathcal{A} \Delta f \bar{e}_i b^\dagger U \quad (4.4.3)$$

To fully evaluate this integral, we need an expression for  $U$ . In general this would be rather complicated, however we only need the value of  $U$  on the boundary, in the limit  $R \rightarrow \infty$ . For a general ADHM matrix

$$\begin{bmatrix} v_1 & v_2 & v_3 & \dots & v_k \\ \tau_1 - x & \sigma_1^* & \sigma_2^* & \dots & \sigma_{k-1}^* \\ \sigma_1 & \tau_2 - x & \sigma_k^* & \dots & \sigma_{2k-3}^* \\ \vdots & & \ddots & & \vdots \\ \sigma_{k-1} & \sigma_{2k-3} & \sigma_{3k-4} & \dots & \tau_k - x \end{bmatrix} \quad (4.4.4)$$

the condition  $\Delta^\dagger U = 0$  gives  $k + N$  equations

$$v_l^\dagger U_1 + (\tau_l^\dagger - x)U_{l+1} + \sum_{i,j \in A} \sigma_i^\dagger U_j + \sum_{i,j \in B} \sigma_i^{\dagger*} U_j \quad (4.4.5)$$

for some index sets  $A$  and  $B$ . These are solved to leading order in  $|x|$  by

$$U_1 \mapsto 1; U_i \mapsto \frac{x}{|x|^2} v_{i-1}^\dagger, i \neq 1 \quad (4.4.6)$$

We might worry here about the issue discussed in section 3.3, where  $U$  may or may not satisfy the completeness relation (3.3.17). In general we would need to worry about this, however if we expand in powers of  $\zeta$ , any terms including a correction of order  $\zeta^n$  would, by dimensional analysis, also have to go as  $|x|^{-2n}$ , and are therefore neglected in this limit. We also need these two results for the behaviour of other quantities in this limit

$$\begin{aligned}\Delta &\mapsto \begin{bmatrix} \Lambda \\ -x\mathbb{1}_k \end{bmatrix} \\ f &\mapsto \frac{1}{|x|^2}\mathbb{1}_k\end{aligned}\tag{4.4.7}$$

We can use these to expand equation (4.4.3), and then multiplying by  $\hat{x}_i$  we get, to leading order

$$\hat{x}_i D_i \phi = \frac{2i}{|x|^3} \left( q\Lambda\Lambda^\dagger - \Lambda P\Lambda^\dagger \right) + \mathcal{O}\left(\frac{1}{|x|^4}\right)\tag{4.4.8}$$

Remembering that  $\phi = iq$  on the boundary, we can then write, to leading order

$$\begin{aligned}\mathcal{V} &= \lim_{R \rightarrow \infty} \int_{|x|=R} dS^3 \hat{x}_i \text{Tr}(\phi D_i \phi) \\ &= -2 \lim_{R \rightarrow \infty} \int_{|x|=R} dS^3 \frac{1}{|x|^3} \left( q^2 \Lambda\Lambda^\dagger - q\Lambda P\Lambda^\dagger \right) + \mathcal{O}\left(\frac{1}{|x|^4}\right) \\ &= -4\pi^2 \text{Tr}\left(q^2 \Lambda\Lambda^\dagger - q\Lambda P\Lambda^\dagger\right)\end{aligned}\tag{4.4.9}$$

Now we have these general expressions and methods for the ADHM solutions, moduli space metric, and potential, we can give specific solutions for different instanton configurations. We will be interesting in  $U(2)$  Yang Mills, and the 2 and 3 Instanton sectors in particular.



## Part II

# Particular Solutions



# Chapter 5

## One and Two Instantons

In this chapter, I derive one of the main results of the thesis- a solution of the noncommutative  $U(2)$  2 instanton theory. First, I review the single  $U(2)$  instanton as presented in [3]. This is necessary to test the two instanton solution in the appropriate limits.

Next I derive the ADHM equations for the two Instanton case, using biquaternion coordinates. I briefly look at the commutative biquaternion equations, and investigate how their solution can be rotated into the quaternion solution found in [1] using the increased symmetry in this case. I explicitly show that this is possible.

Then I move on to the noncommutative biquaternion equations. I begin by showing that the solution derived in [37] is incorrect, and then explore alternate strategies to solve the equations. I was unable to find a solution for the full moduli space, however I was able to find a solution for the geodesic submanifold discussed in section 4.2.1. After finding this solution I use it to derive the metric and potential for the relevant moduli space. I show that the metric and potential behave suitably in the commutative limit and in the limit of the instantons being far separated.



## 5.1 The Single $U(2)$ Instanton

First, we derive the solution for a single  $U(2)$  instanton in noncommutative space. I then use this solution to derive the moduli space metric and potential. This is useful as it allows us to check the two instanton solution behaves correctly in various limits. We will follow the presentation of the solution in [3], however for their purposes they use a very different notation to the one developed here, and even a different method of calculating the metric, which I will discuss below. I rederive their solution in the notation I have used elsewhere. Other discussions of the solution can be found in [12] and [17]. First, for the single noncommutative  $U(2)$  instanton, the ADHM data has the form

$$\begin{bmatrix} v \\ X - x' \end{bmatrix}; \quad v, X, x' \in \mathbb{H} \quad (5.1.1)$$

We can define  $X - x' = -x$ , and write

$$\Delta = \begin{bmatrix} v \\ -x \end{bmatrix} \quad (5.1.2)$$

Then, using the method outlined in section 3.3.2, in particular equation (3.3.52), the noncommutative ADHM equation is

$$v^\dagger v = A\mathbb{1} - 4i\zeta\sigma_3 \quad (5.1.3)$$

where  $v = v_R + iv_I$ . We can solve this by

$$v_I = -\frac{2\zeta v_R \sigma_3}{|v_R|^2}; \quad v_R \in \mathbb{H} \quad (5.1.4)$$

The solution in [3] (in the form from Appendix E) is

$$v = \hat{g} \begin{bmatrix} \sqrt{\rho^2 + 2\zeta'} & 0 \\ 0 & \sqrt{\rho^2 - 2\zeta'} \end{bmatrix} \quad (5.1.5)$$

where  $\hat{g}$  is a unit quaternion and the relation between their  $\zeta'$  and our  $\zeta$  is  $\zeta' = 2\zeta$ . After some calculation it turns out that this is

$$v_I = \frac{-2\zeta v_R \sigma_3}{|v_R|^2}; \quad v_R \in \mathbb{H} \quad (5.1.6)$$

Now we have this, we can try and calculate the metric and potential using our method developed in sections 3.4.1 and 4.4

### 5.1.1 The Potential

The first step is to calculate the scalar field. We use the ansatz (3.4.12), which in this case is

$$\phi = \begin{bmatrix} q & 0 \\ 0 & \psi \end{bmatrix} \quad (5.1.7)$$

Where  $q \in U(2)$ , and  $\psi \in U(1)$ . Then we find the equation of motion for  $\phi$ , (3.4.18), reduces to

$$2\text{Tr}_2(\Lambda^\dagger q \Lambda) = \text{Tr}_2(\{\psi, \Lambda^\dagger \Lambda\}) \quad (5.1.8)$$

In our case,  $\Lambda = v$ , and  $\psi$  commutes with everything, so we have

$$\text{Tr}_2(v^\dagger q v) = \psi \text{Tr}_2(v^\dagger v) \quad (5.1.9)$$

This is solved by

$$\psi = \frac{i q_0 (|v_R|^2 + |v_I|^2) + 2i \text{Re}(\bar{v}_R \mathbf{q} v_I)}{|v_R|^2 + |v_I|^2} \quad (5.1.10)$$

We now use this to calculate the potential. Note that, as  $|x|$  tends to infinity,

$$\Delta U = 0 \quad (5.1.11)$$

is solved by

$$U_1 \mapsto 1; \quad U_2 \mapsto \frac{x}{|x|^2} v^\dagger \quad (5.1.12)$$

Note that, specifically in the U(1) case, this is true not just in the infinite limit, but for all  $x$ . As outlined in section 4.4, we can use this solution for  $U$  to calculate

$$\hat{x}_i D_i \phi = \frac{i}{|x|^3} \left( v v^\dagger q + q v v^\dagger - 2v \psi v^\dagger \right) \quad (5.1.13)$$

which can be expanded into real and imaginary parts as

$$\frac{i}{|x|^3} \left( 2q(|v_R|^2 + |v_I|^2) + 2iq \operatorname{Im}(v_I \bar{v}_R) + 2i \operatorname{Im}(v_I \bar{v}_R) q - 2\psi(|v_R|^2 + |v_I|^2 + 2i \operatorname{Im}(v_I \bar{v}_R)) \right) \quad (5.1.14)$$

So

$$\begin{aligned} \mathcal{V} = & -\lim_{R \rightarrow \infty} \int_{|x|=R} \frac{d^3 S}{|x|^3} \operatorname{Tr} \left( 2q^2(|v_R|^2 + |v_I|^2) \right. \\ & \left. + 2iq^2 \operatorname{Im}(v_I \bar{v}_R) + 2iq \operatorname{Im}(v_I \bar{v}_R) q - 2\psi q(|v_R|^2 + |v_I|^2 + 2i \operatorname{Im}(v_I \bar{v}_R)) \right) \end{aligned} \quad (5.1.15)$$

evaluating the integral, this becomes

$$\mathcal{V} = -8\pi^2 \operatorname{Tr} \left( q^2(|v_R|^2 + |v_I|^2) + iq^2 \operatorname{Im}(v_I \bar{v}_R) + iq \operatorname{Im}(v_I \bar{v}_R) q - \psi q(|v_R|^2 + |v_I|^2 + 2i \operatorname{Im}(v_I \bar{v}_R)) \right) \quad (5.1.16)$$

Using the properties of the trace, this becomes

$$\mathcal{V} = 8\pi^2 \operatorname{Tr} \left( (|\mathbf{q}|^2 + q_0^2)(|v_R|^2 + |v_I|^2) + 4q_0 \mathbf{q} \operatorname{Im}(v_I \bar{v}_R) + i\psi \left( q_0(|v_R|^2 + |v_I|^2) + 2\mathbf{q} \operatorname{Im}(v_I \bar{v}_R) \right) \right) \quad (5.1.17)$$

which we can rearrange as

$$\mathcal{V} = 8\pi^2 \left( (q_0^2 + |\mathbf{q}|^2)(|v_R|^2 + |v_I|^2) + 4q_0 \operatorname{Re}(\bar{v}_R \mathbf{q} v_I) - \frac{(q_0(|v_R|^2 + |v_I|^2) + 2\operatorname{Re}(\bar{v}_R \mathbf{q} v_I))^2}{|v_R|^2 + |v_I|^2} \right) \quad (5.1.18)$$

Now, note that the parts proportional to  $q_0$  cancel and so we are left with

$$\mathcal{V} = 8\pi^2 \left( |\mathbf{q}|^2(|v_R|^2 + |v_I|^2) - \frac{4\operatorname{Re}^2(\bar{v}_R \mathbf{q} v_I)}{|v_R|^2 + |v_I|^2} \right) \quad (5.1.19)$$

Putting in the expression for  $v_I$  and taking  $\mathbf{q} = |\mathbf{q}| \sigma_3$  we get

$$\mathcal{V} = 8\pi^2 |\mathbf{q}|^2 \left( \rho^2 - \frac{4\zeta^2}{\rho^2} \operatorname{Re}^2(\hat{v}_R \sigma_3 \hat{v}_R \sigma_3) \right) \quad (5.1.20)$$

where

$$\rho^2 = |v_R|^2 + |v_I|^2 = |v_R|^2 + \frac{4\zeta^2}{|v_R|^2} \quad (5.1.21)$$

and  $\hat{v}_R$  is the unit vector in the  $v_R$  direction. Now,  $\mathbf{q} \in SU(2)$  and so  $\bar{\mathbf{q}} = -\mathbf{q}$ . Therefore  $\mathbf{q}\hat{v}_R\mathbf{q} = -\bar{\mathbf{q}}\hat{v}_R\mathbf{q}$ , and the latter expression is a rotation of  $\hat{v}_R$  by  $\mathbf{q}$ . If we set  $\mathbf{q} = |\mathbf{q}|\sigma_3$ , we can therefore express this rotation as  $\hat{v}_R(\cos(\theta) + i\sin(\theta))$ , where  $\theta$  is the rotation around the  $\sigma_3$  axis. Then the potential is equal to

$$\mathcal{V} = 8\pi^2|\mathbf{q}|^2\left(\rho^2 - \frac{16\zeta^2}{\rho^2}\cos^2(\theta)\right) \quad (5.1.22)$$

which is exactly the potential in [3] with  $16\zeta^2 = 4\zeta'^2$ .

### 5.1.2 The Metric

We start by splitting  $\Delta$  into

$$a = \begin{bmatrix} v \\ 0 \end{bmatrix}; b = \begin{bmatrix} 0 \\ 1 \end{bmatrix} \quad (5.1.23)$$

with  $v = v_R + iv_I$ , we find that  $a^\dagger b = 0$  and so we have to solve

$$a^\dagger da - (a^\dagger da)^{T^*} = -a^\dagger a(dR) + (a^\dagger a(dR))^{T^*} \quad (5.1.24)$$

In this case,  $dR \in U(1)$ , as we have a single instanton, and if we write  $dR = id\xi$ , we can solve for it as

$$d\xi = \frac{v_R dv_I - \bar{v}_I dv_R}{|v_R|^2 + |v_I|^2} \quad (5.1.25)$$

We use the method in section 4.3. It is worth pointing out here that the method used is an alternative to that in [3]. When considering the residual symmetries 3.3.33, recall we set the rotation  $q$  to be locally constant (note that this  $q$  is a residual symmetry and is not to be confused with  $\mathbf{q}$  the scalar field vev!). I have used a slightly different method – that considered in section (4.3). This method is mentioned in [3] and they confirm it gives the same answer as the one they calculate.

Regardless, if we use our formula

$$ds^2 = ds_1^2 + ds_2^2 = 2\pi^2 \left( \text{Tr}^* (2d\Lambda^\dagger d\Lambda + d\Omega^\dagger d\Omega) + \text{Tr}^* \left( (a^\dagger da - (a^\dagger da)^{T^*}) dR \right) \right) \quad (5.1.26)$$

We get the final result, noting that the  $i$  from  $dR$  cancels the  $i$  from  $a^\dagger da - (a^\dagger da)^{T^*}$

$$ds^2 = 8\pi^2 \left( dv_R^2 + dv_I^2 - \frac{(v_R dv_I - \bar{v}_I dv_R)^2}{|v_R|^2 + |v_I|^2} \right) \quad (5.1.27)$$

## 5.2 Two U(2) Instantons

We now move on to the case of two  $U(2)$  instantons. In the commutative case, a solution was found for the real quaternions (and with gauge group  $SU(2)$ ) in [1]. I begin by showing that a solution can also be found for the commutative case with gauge group  $U(2)$  beginning with the Biquaternions and then enforcing reality conditions via the symmetries. This provides a specific example of the equivalence of these two approaches, discussed in the abstract in section 3.3.2. Next I move on to the noncommutative  $U(2)$  case. Here a solution was put forward in [37], however I will show that this solution is not in fact correct.

I was unable to find the solution for the full moduli space, however I was able to find a solution for the geodesic submanifold discussed in section 4. After outlining this solution, I will go on to derive the scalar field, moduli space metric and potential as discussed above.

## 5.3 ADHM Constraints

We begin with solving the ADHM equations. For the case of two  $U(2)$  instantons, the ADHM data has the form

$$\Delta = a - bx; \quad a = \begin{bmatrix} \Lambda \\ \Omega \end{bmatrix} = \begin{bmatrix} v & w \\ \tau & \sigma^* \\ \sigma & -\tau \end{bmatrix}, \quad b = \begin{bmatrix} 0 & 0 \\ 1 & 0 \\ 0 & 1 \end{bmatrix} \quad (5.3.1)$$

Note that here  $\Omega$  is constrained to be hermitian (under complex conjugation) rather than symmetric, as in the real ADHM construction.  $v, w$  and  $\sigma$  lie in the biquaternions, however due to the requirement that  $\Omega$  be hermitian,  $\tau$  remains a member of  $\mathbb{H}$ . Proceeding as in section (3.3.2), equation (3.3.2) gives the following. We begin by looking at the commutative equations, so  $\zeta = 0$ . First, the diagonal equations

$$\begin{aligned} v^\dagger v + |\tau|^2 + \sigma^\dagger \sigma &= f_{11}^{-1} \mathbb{1} \\ w^\dagger w + |\tau|^2 + (\sigma^\dagger \sigma)^* &= f_{11}^{-1} \mathbb{1} \end{aligned} \quad (5.3.2)$$

Next, the off diagonal constraints are given by

$$\begin{aligned} v^\dagger w + \bar{\tau} \sigma^* - \sigma^\dagger \tau &= f_{12}^{-1} \mathbb{1} \\ w^\dagger v + (\sigma^\dagger)^* \tau - \bar{\tau} \sigma &= f_{12}^{-1*} \mathbb{1} \end{aligned} \quad (5.3.3)$$

This information can be put into a more convenient form – we shall look at the off-diagonal equations first. Again, we expand into quaternion real and imaginary parts

$$\begin{aligned} \bar{v}_R w_R + \bar{v}_I w_I + i (\bar{v}_R w_I - \bar{v}_I w_R) + \bar{\tau} \sigma_R - \bar{\sigma}_R \tau + i (\bar{\sigma}_I \tau - \bar{\tau} \sigma_I) &= f_{12}^{-1} \mathbb{1} \\ \bar{w}_R v_R + \bar{w}_I v_I + i (\bar{w}_R v_I - \bar{w}_I v_R) - (\bar{\tau} \sigma_R - \bar{\sigma}_R \tau) + i (\bar{\sigma}_I \tau - \bar{\tau} \sigma_I) &= f_{12}^{-1*} \mathbb{1} \end{aligned}$$

We can add these two equations together to get

$$\bar{v}_R w_R + \bar{w}_R v_R + \bar{v}_I w_I + \bar{w}_I v_I + i (\bar{v}_R w_I - \bar{w}_I v_R + \bar{w}_R v_I - \bar{v}_R w_R) + 2i (\bar{\sigma}_I \tau - \bar{\tau} \sigma_I) = 2 \operatorname{Re}_{\mathbb{C}}(f_{12}^{-1}) \mathbb{1} \quad (5.3.4)$$

This is equivalent to

$$\operatorname{Re}_{\mathbb{H}}(\bar{w}_R v_R) + \operatorname{Re}_{\mathbb{H}}(\bar{w}_I v_I) + i \operatorname{Im}_{\mathbb{H}}(\bar{w}_R v_I + \bar{v}_R w_I) + 2i \operatorname{Im}_{\mathbb{H}}(\bar{\sigma}_I \tau) = 2 f_{12}^{-1} \mathbb{1} \quad (5.3.5)$$

Since  $f$  is arbitrary we don't care about the real quaternion part of the constraints, so this gives us the equation

$$\operatorname{Im}_{\mathbb{H}}(\bar{\tau} \sigma_I) = \frac{\operatorname{Im}_{\mathbb{H}}(\bar{w}_R v_I + \bar{v}_R w_I)}{2} \quad (5.3.6)$$

As before we can also take the two equations away to get

$$\bar{v}_R w_R - \bar{w}_R v_R + \bar{v}_I w_I - \bar{w}_I v_I + i \left( \bar{v}_R w_I + \bar{w}_I v_R - \bar{v}_I w_R - \bar{w}_R v_I \right) + 2 \left( \bar{\tau} \sigma_R - \bar{\sigma}_R \tau \right) = f_{12} - f_{12}^* \quad (5.3.7)$$

This is

$$\text{Im}_{\mathbb{H}}(\bar{w}_R v_R) + \text{Im}_{\mathbb{H}}(\bar{w}_I v_I) + i \left( \text{Re}_{\mathbb{H}}(\bar{w}_R v_I) - \text{Re}_{\mathbb{H}}(\bar{w}_I v_R) \right) - 2 \text{Im}_{\mathbb{H}}(\bar{\sigma}_R \tau) = 2 \text{Im}_{\mathbb{C}}(f) \quad (5.3.8)$$

Where  $\text{Im}_{\mathbb{C}}(f)$  is the complex imaginary part of  $f$ , which is a complex function. We can therefore again ignore the real quaternion part of this equation, which is a purely imaginary number. This leaves us with the following equation for the quaternion imaginary part:

$$\text{Im}_{\mathbb{H}}(\bar{\tau} \sigma_R) = \frac{\text{Im}_{\mathbb{H}}(\bar{w}_R v_R + \bar{w}_I v_I)}{2} \quad (5.3.9)$$

We now look at the diagonal equations. Expanding the biquaternions into their real and imaginary parts, we can rewrite them as

$$\begin{aligned} |v_R|^2 + |v_I|^2 + i \left( \bar{v}_R v_I - \bar{v}_I v_R \right) + |\tau_R|^2 + |\sigma_R|^2 + |\sigma_I|^2 + i \left( \bar{\sigma}_R \sigma_I - \bar{\sigma}_I \sigma_R \right) &= f_{22} \mathbb{1} \\ |w_R|^2 + |w_I|^2 + i \left( \bar{w}_R w_I - \bar{w}_I w_R \right) + |\tau_R|^2 + |\sigma_R|^2 + |\sigma_I|^2 - i \left( \bar{\sigma}_R \sigma_I - \bar{\sigma}_I \sigma_R \right) &= f_{11} \mathbb{1} \end{aligned} \quad (5.3.10)$$

Since  $f$  is arbitrary we don't care about the real quaternion parts of these equations.

Adding them and taking the quaternion imaginary part we get

$$\text{Im}_{\mathbb{H}}(\bar{w}_R w_I) + \text{Im}_{\mathbb{H}}(\bar{v}_R v_I) = 0 \quad (5.3.11)$$

Taking them away and again taking the quaternion imaginary part we have

$$2 \text{Im}_{\mathbb{H}}(\bar{\sigma}_R \sigma_I) - \text{Im}_{\mathbb{H}}(\bar{w}_R w_I) + \text{Im}_{\mathbb{H}}(\bar{v}_R v_I) = 0 \quad (5.3.12)$$

This gives a total of four equations for the complex ADHM constraints. For completeness we list them here

$$2 \text{Im}_{\mathbb{H}}(\bar{\sigma}_R \sigma_I) - \text{Im}_{\mathbb{H}}(\bar{w}_R w_I) + \text{Im}_{\mathbb{H}}(\bar{v}_R v_I) = 0$$

$$\begin{aligned}
\operatorname{Im}_{\mathbb{H}}(\bar{w}_R w_I) + \operatorname{Im}_{\mathbb{H}}(\bar{v}_R v_I) &= 0 \\
\operatorname{Im}_{\mathbb{H}}(\bar{\tau} \sigma_I) &= \frac{\operatorname{Im}_{\mathbb{H}}(\bar{w}_R v_I + \bar{v}_R w_I)}{2} \equiv \frac{\Upsilon}{2} \\
\operatorname{Im}_{\mathbb{H}}(\bar{\tau} \sigma_R) &= \frac{\operatorname{Im}_{\mathbb{H}}(\bar{w}_R v_R + \bar{w}_I v_I)}{2} \equiv \frac{\Lambda}{2}
\end{aligned} \tag{5.3.13}$$

Note that these are complex equations for the *commutative* ADHM solutions, not the noncommutative ones. In the noncommutative case, only one of these equations changes – the second one, which becomes

$$\operatorname{Im}_{\mathbb{H}}(\bar{w}_R w_I) + \operatorname{Im}_{\mathbb{H}}(\bar{v}_R v_I) = -4\zeta\sigma_3 \tag{5.3.14}$$

As a check, if we assume that our solutions to the ADHM equations are entirely real, we have the complex imaginary parts of all our variables being 0, and we have only the one equation which is not trivially satisfied (just as in [1])

$$\operatorname{Im}_{\mathbb{H}}(\bar{\tau} \sigma_R) = \frac{\operatorname{Im}_{\mathbb{H}}(\bar{w}_R v_R)}{2} \tag{5.3.15}$$

It should be noted, as discussed in section 3.3.2, that no new degrees of freedom are introduced compared to the real ADHM equations. Complexifying  $v, w$  and  $\sigma$  adds twelve degrees of freedom. However, each of the 3 new equations affecting the imaginary part of an expression adds 3 constraints, giving 9. Recall that we have a residual  $O(2)$  symmetry on our solutions to the ADHM equation in the quaternion case, which is promoted to a  $U(2)$  symmetry in the biquaternion case allows us to remove a further three degrees of freedom. This gives a total of 12 degrees of freedom removed, cancelling the number of new parameters and showing that there are no new solutions.

### 5.3.1 Finding biquaternion solutions

That being said, any quaternion solution should be able to be turned into a biquaternion solution by a different choice of the  $U(2)$  symmetry, implemented by an



$SU(2)$  rotation as in equation (3.3.34) with  $R \in SU(2)$ . The rotation is  $SU(2)$  rather than  $U(2)$  as the standard solutions in the real case have already have  $O(2)$  ( $= U(1)$ ) fixed. That is what I shall proceed to show explicitly. I begin by giving a general form of the transformation under  $R$ . I then show how a particular solution to the biquaternion equations can be rotated to a pure quaternion form, exactly corresponding with [1].

The reason this is worth doing is that the non-commutative ADHM equations only have complex solutions, and having the commutative solutions in a complex form might make it easier to spot a generalisation, or to construct a solution via deformation.

We start with the standard real solution to the commutative ADHM equations [1], where  $\Delta$  is put in the canonical form,  $a + bx$ , with  $b$  as in equation (3.3.2) and

$$a = \begin{bmatrix} \mathbf{v} \\ \Omega_{2 \times 2} \end{bmatrix} = \begin{bmatrix} v & w \\ \tau & \frac{\tau\Lambda}{4|\tau|^2} \\ \frac{\tau\Lambda}{4|\tau|^2} & -\tau \end{bmatrix} \quad (5.3.16)$$

where the entries are all quaternions. To get the form of the complex solutions we undo our specification of the real line by rotating with an arbitrary element so  $SU(2)$ , given by either

$$\begin{bmatrix} a & b \\ -\bar{b} & \bar{a} \end{bmatrix}, \quad a, b \in \mathbb{C}; |a|^2 + |b|^2 = 1 \quad (5.3.17)$$

or

$$\begin{bmatrix} y_0 + iy_3 & y_1 + iy_2 \\ -y_1 + iy_2 & y_0 - iy_3 \end{bmatrix}, \quad y_i \in \mathbb{R}; \sum y_i^2 = 1 \quad (5.3.18)$$

The first of these is easier to work with, as there are less symbols, however the second seems to me more illuminating since we are thinking of the (complex) quaternions as modules over  $\mathbb{R}$  rather than  $\mathbb{C}$ . I will therefore give the general solution in terms of both parametrisations of  $SU(2)$ . Applying

$$\Delta \mapsto \begin{bmatrix} 1 & \vec{0} \\ \vec{0} & R^T \end{bmatrix} \cdot \Delta \cdot R, \quad f \mapsto R^T \cdot f \cdot R, \quad U \mapsto RU$$

with  $R$  as given above, we find the general complex solution is given by

$$\begin{bmatrix} av - \bar{b}w & bv + \bar{a}w \\ \left( |a|^2 - |b|^2 - (ab + \bar{a}\bar{b}) \frac{\Lambda}{|\tau|^2} \right) \tau & 2\bar{a}b\tau + (\bar{a}^2 - b^2) \frac{\tau\Lambda}{|\tau|^2} \\ 2\bar{b}a\tau + (a^2 - \bar{b}^2) \frac{\tau\Lambda}{|\tau|^2} & - \left( |a|^2 - |b|^2 - (ab + \bar{a}\bar{b}) \frac{\Lambda}{|\tau|^2} \right) \tau \end{bmatrix} \quad (5.3.19)$$

We can see that this has the correct form

$$\begin{bmatrix} v' & w' \\ \tau' & \sigma'^* \\ \sigma' & -\tau \end{bmatrix} \quad (5.3.20)$$

which we would expect for a complex solution to the ADHM equations. Using the real representation for  $SU(2)$  the solutions cannot be usefully put into matrix form as they are too long, but are given by

$$\begin{aligned} \mathbf{v}' &= \left[ (y_0 + iy_3)v - (y_1 - iy_2)w \quad (y_1 + iy_2)v + (y_0 - iy_3)w \right] \\ \tau' &= \left( (y_0^2 + y_3^2 - y_1^2 - y_2^2) + 2(y_2y_3 - y_0y_1) \frac{\Lambda}{|\tau|^2} \right) \tau \\ \sigma' &= \left( 2(y_0y_1 + y_3y_2 - i(y_0y_2 - y_3y_1)) + (y_0^2 + y_2^2 - y_1^2 - y_3^2 + 2i(y_0y_3 + y_1y_2)) \frac{\tau\Lambda}{|\tau|^2} \right) \tau \end{aligned}$$

### 5.3.2 Using the Symmetries

The above expressions are not particularly illuminating, not least because they are in terms of the old parameters, not the new ones. Ideally, we want  $\sigma'$  in terms of  $\sigma$ . However I was unable to use the above expressions to do this. I next tried directly solving the equations (5.3.13). Again, I could not find a full solution. Solving the last two equations we get

$$\sigma_R = \frac{\tau}{|\tau|^2} \left( \alpha + \frac{\Lambda}{2} \right) \quad (5.3.21)$$

and

$$\sigma_I = \frac{\tau}{|\tau|^2} \left( \gamma + \frac{\Upsilon}{2} \right) \quad (5.3.22)$$

For arbitrary real functions  $\alpha$  and  $\gamma$ . We can then use the second equation to get

$$\bar{w}_R w_I = \beta + \bar{v}_R v_I \quad (5.3.23)$$

which can then be used to define

$$w_I = \frac{\beta w_R + w_R \bar{v}_R v_I}{|w_R|^2} \quad (5.3.24)$$

For some arbitrary real function  $\beta$ . However trying to use these to solve the first equation has not met with success thus far, and therefore we adopt the method of finding the infinitesimal forms of the transformation, and using these to show we can set the functions  $\alpha$  and  $\gamma$  to be zero. We will then use an expansion in  $\frac{1}{|\tau|^2}$  to solve the remaining equations, before using the remaining 2 degrees of freedom to arrive back at the real solution we are familiar with. This ensures the consistency of our equations with the existing real ADHM equations, and enables us to extend the solutions of those real commutative equation to the complex noncommutative case. To start with, we consider the infinitesimal form of our transformation (3.3.2). To do this, we first note that  $R \in SU(2)$  can be written as  $\exp(\mathfrak{r}t)$ ,  $\mathfrak{r} \in \mathfrak{su}(2)$ , and similarly for  $\mathfrak{u}(1)$ . We write an element of  $\mathfrak{u}(1)$  as a phase  $i\theta$ , and an element of  $\mathfrak{su}(2)$  as

$$\begin{bmatrix} ai & b + ci \\ -b + ci & -ia \end{bmatrix} \quad (5.3.25)$$

Then the transformation, to linear order is given by

$$\Delta \mapsto \begin{bmatrix} 1 - i\theta & \vec{0} \\ \vec{0} & \mathbb{1} + \mathfrak{r}^\dagger \end{bmatrix} \cdot \begin{bmatrix} \mathbf{v} \\ \Omega \end{bmatrix} \cdot (\mathbb{1} + \mathfrak{r}) \quad (5.3.26)$$

Then to linear order

$$\delta \vec{v} = -i\theta \vec{v} + \vec{v} \mathfrak{r} \quad (5.3.27)$$

and

$$\delta \Omega = \mathfrak{r}^\dagger \Omega + \Omega \mathfrak{r} \quad (5.3.28)$$

First of all, we look at  $\delta \vec{v}$ . Expanding into components, we find that this is equal to

$$\left[ i(a - \theta)v + w(-b + ci) \quad (b + ci)v - i(a + \theta)w \right] \quad (5.3.29)$$

We now write  $v = v_R + iv_I$ , and the same for  $w$ , and group the (complex) real and imaginary parts to get (separately now for  $v$  and  $w$ )

$$\left( (\theta - a)v_I - bw_R - cw_I \right) + i \left( (a - \theta)v_R - bw_I + cw_R \right) \equiv \delta v_R + i\delta v_I \quad (5.3.30)$$

and

$$\left( w_I(a + \theta) + bv_R - cv_I \right) + i \left( -(a + \theta)w_R + bw_I + cv_R \right) \equiv \delta w_R + i\delta w_I \quad (5.3.31)$$

Now we look at  $\delta\Omega$ . Componentwise, this turns out as

$$\begin{bmatrix} -b(\sigma + \sigma^*) + ic(\sigma^* - \sigma) & -2ia\sigma^* + 2\tau(b + ci) \\ 2ia\sigma + 2\tau(b - ci) & b(\sigma + \sigma^*) - ic(\sigma^* - \sigma) \end{bmatrix} \quad (5.3.32)$$

As a consistency check we can note that this matrix has the form

$$\begin{bmatrix} \tau' & (\sigma')^* \\ \sigma' & -\tau' \end{bmatrix} \quad (5.3.33)$$

Using  $\sigma = \sigma_R + i\sigma_I$ , we can immediately read off that

$$\delta\tau = -2b\sigma_R + 2c\sigma_I \quad (5.3.34)$$

Note that this is a real quaternion, as expected. As for  $\delta\sigma$ , expanding and collecting (complex) real and imaginary parts, we get

$$2 \left( b\tau - a\sigma_I \right) + 2i \left( a\sigma_R - c\tau \right) \equiv \delta\sigma_R + i\delta\sigma_I \quad (5.3.35)$$

We want to show that we can always make the symmetry choice  $\alpha = \gamma = 0$ . Therefore we want expressions for  $\delta\alpha$  and  $\delta\gamma$ , as these are the quantities we want to set to zero. We can combine finding them with a check of consistency. Looking first at  $\delta\alpha$ , if we

write

$$\sigma_R = \frac{\tau}{|\tau|^2} \left( \alpha + \frac{\Lambda}{2} \right) \quad (5.3.36)$$

Then we get

$$\delta(\bar{\tau}\sigma_R) = \delta\alpha + \frac{\delta\Lambda}{2} \quad (5.3.37)$$

We can then compare this to  $\delta(\bar{\tau}\sigma_R)$  calculated directly from  $\delta\Omega$  as

$$(\delta\bar{\tau})\sigma_R + \bar{\tau}\delta\sigma_R \quad (5.3.38)$$

There is one unknown between the two equations,  $\delta\alpha$ , and by comparing the two we can determine what this is (in fact, as  $\Lambda$  is imaginary quaternionic, the real part of equation will be  $\delta\alpha$ ). The consistency check comes in comparing  $2\text{Im}_{\mathbb{H}}(\delta(\bar{\tau}\sigma_R))$  to  $\delta\Lambda$ , as these should be identical. That is what we will now proceed to do. We start with

$$\delta\Lambda = \text{Im}_{\mathbb{H}}\left((\delta\bar{w}_R)v_R + \bar{w}_R\delta v_R + (\delta\bar{w}_I)v_I + \bar{w}_I(\delta v_I)\right) \quad (5.3.39)$$

Looking at each individual part we find

$$\begin{aligned} (\delta\bar{w}_R)v_R &= (a + \theta)\bar{w}_I v_R + b|v_R|^2 - c\bar{v}_I v_R \\ \bar{w}_R\delta v_R &= (\theta - a)\bar{w}_R v_I - b|w_R|^2 - c\bar{w}_R w_I \\ (\delta w_I)v_I &= -(a + \theta)\bar{w}_R v_I + b|v_I|^2 + c\bar{v}_R v_I \\ \bar{w}_I\delta v_I &= (a - \theta)\bar{w}_I v_R - b|w_I|^2 + c\bar{w}_I w_R \end{aligned} \quad (5.3.40)$$

Putting this all together we get

$$\delta\Lambda = 2a\text{Im}_{\mathbb{H}}(\bar{w}_I v_R - \bar{w}_R v_I) + 2c\text{Im}_{\mathbb{H}}(\bar{v}_R v_I - \bar{w}_R w_I) \quad (5.3.41)$$

Note that the terms depending on  $\theta$ , which only acts on  $\mathbf{v}$  and not  $\Omega$ , cancel. This is a good sign that the two forms might be consistent. Using the equations in (5.3.13), we can rewrite this as

$$\delta\Lambda = -2a\Upsilon + 4c\text{Im}_{\mathbb{H}}(\bar{v}_R v_I) \quad (5.3.42)$$

Now we compare this to  $\delta(\bar{\tau}\sigma_R)$  calculated directly. We find

$$\delta\bar{\tau}\sigma_R = 2b(|\tau|^2 - |\sigma_R|^2) - 2a\bar{\tau}\sigma_I + 2c\bar{\sigma}_I\sigma_R \quad (5.3.43)$$

and the part we are interested in for the comparison

$$\text{Im}_{\mathbb{H}}(\delta\bar{\tau}\sigma_R) = -2c\text{Im}_{\mathbb{H}}(\bar{\sigma}_R\sigma_I) - 2a\text{Im}_{\mathbb{H}}(\bar{\tau}\sigma_I) \quad (5.3.44)$$

Now, note that by the constraints (5.3.13),  $\text{Im}_{\mathbb{H}}(\bar{\tau}\sigma_I) = \frac{\Upsilon}{2}$  and  $\text{Im}_{\mathbb{H}}(\bar{\sigma}_R\sigma_I) = -\text{Im}_{\mathbb{H}}(\bar{v}_R v_I)$ . Therefore

$$2\text{Im}_{\mathbb{H}}(\delta\bar{\tau}\sigma_R) = -2a\Upsilon + 4c\text{Im}_{\mathbb{H}}(\bar{v}_R v_I) \quad (5.3.45)$$

in perfect agreement with the result for  $\delta\Lambda$  in (5.3.42). Therefore this part of the transformation is consistent, and we can define

$$\delta\alpha \equiv \text{Im}_{\mathbb{H}}(\delta\bar{\tau}\sigma_R) = 2b(|\tau|^2 - |\sigma_R|^2) - 2a\gamma - 2c\text{Re}_{\mathbb{H}}(\bar{\sigma}_R\sigma_I) \quad (5.3.46)$$

where I have used the fact that  $\text{Re}_{\mathbb{H}}(\bar{\tau}\sigma_I) = \gamma$ . The next stage is to derive a similar result for  $\delta\gamma$ . This is, in fact, not too hard. In a similar way we calculate

$$\delta\Upsilon = 2a\Lambda + 4b\text{Im}_{\mathbb{H}}(\bar{v}_R v_I) \quad (5.3.47)$$

and

$$\delta(\bar{\tau}\sigma_I) = 2c(|\sigma_I|^2 - |\tau|^2) + 2a\alpha + a\Lambda - 2b\bar{\sigma}_R\sigma_I \quad (5.3.48)$$

Again using  $\text{Im}_{\mathbb{H}}(\bar{\sigma}_R\sigma_I) = -\text{Im}_{\mathbb{H}}(\bar{v}_R v_I)$  we can see that the imaginary parts of these equations are consistent, and so we can define

$$\delta\gamma = 2c(|\sigma_I|^2 - |\tau|^2) + 2a\alpha - 2b\text{Re}_{\mathbb{H}}(\bar{\sigma}_R\sigma_I) \quad (5.3.49)$$

The final check at this stage is to make sure that  $\delta\alpha$  and  $\delta\gamma$  are linearly independent, so that we can set both  $\gamma$  and  $\alpha$  simultaneously to zero. Considering the combination  $A\delta\alpha + B\delta\gamma$  and finding the coefficients of  $a$ ,  $b$  and  $c$ , we find that the only way the

combination can be zero is if we have everywhere that

$$\frac{\gamma}{\alpha}|\sigma_I|^2 = \frac{\alpha}{\gamma}|\sigma_R|^2 - |\tau|^2\left(\frac{\gamma}{\alpha} + \frac{\alpha}{\gamma}\right) = 0 \quad (5.3.50)$$

But  $\sigma_R$  and  $\sigma_I$  depend on  $v$  and  $w$ , and  $\tau$  is independent from them. Hence this expression cannot be identically zero and so the variations are linearly independent. Alternative, looking at the expression for  $\delta\alpha$ , (5.3.46), we see that we can tune it using  $a$  in order to set  $\alpha$  to be zero. Then we have ,‘used up’ the variable  $a$ , so it does not contribute to the variation of  $\gamma$ . Instead we can use one of  $b$  or  $c$  to tune  $\gamma$  to be zero too.

Therefore we can set  $\delta\alpha$  and  $\delta\gamma$  to be anything we want, using the parameters  $b$  and  $c$ . In particular we can set  $\alpha$  and  $\gamma$  themselves to zero using successive transformations. For completeness we list all the useful transformations here

$$\begin{aligned} \delta v_R &= (\theta - a)v_I - bw_R - cv_I \\ \delta v_I &= (a - \theta)v_R - bw_I + cw_R \\ \delta w_R &= w_I(a + \theta) + bv_R - cv_I \\ \delta w_I &= -(a + \theta)w_R + bv_I + cv_R \\ \delta\tau &= -2(b\sigma_R + c\sigma_I) \\ \delta\alpha &= 2b(|\tau|^2 - |\sigma_R|^2) - 2a\gamma - 2c\text{Re}(\bar{\sigma}_R\sigma_I) \\ \delta\Lambda &= -2a\Upsilon + 4c\text{Im}(\bar{v}_Rv_I) \\ \delta\gamma &= 2c(|\sigma_I|^2 - |\tau|^2) + 2a\alpha - 2b\text{Re}(\bar{\sigma}_R\sigma_I) \\ \delta\Upsilon &= 2a\Lambda + 4b\text{Im}(\bar{v}_Rv_I) \end{aligned} \quad (5.3.51)$$

We now attempt to solve the second of equations (5.3.13) using an expansion in  $\frac{1}{|\tau|^2}$ . We do this because if we expand the left hand side in terms of our solutions for  $\sigma_R$  and  $\sigma_I$  we get

$$\text{Im}_{\mathbb{H}}(\bar{\sigma}_R\sigma_I) = \text{Im}_{\mathbb{H}}\left(-\frac{\Lambda\Upsilon}{|\tau|^2} + \frac{1}{2|\tau|^2}(\alpha\Upsilon - \gamma\Lambda)\right) = \text{Im}_{\mathbb{H}}(\bar{v}_Rv_I) \quad (5.3.52)$$

The right hand side must also depend on  $\frac{1}{|\tau|^2}$  and so we expand

$$v_I = A_0 v_R + \sum_{i=1}^{\infty} \frac{\hat{A}_i}{|\tau|^{2i}} \quad (5.3.53)$$

where the  $\hat{A}_i$  are quaternions, but  $A_0$  is a real function. Note that the  $A_0$  term does not depend on  $|\tau|^2$ , however this does not matter since  $\text{Im}(\bar{v}_R A_0 v_R) = 0$  and so it does not appear explicitly in the RHS of the equation. The fact that the LHS is one power of  $\frac{1}{|\tau|^2}$  higher than the RHS does mean that we can try and solve the equation iteratively, as when we match the terms in  $\frac{1}{|\tau|^{2i}}$  we find that the LHS depends on  $\frac{1}{|\tau|^{2(i-1)}}$  whenever the RHS depends on  $\frac{1}{|\tau|^{2i}}$ . First of all, we substitute  $v_I = A v_R$  into the LHS to find  $\text{Im}_{\mathbb{H}}(\bar{v}_R \hat{A}_1)$ .

A somewhat long and not very illuminating calculation tells us in this case  $\text{Im}_{\mathbb{H}}(\Lambda \Upsilon) = 0$ . Then we have  $\text{Im}_{\mathbb{H}}(\alpha \Upsilon - \gamma \Lambda) = -2 \text{Im}_{\mathbb{H}}(\bar{v}_R \hat{A}_i)$ . Expanding using the definitions of  $\Lambda$  and  $\Upsilon$ , and equation (5.3.24), we get that

$$\hat{A}_i = (\alpha(A_0 - K) - \gamma(1 + K A_0)) w_R \equiv m w_R; \quad K = \frac{\beta + A_0 |v_R|^2}{|w_R|^2} \quad (5.3.54)$$

Repeating the process by plugging  $\hat{A}_1 = m w_R$  into the LHS, we find that again  $\text{Im}_{\mathbb{H}}(\Lambda \Upsilon) = 0$ . But this time, there is not such a simple form for  $\hat{A}_2$ :

$$\hat{A}_2 = (m - 1) \gamma w_R - \alpha m \bar{w}_R v_R \bar{w}_R \quad (5.3.55)$$

I decided that continuing the series expansion would not be particularly illuminating. Instead notice that if  $\alpha$  and  $\gamma$  are zero, then we have

$$\text{Im}_{\mathbb{H}}(\bar{v}_R \hat{A}_1) = 0 \implies \hat{A}_1 = A_1 v_R \quad (5.3.56)$$

Where  $A_1$  is again a real function. But by iteration, this tells us that  $\hat{A}_i = A_i v_R$ ,  $\forall i \in \mathbb{Z}$  and therefore

$$v_I = v_R \sum_{i=0}^{\infty} \frac{A_i}{|\tau|^{2i}} \equiv A v_R \quad (5.3.57)$$

where we are assuming that the sum converges to a real function  $A$ . So

$$v = v_R(1 + iA) \quad (5.3.58)$$



Using (5.3.24), we find also that

$$w = w_R(1 + iB), B = \frac{\beta - A|v_R|^2}{|w_R|^2} \quad (5.3.59)$$

Now the goal is to use the remaining parameters  $a$  and  $\theta$  to set  $A$  and  $B$  to zero, whilst keeping  $\alpha$  and  $\gamma$  zero. If this is the case, we will have recovered the solution to the real AHDM equations in [1] as a solution to the complex equations when the  $U(2)$  symmetry is modded out, as expected. To see if this is possible, first we write the intermediate solution:

$$\begin{aligned} v &= v_R(1 + iA) \\ w &= w_R(1 + iB) \\ \tau &= \tau \\ \sigma_R &= \frac{\tau\Lambda}{|\tau|^2}, \quad \Lambda = (1 + AB) \operatorname{Im}_{\mathbb{H}}(\bar{w}_R v_R) \\ \sigma_I &= \frac{\tau\Upsilon}{|\tau|^2}, \quad \Upsilon = (A - B) \operatorname{Im}_{\mathbb{H}}(\bar{w}_R v_R) \end{aligned} \quad (5.3.60)$$

We also give the relevant transformations

$$\begin{aligned} \delta v_R &= A(\theta - a)v_R - (b + cB)w_R \\ \delta(Av_R) &= (a - \theta)v_R - (bB - c)w_R \\ \delta w_R &= w_R B(a + \theta) + (b - cA)v_R \\ \delta(Bw_R) &= -(a + \theta)w_R + (Ab + c)v_R \\ \delta\tau &= -2(b\sigma_R + c\sigma_I) \\ \delta\alpha &= 2b(|\tau|^2 - |\sigma_R|^2) - 2Ac\operatorname{Re}(\bar{\sigma}_R\sigma_I) \\ \delta\Lambda &= -2a\Upsilon \\ \delta\gamma &= 2c(|\sigma_I|^2 - |\tau|^2) - 2bA\operatorname{Re}(\bar{\sigma}_R\sigma_I) \\ \delta\Upsilon &= 2a\Lambda \end{aligned} \quad (5.3.61)$$

Where we can simply insert our solutions into the transformation formulae as we showed above that the transformations were consistent with our constraint equations.

At first sight there seems to be an issue with consistency, as

$$\delta A = \frac{\bar{v}_R}{|v_R|} (\delta(Av_R) - A\delta v_R) \quad (5.3.62)$$

This gives

$$\delta A = (a - \theta)(1 + A^2) + \bar{v}_R w_R (b(B - A) - c(1 + AB)) \quad (5.3.63)$$

The problem is that  $A$  is a real function, and therefore  $\delta A$  should be real. But here  $\delta A$  is a quaternion. In fact, we have

$$\text{Im}_{\mathbb{H}}(\delta A) = b\Upsilon + c\Lambda \quad (5.3.64)$$

The solution to this difficulty is that the validity of this intermediate solution depends on  $\alpha$  and  $\gamma$  remaining zero. However we can only make their variations vanish everywhere by setting  $b$  and  $c$  equal to zero. This follows from the linear independence of  $\delta\alpha$  and  $\delta\gamma$ . Then we have

$$\delta A = (a - \theta)(1 + A^2) \quad (5.3.65)$$

which is real, as required. If  $b$  and  $c$  are zero, the remaining transformations become

$$\begin{aligned} \delta v_R &= A(\theta - a)v_R \\ \delta(Av_R) &= (a - \theta)v_R \\ \delta w_R &= w_R B(a + \theta) \\ \delta(Bw_R) &= -(a + \theta)w_R \\ \delta\tau &= 0 \\ \delta\alpha &= 0 \\ \delta\Lambda &= -2a\Upsilon \\ \delta\gamma &= -0 \\ \delta\Upsilon &= 2a\Lambda \end{aligned} \quad (5.3.66)$$

Then we can also see that

$$\delta B = \frac{\bar{w}_R(\delta(Bw_R) - B\delta w_R)}{|w_R|^2} = (a + \theta)(1 + B^2) \quad (5.3.67)$$

There are two more consistency checks we must perform. First of all, are  $\delta A$  and  $\delta\gamma$  independent? Second, is  $\delta B$  to linear order the same as we'd get by varying the definition of  $B$  in equation (5.3.59)? It is not too difficult to see the first of these is true – one simply multiplies out the expression  $C\delta A + D\delta B$  and looks at the coefficients of  $a$  and  $\theta$ . The second condition is also guaranteed because we can simply define

$$\delta\beta \equiv \delta(|w_R|^2 B) + \delta(A|v_R|^2) = B\delta|w_R|^2 + (\delta B)|w_R|^2 + A\delta|v_R|^2 + (\delta A)|v_R|^2 \quad (5.3.68)$$

The only thing we require of  $\delta\beta$  is that it be real, but this is guaranteed as all the quantities on the RHS, and hence their variations, are real. Therefore we can use the two parameters  $a$  and  $\theta$  to set  $A$  and  $B$  equal to zero. This gives us the solution

$$v, w, \tau, \sigma = \frac{\tau\Lambda}{|\tau|^2}; \Lambda = \text{Im}_{\mathbb{H}}(\bar{w}v) \quad (5.3.69)$$

This is the same as the solution in [1]. We now move on to trying to solve the noncommutative equations.

## 5.4 The Noncommutative solution

In this section I explore the solution to the noncommutative deformation of the above ADHM equations. The first step is to review the solution suggested in [37]. I show that this solution is incorrect, and outline several strategies I used to try and find a full solution. I was unable to find such a full solution, however I was able to find a solution on a subspace of the full moduli space. Once I have this partial solution, I use it to calculate the metric and potential for this subspace of the moduli space, as well as the scalar field.

To begin with , consider the noncommutative ADHM equations. As stated above,

they are very similar to the commutative ones and are given by

$$\begin{aligned}
2\mathrm{Im}_{\mathbb{H}}(\bar{\sigma}_R\sigma_I) - \mathrm{Im}_{\mathbb{H}}(\bar{w}_R w_I)\mathrm{Im}_{\mathbb{H}}(\bar{v}_R v_I) &= 0 \\
\mathrm{Im}_{\mathbb{H}}(\bar{w}_R w_I) + \mathrm{Im}_{\mathbb{H}}(\bar{v}_R v_I) &= -4\zeta\sigma_3 \\
\mathrm{Im}_{\mathbb{H}}(\bar{\tau}\sigma_I) &= \frac{\mathrm{Im}_{\mathbb{H}}(\bar{w}_R v_I + \bar{v}_R w_I)}{2} \equiv \frac{\Upsilon}{2} \\
\mathrm{Im}_{\mathbb{H}}(\bar{\tau}\sigma_R) &= \frac{\mathrm{Im}_{\mathbb{H}}(\bar{w}_R v_R + \bar{w}_I v_I)}{2} \equiv \frac{\Lambda}{2}
\end{aligned} \tag{5.4.1}$$

Where the second equation is the one which has changed, and  $\sigma_3$  is the quaternion basis element

$$\begin{bmatrix} i & 0 \\ 0 & -i \end{bmatrix} \tag{5.4.2}$$

We can try to solve this using the same method we used for the complex commutative equations. The initial steps are the same. We can solve the third and fourth equations as

$$\sigma_R = \frac{\tau}{|\tau|^2} \left( \alpha + \frac{\Lambda}{2} \right) \tag{5.4.3}$$

and

$$\sigma_I = \frac{\tau}{|\tau|^2} \left( \gamma + \frac{\Upsilon}{2} \right) \tag{5.4.4}$$

just as before. We can use the second equation to deduce that

$$\bar{w}_R w_I = \beta - \bar{v}_R v_I - 4i\zeta\sigma_3 \tag{5.4.5}$$

and so

$$w_I = \frac{w_R\beta - w_R\bar{v}_R v_I - 4i\zeta w_R\sigma_3}{|w_R|^2} \tag{5.4.6}$$

Getting any further than this, however, is rather non trivial.

### 5.4.1 Checking the previous solution

A good starting point is checking the solution given in [37]. There the solution for the biquaternionic noncommutative parameters  $w'$  &  $v'$  is given in terms of the

quaternions  $w$  and  $v$  as

$$w' = \frac{w}{|w|} \begin{bmatrix} \sqrt{|w|^2 + \alpha\zeta} & 0 \\ 0 & \sqrt{|w|^2 - \alpha\zeta} \end{bmatrix} \quad (5.4.7)$$

and the obvious equivalent for  $v'$  in terms of  $v$ . In the notation we've been using this is

$$\begin{aligned} v' &= v(A + iC\sigma_3) \\ w' &= w(B + iD\sigma_3) \end{aligned} \quad (5.4.8)$$

where

$$\begin{aligned} A &= \frac{\sqrt{|v|^2 - \alpha\zeta} + \sqrt{|v|^2 + \alpha\zeta}}{2|v|} \\ C &= \frac{\sqrt{|v|^2 - \alpha\zeta} - \sqrt{|v|^2 + \alpha\zeta}}{2|v|} \\ B &= \frac{\sqrt{|w|^2 - \alpha\zeta} + \sqrt{|w|^2 + \alpha\zeta}}{2|w|} \\ D &= \frac{\sqrt{|w|^2 - \alpha\zeta} - \sqrt{|w|^2 + \alpha\zeta}}{2|w|} \end{aligned} \quad (5.4.9)$$

This gives

$$\begin{aligned} v'_R &= Av \\ v'_I &= Cv\sigma_3 \\ w'_R &= Bw \\ w'_I &= Dw\sigma_3 \end{aligned} \quad (5.4.10)$$

The claim in [37] is that propagating these definitions through  $\sigma$  solves the noncommutative ADHM equations. However I want to check if this is true, using the more rigorous method of splitting into complex real and imaginary parts defined above. First of all, we need to work out what  $\Lambda$  and  $\Upsilon$  are. We can solve equations 3 and 4 of (5.4.1) to get

$$\Lambda = \text{Im}_{\mathbb{H}}(w'_R v'_R + w'_I v'_I) = AB \text{Im}_{\mathbb{H}}(\bar{w}v) + CD \text{Im}_{\mathbb{H}}(\bar{\sigma}_3 \bar{w}v\sigma_3)$$

$$\Upsilon = \text{Im}_{\mathbb{H}}(\bar{w}'_R v'_I + \bar{v}'_R w'_I) = BC \text{Im}_{\mathbb{H}}(\bar{w}v\sigma_3) + AD \text{Im}_{\mathbb{H}}(\bar{v}w\sigma_3) \quad (5.4.11)$$

What about the other equations? First we look at the second one. Then

$$-4\zeta\sigma_3 = \text{Im}_{\mathbb{H}}(\bar{w}'_R w'_I) + \text{Im}_{\mathbb{H}}(\bar{v}'_R v'_I) = (BD|w|^2 + AC|v|^2)\sigma_3 \quad (5.4.12)$$

We can see that

$$BD|w|^2 = AC|v|^2 = -\frac{\alpha\zeta}{2} \quad (5.4.13)$$

and so we have

$$\alpha = 4 \quad (5.4.14)$$

Now for the final equation. Assuming that, as in [37], we have used the symmetries to set  $\sigma_R = \frac{\tau\Lambda}{2|\tau|^2}$  and  $\sigma_I = \frac{\tau\Upsilon}{2|\tau|^2}$ , this equation becomes

$$\text{Im}_{\mathbb{H}}(\bar{\sigma}_R \sigma_I) = -\frac{1}{4|\tau|^2} \text{Im}_{\mathbb{H}}(\Lambda\Upsilon) = \text{Im}_{\mathbb{H}}(\bar{v}'_R v'_I) - \text{Im}_{\mathbb{H}}(\bar{w}'_R w'_I) \quad (5.4.15)$$

But this left hand side is equal to

$$(AC|v|^2 - BD|w|^2)\sigma_3 = (-2\zeta + 2\zeta)\sigma_3 = 0 \quad (5.4.16)$$

So we are trying to solve

$$\text{Im}_{\mathbb{H}}(\Lambda\Upsilon) = 0 \quad (5.4.17)$$

Using (5.4.11), we can expand  $\Lambda\Upsilon$  as

$$\begin{aligned} & ACB^2 \text{Im}_{\mathbb{H}}(\bar{w}v) \text{Im}(\bar{w}v\sigma_3) \\ & + BDA^2 \text{Im}_{\mathbb{H}}(\bar{w}v) \text{Im}(\bar{v}w\sigma_3) \\ & + BDC^2 \text{Im}_{\mathbb{H}}(\bar{\sigma}_3 \bar{w}v\sigma_3) \text{Im}_{\mathbb{H}}(\bar{w}v\sigma_3) \\ & + ACD^2 \text{Im}_{\mathbb{H}}(\bar{\sigma}_3 \bar{v}w\sigma_3) \text{Im}_{\mathbb{H}}(\bar{v}w\sigma_3) \end{aligned} \quad (5.4.18)$$

For convenience of notation, we write this as

$$ACB^2 \mathbf{X} + BDA^2 \mathbf{Y} + BDC^2 \mathbf{W} + ACD^2 \mathbf{Z} \quad (5.4.19)$$

and look at each term, one at a time. In general, we'll use (5.4.13), as well as the facts that

$$\begin{aligned}
A^2 &= \frac{1}{2} + \frac{\sqrt{|v|^4 - \alpha^2 \zeta^2}}{2|v|^2} \\
C^2 &= \frac{1}{2} - \frac{\sqrt{|v|^4 - \alpha^2 \zeta^2}}{2|v|^2} \\
B^2 &= \frac{1}{2} + \frac{\sqrt{|w|^4 - \alpha^2 \zeta^2}}{2|w|^2} \\
D^2 &= \frac{1}{2} - \frac{\sqrt{|w|^4 - \alpha^2 \zeta^2}}{2|w|^2}
\end{aligned} \tag{5.4.20}$$

Then

$$\begin{aligned}
ACB^2 \mathbf{X} &= -\left(\frac{1}{2} + \frac{\sqrt{|w|^4 - \alpha^2 \zeta^2}}{2|w|^2}\right) \frac{\alpha \zeta}{2|v|^2} (\bar{w}v\bar{w}v\sigma_3 - |v|^2|w|^2\sigma_3 - \bar{w}v\bar{\sigma}_3\bar{v}w + \bar{v}w\bar{\sigma}_3\bar{v}w) \\
BDA^2 \mathbf{Y} &= -\left(\frac{1}{2} + \frac{\sqrt{|v|^4 - \alpha^2 \zeta^2}}{2|v|^2}\right) \frac{\alpha \zeta}{2|w|^2} (|w|^2|v|^2\sigma_3 - \bar{v}w\bar{v}w\sigma_3 - \bar{w}v\bar{\sigma}_3\bar{w}v + \bar{v}w\bar{\sigma}_3\bar{w}v) \\
BDC^2 \mathbf{W} &= -\left(\frac{1}{2} - \frac{\sqrt{|v|^4 - \alpha^2 \zeta^2}}{2|v|^2}\right) \frac{\alpha \zeta}{2|w|^2} (\bar{\sigma}_3\bar{w}v\sigma_3\bar{w}v\sigma_3 - \bar{\sigma}_3\bar{v}w\sigma_3\bar{w}v\sigma_3 - \bar{\sigma}_3|w|^2|v|^2 + \bar{\sigma}_3\bar{v}w\bar{v}w) \\
ACD^2 \mathbf{Z} &= -\left(\frac{1}{2} - \frac{\sqrt{|w|^4 - \alpha^2 \zeta^2}}{2|w|^2}\right) \frac{\alpha \zeta}{2|v|^2} (\bar{\sigma}_3\bar{w}v\sigma_3\bar{v}w\sigma_3 - \bar{\sigma}_3\bar{v}w\sigma_3\bar{v}w\sigma_3 - \bar{\sigma}_3\bar{w}v\bar{w}v + \bar{\sigma}_3|w|^2|v|^2)
\end{aligned} \tag{5.4.21}$$

We can group these terms as

$$-\frac{\alpha \zeta}{4|v|^2} (\mathbf{X} + \mathbf{Z}) - \frac{\alpha \zeta}{4|w|^2} (\mathbf{Y} + \mathbf{W}) + \frac{\alpha \zeta \sqrt{|w|^4 - \alpha^2 \zeta^2}}{4|w|^2|v|^2} (\mathbf{X} - \mathbf{Z}) - \frac{\alpha \zeta \sqrt{|v|^4 - \alpha^2 \zeta^2}}{4|w|^2|v|^2} (\mathbf{Y} - \mathbf{W}) \tag{5.4.22}$$

We can Taylor expand

$$\sqrt{|v|^4 - \alpha^2 \zeta^2} \approx |v|^2 + \frac{\alpha^2 \zeta^2}{|v|^2} + \dots \tag{5.4.23}$$

and similarly for  $\sqrt{|w|^4 - \alpha^2 \zeta^2}$ . Then

$$\bar{\sigma}_R \sigma_I \approx -\frac{\alpha \zeta}{2} \left( \frac{\mathbf{X}}{|v|^2} + \frac{\mathbf{Y}}{|w|^2} \right) - \frac{\alpha^3 \zeta^3}{4|v|^2|w|^2} \left( \frac{\mathbf{X} - \mathbf{Z}}{|w|^2} + \frac{\mathbf{Y} - \mathbf{W}}{|v|^2} \right) + \dots \tag{5.4.24}$$

Now, to show that the solution doesn't work, we need only show that the term linear in  $\zeta$  is non-zero, that is, we need to show that it cannot be the case that

$$\operatorname{Im}_{\mathbb{H}}\left(\frac{\mathbf{X}}{|v|^2} + \frac{\mathbf{Y}}{|w|^2}\right) = 0 \quad (5.4.25)$$

Now,

$$\frac{\mathbf{X}}{|v|^2} + \frac{\mathbf{Y}}{|w|^2} = \operatorname{Im}(\bar{w}v)\left(\operatorname{Im}\left(\frac{\bar{w}v\sigma_3}{|w|^2}\right) + \operatorname{Im}\left(\frac{\bar{v}w\sigma_3}{|v|^2}\right)\right) \quad (5.4.26)$$

Now, (5.4.25) being satisfied implies that either (5.4.26) is identically zero, or that it is always a real number. We look at the former case first. Since the quaternions are a field, there are no zero divisors, so (5.4.25) being satisfied implies either that

$$\operatorname{Im}_{\mathbb{H}}(\bar{w}v) \equiv 0 \quad (5.4.27)$$

or

$$\operatorname{Im}_{\mathbb{H}}\left(\frac{\bar{w}v\sigma_3}{|w|^2}\right) + \operatorname{Im}_{\mathbb{H}}\left(\frac{\bar{v}w\sigma_3}{|v|^2}\right) \equiv 0 \quad (5.4.28)$$

The first of these clearly cannot be true in general, so we look at the second. We can rewrite it as

$$\operatorname{Im}_{\mathbb{H}}\left(\left(\frac{\bar{w}v}{|w|^2} + \frac{\bar{v}w}{|v|^2}\right)\sigma_3\right) \quad (5.4.29)$$

The above expression can only vanish if  $\frac{\bar{w}v}{|w|^2} + \frac{\bar{v}w}{|v|^2} \propto \sigma_3$  which will not be true for general  $v$  and  $w$ . Therefore (5.4.26) cannot be identically zero.

We now have to check the case where (5.4.26) is real. This requires that

$$\frac{\bar{w}v}{|w|^2} + \frac{\bar{v}w}{|v|^2} \propto \bar{w}v\sigma_3 \quad (5.4.30)$$

so that

$$\operatorname{Im}\left(\left(\frac{\bar{w}v}{|w|^2} + \frac{\bar{v}w}{|v|^2}\right)\sigma_3\right) \propto \operatorname{Im}_{\mathbb{H}}(\bar{w}v) \quad (5.4.31)$$

and

$$\frac{\mathbf{X}}{|v|^2} + \frac{\mathbf{Y}}{|w|^2} \propto \operatorname{Im}_{\mathbb{H}}^2(\bar{w}v) \in \mathbb{R} \quad (5.4.32)$$

multiplying both sides of (5.4.30) by  $\bar{v}w$  and rearranging, we find this would imply that

$$\bar{v}w\bar{v}w = -|v|^4\mathbb{1} + \kappa|w|^2|v|^4\sigma_3 \quad (5.4.33)$$



For some real function  $\kappa$ . Again, this will not be true for arbitrary  $v$  and  $w$ . So we see that the solution given in [37] is not a solution to the noncommutative ADHM equations

### 5.4.2 The Noncommutative Case

If this is not the solution, then what is? I tried many methods, but was unable to find a solution for the full quaternion moduli space. However I was able to find a solution on a complex subspace, which I present here. This subspace comes from restricting the the quaternions to the subspace consisting of elements  $z \in \mathbb{C}$  written as  $x + y\sigma_3$ , for  $x, y \in \mathbb{R}$  and  $\sigma_3$  the usual Pauli matrix

$$\sigma_3 = \begin{bmatrix} i & 0 \\ 0 & -i \end{bmatrix} \quad (5.4.34)$$

Note that  $\sigma_3^2 = -\mathbf{1}_{\mathbb{H}}$ , and therefore  $\sigma_3$  can play the role of the imaginary unit. We start with the second ADHM equation, now for complex variables

$$\mathrm{Im}_{\mathbb{C}}(\bar{v}_R v_I) + \mathrm{Im}_{\mathbb{C}}(\bar{w}_R w_I) = -4\zeta\sigma_3 \quad (5.4.35)$$

Recall that we are using the notation  $\mathrm{Im}_{\mathbb{H}}$  to mean the imaginary quaternion part of an element of  $\mathbb{H}$ ; e.g. for  $q = q_0 + \mathbf{q} \in \mathbb{H}$ ,

$$\mathrm{Im}_{\mathbb{H}}(q) = \mathbf{q} \quad (5.4.36)$$

On the other hand,  $\mathrm{Im}_{\mathbb{C}}$  takes the imaginary component of an element of  $\mathbb{C}$ . If  $z \in \mathbb{C}$ ;  $z = a + ib$

$$\mathrm{Im}_{\mathbb{C}}(z) = b \quad (5.4.37)$$

With these definitions in mind, we can solve this for  $w_I$  and  $v_I$  in terms of the other variables by finding a particular solution, then by adding the null space, found by solving

$$\mathrm{Im}_{\mathbb{C}}(\bar{v}_R v_I) + \mathrm{Im}_{\mathbb{C}}(\bar{w}_R w_I) = 0 \quad (5.4.38)$$

It isn't too hard to see that a particular solution is given by

$$v_{Ip} = \frac{-2\zeta v_R \sigma_3}{|v_R|^2}; \quad w_{Ip} = \frac{-2\zeta w_R \sigma_3}{|w_R|^2} \quad (5.4.39)$$

We already know the solution to the null equation; it is

$$\tilde{v}_I = \frac{v_R}{|v_R|^2} \left( \beta - \bar{w}_R \tilde{w}_I \right) \quad (5.4.40)$$

For arbitrary real  $\beta$  and arbitrary quaternion  $\tilde{w}_I$ . Therefore we have the general solution

$$\begin{aligned} v_I &= \frac{-2\zeta v_R \sigma_3}{|v_R|^2} + \frac{v_R}{|v_R|^2} \left( \beta - \bar{w}_R \tilde{w}_I \right) \\ w_I &= \frac{-2\zeta w_R \sigma_3}{|w_R|^2} + \tilde{w}_I \end{aligned} \quad (5.4.41)$$

To complete this general solution we need to solve for  $\tilde{w}_I$ . This is done by solving the first ADHM equation

$$\text{Im}_{\mathbb{C}}(\bar{\sigma}_R \sigma_I) = \text{Im}_{\mathbb{C}}(\bar{v}_R v_I) - \text{Im}_{\mathbb{C}}(\bar{w}_R w_I) \quad (5.4.42)$$

We can use two of the symmetries to set  $\text{Re}(\bar{\tau}\sigma) = 0$ , by analogy to [1]. This corresponds to removing any component proportional to  $\tau$  from  $\sigma$ . If we do this, then the equation becomes

$$-\frac{\text{Im}_{\mathbb{C}}(\Lambda\Upsilon)}{|\tau|^2} = \text{Im}_{\mathbb{C}}(\bar{v}_R v_I) - \text{Im}_{\mathbb{C}}(\bar{w}_R w_I) \quad (5.4.43)$$

In general I have been unable to find a solution, however if we restrict to the complex plane spanned by  $\mathbb{1}$  and  $\sigma_3$  the LHS becomes zero, since  $\Lambda$  and  $\Upsilon$  are both proportional to  $\sigma_3$ , and hence their product is real and  $\text{Im}_{\mathbb{C}}(\Lambda\Upsilon) = 0$ . Putting the solutions in (5.4.41) into the RHS we get

$$\text{Im}_{\mathbb{C}}(\bar{w}_R \tilde{w}_I) = 0 \quad (5.4.44)$$

This leads to the solution

$$v_I = \frac{-2\zeta v_R \sigma_3}{|v_R|^2} + B v_R \quad (5.4.45)$$

$$w_I = \frac{-2\zeta w_R \sigma_3}{|w_R|^2} + A w_R$$

Following the discussion in section 5.3.2, we can use the remaining two symmetries to set  $A$  and  $B$  above to zero, we get the full solution for the complex subspace

$$\begin{aligned} v_I &= \frac{-2\zeta v_R \sigma_3}{|v_R|^2} \\ w_I &= \frac{-2\zeta w_R \sigma_3}{|w_R|^2} \\ \sigma_R &= \frac{\tau \operatorname{Im}(\bar{w}_R v_R + \bar{w}_I v_I)}{2|\tau|^2} = \frac{(|v_R|^2 |w_R|^2 + 4\zeta^2)}{2|\tau|^2 |v_R|^2 |w_R|^2} \tau \operatorname{Im}_{\mathbb{C}}(\bar{w}_R v_R) \sigma_3 \\ \sigma_I &= \frac{\tau \operatorname{Im}_{\mathbb{C}}(\bar{w}_R v_I + \bar{v}_R w_I)}{2|\tau|^2} = -\frac{\zeta(|w_R|^2 + |v_R|^2)}{|\tau|^2 |v_R|^2 |w_R|^2} \tau \operatorname{Im}_{\mathbb{C}}(\bar{w}_R v_R \sigma_3) \sigma_3 \end{aligned} \quad (5.4.46)$$

We can check our assumption about the symmetries by checking both that our solution really does solve the ADHM equations, and that there are no residual symmetries remaining. By this I mean that there should be no symmetry transformations of the solution which also solve the ADHM equations, since this would imply that there were degrees of freedom which our solution had not accounted for. It is straightforward to check the first part. To show there are no residual symmetries remaining, we consider a general linear order  $U(2)$  transformation, as discussed earlier

$$\Delta \mapsto \begin{bmatrix} 1 & 0 \\ 0 & R^\dagger \end{bmatrix} \Delta R; \quad R = \begin{bmatrix} a & b \\ -\bar{b} & \bar{a} \end{bmatrix}; \quad a, b \in \mathbb{C}, \quad |a|^2 + |b|^2 = 1 \quad (5.4.47)$$

This generates the transformation

$$\begin{bmatrix} v & w \\ \tau & \sigma^* \\ \sigma & -\tau \end{bmatrix} \mapsto \begin{bmatrix} av - \bar{b}w & bv + \bar{a}w \\ (|a|^2 - |b|^2)\tau - ab\sigma - \bar{a}\bar{b}\sigma^* & 2\bar{a}b\tau - b^2\sigma + \bar{a}^2\sigma^* \\ 2a\bar{b}\tau + a^2\sigma - \bar{b}^2\sigma^* & -(|a|^2 - |b|^2)\tau + ab\sigma + \bar{a}\bar{b}\sigma^* \end{bmatrix} \quad (5.4.48)$$

Now, to preserve the symmetry we require two things. First, we require that  $\operatorname{Re}_{\mathbb{C}}(\bar{\tau}\sigma) = 0$  has no component proportional to  $\tau$ . We also require that  $\bar{w}_R w_I = \bar{v}_R v_I$ . The first of these conditions requires that

$$\begin{aligned} (|a|^2 - |b|^2)a\bar{b} &= 0 \\ a^3b - \bar{a}\bar{b}^3 &= 0 \end{aligned} \quad (5.4.49)$$

If we write

$$\begin{aligned} a &= \cos\chi(\cos\theta + i\sin\theta) \\ b &= \sin\chi(\cos\phi + i\sin\phi) \end{aligned} \quad (5.4.50)$$

Then the first of the conditions in equation 5.4.49 gives the equation

$$\frac{1}{2} \cos(2\chi) \sin(2\chi) \left( \cos(\theta - \phi) + i \sin(\theta - \phi) \right) = 0 \quad (5.4.51)$$

This requires that  $\chi = \frac{n\pi}{4}$ . We can now look at the second equation of (5.4.49), which gives

$$\sin(\chi) \cos^3(\chi) \left( \cos(3\theta + \phi) + i \sin(3\theta + \phi) \right) - \sin^3(\chi) \cos(\chi) \left( \cos(\theta + 3\phi) + i \sin(\theta + 3\phi) \right) \quad (5.4.52)$$

When  $\chi = \frac{n\pi}{4}$  with  $n$  even then this will vanish automatically, however when  $n$  is odd we have

$$\left( \cos(3\theta + \phi) - \cos(\theta + 3\phi) + i \left( \sin(3\theta + \phi) + \sin(\theta + 3\phi) \right) \right) - \left( \cos(\theta + 3\phi) + i \right) \quad (5.4.53)$$

For this to vanish we require  $\theta = -\phi$ . Thus satisfying the condition on  $\text{Re}_{\mathbb{C}}(\bar{\tau}\sigma)$  gives the constraints

$$\chi = \frac{n\pi}{4}; \quad \theta = -\phi \quad (5.4.54)$$

for  $n$  from 1 to 7. The condition on  $\chi$  gives the dihedral group of order 16 as a group of discrete rotations. The implications of this are discussed in [1]. Now, we look at the second part of our symmetry. After the transformation,

$$\begin{aligned} \bar{w}_R w_I &= |b|^2 \bar{v}_R v_I + |a|^2 \bar{w}_R w_I + \bar{b}a \bar{v}_R w_I + ab \bar{w}_R v_I \\ \bar{w}_R w_I &= (|a|^2 - |b|^2) \bar{w}_R w_I + \bar{b}a \bar{v}_R w_I + ab \bar{w}_R v_I \end{aligned}$$

Keeping  $\bar{w}_R w_I = -\bar{v}_R v_I$  requires

$$2ab\bar{w}_R w_I = 0 \quad (5.4.55)$$

This requires  $ab = 0$ , which is satisfied if  $\cos(2\theta) + i \sin(2\theta) = 0$ . This leads to

$$\theta = 0, \frac{\pi}{2}, \pi, \frac{3\pi}{2} \quad (5.4.56)$$

$\theta = \frac{n\pi}{2}$  multiplies  $a, b$  by  $\pm 1$  and so does not change the symmetries in [1]. If we set  $\theta = 0, \pi$  we multiply  $a$  and  $b$  by  $\pm i$  and  $\mp i$  respectively. This doesn't change  $\tau$ , but sends  $\sigma \rightarrow -\sigma$ . It also interchanges the complex real and imaginary parts of  $v'$  and  $w'$ .

## 5.5 The Scalar Field

Once we have the solution to the constraints, the next step is to calculate the scalar field. Insofar as we do not substitute in the solutions in the above section, 5.4.2, this solution for the scalar field is valid for the whole quaternion subspace, albeit with  $v_I, w_I, \sigma_R, \sigma_I$  as unspecified functions of the moduli space coordinates  $v_R, v_I$  and  $\tau$ , as well as the parameter  $\zeta$ . If we substitute in the solutions from section 5.4.2 then the scalar field derived would only be valid for the complex subspace. This also applies to the Potential and Metric derived below.

With these comments in mind, our ansatz is

$$\phi = U^\dagger \mathcal{A} U; \quad \mathcal{A} = \begin{bmatrix} q & 0 \\ 0 & P \end{bmatrix} \quad (5.5.1)$$

Here  $q$  is in the odd graded part of  $\mathbb{C} \times \mathbb{H}$ ; i.e.  $q = iq_0 + \mathbf{q}$ , where  $q_0 \in \mathbb{R}$  and  $\mathbf{q} \in \text{Im}_{\mathbb{H}}\mathbb{H}$ . This is isomorphic to  $U(2)$ . The matrix  $P$  is given by

$$\begin{bmatrix} ai & ci - b \\ ci + b & di \end{bmatrix} \quad (5.5.2)$$

Following the method in section 3.4.1 we arrive at the equation of motion for the scalar field:

$$2\text{Tr}_2(\Lambda^\dagger q \Lambda) + \text{Tr}_2([\Omega^\dagger, P]\Omega - \Omega^\dagger[\Omega, P]) - \text{Tr}_2(\{P, \Lambda^\dagger \Lambda\}) = 0 \quad (5.5.3)$$

Solving the equation is a lengthy calculation, which I have therefore relegated to appendix A. The solution is

$$\begin{aligned}
a &= -\frac{1}{\Theta} \left( A(3)(g^2 N_{AI} - f^2 N_{AR}) + A(2)w(4gP - fN_{AR}) + A(1)w(4fP - gN_{AI}) \right. \\
&\quad \left. - \left( (16P^2 - N_{AR}N_{AI}) \left( A(3)(2s + w) + wA(4) \right) \right) \right) \\
b &= \frac{1}{2\Theta} \left( A(1) \left( f^2(v + w) - 2N_{AI}(sv + sw + vw) \right) + A(2)(fg(v + w) + 8P(sv + sw + vw)) \right. \\
&\quad \left. + (4fP + gN_{AI}) \left( A(3)(v - w) - A(4)(v + w) \right) \right) \\
c &= \frac{1}{2\Theta} \left( A(1) \left( fg(v + w) - 8P(sv + sw + vw) \right) + A(2) \left( g^2(v + w) + 2N_{AR}(sv + sw + vw) \right) \right. \\
&\quad \left. + (fN_{AR} + 4gP) \left( A(3)(v - w) + A(4)(v + w) \right) \right) \\
d &= -\frac{1}{\Theta} \left( A(3)(f^2 N_{AR} - g^2 N_{AI}) + A(2)v(4gP - fN_{AR}) + A(1)v(4fP - gN_{AI}) \right. \\
&\quad \left. + (A(3)(2s + v) - A(4)v)(16P^2 - XY) \right) \tag{5.5.4}
\end{aligned}$$

where

$$\begin{aligned}
A(1) &= 4q_0 \operatorname{Re}_{\mathbb{H}}(\bar{v}_R w_I - \bar{v}_I w_R) - 4 \operatorname{Re}_{\mathbb{H}}(\bar{v}_R \mathbf{q} w_R + \bar{v}_I \mathbf{q} w_I) \\
A(2) &= 4q_0 \operatorname{Re}_{\mathbb{H}}(\bar{v}_R w_R + \bar{v}_I w_I) + 4 \operatorname{Re}_{\mathbb{H}}(\bar{v}_R \mathbf{q} w_I - \bar{v}_I \mathbf{q} w_R) \\
A(3) &= q_0 \left( |v_R|^2 + |v_I|^2 - |w_R|^2 - |w_I|^2 \right) + 2 \operatorname{Re}_{\mathbb{H}}(\bar{v}_R q v_I - \bar{w}_R q w_I) \\
A(4) &= q_0 \left( |v_R|^2 + |v_I|^2 + |w_R|^2 + |w_I|^2 \right) + 2 \operatorname{Re}_{\mathbb{H}}(\bar{v}_R v_I + \bar{w}_R w_I) \\
f &= \operatorname{Re}_{\mathbb{H}}(\bar{w}_R v_R + \bar{w}_I v_I) \\
g &= \operatorname{Re}_{\mathbb{H}}(\bar{w}_I v_R - \bar{w}_R v_I) \\
x &= |\sigma_R|^2 \\
y &= |\sigma_I|^2 \\
P &= \operatorname{Re}_{\mathbb{H}}(\bar{\sigma}_R \sigma_I) \\
v &= |v_R|^2 + |v_I|^2 \\
w &= |w_R|^2 + |w_I|^2 \\
N_{AR} &= |v_R|^2 + |v_I|^2 + |w_R|^2 + |w_I|^2 + 4(|\tau|^2 + |\sigma_R|^2)
\end{aligned}$$

$$\begin{aligned}
N_{AI} &= |v_R|^2 + |v_I|^2 + |w_R|^2 + |w_I|^2 + 4(|\tau|^2 + |\sigma_I|^2) \\
\Theta &= (v + w)(f^2 N_{AR} - g^2 N_{AI}) + 2(16P^2 - N_{AR} N_{AI})(sv + sw + vw) \quad (5.5.5)
\end{aligned}$$

In the commutative limit from [1], that is,  $\zeta = 0$  and the imaginary quaternion parts  $q_I$  set to zero, this becomes

$$b = \frac{-2\text{Re}_{\mathbb{H}}(\bar{v}\mathbf{q}w)}{\Sigma_+ + 4(|\tau|^2 + |\sigma_R|^2)}; \quad a, b, d = 0 \quad (5.5.6)$$

which is precisely the result in that paper.

Another useful limit is that in which  $|\tau| \mapsto \infty$ . In this case

$$\begin{aligned}
a &= \frac{q_0(|v_R|^2 + |v_I|^2) + 2\text{Re}(\bar{v}_R\mathbf{q}v_I)}{|v_R|^2 + |v_I|^2} \\
d &= \frac{q_0(|w_R|^2 + |w_I|^2) + 2\text{Re}(\bar{w}_R\mathbf{q}w_I)}{|w_R|^2 + |w_I|^2} \quad (5.5.7)
\end{aligned}$$

With  $b, c = 0$ . This corresponds to the two instantons being far separated. In this case we would expect them to look like two single  $U(2)$  instantons, and we see from comparison with (5.1.10) that this is precisely the case.

## 5.6 The Potential

The next step is to use this to explicitly calculate the potential. Recall from section 4.4 that the potential is given by

$$V = \int d^4x \text{Tr}(D_i\phi D_i\phi) \quad (5.6.1)$$

Integrating by parts, and using the equation of motion for  $\phi$

$$D^2\phi = 0 \quad (5.6.2)$$

We get

$$V = \lim_{R \rightarrow \infty} \int_{|x|=R} dS^3 \hat{x}_i \text{Tr}(\phi D_i\phi) \quad (5.6.3)$$

We know that the vector  $U$ , being a null vector of  $\Delta$ , must solve

$$\begin{aligned} v^\dagger U_1 + (\tau^\dagger - x^\dagger)U_2 + \sigma^\dagger U_3 &= 0 \\ w^\dagger U_1 + \sigma^\dagger U_2 - (\tau^\dagger + x^\dagger)U_3 &= 0 \end{aligned} \quad (5.6.4)$$

This is solved on the boundary by

$$\begin{aligned} U_1 &\mapsto 1 \\ U_2 &\mapsto \frac{x}{|x|^2}v^\dagger \\ U_3 &\mapsto \frac{x}{|x|^2}w^\dagger \end{aligned} \quad (5.6.5)$$

The full calculation is in the appendix B. The result is

$$\begin{aligned} &8\pi^2 \left( |q|^2 (|v_R|^2 + |v_I|^2 + |w_R|^2 + |w_I|^2) \right. \\ &+ 4q_0 \operatorname{Re}_{\mathbb{H}}(\bar{v}_R \vec{q} v_I + \bar{w}_R \vec{q} w_I) - a \left( q_0 (|v_R|^2 + |v_I|^2 + 2\operatorname{Re}_{\mathbb{H}}(\bar{v}_R \mathbf{q} v_I)) \right. \\ &- d \left( q_0 (|w_R|^2 + |w_I|^2) + 2\operatorname{Re}_{\mathbb{H}}(\bar{w}_R \vec{q} w_I) \right) + 2b \operatorname{Re}_{\mathbb{H}}(\bar{v}_R \vec{q} w_R + \bar{v}_I \vec{q} w_I) \\ &\left. \left. - 2bq_0 \operatorname{Re}_{\mathbb{H}}(w_I \bar{v}_R - w_R \bar{v}_I) - 2cq_0 \operatorname{Re}_{\mathbb{H}}(w_R \bar{v}_R + w_I \bar{v}_I) - 2c \operatorname{Re}_{\mathbb{H}}(\bar{v}_R \vec{q} w_I - \bar{v}_I \vec{q} w_R) \right) \right) \end{aligned} \quad (5.6.6)$$

Since we can choose the  $q_0$  to be zero by requiring the vev to lie in  $SU(2)$  (as discussed in section 4), we can make this choice and simplify to

$$\begin{aligned} &8\pi^2 \left( |q|^2 (|v_R|^2 + |v_I|^2 + |w_R|^2 + |w_I|^2) - a \left( 2\operatorname{Re}(\bar{v}_R \mathbf{q} v_I) \right) - d \left( 2\operatorname{Re}(\bar{w}_R \vec{q} w_I) \right) \right. \\ &\left. + 2b \operatorname{Re}(\bar{v}_R \vec{q} w_R + \bar{v}_I \vec{q} w_I) - 2c \operatorname{Re}(\bar{v}_R \vec{q} w_I - \bar{v}_I \vec{q} w_R) \right) \end{aligned} \quad (5.6.7)$$

Where  $a, b, c, d$  are given above.



### 5.6.1 The Large $\tau$ limit

If we go back to the large  $\tau$  limit, using (5.5.7)

$$\begin{aligned} \mathcal{V} = 8\pi^2 & \left( |q|^2 (|v_R|^2 + |v_I|^2 + |w_R|^2 + |w_I|^2) + 4q_0 \operatorname{Re}(\bar{v}_R \vec{q} v_I + \bar{w}_R \vec{q} w_I) \right. \\ & \left. - \frac{(q_0 (|v_R|^2 + |v_I|^2 + 2\operatorname{Re}(\bar{v}_R \vec{q} v_I)))^2}{|v_R|^2 + |v_I|^2} - \frac{(q_0 (|w_R|^2 + |w_I|^2 + 2\operatorname{Re}(\bar{w}_R \vec{q} w_I)))^2}{|w_R|^2 + |w_I|^2} \right) \end{aligned} \quad (5.6.8)$$

In this case, the  $q_0$  parts cancel explicitly, and we get

$$\mathcal{V} = 8\pi^2 |\mathbf{q}|^2 \left( \hat{\mathbf{q}} (|v_R|^2 + |v_I|^2 + |w_R|^2 + |w_I|^2) - \frac{4\operatorname{Re}^2(\bar{v}_R \hat{\mathbf{q}} v_I)}{|v_R|^2 + |v_I|^2} - \frac{4\operatorname{Re}^2(\bar{w}_R \hat{\mathbf{q}} w_I)}{|w_R|^2 + |w_I|^2} \right) \quad (5.6.9)$$

We would expect this is the potential for two copies of the single U(1) instanton, and if we compare to the result in section 5.1.1 we can easily see that this is the case.

## 5.7 The Metric

As in section 4.3, we begin by calculating,  $a^\dagger \delta C_r$ , and impose the condition

$$a^\dagger \delta C_r = (a^\dagger \delta C_r)^{T\star} \quad (5.7.1)$$

Once again, we carefully note that  $T$  involves taking the transpose considered as a  $2 \times 2$  matrix of complex quaternions. It does not affect the quaternions themselves. The operation  $\star$  takes the complex conjugate of each element, which again does not affect the quaternions but only their complex coefficients.

This should give us one equation for each component. We can expand  $\delta R$  in the  $u(2)$  basis as

$$\begin{bmatrix} id\phi & id\psi - d\theta \\ id\psi + d\theta & id\chi \end{bmatrix} \quad (5.7.2)$$

this should give 3 simultaneous equations for the derivations in the different gauge directions. We can then solve these to find  $\delta R$  in full. The details of the calculation are in appendix C, however the result is

$$\begin{aligned}
d\phi &= \frac{1}{\Phi} \left( -2B(1)(2s+w)(4fP - gN_{AI}) + 2B(2)((2s+w)(4gP - fN_{AR}) \right. \\
&\quad \left. - (B(3)(2s+w) + B(4)w) (16P^2 - N_{AR}N_{AI}) - 2B(4) (f^2N_{AR} - 8fgP + g^2N_{AI}) \right) \\
d\theta &= \frac{1}{\Phi} \left( 2B(1) (f^2(4s+v+w) - N_{AI}(sv+sw+vw)) \right. \\
&\quad + 2B(2)(fg(4s+v+w) - 4P(sv+sw+vw)) \\
&\quad \left. + (B(3)(4s+v+w) - B(4)(v-w))(4fP - gN_{AI}) \right) \\
d\psi &= \frac{1}{\Phi} \left( -2B(1)(fg(4s+v+w) - 4P(sv+sw+vw)) \right. \\
&\quad - 2B(2) (g^2(4s+v+w) - 2N_{AR}(sv+sw+vw)) \\
&\quad \left. + (B(3)(4s+v+w) - B(4)(v-w))(4gP - fN_{AR}) \right) \\
d\chi &= \frac{1}{\Phi} \left( -2B(1)(2s+v)(4fP - gN_{AI}) + 2B(2)(2s+v)(4gP - fN_{AR}) \right. \\
&\quad \left. - (16P^2 - N_{AR}N_{AI}) (B(3)(2s+v) - B(4)v) + 2B(4) (f^2N_{AR} - 8fgP + g^2N_{AI}) \right)
\end{aligned} \tag{5.7.3}$$

Where the terms are defined in (5.5.5) with the addition of

$$B(1) = \bar{v}_R dw_R + \bar{v}_I dw_I - \bar{w}_R dv_R - w_I dv_I + 2(\bar{\tau} d\sigma_R - \bar{\sigma}_R d\tau)$$

$$B(2) = \bar{v}_R dw_I - \bar{v}_I dw_R + \bar{w}_R dv_I - \bar{w}_I dv_R + 2(\bar{\sigma}_I d\tau - \bar{\tau} d\sigma_I)$$

$$B(3) = \bar{v}_R dv_I - \bar{v}_I dv_R + \bar{w}_R dw_I - \bar{w}_I dw_R$$

$$B(4) = \bar{v}_R dv_I - \bar{v}_I dv_R - \bar{w}_R dw_I + \bar{w}_I dw_R + 2(\bar{\sigma}_R d\sigma_I - \bar{\sigma}_I d\sigma_R)$$

$$\Phi = 4 \left( (4s+v+w) (f^2X - 8fgP + g^2Y) + (16P^2 - XY) (sv+sw+vw) \right)$$

$$\tag{5.7.4}$$

### 5.7.1 The metric itself

Once again we have our formula

$$ds^2 = ds_1^2 + ds_2^2 = 2\pi^2 \left( \text{Tr}^* \left( 2d\Lambda^\dagger d\Lambda + d\Omega^\dagger d\Omega \right) + \text{Tr}^* \left( \left( a^\dagger da - (a^\dagger da)^{T*} \right) dR \right) \right) \quad (5.7.5)$$

First we have that  $a^\dagger da - (a^\dagger da)^{T*}$  is

$$\begin{aligned} & \begin{bmatrix} 0 & \bar{v}_R dw_R + \bar{v}_I dw_I - \bar{w}_R dv_R - \bar{w}_I dv_I + 2(\bar{\tau} d\sigma_R - \bar{\sigma}_R d\tau) \\ -(\bar{v}_R dw_R + \bar{v}_I dw_I - \bar{w}_R dv_R - \bar{w}_I dv_I + 2(\bar{\tau} d\sigma_R - \bar{\sigma}_R d\tau)) & 0 \end{bmatrix} \\ + i & \begin{bmatrix} 2(\bar{v}_R dv_I - \bar{v}_I dv_R + \bar{\sigma}_R d\sigma_I - \bar{\sigma}_I d\sigma_R) & \bar{v}_R dw_I - \bar{v}_I dw_R + \bar{w}_R dv_I - \bar{w}_I dv_R + 2(\bar{\sigma}_I d\tau - \bar{\tau} d\sigma_I) \\ \bar{v}_R dw_I - \bar{v}_I dw_R + \bar{w}_R dv_I - \bar{w}_I dv_R + 2(\bar{\sigma}_I d\tau - \bar{\tau} d\sigma_I) & 2(\bar{w}_R dw_I - \bar{w}_I dw_R - \bar{\sigma}_R d\sigma_I + \bar{\sigma}_I d\sigma_R) \end{bmatrix} \end{aligned} \quad (5.7.6)$$

Once we have this it is fairly straightforward to calculate the metric as

$$\begin{aligned} & 8\pi^2 \left( d^2 v_R + d^2 v_I + d^2 w_R + d^2 w_I + d^2 \tau + d^2 \sigma_R + d^2 \sigma_I \right. \\ & - \text{Re}_{\mathbb{H}} \left( \left( \bar{v}_R dv_I - \bar{v}_I dv_R + \bar{\sigma}_R d\sigma_I - \bar{\sigma}_I d\sigma_R \right) d\phi + \left( \bar{w}_R dw_I - \bar{w}_I dw_R - \bar{\sigma}_R d\sigma_I + \bar{\sigma}_I d\sigma_R \right) d\chi \right. \\ & + \left. \left( \bar{v}_R dw_R + \bar{v}_I dw_I - \bar{w}_R dv_R - \bar{w}_I dv_I + 2(\bar{\tau} d\sigma_R - \bar{\sigma}_R d\tau) \right) d\theta \right. \\ & \left. + \left( \bar{v}_R dw_I - \bar{v}_I dw_R + \bar{w}_R dv_I - \bar{w}_I dv_R + 2(\bar{\sigma}_I d\tau - \bar{\tau} d\sigma_I) \right) d\psi \right) \end{aligned} \quad (5.7.7)$$

### 5.7.2 Checking the Solution

We can check the behaviour of this solution in various limits. First of all, the commutative real limit, where the various imaginary quaternion parts  $q_I$  and the noncommutative parameter  $\zeta$  are set to zero. In this limit we have

$$d\phi = d\psi = d\chi = 0; d\theta = \frac{\bar{v}_R dw_R - \bar{w}_R dv_R - \bar{w}_R dv_R + 2(\bar{\tau} d\sigma_R - \bar{\sigma}_R d\tau)}{|v_R|^2 + |w_R|^2 + 4(|\tau|^2 + |\sigma_R|^2)} \quad (5.7.8)$$

This allows us to calculate the metric to be

$$8\pi^2 \left( d^2 v_R + d^2 w_R + d^2 \tau + d^2 \sigma_R - \frac{dk^2}{N_A} \right) \quad (5.7.9)$$

with

$$N_A = |v_R|^2 + |w_R|^2 + 4(|\tau|^2 + |\sigma_R|^2) \quad (5.7.10)$$

$$dk = \bar{v}_R dw_R - \bar{w}_R dv_R - \bar{w}_R dv_R + 2(\bar{\tau} d\sigma_R - \bar{\sigma}_R d\tau)$$

exactly as in [1]. The second limit we can check is the limit in which  $|\tau| \mapsto \infty$ . Since this corresponds to the two instantons becoming far separated, in this limit, we would expect to get two copies of the solution for a single  $U(2)$  instanton. We in fact get

$$d\phi = \frac{v_R dv_I - \bar{v}_I dv_R}{|v_R|^2 + |v_I|^2}; \quad d\chi = \frac{w_R dw_I - \bar{w}_I dw_R}{|w_R|^2 + |w_I|^2} \quad (5.7.11)$$

This gives the metric

$$ds^2 = 8\pi^2 \left( d^2 v_R + d^2 v_I + d^2 w_R + d^2 w_I - \frac{(v_R dv_I - \bar{v}_I dv_R)^2}{|v_R|^2 + |v_I|^2} - \frac{(w_R dw_I - \bar{w}_I dw_R)^2}{|w_R|^2 + |w_I|^2} \right) \quad (5.7.12)$$

This is precisely the sum of two copies of the form in section 5.1.2 above, equation (5.1.27).

## 5.8 Conclusion

I shall end the chapter by reviewing the main results. I have explicitly derived biquaternion valued ADHM equations for the commutative and non-commutative  $U(2)$  2 instanton case. I have shown that a solution to the commutative biquaternion valued equations can always be rotated to a purely quaternion valued form.

I have then moved on to the noncommutative case. I showed that the existing solution in [37] was incorrect. I then derived a partial solution for the complex valued subspace of the whole Instanton moduli space. I used this to calculate the metric, scalar field and potential for this subspace, and checked that in the correct limits my solutions matched up with the solutions in [1] and [3]. Now I will go on to investigate the dynamics on the moduli space via numerical methods.



# Chapter 6

## Two Instanton Dynamics

In this section we discuss the dynamics of the instantons on the noncommutative two Instanton moduli space we have constructed. The graphs in this section were produced using the same basic code as [1], but modified for the non commutative metric and potential we derived.

### 6.1 The Setup

I will now give a general overview of the method we used to scatter two Instantons. The parametrisation is as shown in figure 6.1. As stated in section 4.2.1, we are working on the subspace of the total moduli space with the collective coordinates in  $\mathbb{C} \times \mathbb{C}$  rather than  $\mathbb{C} \times \mathbb{H}$ . Therefore the coordinates shown in the diagram are complex numbers. In the noncommutative case, the instanton size  $\rho_i$  is defined as

$$\tilde{\rho}_i = \sqrt{\rho_i^2 + \frac{4\zeta}{\rho_i^2}} \quad (6.1.1)$$

Where the index  $i$  in  $\rho_i$  is either 1 or 2, referring to the magnitude of  $v$  or  $w$  respectively. Calculating the scattering with general  $\rho_1$  and  $\rho_2$ , and with general gauge embedding is very computationally expensive for the noncommutative case. Therefore we did a lot of the simulations in the, ‘Orthogonal’ case where  $\rho_1 = \rho_2$  and the relative gauge angle between the two instantons is  $\pi/2$ . The relation between

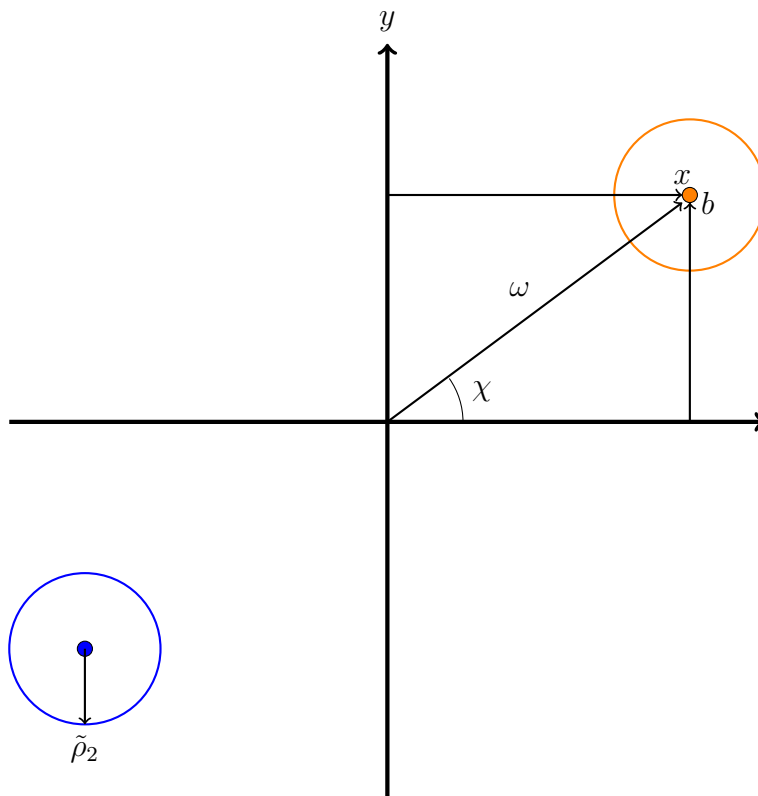


Figure 6.1: The setup of the Instantons. The instantons are located at  $\pm(x, b) = (\omega \cos(\chi), \omega \sin(\chi))$ . They have size  $\tilde{\rho}_i = \sqrt{\rho_i^2 + \frac{4\zeta^2}{\rho_i^2}}$

the new coordinates  $\rho_i, \theta_i, \omega, \chi$  and  $v, w, \tau$  is given by

$$\begin{aligned} v &= \rho_1 \left( \cos(\theta_1) + i \sin(\theta_1) \right) \\ w &= \rho_2 \left( \cos(\theta_2) + i \sin(\theta_2) \right) \\ \tau &= \omega \left( \cos(\chi) + i \sin(\chi) \right) \end{aligned} \quad (6.1.2)$$

The relation between the coordinates  $b, x$  and  $\omega, \chi$  is

$$\begin{aligned} x &= \omega \cos(\chi) \\ b &= \omega \sin(\chi) \\ \omega &= \sqrt{b^2 + x^2} \\ \chi &= \arctan(b/x) \end{aligned} \quad (6.1.3)$$

There are several technical issues which emerged. First of all, around the point of collision there is a discontinuous jump between the different, ‘paths’ the instantons can take – there is no *a priori* reason why any two of the paths should be connected rather than the alternative option. This can be seen on several of the graphs around the origin.

The second issue is with the parameterisation of the Instanton position in terms of  $\tau$ . The position of the Instanton is given by the eigenvalues of the submatrix

$$\begin{bmatrix} \tau & \sigma^* \\ \sigma & -\tau \end{bmatrix} \quad (6.1.4)$$

of the ADHM data [1]. Recall that

$$\begin{aligned} \sigma_R &= \frac{\text{Im}(\bar{w}_R v_R + \bar{w}_I v_I)}{2} = \frac{(|v_R|^2 |w_R|^2 + 4\zeta^2)}{2|\tau|^2 |v_R|^2 |w_R|^2} \tau \text{Im}(\bar{w}_R v_R) \\ \sigma_I &= \frac{\text{Im}(\bar{w}_R v_I + \bar{v}_R w_I)}{2} = -\frac{\zeta(|w_R|^2 + |v_R|^2)}{|\tau|^2 |v_R|^2 |w_R|^2} \tau \text{Im}(\bar{w}_R v_R \sigma_3) \end{aligned} \quad (6.1.5)$$

In the subspace under discussion, and in the coordinates we are using, this becomes

$$\sigma_R = \frac{i(\rho_1^2 \rho_2^2 + 4\zeta^2) \left( \cos(\chi) + i \sin(\chi) \right) \sin(\theta_1 - \theta_2)}{2\rho_1 \rho_2 \omega}$$



$$\sigma_I = \frac{-i\zeta(\rho_1^2 + \rho_2^2)(\cos(\chi) + i\sin(\chi))\cos(\theta_1 - \theta_2)}{\rho_1\rho_2\omega} \quad (6.1.6)$$

At large  $\tau$ , the matrix is effectively diagonal, and so the positions of the two Instantons can be approximated by  $\tau$  and  $-\tau$  respectively. At small values of  $\tau$ , however,  $\sigma$  becomes very large and therefore  $\pm\tau$  is no longer a good description. A better approximation is to diagonalise the full matrix which gives the parametrisation  $\sqrt{\tau^2 + \sigma^2}$  for the position (note that this is in general a complex number), though this can give a discontinuity at the origin to the presence of the square root, with both positive and negative values. In practice, different plottings are clearly better for different cases – usually for the noncommutative case it made more sense to use the more complicated parametrisation, as the presence of  $\zeta$  in  $\sigma$  means that this becomes more important (as shown in figure 6.2).

### 6.1.1 Numerical Checks

We performed several checks on the numerical accuracy of our results. There were two basic programmes used. The first was developed from the code used for [1], and was used for the orthogonal instantons. The second was used for the 6-parameter case, and was written by Mr. Joseph Farrow. In both cases, I made sure that I could reproduce the results from [1] when I set  $\zeta = 0$ . I also made sure that the second code reproduced the results of the first when I set the six parameters to the same values as individual graphs in the four parameter case. Additionally, I checked that, e.g. there was no interaction when the instantons were far separated. Finally, I checked that for small values of  $\zeta$  there was no observable change from the commutative case.

I also looked at how changing the numerical precision of the method affected the results. For the first code, I implemented this by changing the precision of the NDSolve algorithm in Mathematica. Here it turned out that the standard precision was enough – there was no appreciable change from increasing the precision beyond this. For the second code, I checked this by manually changing the step size and

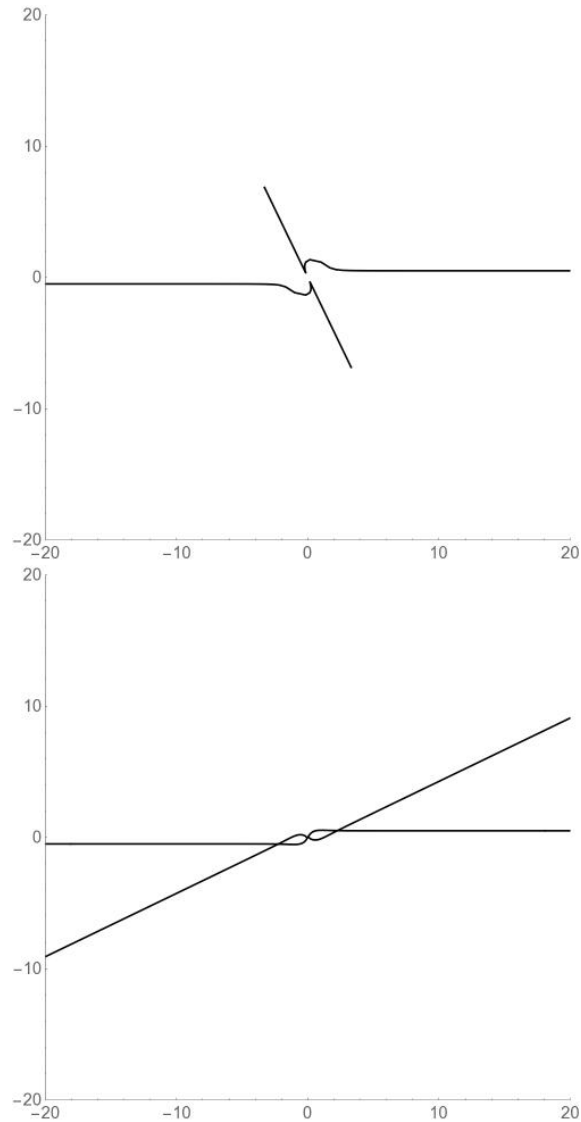


Figure 6.2: Scattering of Dyonic instantons with  $b = 0.5$  and  $\zeta = 1.15$ . The upper plot shows the  $|\tau|$  parametrisation, the lower shows  $\sqrt{|\tau|^2 + |\sigma|^2}$ . The radii of the instantons are not shown. In this case the  $\sigma$  behaviour dominates and after the interaction the position of the instantons goes as  $\frac{1}{|\tau|^2}$  – the  $\tau$  case had to be run for many more time steps (50000 as opposed to 2400). This is presumably because the size of the instantons becomes very large and so  $\sigma$  continues to dominate  $\tau$  in the definition of the instanton position

number of steps. I increased it until further changes no longer seemed to have any effect on the graphs produced.

## 6.2 Pure Instantons

We start with the four parameter orthogonal instantons. The first thing we could do is look at the scalar field profiles for the instantons. This will give us an idea whether the interpretation of the parameters for the noncommutative instantons makes sense in terms of the interpretation for the commutative instantons. This is made more difficult by the fact that the calculation of the scalar field involves the Moyal product. We used a first order expansion in the Moyal product, which ought to be valid for small  $\zeta$ . We found that for small zeta (up to about 0.025) there was no observable difference with the commutative case (See figures 6.3 and 6.4). However, if we increased  $\zeta$  even as far as 0.1, some differences emerged. The first is the presence of a discontinuity in the left hand graph. This is almost certainly an error due to only going to first order in the Moyal product. The second difference is the presence of a ring structure in the separate peaks in figure 6.5. This can be seen more clearly if we plot a two dimensional plot as in figure 6.6. Increasing  $\zeta$  increases the size of the rings, as in figure 6.7. I think that this is less likely to be numerical error and may be a genuinely new feature of the noncommutative case, however future work calculating the Moyal product to higher orders in the scalar field would be required. Now we move to look at the scattering. We will first compare some particular scattering cases for different values of  $\zeta$ , then I will conduct a more systematic analysis and search for interesting behaviour. Choosing a value for the noncommutative parameter  $\zeta$  sets an overall scale, so we can, ‘scan’ the parameter space by changing one of the other parameters at a time to look for abrupt changes in the scattering angle. We can then focus on these areas to look at the scattering behaviour around these points on the moduli space. It should be noted that this scanning process is not in itself sensitive to periodic ambiguities

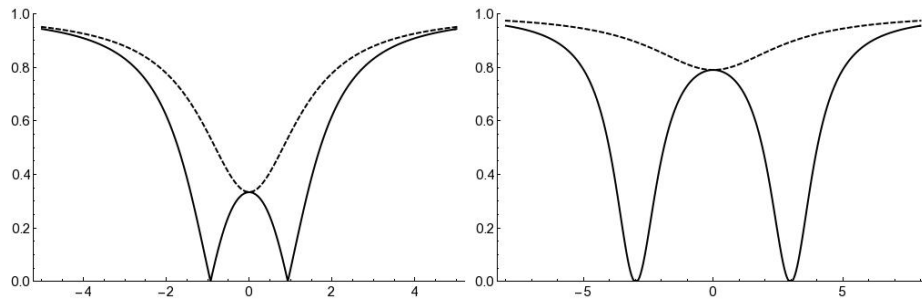


Figure 6.3: The scalar field profile for the Commutative instantons. The left graph is when they are nearly coincident, the right when they are separated. The solid line shows the profile along the imaginary direction of the complex subspace; the dotted line shows the profile off the complex subspace we are elsewhere considering.

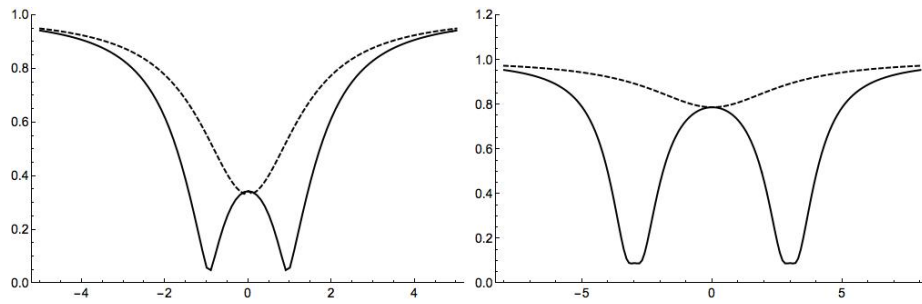


Figure 6.4: The scalar field profile for the Noncommutative instantons with  $\zeta=0.025$ . The left graph is when they are nearly coincident, the right when they are separated. The solid line shows the profile along the imaginary direction of the complex subspace; the dotted line shows the profile off the complex subspace we are elsewhere considering.

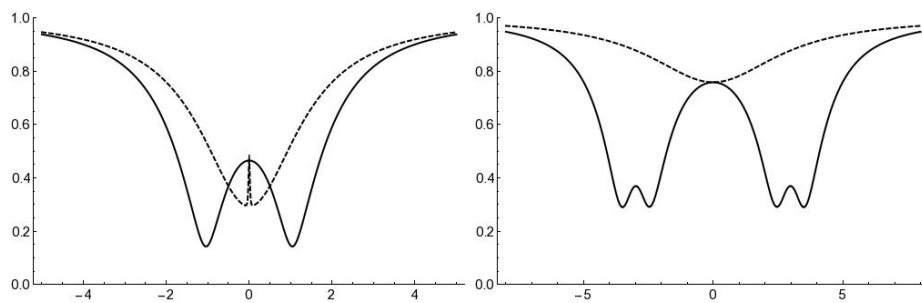


Figure 6.5: The scalar field profiles for coincident (left) and separated (right) Instantons with  $\zeta = 0.1$ . The dotted and solid lines have the same meaning as before. As discussed in the main text these graphs are probably not reliable due to being calculated only to first order in the Moyal product

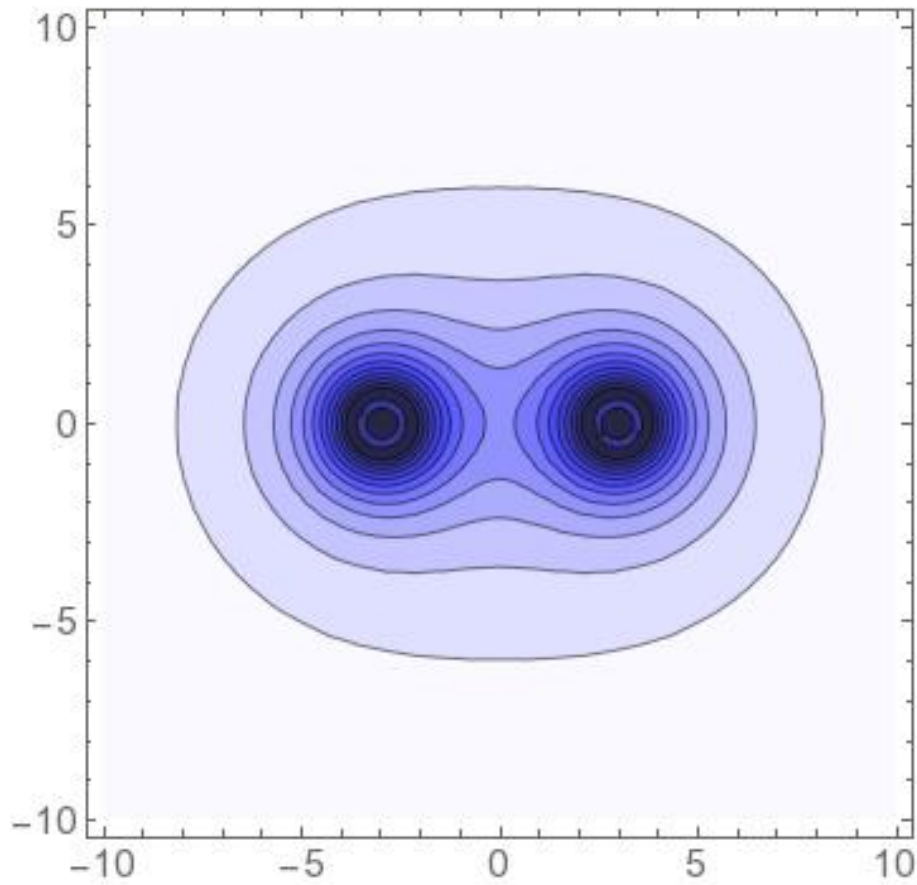


Figure 6.6: A top down 2D contour plot of the noncommutative part of figure 6.5. The brighter circles in the dark spots show that the splitting of the two peaks really does indicate a ring structure

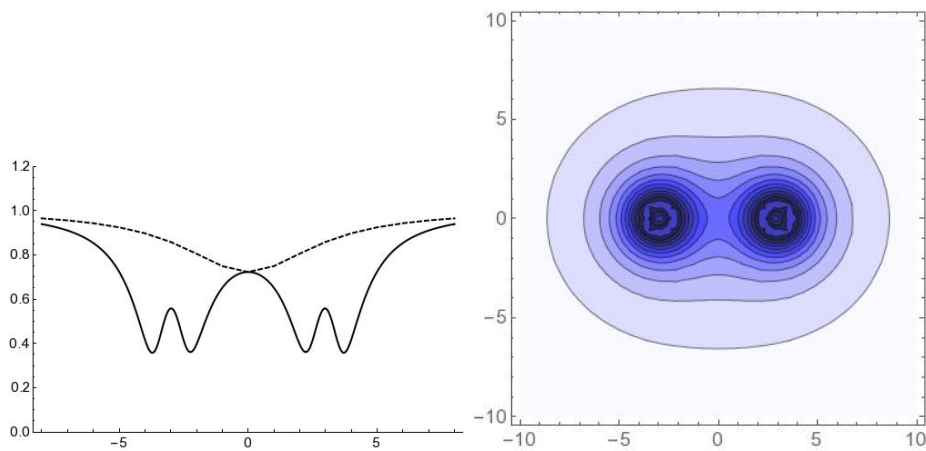


Figure 6.7: The scalar field profiles in 1D and 2D for the case in figure 6.5, but with  $\zeta=0.15$ . Note that increasing  $\zeta$  has increased the size of the rings.

in the scattering angles – e.g. instantons moving parallel and not interacting and instantons reflecting directly off each other would both register a scattering angle of zero. Therefore we must supplement this scanning by looking at individual plots to check the interpretation of the scattering angles we have found.

To begin with, I will look at how a typical example of scattering in the commutative case changes as we turn the noncommutativity on. In this case, the parameters  $\{\rho, \theta, b, x\}$  take the values  $\{1, 0, 0.5, 50\}$  and their initial derivatives are  $\{0, 0, 0, -0.03\}$ . The change in scattering angle as we change the value of  $\zeta$  from 0 to 5 is shown in figure 6.8. The presence of the peak itself is notable and bears further examination.

The first thing to note is that the peak is quite hard to resolve numerically – there seems to be a discontinuity. To analyse this we can zoom in on that section of the graph (figure 6.9). Then there seem to be two parts to the discontinuity. The first moves between  $\pm\pi/4$  faster than the scanning programme can pick up. The second seems to jump between  $\pm\pi/2$ . This second one seems to be an artificial discontinuity since the code is not always able to consistently identify the instantons in the same way before and after the solution. This would cause just such a jump of  $\pi$  radians to be observed. The first discontinuity seems to be a genuine feature of the scattering behaviour, where the angle changes too fast to be resolved correctly by the graph. This interpretation is borne out by looking at individual scattering graphs. In figure 6.10 we can look at the behaviour to the left of the peak and around the peak in figure 6.8. At the peak itself the  $\tau$  description of the position breaks down and it is essential to use the combined  $\sigma$  and  $\tau$  definition for the position. The behaviour at the peak itself is shown in figure 6.11. We analyse the behaviour to the right of the peak in figure 6.12.

The overall effect of the noncommutativity is to increase the repulsion between the instantons; however this is done in a non-linear way. Initially, the instanton scattering angle seems to rotate anticlockwise, going from glancing off each other, to moving parallel, to crossing over. This first change occurs rapidly as  $\zeta$  changes from

0.85 until about 0.88 (figure 6.10).

At the first apparent discontinuity, the instantons change from moving across each others paths, to repelling and turning back on themselves, so that their paths form a loop near the interaction point. This change happens between  $\zeta = 0.8818695$  and  $\zeta = 0.88187$  however I have been unable to capture any intermediate behaviour. The beginnings of the looping behaviour can be seen in the first graph in figure 6.11, however as can be seen in the second graph there seems to be some kind of numerical difficulty in assigning the trajectories to different instantons. I think on examination, one can discern the two instantons looping and deflecting however.

The second part of the discontinuity seems to be artificial due to inconsistently identifying the instantons, as can be seen from the bottom two graphs in figure 6.11, where the loops are joined in two different ways. Comparison to the behaviour on the right of the peak, and in the first graph in figure 6.11 leads me to conclude that the correct behaviour is shown in the final graph – the particles loop back on themselves – and therefore the discontinuities in the scattering angle graph 6.9 are based on a breakdown (at least numerically) of the notion of the instanton positions. Increasing the numerical precision does not seem to affect these results.

After the peak (figure 6.12), the scattering angle appears to rotate clockwise – the loop at the interaction point is, ‘unwound’. This leads to them then repelling entirely before the angle widens to about  $\pi/4$ , with the instantons repelling rather than glancing off each other as they did at the start.

Another thing we can do is to start off with a commutative case where there is no interaction, and see what happens when we turn on the noncommutative parameter. The overall plot is given in figure 6.13, and the scattering is shown in more detail for particular cases in 6.15. The behaviour is similar to the previous case. As zeta is increased the force between the instantons increases, until they begin to cross over. Then, at the peak, there is a rapid change in behaviour where the instantons loop back on themselves. As  $\zeta$  is further increased, the loop unwinds until the instantons are now fully repelled by one another. A new feature is the apparent presence of

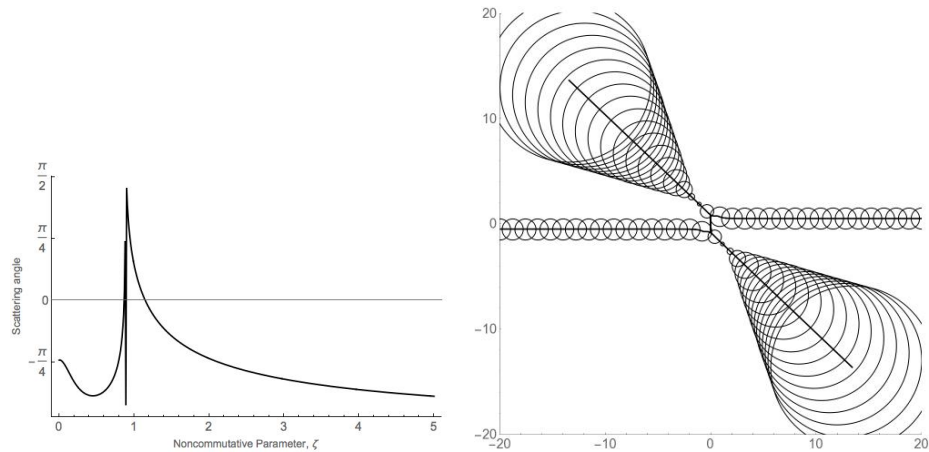


Figure 6.8: Change of scattering angle (left) with noncommutative parameter  $\zeta$  for  $b = 0.5$ , with the other parameters as discussed in the main body of the text. On the right is the commutative case, with  $\zeta = 0$ . Increasing either  $b$  or the parameter  $\rho$  moves the peak to higher values of  $\zeta$ . In the case of  $b$  this is because we need a larger size, and hence larger  $\zeta$  to compensate for the same separation. It is less clear what the explanation is in the case of  $\rho$ , though the nonlinear dependence of the instanton size on both  $\rho$  and  $\zeta$  almost certainly plays a role.

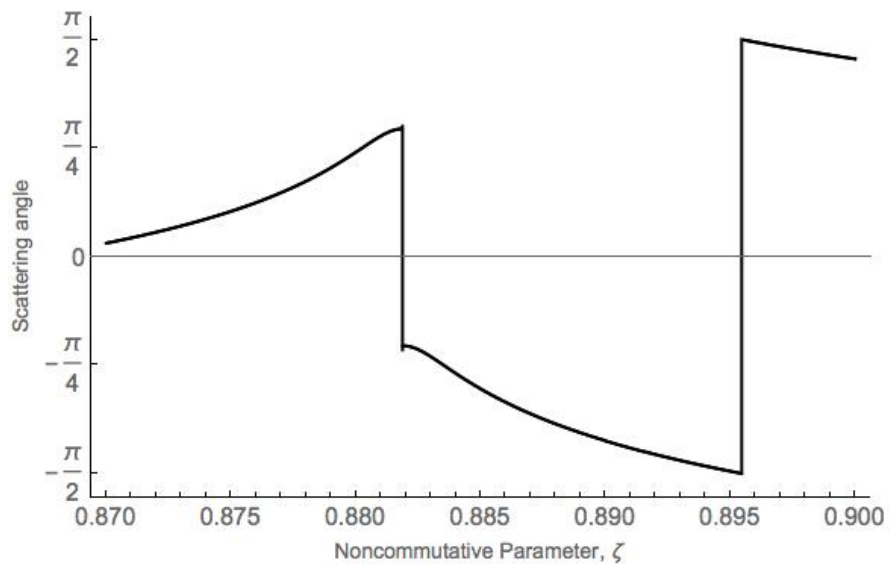


Figure 6.9: Zooming in on the discontinuity in figure 6.8. Individual scattering examples from this graph are shown in figure 6.11



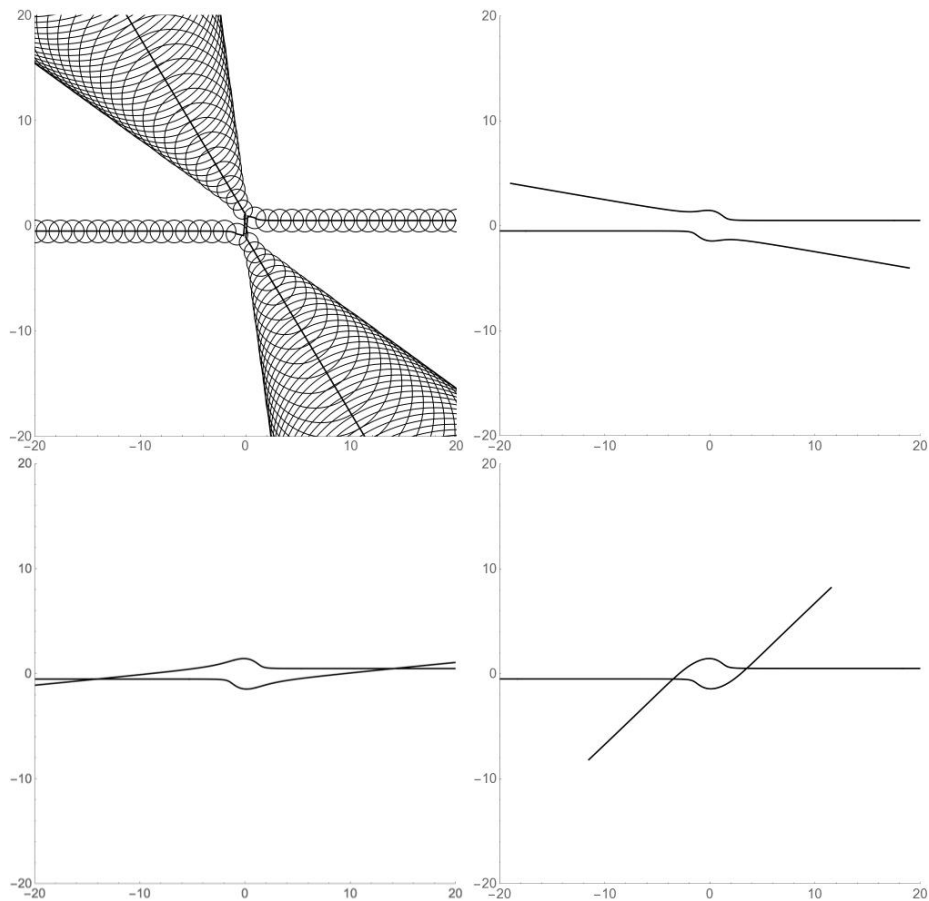


Figure 6.10: Scattering for two instantons with  $b = 0.5$ , and, moving in each row from left to right,  $\zeta = \{0.1, 0.86, 0.87, 0.88\}$ ; This corresponds to the region to the left of and around the peak in figure 6.8. Where the sizes are not shown this is in order to make the trajectories clearer. Note that the instantons go from glancing off one another, to moving parallel, to crossing over, and then deflecting

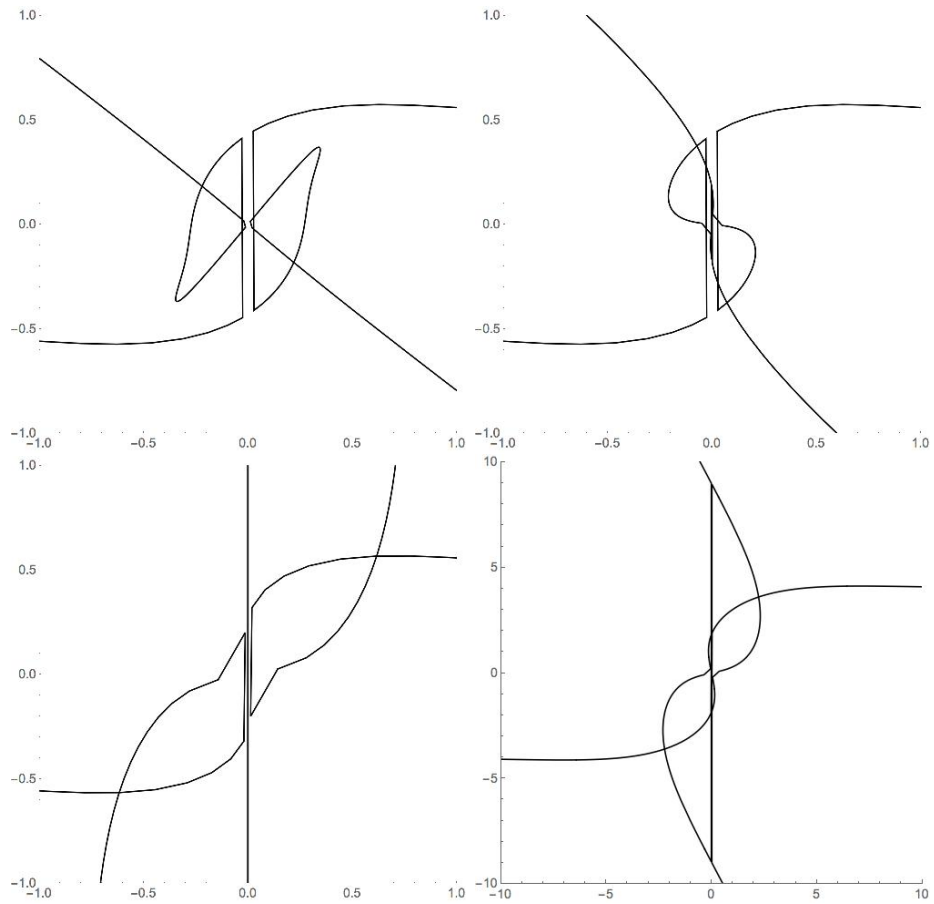


Figure 6.11: Graphs of the interaction around the peak, zoomed in at the center, with  $\zeta = \{0.8187, 0.882, 0.89, 0.9\}$ . The vertical lines on the graph are the results of confusion about which parts of the trajectory belong to which instanton, and can be ignored. More detailed interpretation of the graphs is given in the main text, however I think that the description of the position is breaking down somewhat, and this explains the discontinuities in the scattering angle graph. I conclude that the correct behaviour is the looping behaviour in the first and last graphs, which rotates in a clockwise direction, and that the connection of the two loops is an error in the plotting.

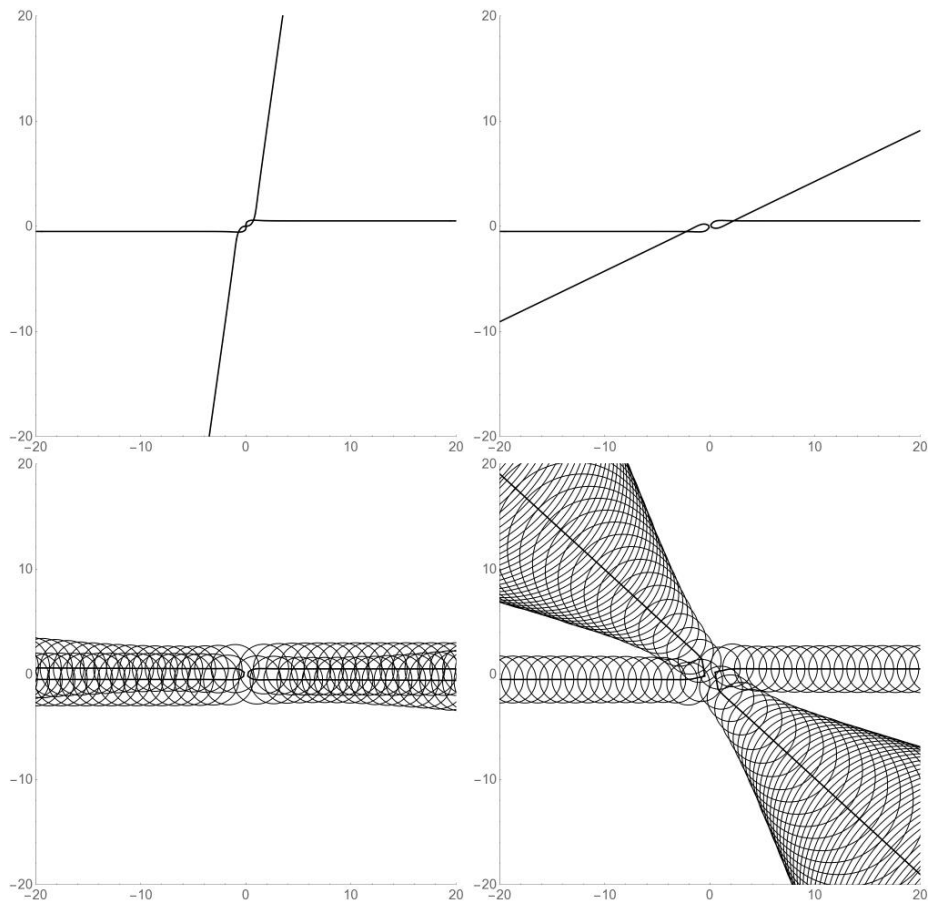


Figure 6.12: Scattering for two instantons with  $b = 0.5$ , and  $\zeta = 0.9, 1, 1.15, 2$ . This corresponds to the right side of the peak. Note that the Instanton angle begins to turn back on itself, until the scattering becomes a direct repulsion  $\zeta = 1.15$ , then opens to about  $\pi/4$

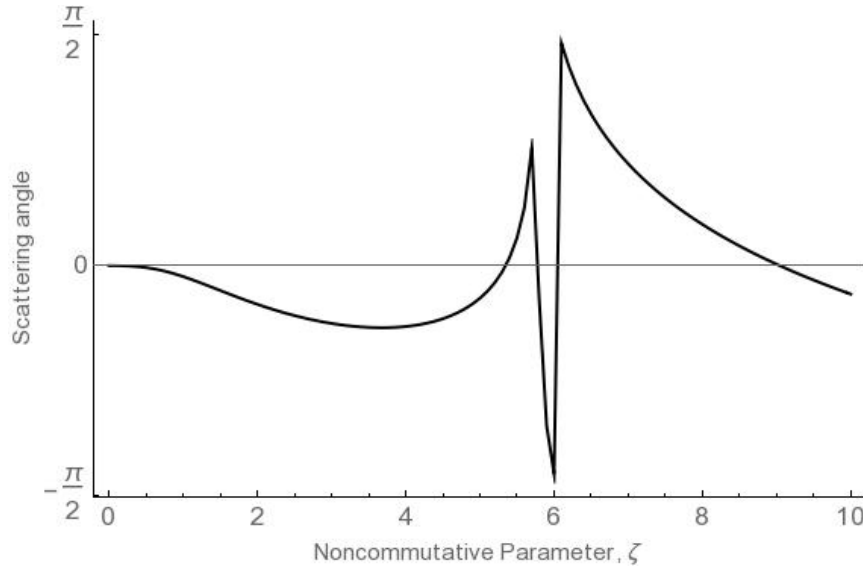


Figure 6.13: Plot of scattering angle vs. noncommutative parameter  $\zeta$  for the initial parallel scattering, shown for particular cases in figure 6.15. The jump at  $\zeta = 6$  is a discontinuity similar to those analysed in figure 6.9, and is shown in more detail in figure 6.14

rapid oscillation of the scattering angle once the loops form, as shown in figure 6.16

An overall feature of all this graphs is that whereas in the commutative case the instantons shrink through zero size then expand again, in the noncommutative case, as we would expect, they shrink to a finite size before expanding; since due to the noncommutativity the zero size point cannot be reached.

We now move onto a systematic analysis of the other parameters. Fixing  $\zeta$  fixes the length scale of the system, therefore I will investigate the behaviour of the system keeping  $\zeta$  at a constant value of 1, and looking at how the scattering angle of the Instantons depends on the other parameters. Plotting the scattering angle for differing values of the impact parameter  $b$  shows some interesting behaviour which seems to be unique to the noncommutative case. There is a distinctive spike for a particular value of  $b$  (figure 6.17). This spike is mirrored if we plot the scattering angle for varying  $\zeta$  whilst keeping  $b$  fixed – the spike appears at the same  $(b, \zeta)$  coordinates in both cases. In fact, this is the same spike as was found in the above cases. These are the points at which the Instantons change from glancing off one another, to repelling one another. From the above cases it seems like there is sometimes some interesting

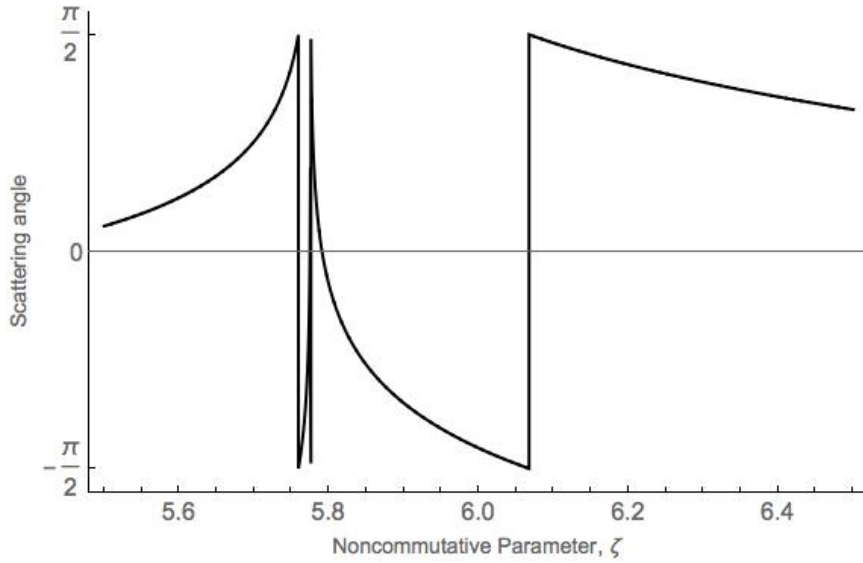


Figure 6.14: Plot of scattering angle vs. noncommutative parameter  $\zeta$  for the initial parallel scattering, zooming in on the discontinuity. Note the splitting on the left hand side—this is analysed in figure 6.16

behaviour at the transition point (i.e. the peak) however the difficulties in defining the positions of the Instantons in cases of very strong interaction make it hard to be too precise. If we plot the graphs of scattering angle vs. impact parameter for different values of  $\zeta$  we see that the overall behaviour stays the same, however the position of the peak moves to the right as  $\zeta$  increases as shown in figure 6.17. There is also evidence of the rapid oscillatory behaviour observed in the  $b = 4$  case as we increase  $\zeta$ .

The next case we will look at is the case where the scattering is orthogonal in the commutative case (so  $b = 0$ ). This remains consistently orthogonal in the noncommutative case. Examples of this scattering in individual graphs are shown in figure 6.20. Overall the scattering keeps its perpendicular character. We can explain this analytically in a similar way as in the commutative case in [1]. As discussed above, the location of the instantons is described by a combination of  $\tau$  and  $\sigma$ . Because  $\sigma$  goes as  $1/|\tau|$ , the change in which parameter dominates happens at  $\tau = 0$ . Going through the point  $\tau = 0$  involves a change in the sign of  $\tau^2 + \sigma^2$ . Since the positions are given by the square root of this quantity, they are rotated by  $\pi/2$  in the complex plane. This corresponds to a 90 degree rotation of the instanton trajectory on the

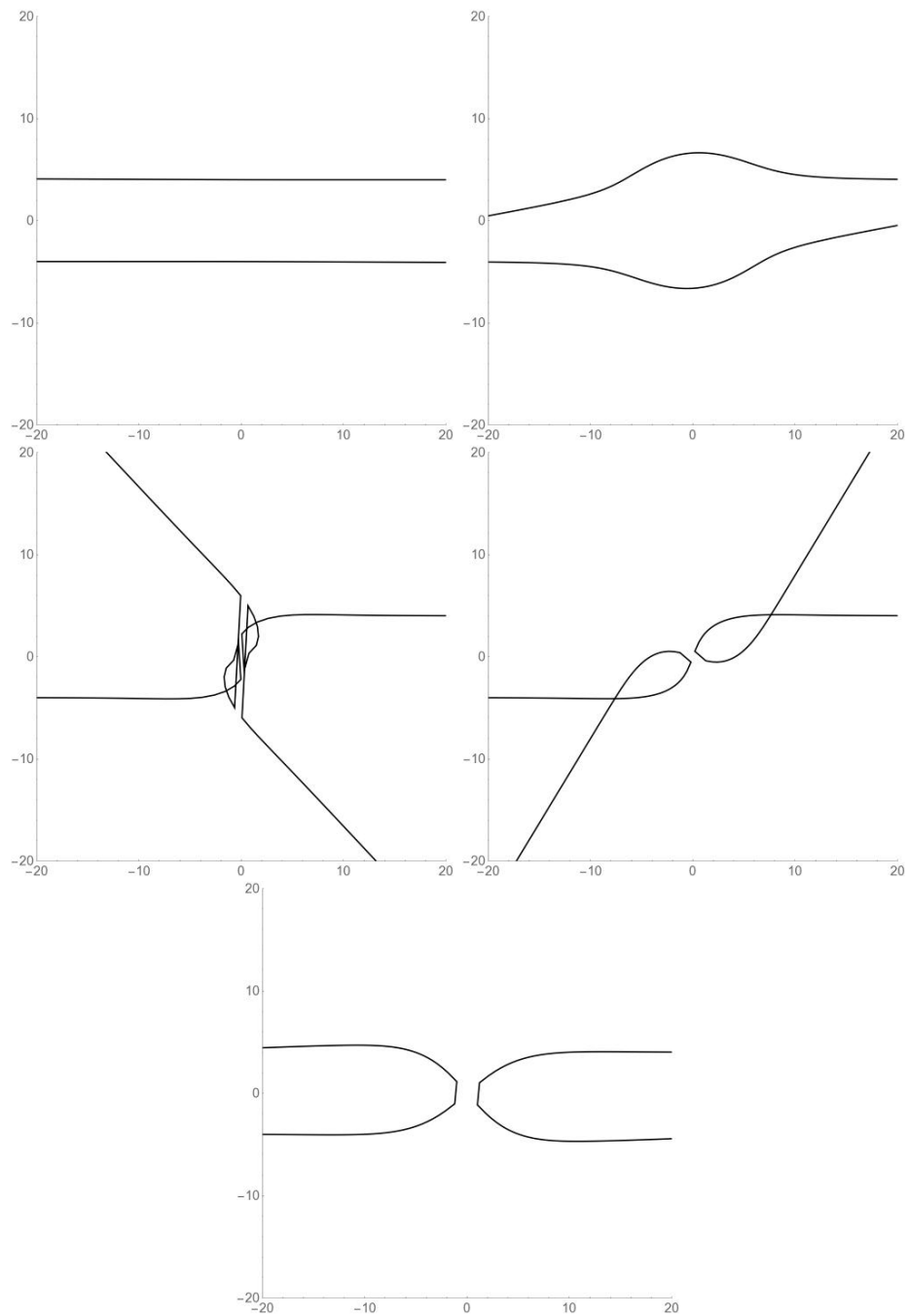


Figure 6.15: Scattering behaviour for the setup in 6.18, for  $\zeta = \{0, 5.5, 8.85, 9.5, 8.85\}$ . The Instantons begin by not interacting in the commutative case, then begin to interact as the noncommutative parameter is increased. At the peak at  $\zeta = 5.85$ , the interaction is complicated and even the  $\sqrt{\sigma^2 + \tau^2}$  description seems to break down. As in the original case, figure 6.12, the instantons then completely reflect off one another. The explanation for this behaviour seems to be that increasing  $\zeta$  increases the size of the instantons, so that they are no longer separated and begin to interact

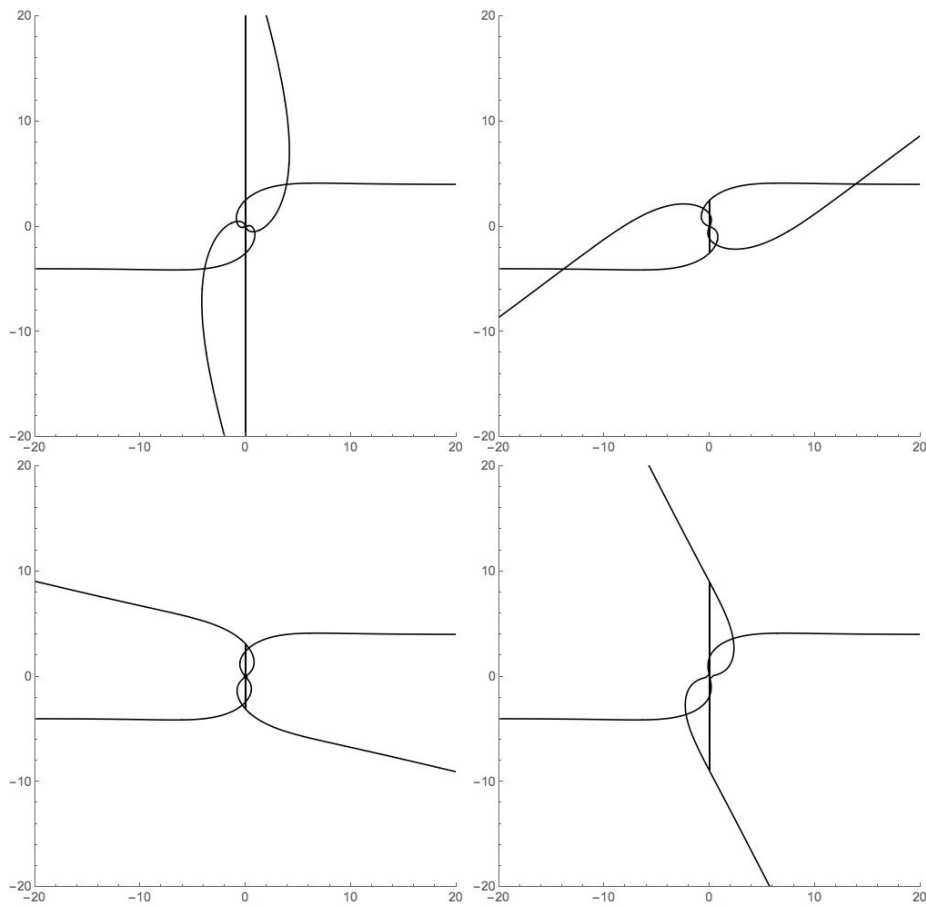


Figure 6.16: Zoomed in graphs showing rapid oscillatory behaviour of in the splitting on the left of figure 6.14. We have  $\zeta = \{5.7757, 5.78, 5.8, 5.9\}$ . The instanton trajectories rotate a full circle over a very small parameter range. This seems to correspond to the removal of a second set of loops from the centre of the interaction. As before, the vertical lines are due to errors in constantly identifying the instanton positions

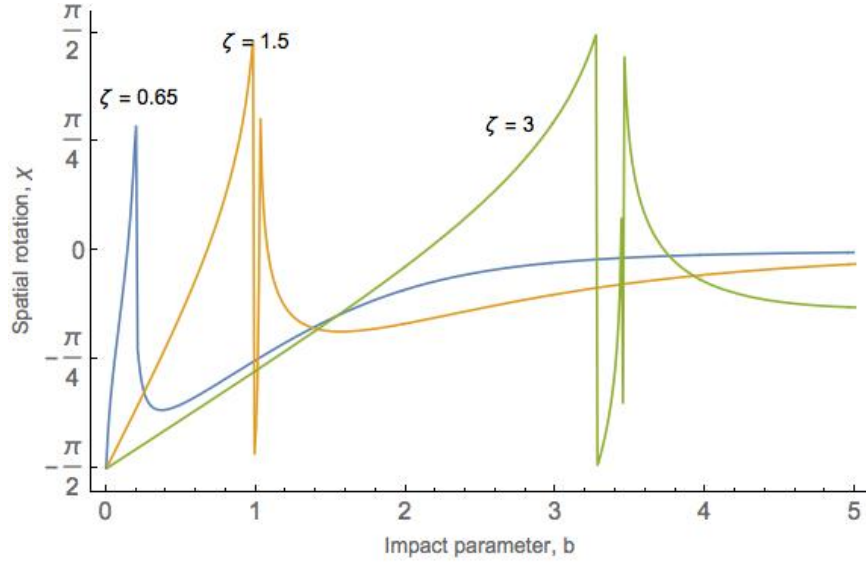


Figure 6.17: Plot of scattering angle vs. impact parameter for different values of  $\zeta$ . From left to right we have  $\zeta = \{0.65, 1.5, 3\}$

plane plotted in the graphs here. Recall the definitions of  $\tau$  and  $\sigma$  in equation (6.1.6). For the case of orthogonal scattering,  $\chi = 0$ . Therefore  $\tau = \omega$ , and so lies entirely on the  $x$  axis. On the contrary,  $\sigma$  is proportional to  $i$  and so lies on the  $y$  axis. Therefore, as the instantons pass through the origin, their motion goes from the  $x$  axis to the  $y$  axis and so the scatter orthogonally.

There is an interesting behaviour where for very small values of  $b$  the scattering stops being orthogonal for a small range of the parameter  $\zeta$ , before returning to the orthogonal behaviour as  $\zeta$  increases. This is shown in figures 6.18 and 6.19. As shown in figure 6.19, this region gets larger as  $\rho$  increases. Individual examples are shown in figure 6.21. I have not been able to determine an analytic reason for this behaviour.

The next thing to consider is the effect of varying  $\theta$ . It turns out however that the effect on the scattering angle has no discernible pattern (figure 6.25). Therefore I moved onto considering  $\rho$ . There is potentially in issue here as in the noncommutative case,  $\rho$  is not directly the size of the instanton, which is given by

$$\tilde{\rho} = \sqrt{\rho^2 + \frac{4\zeta^2}{\rho^2}} \quad (6.2.1)$$



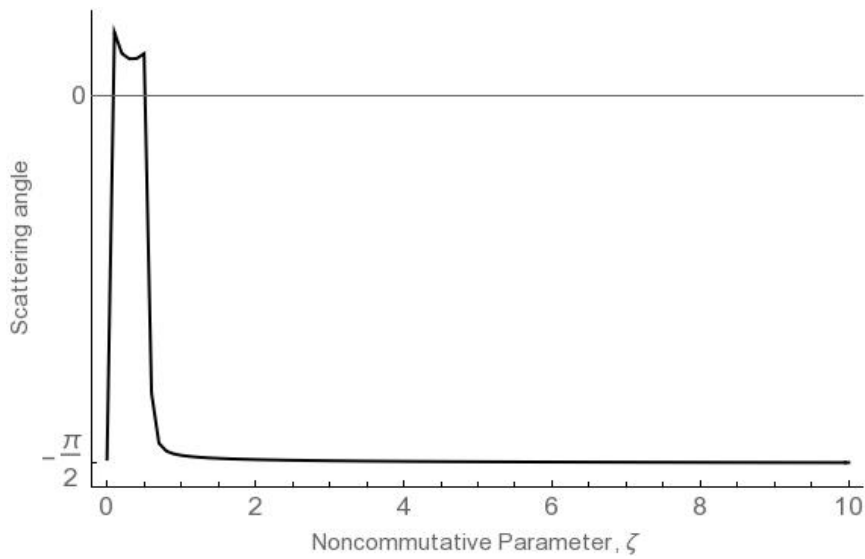


Figure 6.18: Plot of scattering angle vs. noncommutative parameter  $\zeta$  for the near orthogonal scattering, with  $b = 0.1$

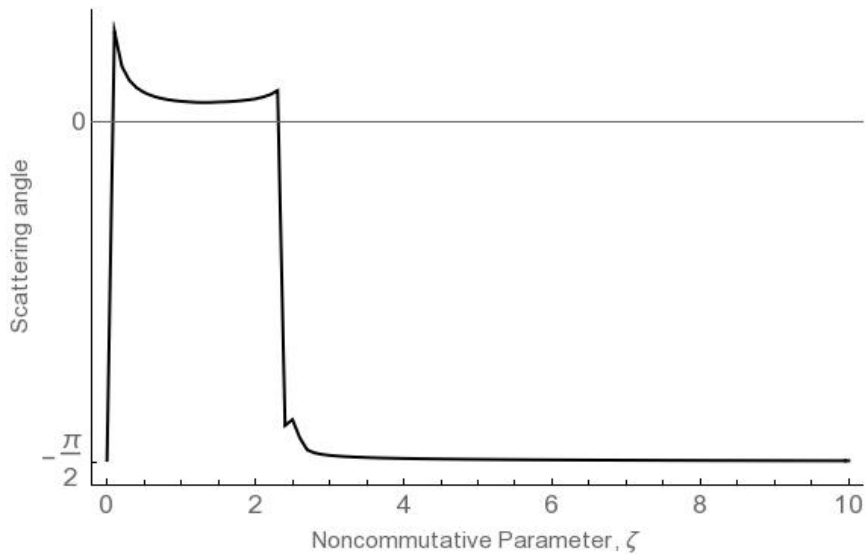


Figure 6.19: Plot of scattering angle vs. noncommutative parameter  $\zeta$  for the nearly orthogonal scattering with  $\rho = 2$  and  $b = 0.1$ , note that the plateau at the start is wider than figure 6.18, where  $\rho = 1$

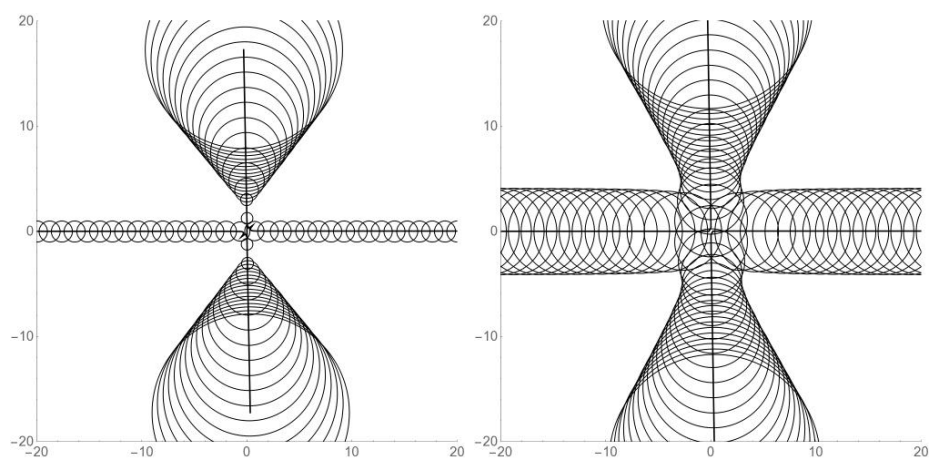


Figure 6.20: Examples of scattering behaviour for the orthogonal scattering with  $b = 0$  for  $\zeta = \{0, 2\}$ .

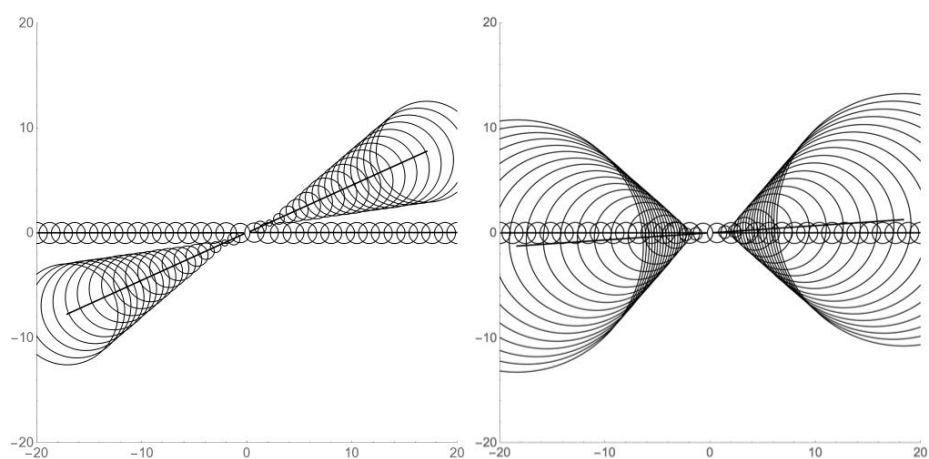


Figure 6.21: Examples of scattering behaviour for the near orthogonal scattering with  $b = \{0.1, 0.01\}$ . Note that the scattering becomes almost completely repulsive for the smaller values of  $b$

However if  $\zeta$  is small these will be very similar and we can do an approximate analysis provided that  $2\zeta/\rho$  is small. There are in theory three separate cases; where  $\zeta$  is small compared to the distance between the instantons (which is twice the impact parameter), where it is comparable to the impact parameter, and where it is large. These are shown in figures 6.22 and 6.23. It turned out the pattern of behaviour was similar in all these cases, and is discussed in figure 6.24. Finally, I conducted a similar analysis varying both  $\dot{\rho}$  and  $\dot{\theta}$ . This showed similarly interesting behaviour in both cases, and so I will discuss them together. As can be seen in figures 6.26 and 6.28, in both cases, a small perturbation in  $\dot{\rho}$  and  $\dot{\theta}$  causes almost orthogonal scattering, no matter what the initial scattering angle. The difference is that, as shown in figure 6.29, there is a jump in the chirality of the scattering for positive and negative  $\dot{\theta}$ , which is not present for  $\dot{\rho}$ . Even if there is no scattering in the ‘base’ case where both are zero, as in figure 6.13, we still get the same orthogonal scattering behaviour (figure 6.27), however there is not the same jump in chirality at the origin. The reason for this behaviour seems to be that changing either of these parameters from zero makes the instanton size very large, causing a high degree of interaction (and hence orthogonal scattering) no matter what the initial separation is. There is a subtlety in that  $\dot{\rho}$  is not the variation in the actual size, but only in the parameter  $\rho$ . The variation in the actual size is give by

$$\dot{\tilde{\rho}} = \frac{\dot{\rho}\rho - \frac{4\zeta^2\dot{\rho}}{\rho^3}}{\sqrt{\rho^2 + \frac{4\zeta^2}{\rho^2}}} \quad (6.2.2)$$

Therefore  $\dot{\tilde{\rho}}$  is a good approximation when  $2\zeta/\rho$  is small. I have been careful to only consider such cases

### 6.3 Dyonic Instantons

If we move to consider Dyonic Instantons, we again see that the noncommutative parameter initially introduces a repulsive effect (figures 6.30 and 6.31). Here, the basic values of the parameters are as in the pure case, except that we give  $\theta$  a

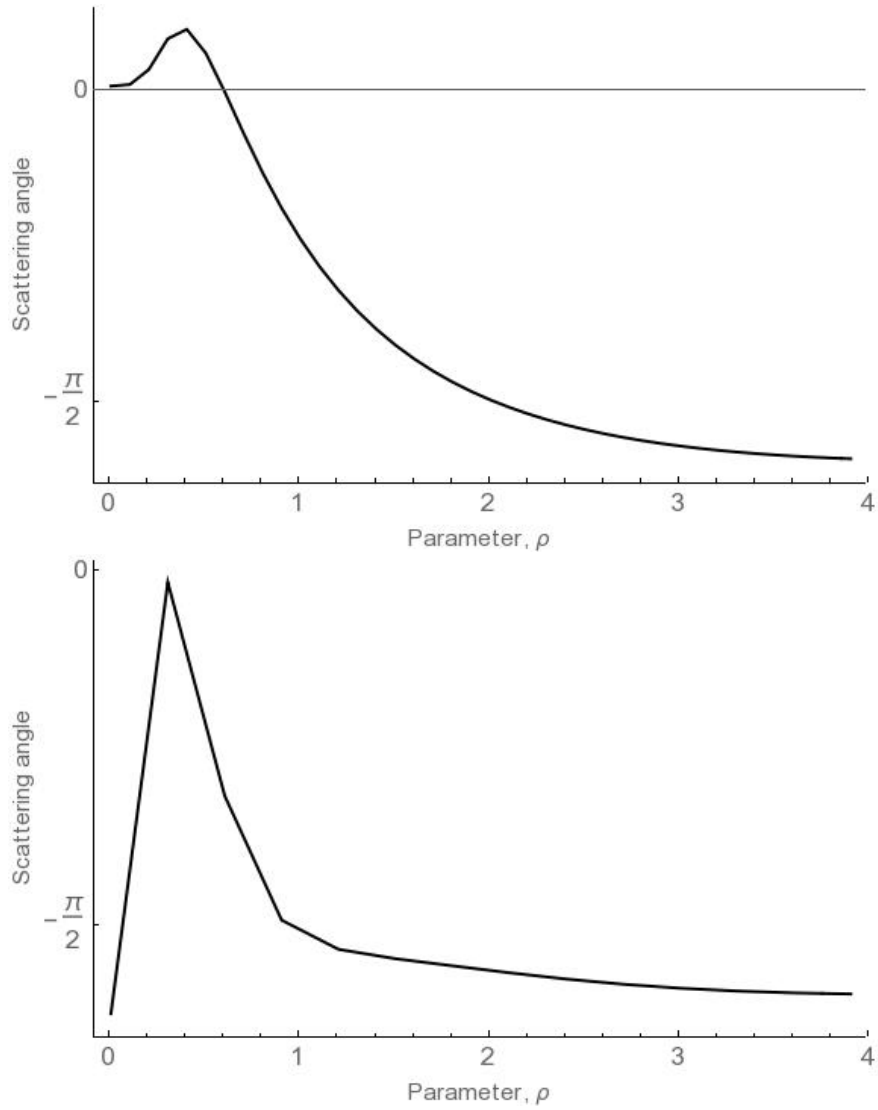


Figure 6.22: Graphs of scattering angle vs. initial Instanton size for  $\zeta = 0$  (above), and  $\zeta = 0.3$  (below). As the distance between the Instantons is 1, this represents the case where  $\zeta$  is small compared to the separation. The true size of the Instanton is within 12% of the  $\rho$  after  $\rho = 0.6$ , which is about the top of the peak in the below graph. I therefore assume the graph is reliable after this point.

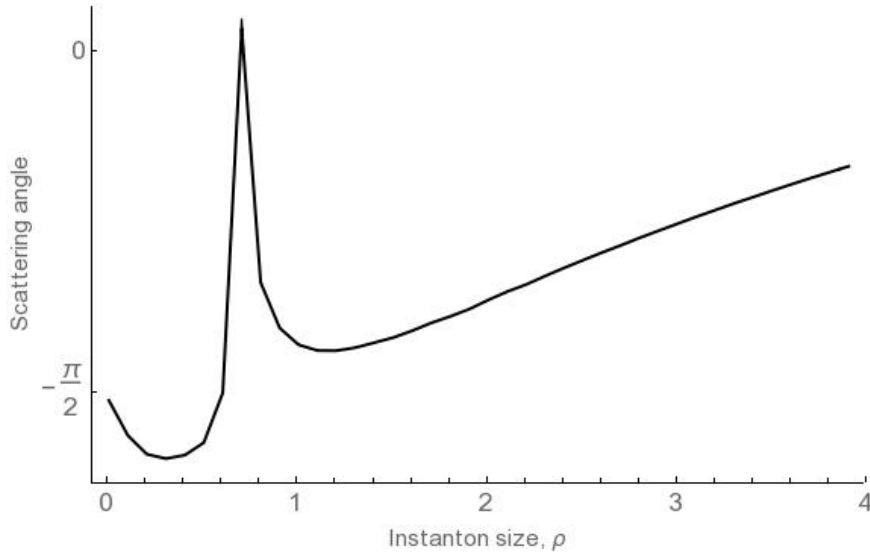


Figure 6.23: Graphs of scattering angle vs. initial Instanton size for  $\zeta = 0.3$ , and  $b = 0.05$ . This represents the cases where  $\zeta$  is greater than the separation. This is shown specifically in figure 6.24. Again, after the initial peak. After the peak, the true size is within 17% of the parameter  $\rho$ , and so the graph is a good description. Hence the qualitative behaviour is the same as in the non-commutative case in figure 6.22

small initial velocity of 0.1 in order to avoid numerical issues. Any changes to these parameters will be discussed in the captions to the graphs. As discussed in [1], Dyon Instantons oscillate along their motion, and this effect is much more observable with the non commutativity turned on. The repulsion seems to be strong enough to significantly change the behaviour (figure 6.32). For higher values of zeta there seems to be a lot of variation in the scattering angle, though this may just be numerical noise (see figure 6.33). In this graph, there does not seem to be any equivalent to the spike which appeared when plotting the scattering angle vs. impact parameter for the pure instanton. However general features of plotting scattering angle vs.  $\zeta$  for different values of the impact parameter are initial spikes – which do not seem to correspond to anything interesting, an extended period of little change where the instantons repel almost completely, and a region of large variation in angle, in which there is a mix of behaviour – including orbiting behaviour. This is shown for the case  $b = 0.5$  in figure 6.34.

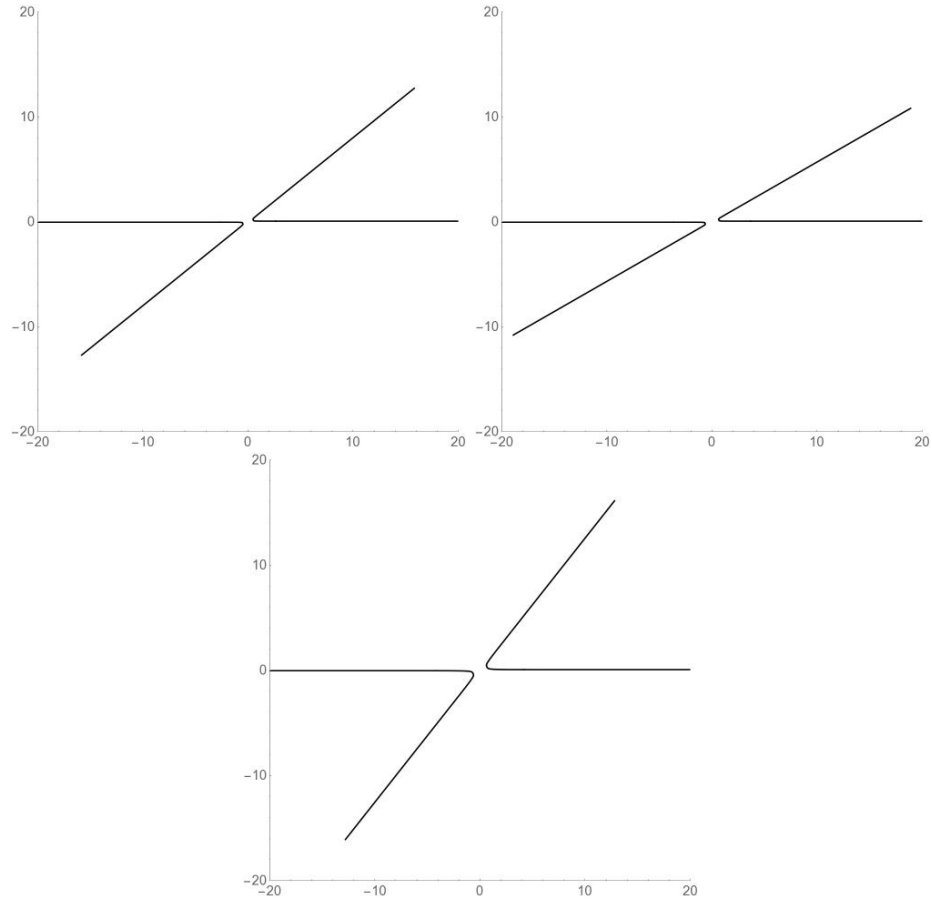


Figure 6.24: This is the evolution of the  $\zeta = 0.3$  system introduced in figure 6.23, for  $\rho = \{0.8, 1.2, 4\}$ . As seen in that figure, the scattering angle decreases slightly to begin with, then increases with the parameter  $\rho$

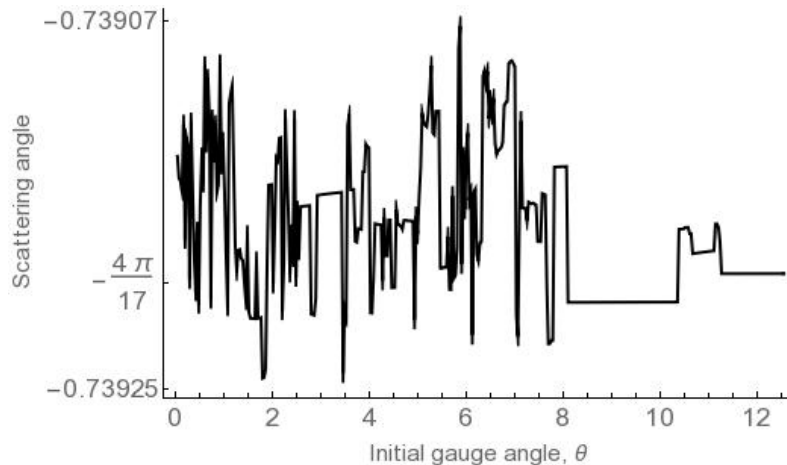


Figure 6.25: Graph showing variation of scattering angle vs. gauge angle  $\theta$  for  $b = 0.5$  and  $\zeta = 2$ . As can be seen, there is very little change in the angle for different  $\theta$  – the overall change is of the order of 0.0001. This is almost certainly just numerical noise, and the true scattering angle remains effectively constant

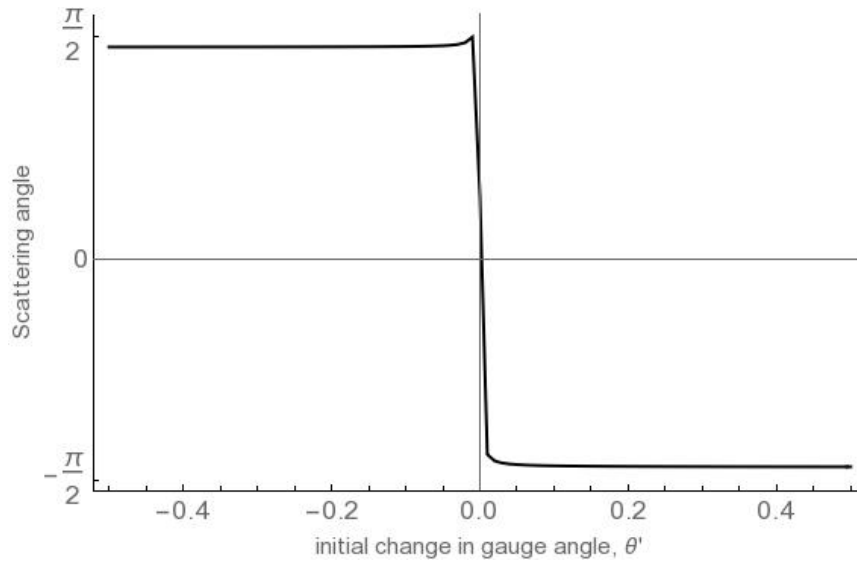


Figure 6.26: Graph showing variation of scattering angle vs. gauge angle  $\theta$  for  $b = 0.5$  and  $\zeta = 1$ . As show in figure 6.29 the jump at the origin is real, and involves a switch in the chirality of the scattering

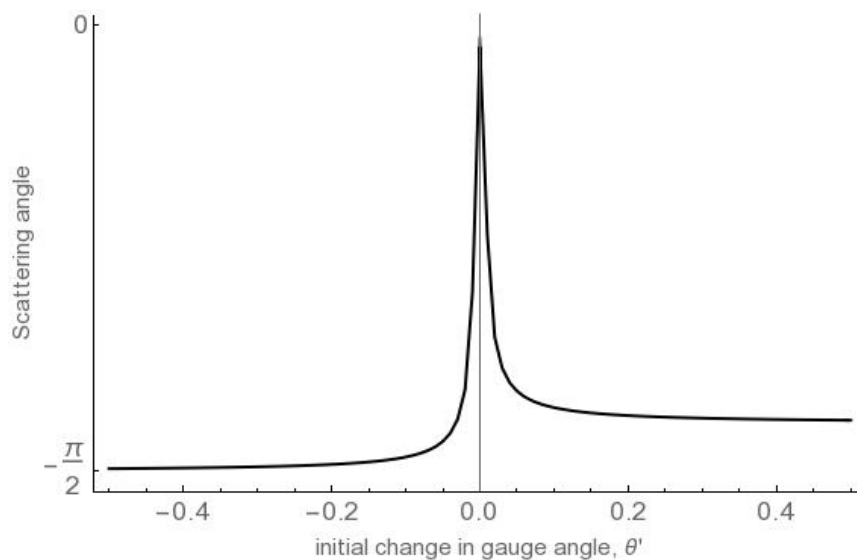


Figure 6.27: Graph showing variation of scattering angle vs. gauge angle  $\theta$  for  $b = 4$  and  $\zeta = 1$ . Note that here there is no jump in the chirality. I have checked this explicitly

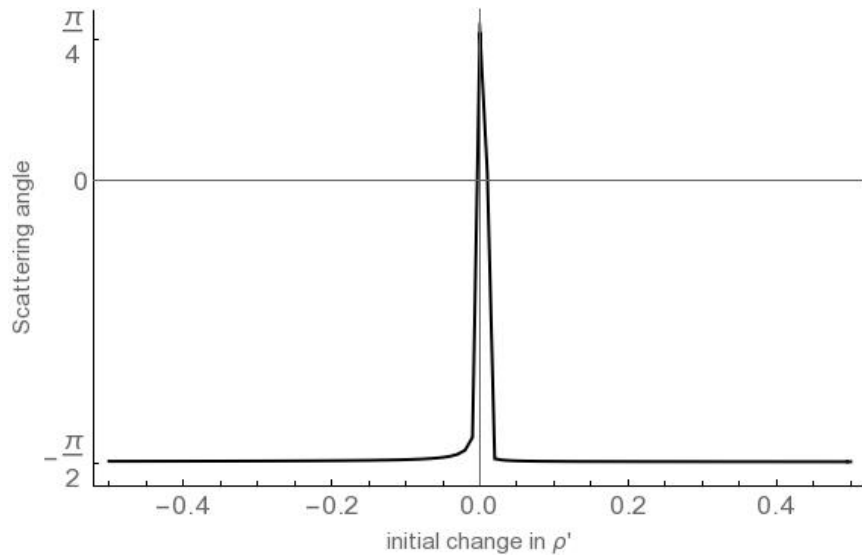


Figure 6.28: Graph showing variation of scattering angle vs. gauge angle  $\theta$  for  $b = 0.5$  and  $\zeta = .1$ . Note that here there is no jump in the chirality, unlike in the case of  $\dot{\theta}$

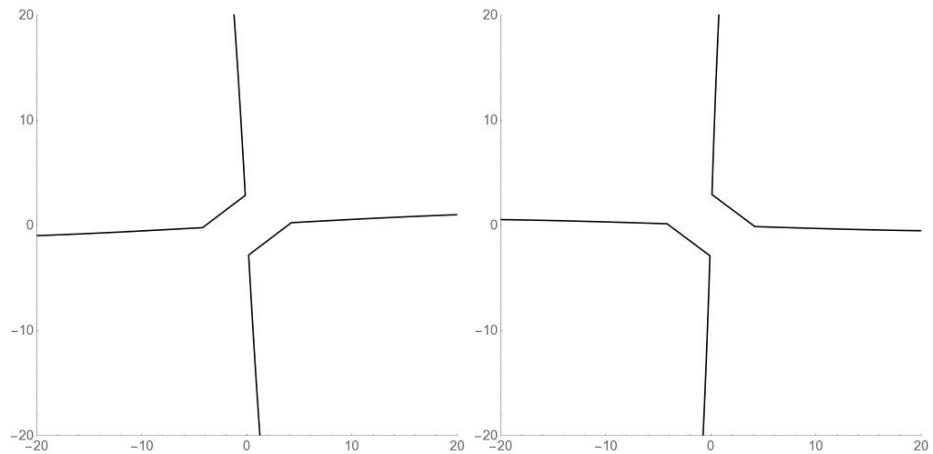


Figure 6.29: Graph showing examples of scattering for cases from figure 6.26. Here,  $\dot{\theta} = -0.2$  on the left, and  $0.2$  on the right. Note the chirality of the scattering has reversed, confirming the discontinuity shown in figure 6.26 is physical



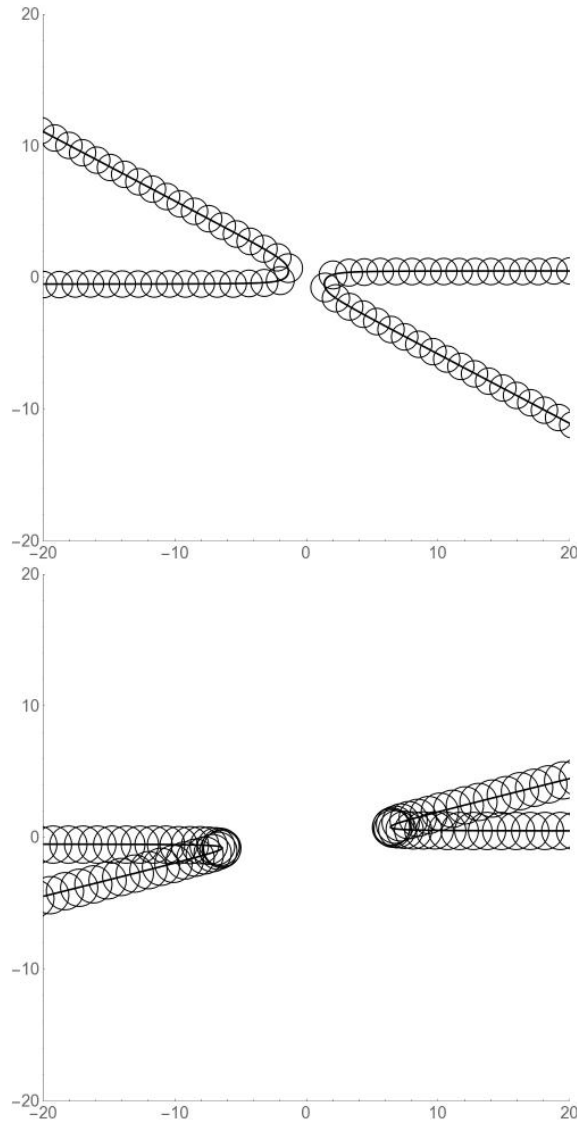


Figure 6.30: Plot of dyonic instanton scattering for  $b = 0.5$ ,  $|q| = 0.1$ ,  $\zeta = 0$  (above),  $\zeta = 0.5$  (below)

However there are some more noteworthy features when plotting the scattering angle vs. the magnitude for the potential  $|q|$ . Recall that for the Dyonic Instanton solutions to be valid we require  $q \ll 1$ . For small zeta, there seems to be no discernible pattern, similar to the commutative case (figure 6.35). However, if we increase  $\zeta$  a distinctive pattern emerges (figure 6.36). I have observed it at  $\zeta = \{0.2, 0.5, 1\}$ . However, the pattern disappears and becomes random noise again by  $\zeta = 2$ . For the graphs where the pattern is present, after some initial fluctuation, the instanton scattering angle increases rapidly and becomes very stable. Zooming in on the very small  $q$  region where the fluctuation occurs, we find a high variation in scattering

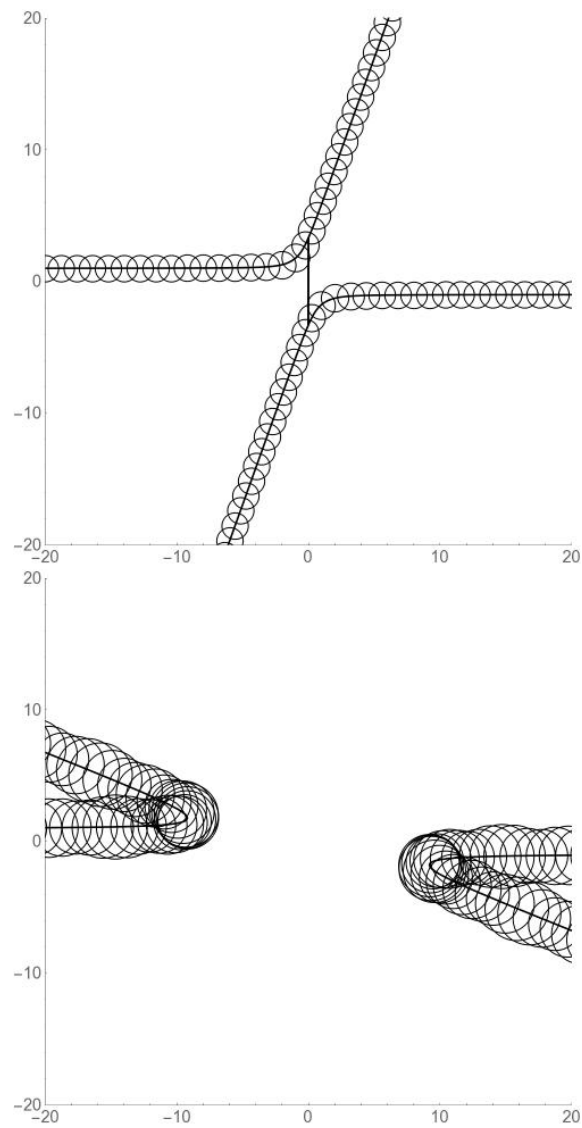


Figure 6.31: Plot of dyonic instanton scattering for  $b = -1$ ,  $|q| = 0.1$ ,  $\zeta = 0$  (above),  $\zeta = 1$  (below). Note the visible oscillations on the right hand graph.

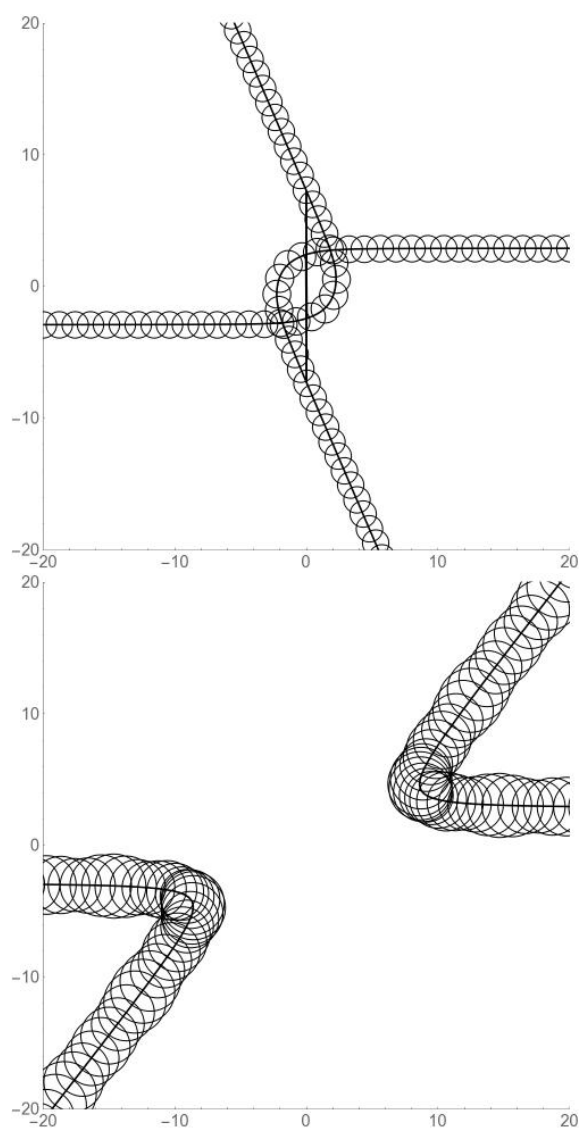


Figure 6.32: Plot of dyonic instanton scattering for  $b = 2.9$ ,  $|q| = 0.1$ ,  $\zeta = 0$  (above),  $\zeta = 1$  (below).

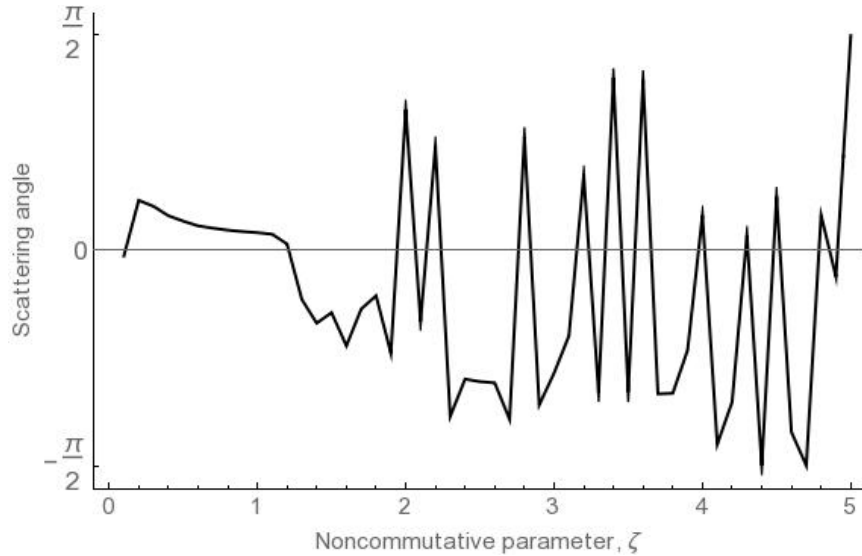


Figure 6.33: Graph of scattering angle vs. noncommutative parameter  $\zeta$  for  $b = 0.5$ . Particular scattering examples from this graph are discussed in figure 6.34

angle, as seen in figure 6.37, though with an overall increasing pattern. Investigation reveals a certain amount of orbiting behaviour, of which the most spectacular example is in figure 6.38.

We can then systematically look for interesting behaviour amongst the remaining parameters. In the Dyonics case, the length scale is still set by the  $\zeta$ , however the scale of the time dimension is no longer arbitrary, but is set by  $|q|$ . Therefore we must consider both.

I started by looking at varying  $\theta$ , but this did not yield any interesting systematic behaviour – only random noise. I then looked at  $\rho$ . Here there seemed to be a window where the behaviour matched the commutative case, e.g. with  $\zeta = 0.1$  and  $q = 0.1$ , as shown in figure 6.39 which has the same kind of shape as in figure 6.22. Exploring around that point showed that the behaviour persisted with roughly  $\zeta < 1$  and with  $q > 0.08$

I then moved onto looking at  $b$ . Here there was similar behaviour. At low  $\zeta$  there did not seem to be any overall pattern, however increasing  $\zeta$  led to graphs having a linear pattern, as in figure 6.40. I think that these are two examples of the same phenomenon, with very different scaling caused by the differences in the relative

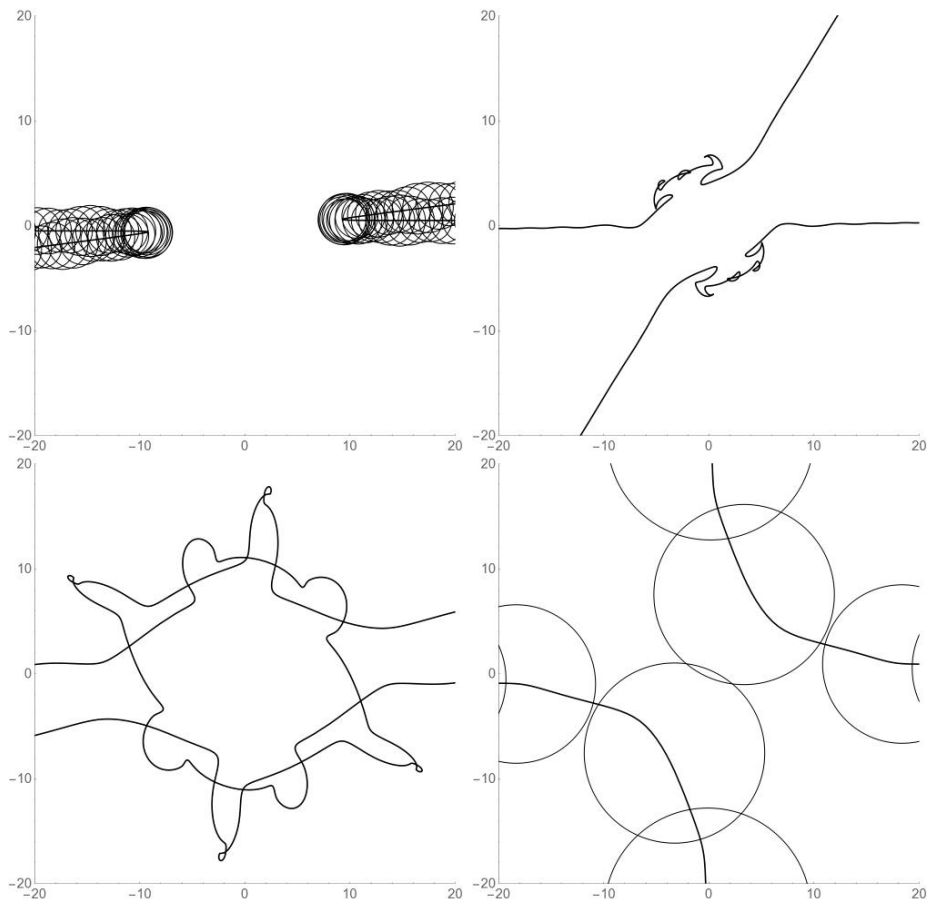


Figure 6.34: Scattering behaviour for the system presented in figure 6.33, for  $\zeta = \{1, 2, 4, 5\}$ . At  $\zeta = 1$ , corresponding to the flat part of that graph, the particles are almost completely reflected. Once the behaviour becomes more chaotic, there is a variety of behaviour with no clear pattern. Examples include deflection at  $\zeta = 2$ , some kind of orbiting at  $\zeta = 4$ , and repulsion at  $\zeta = 5$

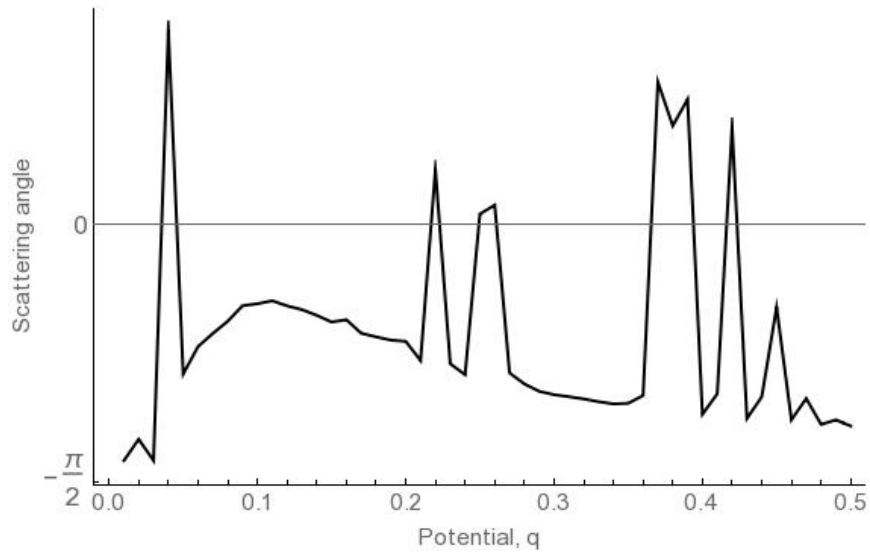


Figure 6.35: Graph showing scattering angle vs. magnitude of potential,  $q$ , in the commutative case ( $\zeta = 0$ ). The graphs for small  $\zeta$  (below 0.3 at most), and large  $\zeta$  (at least above 2) show the same behaviour. Note that these bounds are not the cut-off points, merely the lowest and highest points I have observed this behaviour.

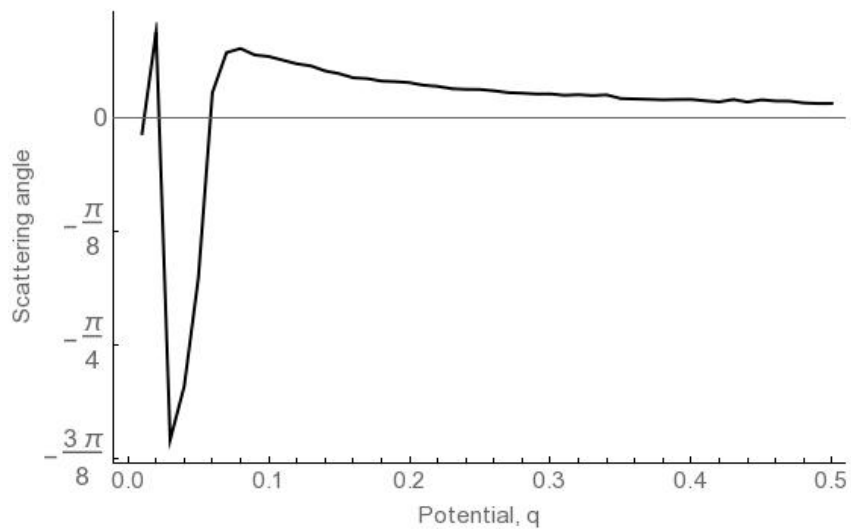


Figure 6.36: Graph showing scattering angle vs.  $q$  for  $\zeta = 0.5$ .

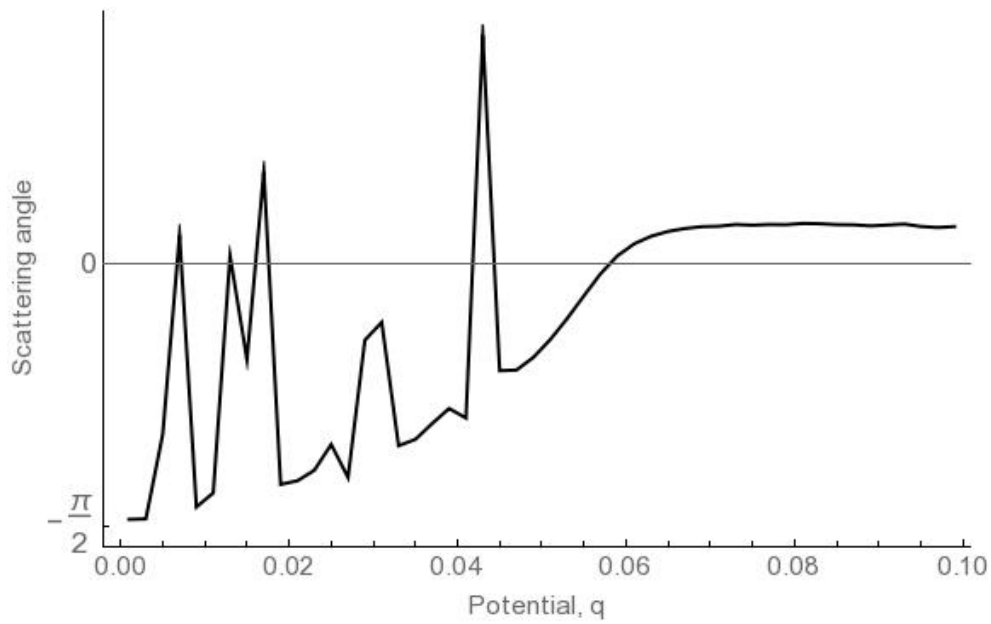


Figure 6.37: Graph showing scattering angle at very low values of  $q$  for  $\zeta = 0.5$ .

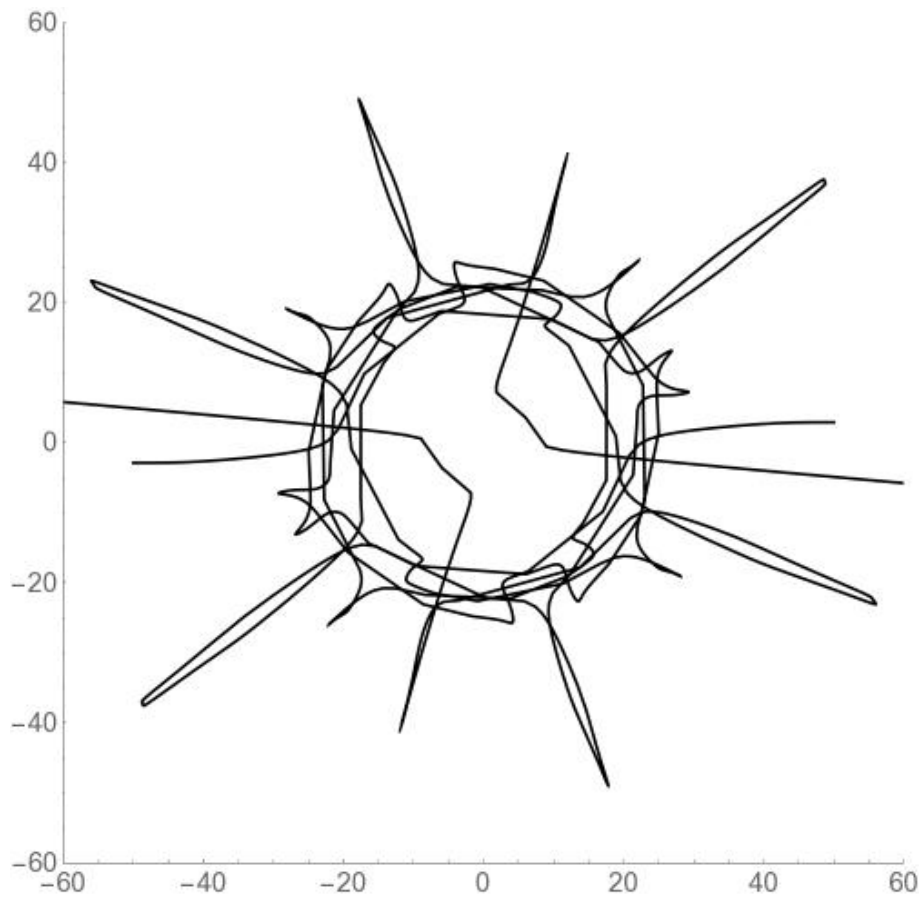


Figure 6.38: Graph of scattering with orbiting behaviour, with  $\zeta = 0.5$ ,  $b = 0.5$ ,  $q = 0.00438$

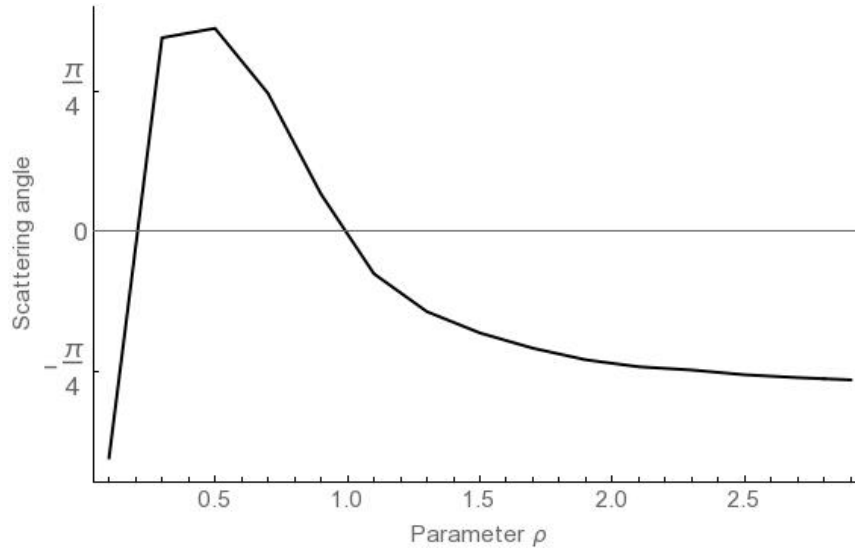


Figure 6.39: Scattering angle vs. parameter  $\rho$  for  $\zeta = q = 0.1$ . As in figures 6.22 and 6.23 I expect  $\rho$  to be a good approximation to the true initial size after the peak

values of  $\zeta$ . The magnitude of  $q$  did not seem to have a major effect on whether the patterned or non patterned behaviour was observed past a certain point, but continuing to make  $\zeta$  larger caused the non patterned behaviour to return.

The final thing is to look at  $\dot{\rho}$  and  $\dot{\theta}$ . Bear in mind though that as we have stated  $\dot{\rho}$  is the variation in the moduli space parameter  $\rho$ , not the actual size of the instanton. It is only a good approximation when  $2\zeta\rho$  is small. However, I was unable to find any non-chaotic behaviour in the region where this approximation was valid. Finally, I did not find any discernible patterns for  $\dot{\theta}$  either. I think this difference as compared to the pure case is because the potential prevents the instanton size from growing large in the dyonic case, and therefore the transition to orthogonal scattering cannot occur.

### 6.3.1 Orbiting Behaviour

We conclude this section by looking at the stability of the orbiting behaviour for some of the graphs we have found in the dyonic case. To clarify, here by, ‘orbiting behaviour’ I mean cases where the trajectory of one or both instantons moves in a roughly circular pattern around the middle of the interaction, with at least one



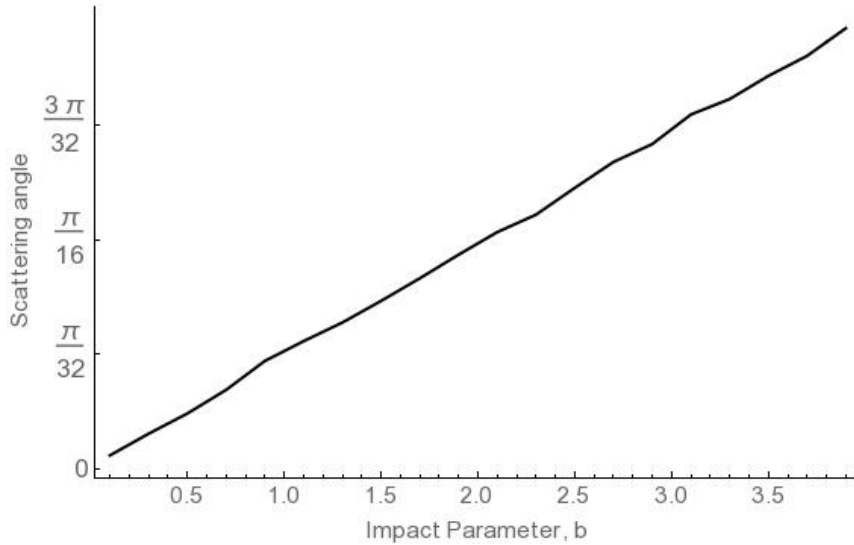


Figure 6.40: Scattering angle vs. Impact parameter for  $\zeta = q = 0.5$

rotation being completed. By stability, I mean the range of parameters for which such orbiting behaviour persists. We are interested in the stability with respect to an orbit we have already found, so are most interested in varying  $\dot{\theta}$  and  $\dot{\rho}$ . I will also see how sensitive the orbit is to the length scale set by  $\zeta$  and the time scale set by  $q$ . It should be noted that there is nothing particularly special about any of these parameters – my aim is to see, having found a solution with orbiting behaviour, how stable that solution is when we move away from it in the parameter space.

We start with the graph first found in figure 6.34. We first vary  $\dot{\theta}$ . Increasing or decreasing it slightly from 0.1 causes the orbit to vanish by 0.102 and 0.098. It was also very similar for  $\dot{\rho}$ . Here there was a definite asymmetry between positive and negative  $\dot{\rho}$ . The orbit vanishes by  $\rho = 0.005$  in the positive direction (though with complicated behaviour shown in figure 6.41) but not until -0.012 in the negative one. We now vary  $\zeta$ . The orbiting exists inside a region bounded by  $\zeta$  in the range (3.993, 4.004). This includes a rather more spectacular orbit at  $\zeta = 4.003$ , shown in figure 6.41. Finally, I found that the orbit is very sensitive to changes in  $q$ , only existing within the range (0.0998, 1.002). We now repeat this analysis for the case found in figure 6.38. First, the orbit existed for  $\dot{\rho}$  within  $(-0.21, 0.32)$  to two decimal places. It therefore seems more stable than the previous one under changes in  $\dot{\rho}$ . There is also greater stability under changes in  $\dot{\theta}$ , though here there was a

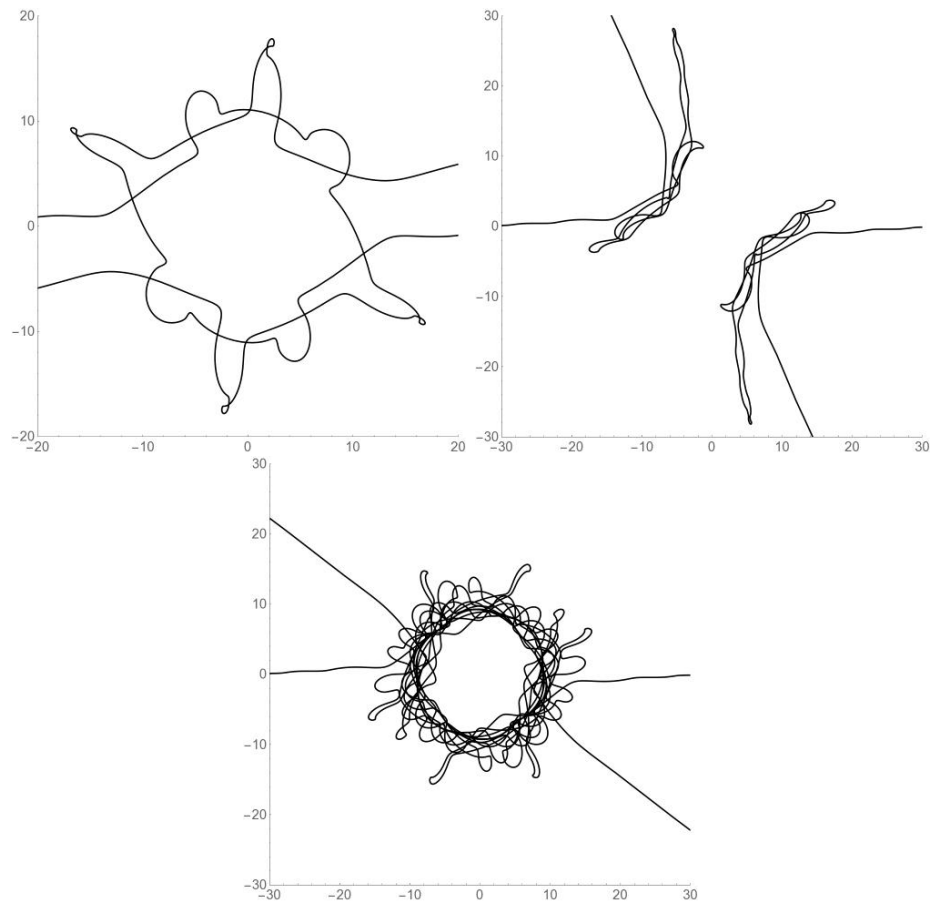


Figure 6.41: The behaviour as described in the text, varying around the first of these graphs. In that graph,  $\zeta = 4$ ,  $q = 0.1$ ,  $b = 0.5$ . The second shows the complicated repulsion behaviour for  $\rho = 0.005$ , and the third shows the orbit at  $\zeta = 0.4003$

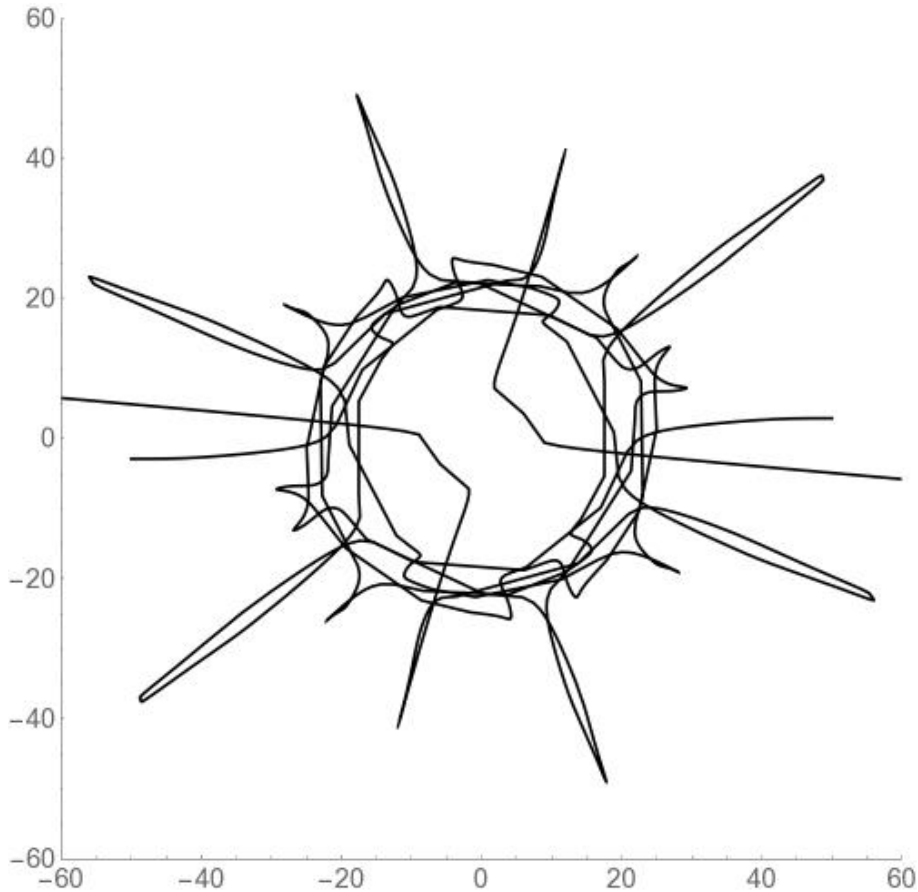


Figure 6.42: Graph of scattering with orbiting behaviour, for the case  $\zeta = 0.5$ ,  $b = 0.2.9$ ,  $q = 0.00438$ .

much greater stability if we decreased the value of  $\dot{\theta}$ , with scattering in the region  $(-0.44, 0.28)$ . Finally, we look at changing the scale via varying  $\zeta$ . Here again, this scattering seems much more stable, with orbiting observed (albeit of decreasing complexity) until  $\zeta = 3.1$  in one direction, and  $\zeta = 0.23$  in the other. This greater range of orbiting as  $\zeta$  is increased fits with the behaviour in figure 6.33 where the scattering angle seemed to vary rapidly as we increased  $\zeta$ . Finally, we look at varying  $q$ . Here, the orbit exists for a region within  $(0.0038, 0.00525)$ .

## 6.4 The Six Parameter Space

We now move on to look at the full six parameter space, where the Instantons are free to have different sizes and to vary in their gauge angle. The additional parameters add greatly to the complexity of the numerics, and we were unable to get results

using the modified code from [1] as we had in the four parameter case. Fortunately I was able to use some code written by Mr. Joe Farrow, which reformatted the metric and potential and used a more optimised method to find the moduli space geodesics, to run some simulations for this part of the moduli space. I have graphs for the pure instanton case, but was not able to make any for the Dyonic case.

There are two parameters to examine here. These are the relative gauge angle  $\phi$  and the relative sizes of the instantons. Unless otherwise stated, the initial conditions for  $\{\rho_1, \rho_2, \theta, x\}$  take the values  $\{1, 1, 0, 50\}$ , and the initial derivatives of all parameters are zero, except  $x' = -0.03$ . In the noncommutative case it is tricky to systematically explore the latter as the Instanton sizes are nonlinear functions of  $\zeta$  and the  $\rho_i$ . Therefore I chose to keep  $\zeta$  fixed to set the overall length scale, and to vary the impact parameter rather than the instanton size, looking at cases where the separation was much smaller than, larger than and of the same order as the sizes of the instantons. Initially I kept the instantons the same size. I then checked how the behaviour in three cases  $\rho_1 < b < \rho_2$ ,  $b < \rho_1 < \rho_2$  and  $\rho_1 < \rho_2 < b$ .

In the commutative case, varying the gauge angle produces a clear sinusoidal variation (figure 6.43). This pattern held for different values of the impact parameter, however when the impact parameter was small compared to the instanton size, the variation takes on more of a, ‘square’ shape (figure 6.44). As can be seen both from these two figures and from the scattering angles in figure 6.45, at  $\phi = n\pi$ , where the instantons are parallel in the gauge group, the interaction between the instantons disappears and they just move past one another. Conversely, the instantons interact most strongly at  $\phi = n\pi/2$ , where they are orthogonal in the gauge group. Changing the relative sizes of the instantons did not seem to affect this sinusoidal behaviour, but it did change the strength of the interaction, with the scattering angle decreasing when the Instantons were different sizes, with smaller sizes making the scattering angle smaller (figure 6.46).

The behaviour in the noncommutative case is not so simple. The outline of the sinusoidal pattern is still present, but it is significantly disrupted, as in figure

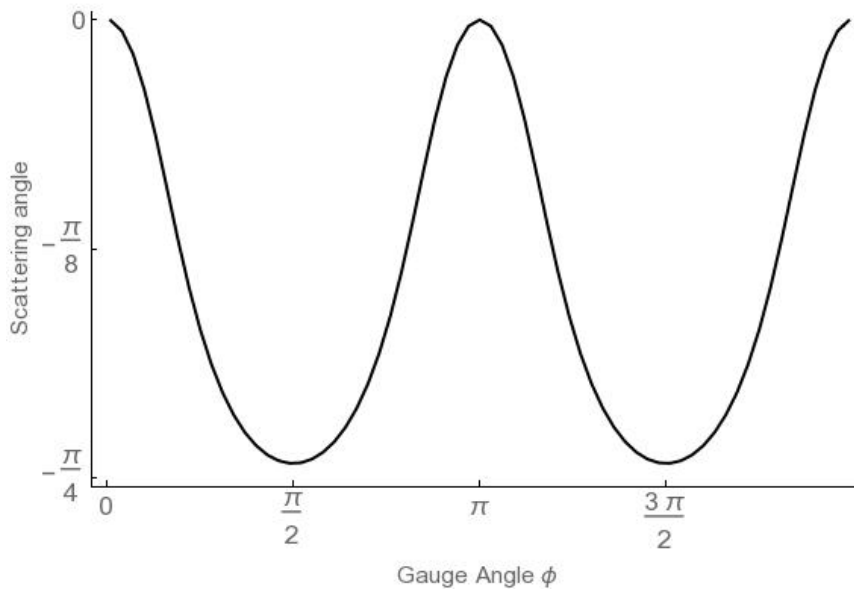


Figure 6.43: Graph showing variation of scattering angle  $\phi$  with  $\zeta = 0$ ,  $\rho_1 = \rho_2 = 1$  and  $b = 0.5$ .

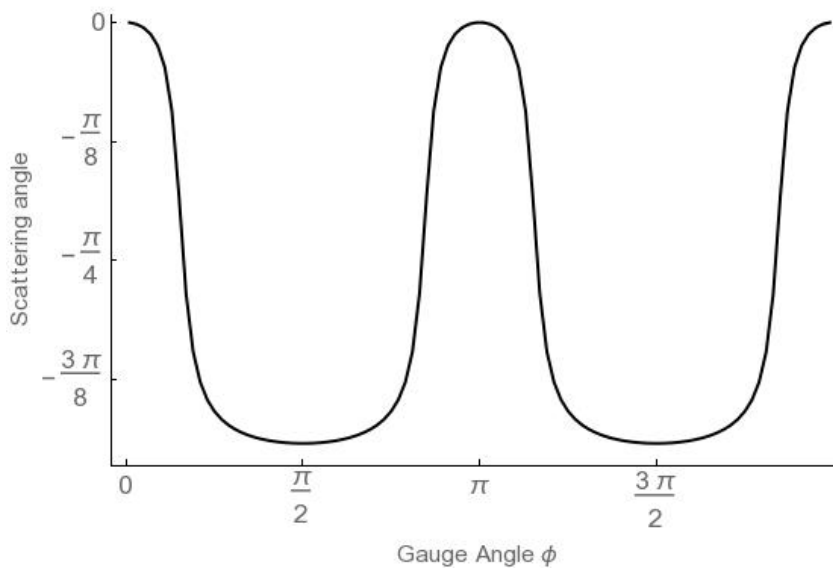


Figure 6.44: Graph showing variation of scattering angle  $\phi$  with  $\zeta = 0$ ,  $\rho_1 = \rho_2 = 1$  and  $b = 0.1$ .

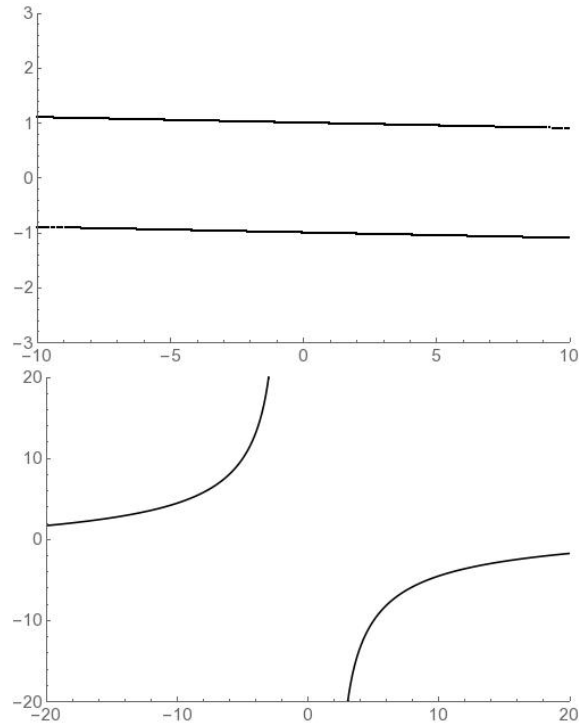


Figure 6.45: Graph showing scattering examples from figure 6.47, with  $\phi = \pi$  above and  $\phi = 3\pi/2$  below. Note that the scales are different on the two graphs, and that the behaviour is extremely different.

6.47. Increasing the impact parameter somewhat restores the behaviour (figure 6.48). There is therefore much less variation in the scattering angle for the noncommutative case, as can be seen in figure 6.49. The Instantons also no longer stop interacting when they are parallel in the gauge group, instead oscillating between minimum and maximum scattering angles, as in figure 6.50. Making one of the instantons smaller than the other and the impact parameter did not seem to have too much of an effect, however, making one larger than the impact parameter further disrupted the sinusoidal pattern, as in figure 6.51.

## 6.5 Conclusions

I shall end this section by reviewing the main results. I looked at both the full six parameter space, and also a four parameter subspace where the instantons were orthogonally embedded in the gauge group. This was necessary to analyse the dyonic

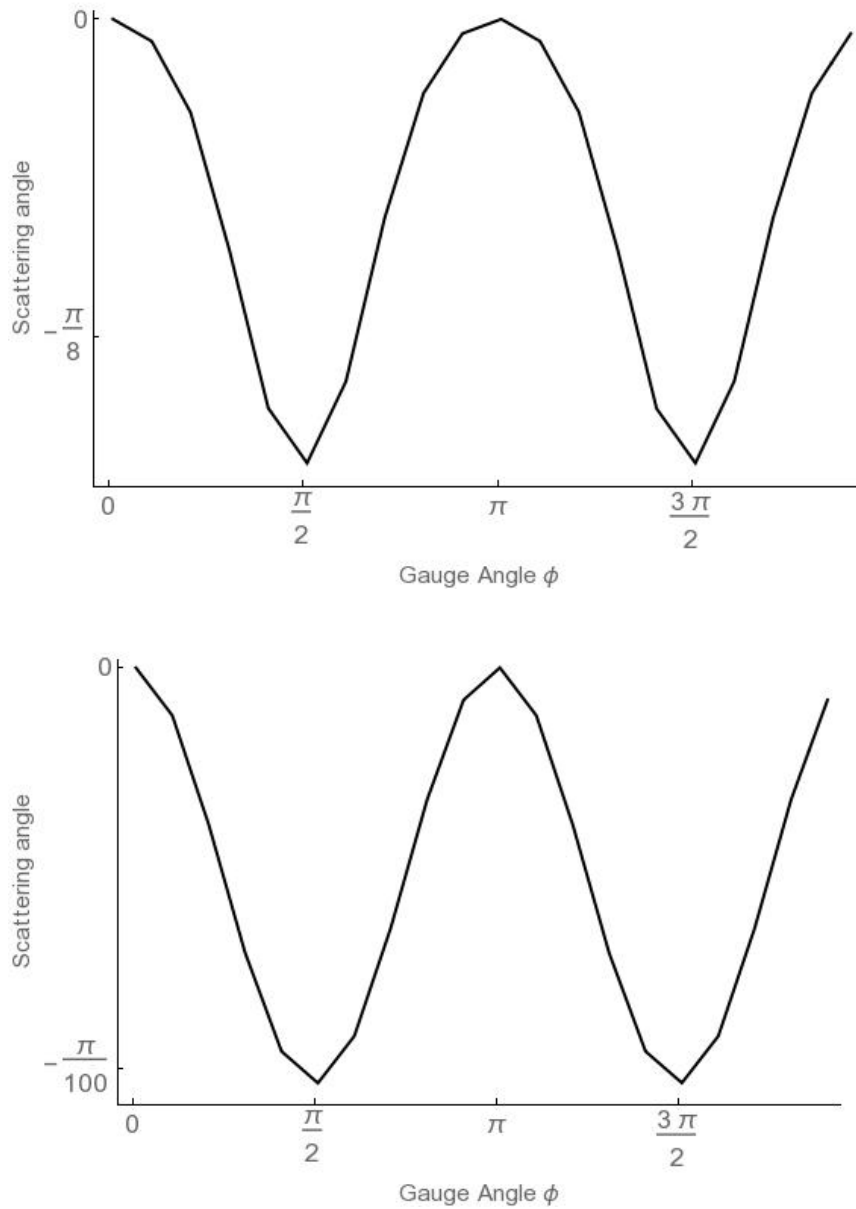


Figure 6.46: Graph showing variation of scattering with gauge angle  $\phi$ , where  $\zeta = 0$  and  $b = 0.5$ . In both graphs  $\rho_1 = 1$ . In the top graph,  $\rho_2 = 5$ , and in the bottom graph  $\rho_2 = 0.1$ . Note that the scattering angle is much smaller in this case.

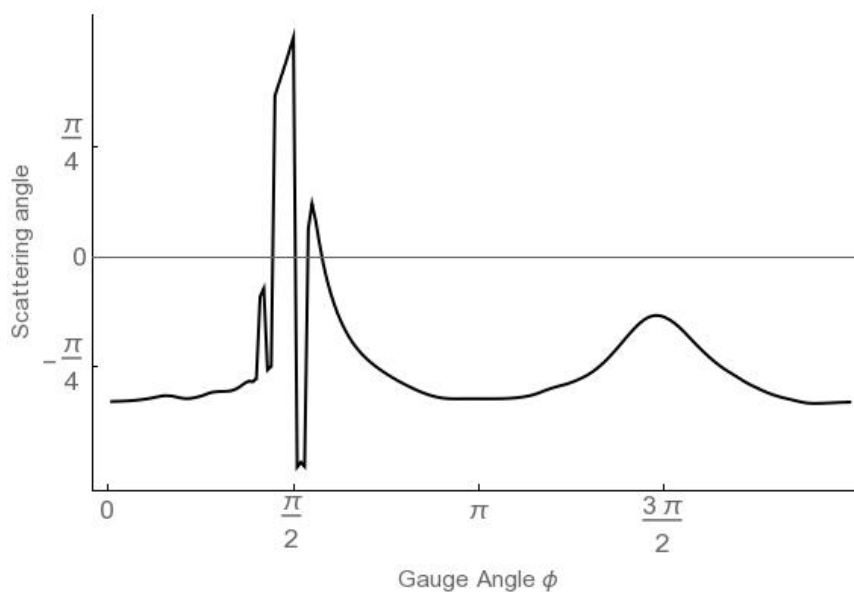


Figure 6.47: Graph showing variation of scattering angle  $\phi$  with  $\zeta = 1$ ,  $\rho_1 = \rho_2 = 1$  and  $b = 0.5$ . The true instanton size is therefore  $\sqrt{2}$ , and so is roughly comparable to the separation. The splitting of the left peak appears to be a numerical error.

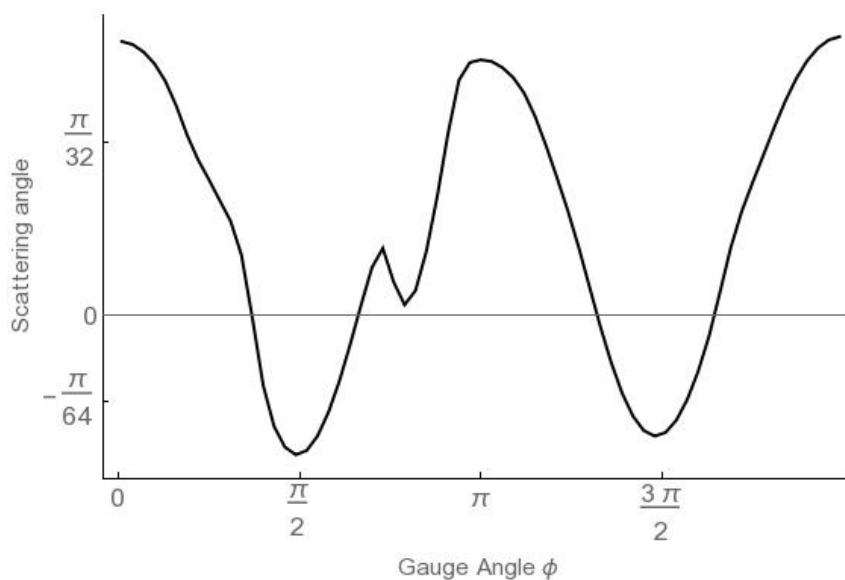


Figure 6.48: Graph showing variation of scattering angle  $\phi$  with  $\zeta = 1$ ,  $\rho_1 = \rho_2 = 1$  and  $b = 4$ . The true instanton size is therefore  $\sqrt{2}$ , and so is much smaller than the separation. Note that the sinusoidal form is much more preserved, but now oscillates around zero rather than away from it



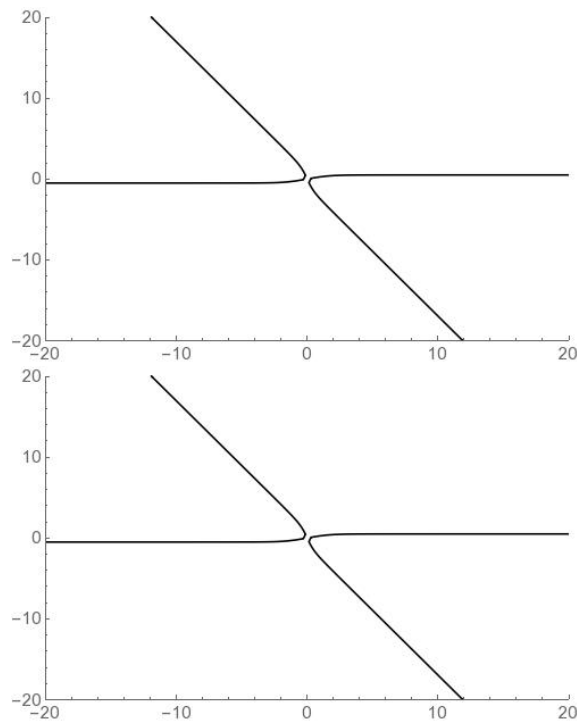


Figure 6.49: Graph showing scattering examples from figure 6.47, with  $\phi = \pi$  above and  $\phi = 3\pi/2$  below. Note that there is very little difference.

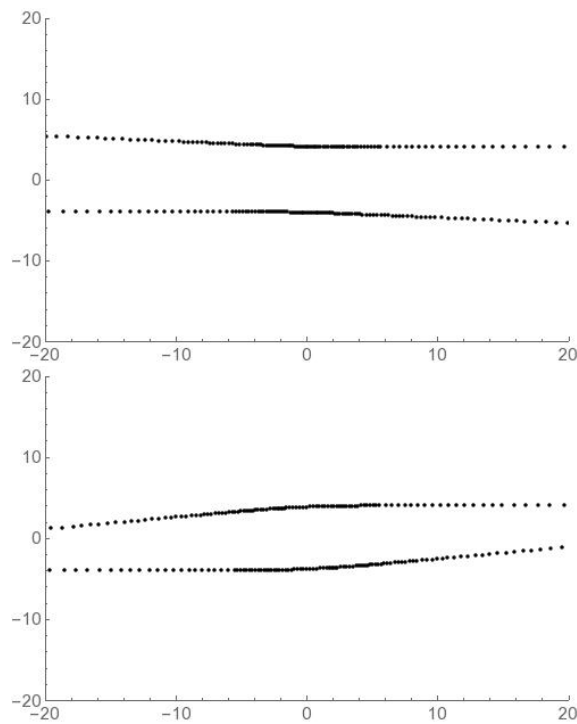


Figure 6.50: Graph showing scattering examples from figure 6.48, with  $\phi = \pi$  above and  $\phi = 3\pi/2$  below

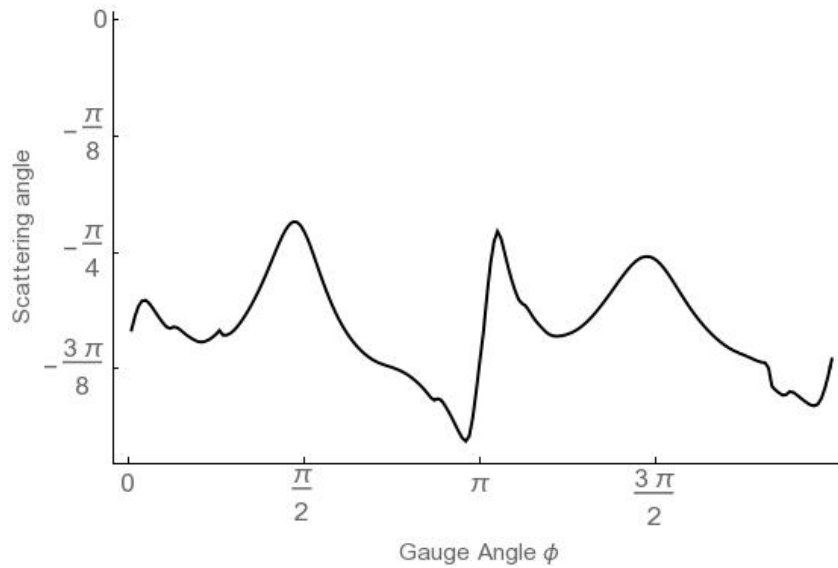


Figure 6.51: Graph showing variation of gauge angle  $\phi$  with  $\zeta = 1$ ,  $\rho_1 = 1$ ;  $\rho_2 = 5$  and  $b = 0.5$ . The true instanton sizes are  $\sqrt{2}$  and just over 25 respectively.

case. Overall, increasing the noncommutative parameter  $\zeta$  increases the repulsion between the instantons. The form this takes is not straightforward, and in the pure instanton case involves a peak with strange behaviour which requires a future, more detailed analysis with more sophisticated plotting programmes. However in general even if the instantons begin by not interacting, they move from glancing off each other, to reflecting entirely as the parameter  $\zeta$  increases.

We found that orthogonal scattering was present in the noncommutative case as well as the commutative case, and postulated an analytical reason for this. Systematically looking at the other parameters, We saw that, as expected, increasing  $\rho$  strengthens the repulsive effect of the scattering, and increasing the separation  $b$  decreases it. Further interesting behaviour was observed seeing how the scattering changed when the quantities  $\dot{\rho}$  and  $\dot{\theta}$  were varied. For any non- zero value of these initial velocities, the scattering rapidly became almost orthogonal. This seems to be because making these parameters nonzero causes a rapid increase in the instanton size, and hence a very strong interaction.

This behaviour is not found in the dyonic case; probably because the presence of the

potential suppresses the instanton size. In the dyonic case there was the additional feature of orbiting behaviour, some of a high winding number and great complexity. Finally, we were able to use the six parameter pure instanton case to analyse changing the gauge embedding. In general we found that the scattering oscillated with the gauge angle, but that this was suppressed as  $\zeta$  was increased.

# Chapter 7

## Three Instantons

We now move on to the case of three instantons in  $SU(2)$  Yang Mills. Here we only consider a commutative background, not a noncommutative one. We also use the usual version of the commutative ADHM construction with the quaternions rather than the biquaternion construction outlined above. This is because the additional complexity of the three instanton case means it makes sense to use the simplest version of the equations. As before, we begin by solving the ADHM constraints. We then calculate the scalar field for the dyonic case and use this to calculate the moduli space potential. Finally, I then calculate the moduli space metric. The results in this section are completely original. There is, however, some related work in [13] and its related papers. Here, some three monopole solutions are found, using two methods involving writing the solution as a reduction of the ADHM equations. The first method is to use the JNR ansatz. This corresponds to taking  $\Omega$  to be diagonal in our notation. The second is to calculate Axial monopoles using ADHM data which has axial symmetry imposed on it via the Manton- Sutcliffe method. In our notation, there is a non-diagonal but specific form for  $\Omega$ , and the instanton size  $v$  is chosen to be zero. These specific symmetries do not seem to match the ones I have chosen, and hence it is not immediately clear how the results in that thesis relate to those presented here, but it would be interesting and worthwhile to pursue this in future work.

## 7.1 Solving the $O(3)$ equations

Since we are in the commutative case, we need to solve the equation  $\Delta^\dagger \Delta = 0$ . For three instantons in  $SU(2)$  Yang Mills, the ADHM data  $\Delta$  is

$$\begin{bmatrix} \Lambda \\ \Omega \end{bmatrix} = \begin{bmatrix} u & v & w \\ \tau_1 & \sigma_1 & \sigma_2 \\ \sigma_1 & \tau_2 & \sigma_3 \\ \sigma_2 & \sigma_3 & \tau_3 \end{bmatrix} \quad (7.1.1)$$

where the entries of  $\Delta$  all lie in  $\mathbb{H}$ . With  $\Delta$  as given above, we have three equations, one for each component of  $o(3)$ . These are

$$\begin{aligned} \operatorname{Im}_{\mathbb{C}}(\bar{u}v + (\bar{\tau}_1 - \bar{\tau}_2)\sigma_1 + \bar{\sigma}_2\sigma_3) &= 0 \\ \operatorname{Im}_{\mathbb{C}}(\bar{u}w + (\bar{\tau}_1 - \bar{\tau}_3)\sigma_2 + \bar{\sigma}_1\sigma_3) &= 0 \\ \operatorname{Im}_{\mathbb{C}}(\bar{v}w + (\bar{\tau}_2 - \bar{\tau}_3)\sigma_1 + \bar{\sigma}_1\sigma_2) &= 0 \end{aligned} \quad (7.1.2)$$

Note that these are now nonlinear in the ADHM data. I was unable to find a solution on the full quaternion moduli space; however, if we restrict to the complex subspace as in the noncommutative 2 instanton case, and use the three residual symmetries to set the real parts of the  $\sigma_i$  to zero, the terms in  $\operatorname{Im}(\bar{\sigma}_i\sigma_j)$  vanish, and we can solve as

$$\begin{aligned} \sigma_1 &= \frac{\tau_1 - \tau_2}{|\tau_1 - \tau_2|^2} \left( \alpha - \operatorname{Im}_{\mathbb{C}}(\bar{u}v) \right) \\ \sigma_2 &= \frac{\tau_1 - \tau_3}{|\tau_1 - \tau_3|^2} \left( \beta - \operatorname{Im}_{\mathbb{C}}(\bar{u}w) \right) \\ \sigma_3 &= \frac{\tau_2 - \tau_3}{|\tau_2 - \tau_3|^2} \left( \gamma - \operatorname{Im}_{\mathbb{C}}(\bar{v}w) \right) \end{aligned} \quad (7.1.3)$$

For constants  $\alpha, \beta, \gamma$ . These are then constrained by the condition  $\operatorname{Re}_{\mathbb{C}}(\sigma_i) = 0$  to be

$$\begin{aligned} \alpha &= -\frac{\operatorname{Im}_{\mathbb{C}}(\tau_1 - \tau_2)\operatorname{Im}_{\mathbb{C}}(\bar{u}v)}{\operatorname{Re}(\tau_1 - \tau_2)} \\ \beta &= -\frac{\operatorname{Im}_{\mathbb{C}}(\tau_1 - \tau_3)\operatorname{Im}_{\mathbb{C}}(\bar{u}w)}{\operatorname{Re}(\tau_1 - \tau_3)} \end{aligned}$$

$$\gamma = -\frac{\text{Im}_{\mathbb{C}}(\tau_2 - \tau_3)\text{Im}_{\mathbb{C}}(\bar{v}w)}{\text{Re}(\tau_2 - \tau_3)} \quad (7.1.4)$$

The minus sign comes from the fact that each  $\text{Im}_{\mathbb{C}}$  comes with a  $\sigma_3$ , which multiply together to give  $-1$ . The above equations give a solution for the complex subspace. We can now move on to the scalar field

## 7.2 The Scalar Field

As in the 2 Instanton case the expressions derived here for the scalar field, metric and potential are in principle valid for the full quaternion parametrisation. However when we substitute in the solutions for the  $\sigma_i$  derived above, that is only valid for that particular complex subspace. Keeping this in mind, we use the same method as before. This time the ansatz is given by

$$\mathcal{A} = \begin{bmatrix} \mathbf{q} & 0 \\ 0 & P \end{bmatrix} \quad (7.2.1)$$

Where  $\mathbf{q} \in su(2)$ , and  $P \in o(3)$ , parametrised as

$$\begin{bmatrix} 0 & -a & b \\ a & 0 & -c \\ -b & c & 0 \end{bmatrix} \quad (7.2.2)$$

The ADHM data  $\Delta$  is given, in this case, by

$$\begin{bmatrix} u & v & w \\ \tau_1 & \sigma_1 & \sigma_2 \\ \sigma_1 & \tau_2 & \sigma_3 \\ \sigma_2 & \sigma_3 & \tau_3 \end{bmatrix} \quad (7.2.3)$$

Where  $\tau_1 + \tau_2 + \tau_3 = 0$ . Now the elements are all quaternions, not complex quaternions.

The equation we want to solve is still

$$2\text{Tr}_2(\Lambda^\dagger \mathbf{q} \Lambda) + \text{Tr}_2([\Omega^\dagger, P]\Omega - \Omega^\dagger[\Omega, P]) - \text{Tr}_2(\{P, \Lambda^\dagger \Lambda\}) = 0 \quad (7.2.4)$$

Proceeding as in the previous cases (see Appendix D for more details), we can solve for the components of  $\mathcal{A}$  as

$$\begin{aligned}
a &= \frac{1}{\Upsilon} \left( C_3(2\Psi_2 M_{A2} - \Psi_1 \Psi_3) + C_2(2\Psi_1 M_{A3} - \Psi_2 \Psi_3) + C_1 \left( - \left( 4M_{A2} M_{A3} - \Psi_3^2 \right) \right) \right) \\
b &= \frac{1}{\Upsilon} \left( - C_3(\Psi_1 \Psi_2 + 2M_{A1} z) + C_1(2\Psi_1 M_{A3} - \Psi_2 \Psi_3) - C_2 \left( 4M_{A1} M_{A3} - \Psi_2^2 \right) \right) \\
c &= \frac{1}{\Upsilon} \left( - C_3 \left( 4M_{A1} M_{A2} - \Psi_1^2 \right) - C_2(\Psi_1 \Psi_2 + 2M_{A1} \Psi_3) + C_1(2\Psi_2 Y - \Psi_1 \Psi_3) \right)
\end{aligned} \tag{7.2.5}$$

Where

$$\begin{aligned}
C_1 &= 4\text{Re}_{\mathbb{H}}(\bar{v}\mathbf{q}u) \\
C_2 &= 4\text{Re}_{\mathbb{H}}(\bar{u}\mathbf{q}w) \\
C_3 &= 4\text{Re}_{\mathbb{H}}(\bar{w}\mathbf{q}v) \\
M_{A1} &= |u|^2 + |v|^2 + 3|\sigma_1|^2 + \Sigma^2 + |\tau_1 - \tau_2|^2 \\
M_{A2} &= |w|^2 + |v|^2 + 3|\sigma_2|^2 + \Sigma^2 + |\tau_1 - \tau_3|^2 \\
M_{A3} &= |w|^2 + |v|^2 + 3|\sigma_3|^2 + \Sigma^2 + |\tau_2 - \tau_3|^2 \\
\Psi_1 &= \text{Re}_{\mathbb{H}}\left(3(\bar{\tau}_1\sigma_3 - \bar{\sigma}_2\sigma_1) - \bar{w}v\right) \\
\Psi_2 &= \text{Re}_{\mathbb{H}}\left(3(\bar{\tau}_2\sigma_2 - \bar{\sigma}_1\sigma_3) - \bar{u}w\right) \\
\Psi_3 &= \text{Re}_{\mathbb{H}}\left(3(\bar{\tau}_3\sigma_1 - \bar{\sigma}_3\sigma_2) - \bar{v}u\right) \\
\Upsilon &= 2 \left( \Psi_1^2 M_{A3} + \Psi_1 \Psi_2 \Psi_3 - 4M_{A1} M_{A2} M_{A3} + M_{A1} \Psi_3^2 + \Psi_2^2 M_{A2} \right)
\end{aligned} \tag{7.2.6}$$

### 7.3 The Potential

We can now use this to calculate the potential, using the formula

$$V = \int d^4x \text{Tr}(D_i \phi D_i \phi) \tag{7.3.1}$$

We can now follow the standard method. Integrating by parts, and using the equation of motion for  $\phi$

$$D^2 \phi = 0 \tag{7.3.2}$$

We get

$$V = \lim_{R \rightarrow \infty} \int_{|x|=R} dS^3 \hat{x}_i \text{Tr}(\phi D_i \phi) \quad (7.3.3)$$

We know that the vector  $U$ , being a null vector of  $\Delta$ , must solve  $\Delta^\dagger U = 0$ , which gives the equations

$$\begin{aligned} \bar{u}U_1 + (\bar{\tau}_1 - \bar{x})U_2 + \bar{\sigma}_1U_3 + \bar{\sigma}_2U_4 &= 0 \\ \bar{v}U_1 + \bar{\sigma}_1U_2 + (\bar{\tau}_2 - \bar{x})U_3 + \bar{\sigma}_3U_4 &= 0 \\ \bar{w}U_1 + \bar{\sigma}_2U_2 + \bar{\sigma}_3U_3 + (\bar{\tau}_3 - \bar{x})U_4 &= 0 \end{aligned} \quad (7.3.4)$$

These can be solved in the  $|x|^2 \mapsto \infty$  limit as

$$U_1 \mapsto 1 ; U_2 \mapsto \frac{x\bar{u}}{|x|^2} ; U_3 \mapsto \frac{x\bar{v}}{|x|^2} ; U_4 \mapsto \frac{x\bar{w}}{|x|^2} \quad (7.3.5)$$

We can continue to calculate the potential as in the previous cases. The details are in Appendix E, however the result is

$$\mathcal{V} = 8\pi^2 \left( |\mathbf{q}|^2 (|u|^2 + |v|^2 + |w|^2) - 2a \text{Re}_{\mathbb{H}}(\bar{v}\mathbf{q}u) - 2b \text{Re}_{\mathbb{H}}(\bar{u}\mathbf{q}w) - 2c \text{Re}_{\mathbb{H}}(\bar{w}\mathbf{q}v) \right) \quad (7.3.6)$$

with  $a, b, c$  given as above.

## 7.4 $O(3)$ Metric

The final thing to calculate is the metric. As in the previous case, we need to calculate  $a^T \delta C_r$ , and impose the condition

$$a^T \delta C_r = (a^T \delta C_r)^{T\star} \quad (7.4.1)$$

Note that here we have the operation  $T$  rather than  $\dagger$  as we are dealing with the usual, real Quaternions rather than the Complexified version. Since in this commutative 3-



instanton case, the remaining symmetry is  $o(3)$ , we can write

$$\delta R = \begin{bmatrix} 0 & -d\phi & d\theta \\ d\phi & 0 & -d\psi \\ -d\theta & d\psi & 0 \end{bmatrix} \quad (7.4.2)$$

We should end up, analogously to the previous case, with three simultaneous equations. As before, we have

$$a^\dagger dC_r = a^\dagger da - a^\dagger b(dR)b^\dagger a + a^\dagger a(dR) \quad (7.4.3)$$

We now follow the same method as before. Again, the details are in Appendix F.

The solution is

$$d\phi = \frac{1}{\Xi} \left( D_1 (M_{A_2} M_{A_3} + \Psi_3^2) + D_2 (M_{A_3} \Psi_1 - \Psi_2 \Psi_3) - D_3 (M_{A_2} \Psi_2 + \Psi_1 \Psi_3) \right) \quad (7.4.4)$$

$$d\theta = \frac{1}{\Xi} \left( -D_1 (M_{A_3} \Psi_1 + \Psi_2 \Psi_3) - D_2 (M_{A_1} M_{A_3} - \Psi_2^2) + D_3 (M_{A_1} \Psi_3 + \Psi_1 \Psi_2) \right)$$

$$d\psi = \frac{1}{\Xi} \left( D_1 (\Psi_1 \Psi_3 - M_{A_2} \Psi_2) + D_2 (M_{A_1} \Psi_3 - \Psi_1 \Psi_2) + D_3 (M_{A_1} M_{A_2} - \Psi_1^2) \right)$$

Where

$$D_1 = \bar{u}dv - \bar{v}du + \bar{\tau}_1 d\sigma_1 - \bar{\sigma}_1 d\tau_1 + \bar{\sigma}_1 d\tau_2 - \bar{\tau}_2 d\sigma_1 + \bar{\sigma}_2 d\sigma_3 - \bar{\sigma}_3 d\sigma_2$$

$$D_2 = \bar{u}dw - \bar{w}du + \bar{\tau}_1 d\sigma_2 - \bar{\sigma}_2 d\tau_1 + \bar{\sigma}_1 d\sigma_3 - \bar{\sigma}_3 d\sigma_1 + \bar{\sigma}_2 d\tau_3 - \bar{\tau}_3 d\sigma_2$$

$$D_3 = \bar{v}dw - \bar{w}dv + \bar{\sigma}_1 d\sigma_2 - \bar{\sigma}_2 d\sigma_1 + \bar{\tau}_2 d\sigma_3 - \bar{\sigma}_3 d\tau_2 + \bar{\sigma}_3 d\tau_3 - \bar{\tau}_3 d\sigma_3$$

$$M_{A_1} = |u|^2 + |v|^2 + 3|\sigma_1|^2 + \Sigma^2 + |\tau_1 - \tau_2|^2$$

$$M_{A_2} = |w|^2 + |v|^2 + 3|\sigma_2|^2 + \Sigma^2 + |\tau_1 - \tau_3|^2$$

$$M_{A_3} = |w|^2 + |v|^2 + 3|\sigma_3|^2 + \Sigma^2 + |\tau_2 - \tau_3|^2$$

$$\Psi_1 = \text{Re}_{\mathbb{H}} \left( 3(\bar{\tau}_1 \sigma_3 - \bar{\sigma}_2 \sigma_1) - \bar{w}v \right)$$

$$\Psi_2 = \text{Re}_{\mathbb{H}} \left( 3(\bar{\tau}_2 \sigma_2 - \bar{\sigma}_1 \sigma_3) - \bar{u}w \right)$$

$$\Psi_3 = \text{Re}_{\mathbb{H}} \left( 3(\bar{\tau}_3 \sigma_1 - \bar{\sigma}_3 \sigma_2) - \bar{v}u \right)$$

$$\Xi = M_{A_1} M_{A_2} M_{A_3} + M_{A_1} \Psi_3^2 - M_{A_2} \Psi_2^2 - M_{A_3} \Psi_1^2 \quad (7.4.5)$$

Once more we use our formula, modified for real quaternions

$$ds^2 = ds_1^2 + ds_2^2 = 2\pi^2 \left( \text{Tr}^*(2d\Lambda^\dagger d\Lambda + d\Omega^\dagger d\Omega) + \text{Tr}^* \left( (a^\dagger da - (a^\dagger da)^T) dR \right) \right) \quad (7.4.6)$$

which enables us to calculate the metric as

$$8\pi^2 \left( d^2u + d^2v + d^2w + d^2\tau_1 + d^2\tau_2 + d^2\tau_3 + d^2\sigma_1 + d^2\sigma_2 + d^2\sigma_3 - \left( D_1 d\phi + D_2 d\theta + D_3 d\psi \right) \right) \quad (7.4.7)$$

## 7.5 3 Instanton Dynamics

The next logical thing to do is to use the metric and potential given above to analyse the dynamics numerically, as was done in the case of two instantons. Unfortunately I was unable to generate enough simulations to carry out a full analysis, however I was able to observe some particular behaviours.

First, I was able to plot the scalar field profiles. When the instantons are far separated, this gives three peaks at the positions of each Instanton, with the position defined as  $\tau_i$  (figure 7.1). This confirms the interpretation of that parameter. If we move one instanton far away from the others (off to the right of the plot, in fact) then we see two peaks which look a lot like the two instanton case (figure 7.2). The splitting in the right peak increases the closer the third instanton gets. In the graph in question, the two instantons shown are at  $(\pm 1, 0)$  and the third is at  $(0, 40)$ . Finally, I was able to approximate some aspects of the scattering by plotting the Topological charge Density (figure 7.3). Here, if one instanton is kept, ‘stationary’ at the origin, and the other instantons are plotted at successively closer values of  $\tau_i$ , there appears to be the kind of right angled scattering that is a familiar part of Soliton Dynamics. The fact that the instantons are moving away at very small values of  $\tau_i$  is a function of the fact that the position depends both upon  $\tau_i$  and  $\sigma_i$ , as in the two instanton case.

Finally, I was able to use Joe Farrow’s code, as in the case of the six parameter

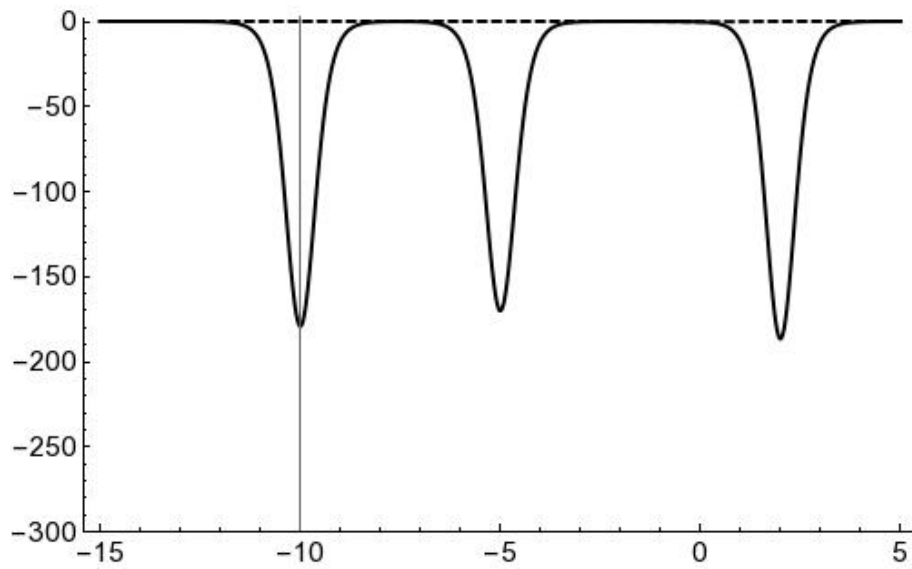


Figure 7.1: Plot of the scalar field profile for three separated instantons

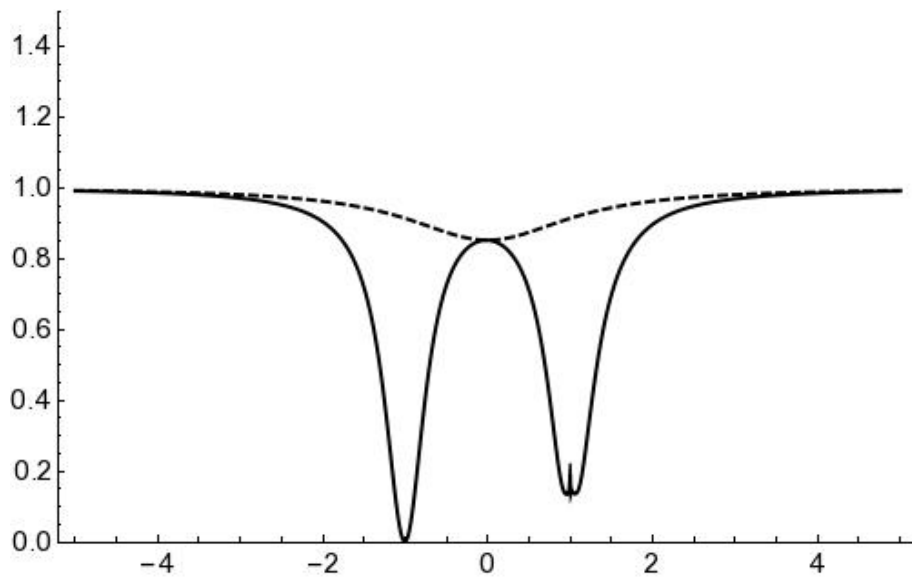


Figure 7.2: Plot of the scalar field profile for two instantons, with the third far separated off to the right

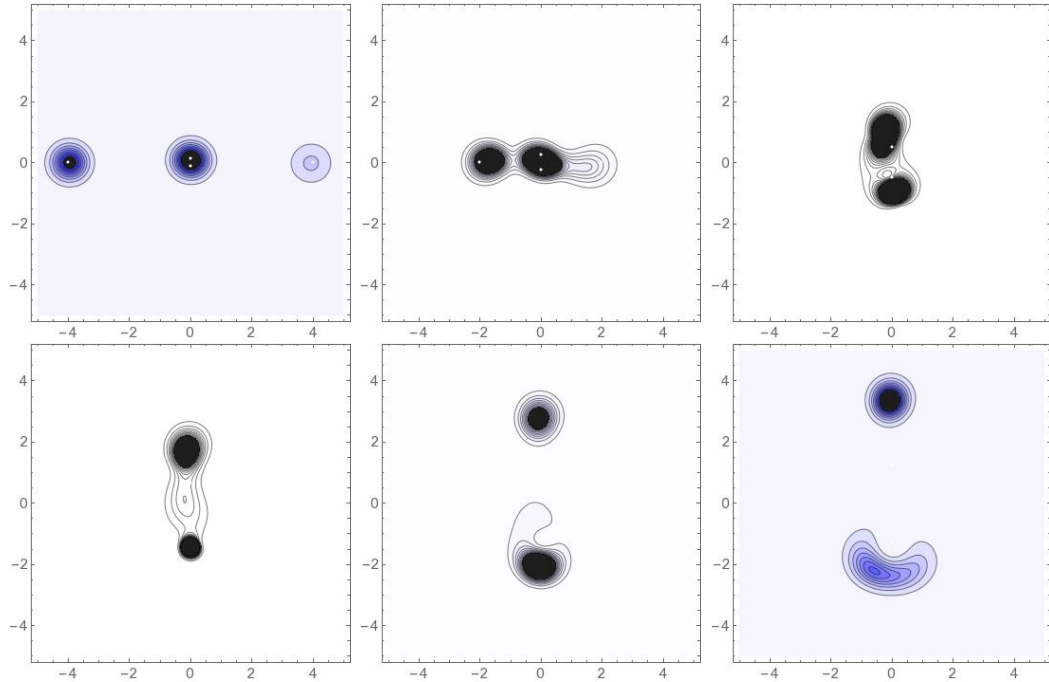


Figure 7.3: Plot of the topological charge density with one instanton at the origin and the other two at decreasing values of  $\tau_i$ . Note the apparent right angled scattering

instantons, to get several plots of the scattering – though only for the case where the potential was zero. It turns out that plotting the scattering is very numerically difficult. When the instantons become very close, the factors in  $1/(\tau_i - \tau_j)$  become very large, leading in various methods to the solution either blowing up, or getting stuck at certain points.

I was able to examine the case where one of the instantons is far away from the other two, and to compare it to the two instanton case I had already derived. There was excellent agreement, as can be seen in figures 7.4 and 7.5. Additionally, I was able to generate one graph with all three instantons interacting – in all my other attempts the instanton trajectories plotted were discontinuous. I think this is because the trajectories are dominated by the off-diagonal elements  $\sigma_i$ , which goes as  $1/(\tau_i - \tau_j)$ . As the difference becomes small, the numerical programme is trying to take smaller increments of the variables  $\tau_i$  to compensate – which leads to large leaps in the actual plotted position between step sizes. Trying to resolve this would be a obvious direction for future work.

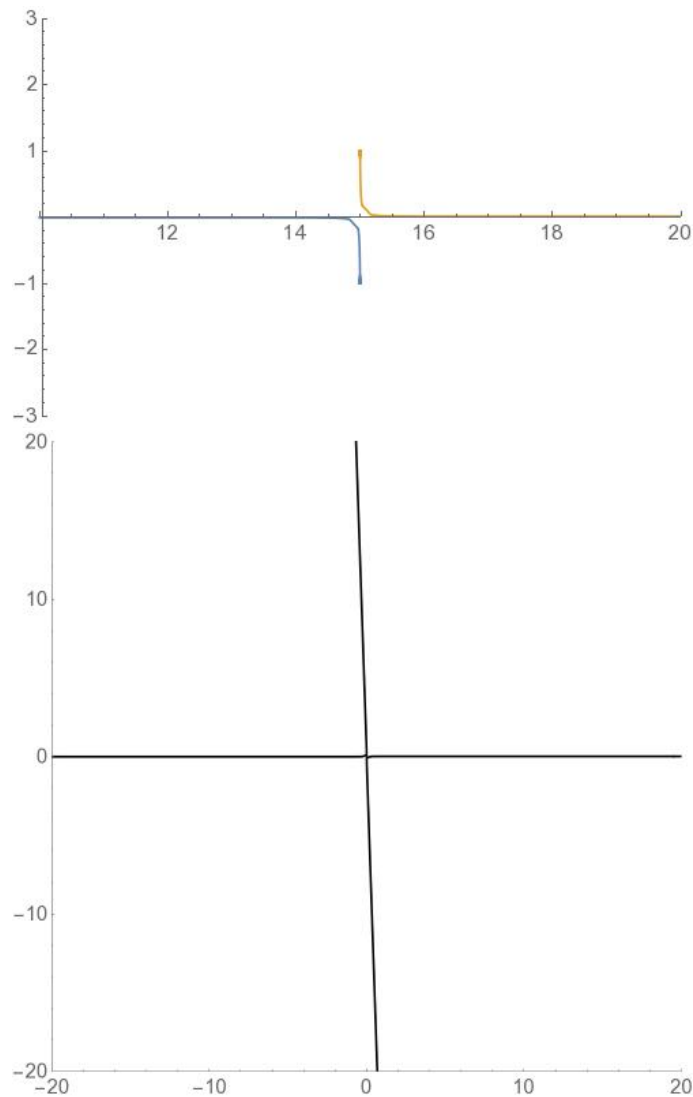


Figure 7.4: Comparison of scattering in three instanton case with one instanton far away from the other two (top), with the 4 parameter (orthogonal) case for two instantons. This is with  $b = 0.1$ . Note the orthogonal scattering in both cases. Here the three instanton initial parameters are  $\{\tau_{1R}, \tau_{1I}, \tau_{1R}, \tau_{1I}, u_R, u_I, v_R, v_I, w_R, w_I\}$  are  $\{10, -0.01, 20, 0.01, 1, 0, 0, 1, 1, 1\}$ , and their initial velocities are  $\{0.03, 0, -0.03, 0, 0, 0, 0, 0, 0, 0\}$ . This means that the two instantons which are interacting are orthogonal in the gauge group, and the third is at  $(-30, 0)$ , which is sufficiently separated not to qualitatively affect the interaction

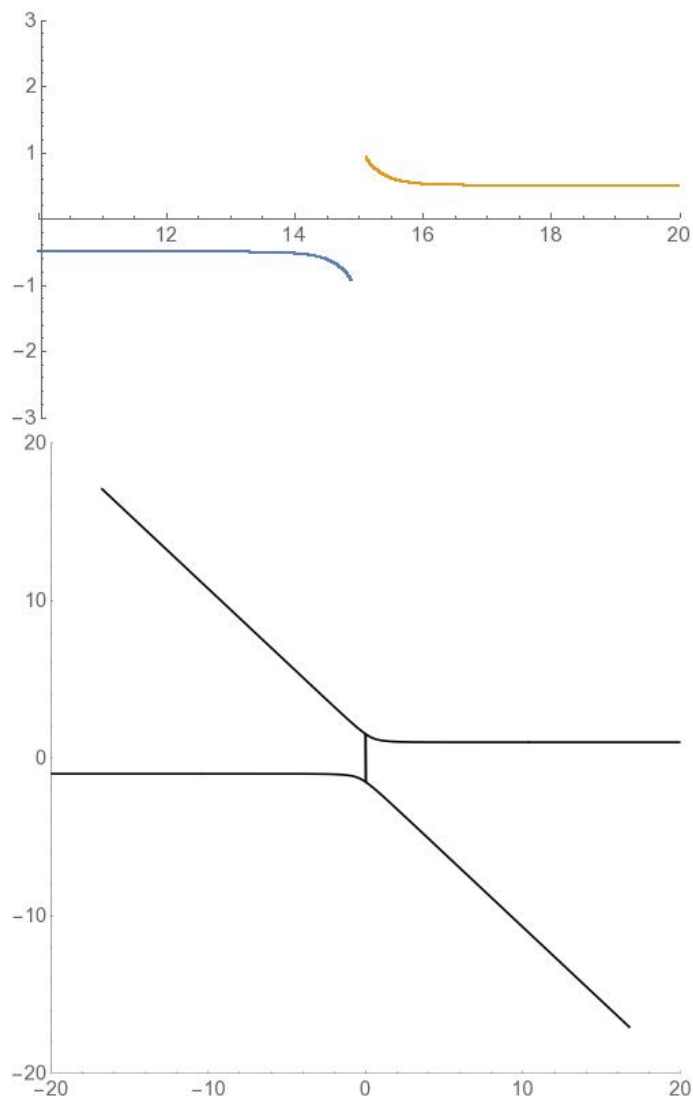


Figure 7.5: Comparison of scattering in three instanton case with one instanton far away from the other two (top), with the 4 parameter (orthogonal) case for two instantons. This is with  $b = 0.5$ .  $\{10, -0.5, 20, 0.5, 1, 0, 0, 1, 1, 1\}$ , and their initial velocities are  $\{0.03, 0, -0.03, 0, 0, 0, 0, 0, 0, 0\}$ . This means that the two instantons which are interacting are orthogonal in the gauge group, and the third is at  $(-30, 0)$ , which is sufficiently separated not to qualitatively affect the interaction

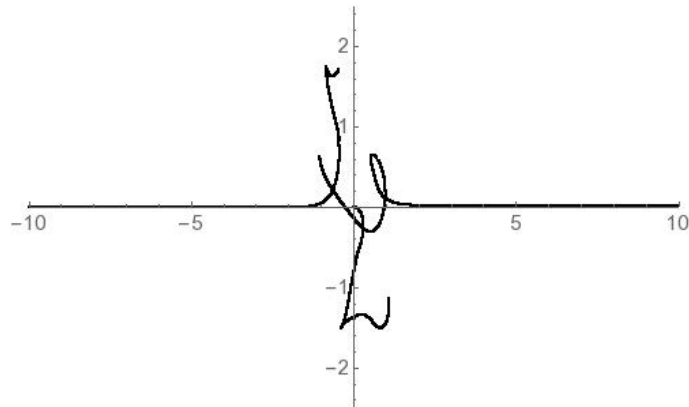


Figure 7.6: Three Instantons scattering. One begins stationary at the origin, whilst the other two move in with equal and opposite positions.  $\{\tau_{1R}, \tau_{1I}, \tau_{1R}, \tau_{1I}, u_R, u_I, v_R, v_I, w_R, w_I\}$  are  $\{10, 0.01, -10, -0.01, 1, 0, 0, 1, 1, 1\}$ , and their initial velocities are  $\{0.05, 0, -0.05, 0, 0, 0, 0, 0, 0, 0\}$ . The two instantons that come in from the sides are orthogonal in the gauge group to each other, but not to the stationary one at the origin

# Chapter 8

## Conclusion

In the first part of my Thesis, I reviewed certain topics in mathematics and physics which underpinned the general topic of Instantons. First I looked at the theory of Fibre Bundles. I explained what they were, I outlined the notion of a connection on a bundle, and I showed how this let us define the curvature. The definition of an Instanton relies on the link between the Topological degree of a map, and the definition of Characteristic classes. This was therefore the topic of the next part of that chapter.

After these more general concepts, the second chapter looked at Instantons themselves. After defining what an instanton was, I gave an overview of noncommutative spacetimes, as a large part of the rest of the thesis dealt with Instantons defined over these spacetimes. I also introduced the biquaternion algebra, and outlined the notation and calculation methods I was using. Once this had been done, I looked at how to actually derive Instanton solutions, using the ADHM construction. Notably, I showed that even in the commutative case one could still begin with the biquaternions. The solution one gets is Complex rather than Real, but the residual symmetry is also complexified from  $SO(2)$  to  $SU(2)$ . This symmetry allows us to, ‘rotate’ our complex solution into a real one. I then looked at Dyonic instantons, and gave a general method for calculating the scalar field for general noncommutative  $U(N)$  instantons.



In the third chapter I reviewed the topic of the Instanton Moduli Space and the Potential which is induced upon it in the Dyon case. Again, I gave a method for calculating both these for noncommutative  $U(N)$  Instantons. This concluded the first part of my thesis.

The second part of the thesis began with a rederivation of the solution for a single noncommutative instanton in [3]. This was done primarily to enable me to check the solution I derived for the two instanton case. First of all, I rederived the commutative solution which was found in [1], but using biquaternions rather than quaternions. This allows us to check for a specific case that the procedure outlined in chapter 2 for doing this works in practice. I then tried to find a solution for the noncommutative case. First of all I checked the solution presented in [37] and showed that this was not a full solution to the ADHM equations. I then looked for a solution. I was unable to find a full solution, however I was able to find one for the subspace of the moduli space spanned by the  $\mathbb{C} \times \mathbb{C}$  subalgebra of  $\mathbb{C} \times \mathbb{H}$ . I used this solution to calculate the metric and potential for that subspace. I checked that in the commutative limit  $\zeta \rightarrow 0$  the noncommutative solution gave the commutative solution in [1], and that in the limit  $\tau \rightarrow \infty$  where the Instantons become far separated, the solution became two copies of the single noncommutative  $U(2)$  instanton.

Once I had these two solutions, I investigated the dynamics on the noncommutative moduli space numerically. First I plotted the profile of the scalar field for separated and nearly-coincident instantons. This showed the same qualitative behaviour as in the commutative case, showing that it made sense to give the various components of the ADHM data the same interpretation in the noncommutative as in the commutative case. With this established, we investigated the scattering of two instantons, both for pure and for Dyon Instantons. I began with the four parameter subspace of the moduli space where the two instantons have the same initial size and are orthogonal. In both cases, pure and dyonic, the presence of the noncommutative parameter seemed to increase the repulsion between the two instantons compared to the commutative case. Additionally, as one might expect, whereas in the com-

mutative case the instantons shrink through zero size then begin to increase, in the noncommutative case they instead shrink (then grow) through a finite minimum size which increases with  $\zeta$ . In the case of pure instantons, if we plot the scattering angle vs. the impact parameter, there is a peak at a specific value of  $\zeta$ . At this peak, there seems to be some kind of orbiting behaviour involving the instantons, however the difficulties in giving a meaningful interpretation to very small instanton separation given the presence of the noncommutative parameter makes it hard to be too certain. In the pure instanton case, varying  $\dot{\theta}$  and  $\dot{\rho}$  away from zero gave very strong orthogonal scattering, since doing this made the instanton size very large. However the presence of the potential prevents this from occurring, and therefore I did not observe this behaviour in the dyonic case. I then looked at the 6 parameter case where the relative gauge angle and size could freely vary. There was a clear oscillatory behaviour in the commutative case with the gauge angle, where the behaviour went in some cases from no interaction to orthogonal scattering. This was suppressed when the noncommutativity was turned on. Though some limited sinusoidal behaviour could still be observed, it did not cover such a wide range of angles, and the overall shape was not nearly so distinct.

In the case of dyonic instantons, I was restricted to looking at the four parameter case. Unlike in the commutative case, there is no peak in the scattering angle vs impact parameter graphs. There is, however, some interesting orbiting behaviour for very low values of the potential, though the same issues regarding interpretation arise as in the pure case. A key difference is that there are two scales to set, the length scale via  $\zeta$  and the time scale via  $q$ , the magnitude of the potential. There was some evidence that there was a particular region where  $\zeta$  was not too large, and  $q$  was not too small, where the scattering behaviour became considerably less chaotic.

Finally, I looked at the case of three  $U(2)$  instantons. Here, to make the calculations easier, I did not use the biquaternions, but specialised to quaternion ADHM data from the beginning. I was again unable to find a solution for the full moduli space,

however I was, again, able to find a solution on the submanifold of the moduli space spanned by the  $\mathbb{C}$  subgroup of  $\mathbb{H}$ . This solution once more allowed me to calculate the metric and potential on that submanifold. First I was able to numerically graph the scalar field profiles, allowing me to interpret the components of the ADHM data in an analogous way to the two instanton case. I was also able to plot the topological charge density, and for the case of one stationary instanton colliding with two moving in opposite directions, plotting this for discrete values of the instanton separation seems to show the orthogonal scattering that is a common feature of soliton dynamics. Finally, I was able to look at examples of the scattering where one instanton was too far away to interact. I showed that these reproduced the behaviour of the two instanton case. Finally, I showed a single example of the scattering of three instantons.

### 8.0.1 Further work

In terms of further work, the most obvious thing to do is to try and improve the efficiency of the numerical evaluations so that we can explore the dyonic six parameter case for the noncommutative two instantons, and to access more of the three particle scattering in the three instanton case. Analytically, we could try and extend our ADHM solutions from the subspaces of the moduli spaces to the full moduli spaces. This would also allow us to calculate the partition functions on the moduli space. To do this, we would analyse the quantum mechanics around the zeros of the potential and calculate its superconformal index. This can be used to count the BPS states in the theory, and it can be argued – as for the single instanton case in [3] – that it also determines the partition function of the theory. The value of this method is that it not only allows for an independent check of the partition function calculation from the field theory point of view, but also could allow us to construct specific wavefunctions, which could not be done from the field theory partition function alone. In the noncommutative  $U(2)$  case the equivalent field theory partition function was

calculated in [40], and this is what we would want to compare any result we derived to.



# Appendix A

## The Two- Instanton Scalar Field

Here Re and Im refer to  $\text{Re}_{\mathbb{H}}$  and  $\text{Im}_{\mathbb{H}}$  unless otherwise stated. We have the equation of motion for the scalar field

$$2\text{Tr}_2(\Lambda^\dagger q \Lambda) + \text{Tr}_2([\Omega^\dagger, P]\Omega - \Omega^\dagger[\Omega, P]) - \text{Tr}_2(\{P, \Lambda^\dagger \Lambda\}) = 0 \quad (\text{A.0.1})$$

We shall now solve this equation. We will calculate each term separately, then derive an equation for each basis element of the resulting  $SU(2)$  matrices. We will then solve this for  $a, b$  and  $c$  in the ansatz (5.5.2). First, we look at  $\text{Tr}_2(\Lambda^\dagger q \Lambda)$ . A long calculation shows this is

$$2 \begin{bmatrix} 0 & \text{Re}(\bar{v}_R \mathbf{q} w_R + \bar{v}_I \mathbf{q} w_I) - q_0 \text{Re}(\bar{v}_R w_I - \bar{v}_I w_R) \\ -\text{Re}(\bar{v}_R \mathbf{q} w_R + \bar{v}_I \mathbf{q} w_I) + q_0 \text{Re}(\bar{v}_R w_I - \bar{v}_I w_R) & 0 \end{bmatrix} \quad (\text{A.0.2})$$

$$+ i \begin{bmatrix} 2q_0(|v_R|^2 + |v_I|^2) + 4\text{Re}(\bar{v}_R \mathbf{q} v_I) & 2q_0 \text{Re}(\bar{v}_R w_R + \bar{v}_I w_I) + 2\text{Re}(\bar{v}_R \mathbf{q} w_I - \bar{v}_I \mathbf{q} w_R) \\ 2q_0 \text{Re}(\bar{v}_R w_R + \bar{v}_I w_I) + 2\text{Re}(\bar{v}_R \mathbf{q} w_I - \bar{v}_I \mathbf{q} w_R) & 2q_0(|w_R|^2 + |w_I|^2) + 4\text{Re}(\bar{w}_R \mathbf{q} w_I) \end{bmatrix}$$

Next, we calculate  $\text{Tr}_2(\{P, \Lambda^\dagger \Lambda\})$ . This is equal to

$$\begin{bmatrix} 0 & -2b\Sigma - (a+d)\alpha \\ 2b\Sigma + (a+d)\alpha & 0 \end{bmatrix} + i \begin{bmatrix} 4a(|v_R|^2 + |v_I|^2) + 4b\alpha + 4c\beta & 2c\Sigma + (a+d)\beta \\ 2c\Sigma + (a+d)\beta & 4d(|w_R|^2 + |w_I|^2) + 4b\alpha + 4c\beta \end{bmatrix} \quad (\text{A.0.3})$$

Where

$$\begin{aligned} \Sigma &= |v_R|^2 + |v_I|^2 + |w_R|^2 + |w_I|^2 \\ \alpha &= \text{Re}(\bar{w}_I v_R - \bar{w}_R v_I) \\ \beta &= \text{Re}(\bar{v}_R w_R + \bar{v}_I w_I) \end{aligned} \quad (\text{A.0.4})$$

Finally, we have  $\text{Tr}_2([\Omega^\dagger, P]\Omega - \Omega^\dagger[\Omega, P])$ . To calculate this we expand it as  $2\Omega^\dagger P\Omega - P\Omega^\dagger\Omega - \Omega^\dagger\Omega P$ . Here, we use our choice of symmetry that  $\text{Re}(\bar{\tau}\sigma_R) = \text{Re}(\bar{\tau}\sigma_I)$ . First, we get  $P\Omega^\dagger\Omega + \Omega^\dagger\Omega P$  as

$$4(|\tau|^2 + |\sigma_R|^2 + |\sigma_I|^2)P \quad (\text{A.0.5})$$

and then  $\Omega^\dagger P\Omega$  is

$$2 \begin{bmatrix} 0 & b(|\tau|^2 + |\sigma_R|^2 - |\sigma_I|^2) + 2c\text{Re}(\bar{\sigma}_R\sigma_I) \\ -b(|\tau|^2 + |\sigma_R|^2 - |\sigma_I|^2) - 2c\text{Re}(\bar{\sigma}_R\sigma_I) & 0 \end{bmatrix} + 2i \begin{bmatrix} a|\tau|^2 - d(|\sigma_R|^2 + |\sigma_I|^2) & -2b\text{Re}(\bar{\sigma}_R\sigma_I) + c(|\sigma_R|^2 - |\sigma_I|^2 - |\tau|^2) \\ -2b\text{Re}(\bar{\sigma}_R\sigma_I) + c(|\sigma_R|^2 - |\sigma_I|^2 - |\tau|^2) & a(|\sigma_R|^2 + |\sigma_I|^2) + d|\tau|^2 \end{bmatrix} \quad (\text{A.0.6})$$

Putting them together, we get

$$8 \begin{bmatrix} 0 & b(|\tau|^2 + |\sigma_R|^2) + c\text{Re}(\bar{\sigma}_R\sigma_I) \\ -b(|\tau|^2 + |\sigma_R|^2) - c\text{Re}(\bar{\sigma}_R\sigma_I) & 0 \end{bmatrix} + 4i \begin{bmatrix} -(a+d)(|\sigma_R|^2 + |\sigma_I|^2) & -2b\text{Re}(\bar{\sigma}_R\sigma_I) - 2c(|\sigma_I|^2 + |\tau|^2) \\ -2b\text{Re}(\bar{\sigma}_R\sigma_I) - 2c(|\sigma_I|^2 + |\tau|^2) & (a+d)(|\sigma_R|^2 + |\sigma_I|^2) \end{bmatrix} \quad (\text{A.0.7})$$

We can now extract one equation for each of the quaternion components and then use Mathematica to solve them.

### A.0.2 Solving the equations

The  $\begin{bmatrix} 0 & -1 \\ 1 & 0 \end{bmatrix}$  component gives

$$4q_0\text{Re}(\bar{v}_R w_I - \bar{v}_I w_R) - 4\text{Re}(\bar{v}_R \mathbf{q} w_R + \bar{v}_I \mathbf{q} w_I) = 2b(|v_R|^2 + |v_I|^2 + |w_R|^2 + |w_I|^2 + 4(|\tau|^2 + |\sigma_R|^2)) - (a+d)\text{Re}(\bar{w}_R v_I - \bar{w}_I v_R) + 8c\text{Re}(\bar{\sigma}_R\sigma_I) \quad (\text{A.0.8})$$

For the  $\begin{bmatrix} 0 & i \\ i & 0 \end{bmatrix}$  component we have

$$4q_0\text{Re}(\bar{v}_R w_R + \bar{v}_I w_I) + 4\text{Re}(\bar{v}_R \mathbf{q} w_I - \bar{v}_I \mathbf{q} w_R) = 8b\text{Re}(\bar{\sigma}_R\sigma_I) + 2c(|v_R|^2 + |v_I|^2 + |w_R|^2 + |w_I|^2 + 4(|\tau|^2 + |\sigma_I|^2)) + (a+d)\text{Re}(\bar{w}_R v_R + \bar{w}_I v_I) \quad (\text{A.0.9})$$

Now we look at  $\begin{bmatrix} i & 0 \\ 0 & 0 \end{bmatrix}$ , which gives

$$\begin{aligned} 2q_0(|v_R|^2 + |v_I|^2) + 4\text{Re}(\bar{v}_R \mathbf{q} v_I) &= 2a(|v_R|^2 + |v_I|^2 + |\sigma_R|^2 + |\sigma_I|^2) \\ &+ 2d(|\sigma_R|^2 + |\sigma_I|^2) + 2b\text{Re}(\bar{w}_I v_R - \bar{w}_R v_I) + 2c\text{Re}(\bar{v}_R w_R + \bar{v}_I w_I) \end{aligned} \quad (\text{A.0.10})$$

Final, we have the new equation from  $\begin{bmatrix} 0 & 0 \\ 0 & -i \end{bmatrix}$  which is

$$\begin{aligned} 2q_0(|w_R|^2 + |w_I|^2) + 4\text{Re}(\bar{w}_R \mathbf{q} w_I) &= 2d(|w_R|^2 + |w_I|^2 + |\sigma_R|^2 + |\sigma_I|^2) \\ &+ 2a(|\sigma_R|^2 + |\sigma_I|^2) + 2b\text{Re}(\bar{w}_I v_R - \bar{w}_R v_I) + 2c\text{Re}(\bar{v}_R w_R + \bar{v}_I w_I) \end{aligned} \quad (\text{A.0.11})$$

To make progress, we get two new equations from adding and taking away the pairs of diagonal and off diagonal equations. Adding the diagonal equations gives

$$\begin{aligned} q_0(|v_R|^2 + |v_I|^2 + |w_R|^2 + |w_I|^2) + 2\text{Re}(\bar{v}_R v_I + \bar{w}_R w_I) &= \\ a(|v_R|^2 + |v_I|^2) + d(|w_R|^2 + |w_I|^2) + 2(a + d)(|\sigma_R|^2 + |\sigma_I|^2) & \\ 2b\text{Re}(\bar{w}_I v_R - \bar{w}_R v_I) + 2c\text{Re}(\bar{v}_R w_R + \bar{v}_I w_I) & \end{aligned} \quad (\text{A.0.12})$$

Taking them away we get

$$q_0(|v_R|^2 + |v_I|^2 - |w_R|^2 - |w_I|^2) + 2\text{Re}(\bar{v}_R q v_I - \bar{w}_R q w_I) = a(|v_R|^2 + |v_I|^2) - d(|w_R|^2 + |w_I|^2) \quad (\text{A.0.13})$$

We can use (A.0.13) to write

$$d = \frac{a(|v_R|^2 + |v_I|^2) - q_0(|v_R|^2 + |v_I|^2 - |w_R|^2 - |w_I|^2) - 2\text{Re}(\bar{v}_R q v_I - \bar{w}_R q w_I)}{|w_R|^2 + |w_I|^2} \quad (\text{A.0.14})$$

Solving these gives the solution in the main text, in (5.5.4).





# Appendix B

## The Two Instanton Potential

As a first step to solving (5.6.3), we calculate

$$\hat{x}_i D_i \phi = \hat{x}_i \left( iU^\dagger e_i b f \Delta^\dagger \mathcal{A} U + iU^\dagger \mathcal{A} \Delta f \bar{e}_i b^\dagger U \right) \quad (\text{B.0.1})$$

in the limit  $|x| \mapsto \infty$ , using the following (see section 4.4)

$$\Delta \mapsto \begin{bmatrix} v & w \\ -x & 0 \\ 0 & -x \end{bmatrix}$$

$$f_{kl} \mapsto \frac{1}{|x|^2} \delta_{kl} \quad (\text{B.0.2})$$

Then we can write

$$\hat{x}_i D_i \phi \mapsto \frac{i}{|x|^2} \left( \hat{x} U^\dagger b \mathbb{1}_2 \begin{bmatrix} v^\dagger & -\bar{x} & 0 \\ w^\dagger & 0 & -\bar{x} \end{bmatrix} \mathcal{A} U + \hat{x} U^\dagger \mathcal{A} \begin{bmatrix} v & w \\ -x & 0 \\ 0 & -x \end{bmatrix} \mathbb{1}_2 b^\dagger U \right) \quad (\text{B.0.3})$$

Where  $\mathcal{A}$ , as above, is

$$\begin{bmatrix} q & 0 & 0 \\ 0 & ai & ci - b \\ 0 & ci + b & di \end{bmatrix} \quad (\text{B.0.4})$$

and

$$b = \begin{bmatrix} 0 & 0 \\ 1 & 0 \\ 0 & 1 \end{bmatrix} \quad (\text{B.0.5})$$

This gives

$$\frac{i}{|x|^2} \left( \hat{x} U^\dagger \begin{bmatrix} 0 & 0 & 0 \\ v^\dagger q & -ai\bar{x} & -(ci-b)\bar{x} \\ w^\dagger q & -(ci+b)\bar{x} & -di\bar{x} \end{bmatrix} U + \hat{x} U^\dagger \begin{bmatrix} 0 & qv & qw \\ 0 & -aix & -(ci-b)x \\ 0 & -(ci+b)x & -dix \end{bmatrix} U \right) \quad (\text{B.0.6})$$

which contracts as

$$\begin{aligned} \hat{x}_i D_i \phi &= \frac{i}{|x|^2} \left( \hat{x} (U_2^\dagger v^\dagger q U_1 + U_3^\dagger w^\dagger q U_1) + \hat{x} (U_1^\dagger q v U_2 + U_1^\dagger q w U_3) \right. \\ &\quad \left. - 2|x| \left( ai U_2^\dagger U_2 + di U_3^\dagger U_3 + b (U_3^\dagger U_2 - U_2^\dagger U_3) + ci (U_3^\dagger U_2 + U_2^\dagger U_3) \right) \right) \end{aligned} \quad (\text{B.0.7})$$

Substituting in the limiting values for the  $U_i$  in (5.6.5) we have

$$\begin{aligned} \hat{x}_i D_i \phi &= \frac{i}{|x|^3} \left( (vv^\dagger + ww^\dagger)q + q(vv^\dagger + ww^\dagger) \right. \\ &\quad \left. - 2 \left( aivv^\dagger + diww^\dagger + b(vv^\dagger - ww^\dagger) + ci(ww^\dagger + vv^\dagger) \right) \right) + \mathcal{O}\left(\frac{1}{|x|^4}\right) \end{aligned} \quad (\text{B.0.8})$$

Finally, we can expand into real and imaginary parts

$$\begin{aligned} \hat{x}_i D_i \phi &= \frac{i}{|x|^3} \left( 2q(|v_R|^2 + |v_I|^2 + |w_R|^2 + |w_I|^2) - 2i \left( \text{Im}(v_R \bar{v}_I + w_R \bar{w}_I)q + q \text{Im}(v_R \bar{v}_I + w_R \bar{w}_I) \right) \right. \\ &\quad - 2 \left( ai(|v_R|^2 + |v_I|^2 - 2i \text{Im}(v_R \bar{v}_I)) + di(|w_R|^2 + |w_I|^2 - 2i \text{Im}(w_R \bar{w}_I)) \right) \\ &\quad \left. + 2b \left( \text{Im}(w_R \bar{v}_R + w_I \bar{v}_I) + i \text{Re}(w_I \bar{v}_R - w_R \bar{v}_I) \right) + 2ci \left( \text{Re}(w_R \bar{v}_R + w_I \bar{v}_I) + i \text{Im}(w_I \bar{v}_R - w_R \bar{v}_I) \right) \right) \\ &\quad + \mathcal{O}\left(\frac{1}{|x|^4}\right) \end{aligned} \quad (\text{B.0.9})$$

We now combine this result with the fact that the scalar field  $\phi$  tends to  $iq$  at infinity, to get

$$V = \lim_{|x|^2 \rightarrow \infty} - \int d^3 S \frac{1}{|x|^3} \text{Tr} \left( 2q^2 (|v_R|^2 + |v_I|^2 + |w_R|^2 + |w_I|^2) \right)$$

$$\begin{aligned}
& -2i\left(q\mathrm{Im}(v_R\bar{v}_I + w_R\bar{w}_I)q + q^2\mathrm{Im}(v_R\bar{v}_I + w_R\bar{w}_I)\right) - 2q\left(ai\left(|v_R|^2 + |v_I|^2 - 2i\mathrm{Im}(v_R\bar{v}_I)\right)\right. \\
& + di\left(|w_R|^2 + |w_I|^2 - 2i\mathrm{Im}(w_R\bar{w}_I)\right) + 2b\left(\mathrm{Im}(w_R\bar{v}_R + w_I\bar{v}_I) + i\mathrm{Re}(w_I\bar{v}_R - w_R\bar{v}_I)\right) \\
& \left. + 2ci\left(\mathrm{Re}(w_R\bar{v}_R + w_I\bar{v}_I) + i\mathrm{Im}(w_I\bar{v}_R - w_R\bar{v}_I)\right)\right) + \mathcal{O}\left(\frac{1}{|x|^4}\right) \tag{B.0.10}
\end{aligned}$$

Here and elsewhere in this appendix  $\mathrm{Re}$  and  $\mathrm{Im}$  refer to  $\mathrm{Re}_{\mathbb{H}}$  and  $\mathrm{Im}_{\mathbb{H}}$  unless otherwise stated. To simplify the trace, we split  $q = iq_0 + \mathbf{q}$  and ignore any of the purely imaginary quaternion terms, which go to zero. Then, also evaluating the integral, we have

$$\begin{aligned}
V = & -4\pi^2\mathrm{Tr}\left(2(-|\vec{q}|^2 - q_0^2)\left(|v_R|^2 + |v_I|^2 + |w_R|^2 + |w_I|^2\right) + 8q_0\mathbf{q}\mathrm{Im}(v_R\bar{v}_I + w_R\bar{w}_I)\right. \\
& + 2a\left(q_0(|v_R|^2 + |v_I|^2) - 2\mathbf{q}\mathrm{Im}(v_R\bar{v}_I)\right) + 2d\left(q_0(|w_R|^2 + |w_I|^2) - 2\mathbf{q}\mathrm{Im}(w_R\bar{w}_I)\right) \\
& - 4b\mathbf{q}\mathrm{Im}(w_R\bar{v}_R + w_I\bar{v}_I) + 4bq_0\mathrm{Re}(w_I\bar{v}_R - w_R\bar{v}_I) \\
& \left. + 4cq_0\mathrm{Re}(w_R\bar{v}_R + w_I\bar{v}_I) + 4c\mathbf{q}\mathrm{Im}(w_I\bar{v}_R - w_R\bar{v}_I)\right) \tag{B.0.11}
\end{aligned}$$

Taking the trace we get the solution (7.3.3)



# Appendix C

## The Two Instanton Metric

In this appendix  $\text{Re}$  and  $\text{Im}$  refer to  $\text{Re}_{\mathbb{H}}$  and  $\text{Im}_{\mathbb{H}}$  unless otherwise stated. To start with, note

$$a^\dagger dC_\tau = a^\dagger da - a^\dagger b(dR)b^\dagger a + a^\dagger a(dR) \quad (\text{C.0.1})$$

We will calculate this term by term. First,  $a^\dagger da$  is

$$\begin{bmatrix} v^\dagger dv + \tau^\dagger d\tau + \sigma d\sigma & v^\dagger dw + \tau^\dagger d\sigma^* - \sigma^\dagger d\tau \\ w^\dagger dv + \sigma^{*\dagger} d\tau - \tau^\dagger d\sigma & w^\dagger dw + \sigma^{*\dagger} d\sigma^* + \tau^\dagger d\tau \end{bmatrix} \quad (\text{C.0.2})$$

which we can expand as

$$\begin{aligned} & \begin{bmatrix} \bar{v}_R dv_R + \bar{v}_I dv_I + \bar{\sigma}_R d\sigma_R + \bar{\sigma}_I d\sigma_I + \bar{\tau} d\tau & \bar{v}_R dw_R + \bar{v}_I dw_I + \bar{\tau} d\sigma_R - \bar{\sigma}_R d\tau \\ \bar{w}_R dv_R + \bar{w}_I dv_I + \bar{\sigma}_R d\tau - \bar{\tau} d\sigma_R & \bar{w}_R dw_R + \bar{w}_I dw_I + \bar{\sigma}_R d\sigma_R + \bar{\sigma}_I d\sigma_I + \bar{\tau} d\tau \end{bmatrix} \\ & + i \begin{bmatrix} \bar{v}_R dv_I - \bar{v}_I dv_R + \bar{\sigma}_R d\sigma_I - \bar{\sigma}_I d\sigma_R & \bar{v}_R dw_I - \bar{v}_I dw_R + \bar{\sigma}_I d\tau - \bar{\tau} d\sigma_I \\ \bar{w}_R dv_I - \bar{w}_I dv_R + \bar{\sigma}_I d\tau - \bar{\tau} d\sigma_I & \bar{w}_R dw_I - \bar{w}_I dw_R + \bar{\sigma}_I d\sigma_R - \bar{\sigma}_R d\sigma_I \end{bmatrix} \end{aligned} \quad (\text{C.0.3})$$

Now we look at the term  $a^\dagger b(dR)b^\dagger a$ . Expanding  $dR$  as in (5.7.2), we get

$$\begin{aligned} & \begin{bmatrix} |\tau|^2 & \tau^\dagger \sigma^* \\ \sigma^{*\dagger} \tau & \sigma^{*\dagger} \sigma^* \end{bmatrix} id\phi + \begin{bmatrix} \tau^\dagger \sigma + \sigma^\dagger \tau & \sigma^\dagger \sigma^* - |\tau|^2 \\ \sigma^{\dagger*} \sigma - |\tau|^2 & -\sigma^{\dagger*} \tau - \tau^\dagger \sigma^* \end{bmatrix} id\psi \\ & + \begin{bmatrix} -\tau^\dagger \sigma + \sigma^\dagger \tau & |\tau|^2 + \sigma^\dagger \sigma^* \\ -\sigma^{*\dagger} \sigma - |\tau|^2 & \sigma^{*\dagger} \tau - \tau^\dagger \sigma^* \end{bmatrix} d\theta + \begin{bmatrix} \sigma^\dagger \sigma & -\sigma^\dagger \tau \\ -\bar{\tau} \sigma & |\tau|^2 \end{bmatrix} id\chi \end{aligned} \quad (\text{C.0.4})$$

We can further expand this as

$$\begin{aligned}
& \begin{bmatrix} |\tau|^2 & \bar{\tau}\sigma_R - i\bar{\tau}\sigma_I \\ \bar{\sigma}_R\tau + i\bar{\sigma}_I\tau & |\sigma_R|^2 + |\sigma_I|^2 + i(\bar{\sigma}_R\sigma_I - \bar{\sigma}_I\sigma_R) \end{bmatrix} id\phi \\
+ & \begin{bmatrix} i(\bar{\tau}\sigma_I - \bar{\sigma}_I\tau) & |\sigma_R|^2 - |\sigma_I|^2 - |\tau|^2 - i(\bar{\sigma}_R\sigma_I + \bar{\sigma}_I\sigma_R) \\ |\sigma_R|^2 - |\sigma_I|^2 - |\tau|^2 + i(\bar{\sigma}_R\sigma_I + \bar{\sigma}_I\sigma_R) & i(\bar{\tau}\sigma_I - \bar{\sigma}_I\tau) \end{bmatrix} id\psi \\
& \begin{bmatrix} \bar{\sigma}_R\tau - \bar{\tau}\sigma_R & |\tau|^2 + |\sigma|^2 - |\sigma_I|^2 - i(\bar{\sigma}_R\sigma_I + \bar{\sigma}_I\sigma_R) \\ |\sigma_I|^2 - |\sigma_R|^2 - |\tau|^2 - i(\bar{\sigma}_R\sigma_I + \bar{\sigma}_I\sigma_R) & \bar{\sigma}_R\tau - \bar{\tau}\sigma_R \end{bmatrix} d\theta \\
& + \begin{bmatrix} |\sigma_R|^2 + |\sigma_I|^2 + i(\bar{\sigma}_R\sigma_I - \bar{\sigma}_I\sigma_R) & -\bar{\sigma}_R\tau + i\bar{\sigma}_I\tau \\ -\bar{\tau}\sigma_R - i\bar{\tau}\sigma_I & |\tau|^2 \end{bmatrix} id\chi
\end{aligned} \tag{C.0.5}$$

Now we calculate the term  $a^\dagger adR$ . First note that due to the ADHM equations, we have

$$a^\dagger a = \begin{bmatrix} A\mathbb{1} + 4i\zeta\sigma_3 & C\mathbb{1} \\ C^*\mathbb{1} & B\mathbb{1} + 4i\zeta\sigma_3 \end{bmatrix} \tag{C.0.6}$$

Where  $A, B, C$  are real functions. We can calculate them to be

$$\begin{aligned}
& \begin{bmatrix} |v_R|^2 + |v_I|^2 + |\sigma_R|^2 + |\sigma_I|^2 + |\tau|^2 & \frac{1}{2}(\bar{v}_R w_R + \bar{w}_R v_R + \bar{v}_I w_I + \bar{w}_I v_I) \\ \frac{1}{2}(\bar{v}_R w_R + \bar{w}_R v_R + \bar{v}_I w_I + \bar{w}_I v_I) & |w_R|^2 + |w_I|^2 + |\sigma_R|^2 + |\sigma_I|^2 + |\tau|^2 \end{bmatrix} \\
+ i & \begin{bmatrix} 4\zeta\sigma_3 & \frac{1}{2}(\bar{v}_R w_I + \bar{w}_I v_R - \bar{v}_I w_R - \bar{w}_R v_I) \\ -\frac{1}{2}(\bar{v}_R w_I + \bar{w}_I v_R - \bar{v}_I w_R - \bar{w}_R v_I) & 4\zeta\sigma_3 \end{bmatrix}
\end{aligned} \tag{C.0.7}$$

expanding  $dR$  as above, we can write  $a^\dagger adR$  as

$$\begin{aligned}
& \left( \begin{bmatrix} |v_R|^2 + |v_I|^2 + |\sigma_R|^2 + |\sigma_I|^2 + |\tau|^2 & 0 \\ \frac{1}{2}(\bar{v}_R w_R + \bar{w}_R v_R + \bar{v}_I w_I + \bar{w}_I v_I) & 0 \end{bmatrix} + i \begin{bmatrix} 4\zeta\sigma_3 & 0 \\ -\frac{1}{2}(\bar{v}_R w_I + \bar{w}_I v_R - \bar{v}_I w_R - \bar{w}_R v_I) & 0 \end{bmatrix} \right) id\phi \\
& + \left( \begin{bmatrix} \frac{1}{2}(\bar{v}_R w_R + \bar{w}_R v_R + \bar{v}_I w_I + \bar{w}_I v_I) & |v_R|^2 + |v_I|^2 + |\sigma_R|^2 + |\sigma_I|^2 + |\tau|^2 \\ |w_R|^2 + |w_I|^2 + |\sigma_R|^2 + |\sigma_I|^2 + |\tau|^2 & \frac{1}{2}(\bar{v}_R w_R + \bar{w}_R v_R + \bar{v}_I w_I + \bar{w}_I v_I) \end{bmatrix} \right. \\
& \left. + i \begin{bmatrix} \frac{1}{2}(\bar{v}_R w_I + \bar{w}_I v_R - \bar{v}_I w_R - \bar{w}_R v_I) & 4\zeta\sigma_3 \\ 4\zeta\sigma_3 & -\frac{1}{2}(\bar{v}_R w_I + \bar{w}_I v_R - \bar{v}_I w_R - \bar{w}_R v_I) \end{bmatrix} \right) id\psi
\end{aligned}$$

$$\begin{aligned}
& + \left( \begin{bmatrix} \frac{1}{2}(\bar{v}_R w_R + \bar{w}_R v_R + \bar{v}_I w_I + \bar{w}_I v_I) & -(|v_R|^2 + |v_I|^2 + |\sigma_R|^2 + |\sigma_I|^2 + |\tau|^2) \\ |w_R|^2 + |w_I|^2 + |\sigma_R|^2 + |\sigma_I|^2 + |\tau|^2 & -\frac{1}{2}(\bar{v}_R w_R + \bar{w}_R v_R + \bar{v}_I w_I + \bar{w}_I v_I) \end{bmatrix} \right. \\
& \left. + i \begin{bmatrix} \frac{1}{2}(\bar{v}_R w_I + \bar{w}_I v_R - \bar{v}_I w_R - \bar{w}_R v_I) & -4\zeta\sigma_3 \\ 4\zeta\sigma_3 & \frac{1}{2}(\bar{v}_R w_I + \bar{w}_I v_R - \bar{v}_I w_R - \bar{w}_R v_I) \end{bmatrix} \right) d\theta \\
& + \left( \begin{bmatrix} 0 & \frac{1}{2}(\bar{v}_R w_R + \bar{w}_R v_R + \bar{v}_I w_I + \bar{w}_I v_I) \\ 0 & |w_R|^2 + |w_I|^2 + |\sigma_R|^2 + |\sigma_I|^2 + |\tau|^2 \end{bmatrix} + i \begin{bmatrix} 0 & \frac{1}{2}(\bar{v}_R w_I + \bar{w}_I v_R - \bar{v}_I w_R - \bar{w}_R v_I) \\ 0 & -4\zeta\sigma_3 \end{bmatrix} \right) id\chi \\
\end{aligned} \tag{C.0.8}$$

We can now take each of these away from their conjugate transpose. First, we look at  $a^\dagger a dR - (a^\dagger a dR)^{T*}$ , which is

$$\begin{aligned}
& \left( \begin{bmatrix} 0 & -\frac{1}{2}(\bar{v}_R w_I + \bar{w}_I v_R - \bar{v}_I w_R - \bar{w}_R v_I) \\ \frac{1}{2}(\bar{v}_R w_I + \bar{w}_I v_R - \bar{v}_I w_R - \bar{w}_R v_I) & 0 \end{bmatrix} \right. \\
& + 2i \left[ \begin{bmatrix} |v_R|^2 + |v_I|^2 + |\sigma_R|^2 + |\sigma_I|^2 + |\tau|^2 & \frac{1}{4}(\bar{v}_R w_R + \bar{w}_R v_R + \bar{v}_I w_I + \bar{w}_I v_I) \\ \frac{1}{4}(\bar{v}_R w_R + \bar{w}_R v_R + \bar{v}_I w_I + \bar{w}_I v_I) & 0 \end{bmatrix} \right] d\phi \\
& + i \left[ \begin{bmatrix} \bar{v}_R w_R + \bar{w}_R v_R + \bar{v}_I w_I + \bar{w}_I v_I & |v_R|^2 + |v_I|^2 + |w_R|^2 + |w_I|^2 + 2(|\sigma_R|^2 + |\sigma_I|^2 + |\tau|^2) \\ |v_R|^2 + |v_I|^2 + |w_R|^2 + |w_I|^2 + 2(|\sigma_R|^2 + |\sigma_I|^2 + |\tau|^2) & \bar{v}_R w_R + \bar{w}_R v_R + \bar{v}_I w_I + \bar{w}_I v_I \end{bmatrix} \right] d\psi \\
& + \left( \begin{bmatrix} 0 & -(|v_R|^2 + |v_I|^2 + |w_R|^2 + |w_I|^2 + 2(|\sigma_R|^2 + |\sigma_I|^2 + |\tau|^2)) \\ |v_R|^2 + |v_I|^2 + |w_R|^2 + |w_I|^2 + 2(|\sigma_R|^2 + |\sigma_I|^2 + |\tau|^2) & 0 \end{bmatrix} \right. \\
& \left. i \begin{bmatrix} (\bar{v}_R w_I + \bar{w}_I v_R - \bar{v}_I w_R - \bar{w}_R v_I) & 0 \\ -0 & (\bar{v}_R w_I + \bar{w}_I v_R - \bar{v}_I w_R - \bar{w}_R v_I) \end{bmatrix} \right) d\theta \\
& + \left( \begin{bmatrix} 0 & -\frac{1}{2}(\bar{v}_R w_I + \bar{w}_I v_R - \bar{v}_I w_R - \bar{w}_R v_I) \\ \frac{1}{2}(\bar{v}_R w_I + \bar{w}_I v_R - \bar{v}_I w_R - \bar{w}_R v_I) & 0 \end{bmatrix} \right. \\
& \left. 2i \begin{bmatrix} 0 & \frac{1}{4}(\bar{v}_R w_R + \bar{w}_R v_R + \bar{v}_I w_I + \bar{w}_I v_I) \\ \frac{1}{4}(\bar{v}_R w_R + \bar{w}_R v_R + \bar{v}_I w_I + \bar{w}_I v_I) & |w_R|^2 + |w_I|^2 + |\sigma_R|^2 + |\sigma_I|^2 + |\tau|^2 \end{bmatrix} \right) d\chi \\
\end{aligned} \tag{C.0.9}$$

Next we look at  $a^\dagger b dR b^\dagger a - (a^\dagger b dR b^\dagger a)^{T*}$

$$\begin{aligned}
& 2i \begin{bmatrix} |\tau|^2 & 0 \\ 0 & |\sigma_R|^2 + |\sigma_I|^2 \end{bmatrix} d\phi + 2i \begin{bmatrix} |\sigma_R|^2 + |\sigma_I|^2 & 0 \\ 0 & |\tau|^2 \end{bmatrix} d\chi \\
& + \left( 2 \begin{bmatrix} 0 & \bar{\sigma}_R \sigma_I + \bar{\sigma}_I \sigma_R \\ -(\bar{\sigma}_R \sigma_I + \bar{\sigma}_I \sigma_R) & 0 \end{bmatrix} + 2i \begin{bmatrix} 0 & |\sigma_R|^2 - |\sigma_I|^2 - |\tau|^2 \\ |\sigma_R|^2 - |\sigma_I|^2 - |\tau|^2 & 0 \end{bmatrix} \right) d\psi \\
& + \left( 2 \begin{bmatrix} 0 & |\tau|^2 + |\sigma_R|^2 - |\sigma_I|^2 \\ |\sigma_I|^2 - |\sigma_R|^2 - |\tau|^2 & 0 \end{bmatrix} + 2i \begin{bmatrix} 0 & -(\bar{\sigma}_R \sigma_I + \bar{\sigma}_I \sigma_R) \\ -(\bar{\sigma}_R \sigma_I + \bar{\sigma}_I \sigma_R) & 0 \end{bmatrix} \right) d\theta \\
\end{aligned} \tag{C.0.10}$$



Now we put them together as

$$a^\dagger adR - (a^\dagger adR)^{T^*} - a^\dagger b dR b^\dagger a + (a^\dagger b dR b^\dagger a)^{T^*} \quad (\text{C.0.11})$$

which becomes

$$\begin{aligned} & \left( \begin{bmatrix} 0 & -\frac{1}{2}(\bar{v}_R w_I + \bar{w}_I v_R - \bar{v}_I w_R - \bar{w}_R v_I) \\ \frac{1}{2}(\bar{v}_R w_I + \bar{w}_I v_R - \bar{v}_I w_R - \bar{w}_R v_I) & 0 \end{bmatrix} \right. \\ & + 2i \left[ \begin{array}{cc} |v_R|^2 + |v_I|^2 + |\sigma_R|^2 + |\sigma_I|^2 & \frac{1}{4}(\bar{v}_R w_R + \bar{w}_R v_R + \bar{v}_I w_I + \bar{w}_I v_I) \\ \frac{1}{4}(\bar{v}_R w_R + \bar{w}_R v_R + \bar{v}_I w_I + \bar{w}_I v_I) & -|\sigma_R|^2 - |\sigma_I|^2 \end{array} \right] d\phi \\ & + \left( 2 \begin{bmatrix} 0 & -\bar{\sigma}_R \sigma_I - \bar{\sigma}_I \sigma_R - 4\zeta \sigma_3 \\ 4\zeta \sigma_3 + \sigma_R \sigma_I + \bar{\sigma}_I \sigma_R & 0 \end{bmatrix} \right. \\ & + i \left[ \begin{array}{cc} \bar{v}_R w_R + \bar{w}_R v_R + \bar{v}_I w_I + \bar{w}_I v_I & |v_R|^2 + |v_I|^2 + |w_R|^2 + |w_I|^2 + 4(|\sigma_I|^2 + |\tau|^2) \\ |v_R|^2 + |v_I|^2 + |w_R|^2 + |w_I|^2 + 4(|\sigma_I|^2 + |\tau|^2) & \bar{v}_R w_R + \bar{w}_R v_R + \bar{v}_I w_I + \bar{w}_I v_I \end{array} \right] \Big) d\psi \\ & \left( \begin{bmatrix} 0 & -(|v_R|^2 + |v_I|^2 + |w_R|^2 + |w_I|^2 + 4(|\tau|^2 + |\sigma_R|^2)) \\ |v_R|^2 + |v_I|^2 + |w_R|^2 + |w_I|^2 + 4(|\tau|^2 + |\sigma_R|^2) & 0 \end{bmatrix} \right. \\ & + \left( \begin{bmatrix} 0 & -\frac{1}{2}(\bar{v}_R w_I + \bar{w}_I v_R - \bar{v}_I w_R - \bar{w}_R v_I) \\ \frac{1}{2}(\bar{v}_R w_I + \bar{w}_I v_R - \bar{v}_I w_R - \bar{w}_R v_I) & 0 \end{bmatrix} \right. \\ & \left. \left. 2i \begin{bmatrix} -|\sigma_R|^2 - |\sigma_I|^2 & \frac{1}{4}(\bar{v}_R w_R + \bar{w}_R v_R + \bar{v}_I w_I + \bar{w}_I v_I) \\ \frac{1}{4}(\bar{v}_R w_R + \bar{w}_R v_R + \bar{v}_I w_I + \bar{w}_I v_I) & |w_R|^2 + |w_I|^2 + |\sigma_R|^2 + |\sigma_I|^2 + \end{bmatrix} \right) \right) d\chi \\ & \quad \quad \quad (\text{C.0.12}) \end{aligned}$$

Now we calculate  $a^\dagger da - (a^\dagger da)^{T^*}$

$$\begin{aligned} & \left[ \begin{array}{cc} 0 & \bar{v}_R dw_R + \bar{v}_I dw_I - \bar{w}_R dv_R - \bar{w}_I dv_I + 2(\bar{\tau} d\sigma_R - \bar{\sigma}_R d\tau) \\ -(\bar{v}_R dw_R + \bar{v}_I dw_I - \bar{w}_R dv_R - \bar{w}_I dv_I + 2(\bar{\tau} d\sigma_R - \bar{\sigma}_R d\tau)) & 0 \end{array} \right] \\ & + i \left[ \begin{array}{cc} 2(\bar{v}_R dv_I - \bar{v}_I dv_R + \bar{\sigma}_R d\sigma_I - \bar{\sigma}_I d\sigma_R) & \bar{v}_R dw_I - \bar{v}_I dw_R + \bar{w}_R dv_I - \bar{w}_I dv_R + 2(\bar{\sigma}_I d\tau - \bar{\tau} d\sigma_I) \\ \bar{v}_R dw_I - \bar{v}_I dw_R + \bar{w}_R dv_I - \bar{w}_I dv_R + 2(\bar{\sigma}_I d\tau - \bar{\tau} d\sigma_I) & 2(\bar{w}_R dw_I - \bar{w}_I dw_R - \bar{\sigma}_R d\sigma_I + \bar{\sigma}_I d\sigma_R) \end{array} \right] \\ & \quad \quad \quad (\text{C.0.13}) \end{aligned}$$

We are now in a position to solve (5.7.1). To do this we solve

$$a^\dagger da - (a^\dagger da)^{T^*} = a^\dagger b(dR)b^\dagger a - (a^\dagger b(dR)b^\dagger a)^{T^*} - a^\dagger a(dR) + (a^\dagger da)^{T^*} \quad (\text{C.0.14})$$

This gives us several equations from the different components of the matrix. First, the  $\begin{bmatrix} 0 & -1 \\ 1 & 0 \end{bmatrix}$  component gives

$$\begin{aligned} \bar{v}_R dv_R + \bar{v}_I dv_I - \bar{w}_R dv_R - w_I dv_I + 2(\bar{\tau} d\sigma_R - \bar{\sigma}_R d\tau) &= 4(\operatorname{Re}(\bar{\sigma}_R \sigma_I)) d\psi \\ + (|v_R|^2 + |v_I|^2 + |w_R|^2 + |w_I|^2 + 4(|\tau|^2 + |\sigma_R|^2)) d\theta &+ \operatorname{Re}(\bar{v}_R w_I - \bar{w}_I v_R)(d\phi + d\chi) \end{aligned} \quad (\text{C.0.15})$$

Next, from the  $\begin{bmatrix} 0 & i \\ i & 0 \end{bmatrix}$  component, we have

$$\begin{aligned} \bar{v}_R dw_I - \bar{v}_I dw_R + \bar{w}_R dv_I - \bar{w}_I dv_R + 2(\bar{\sigma}_I d\tau - \bar{\tau} d\sigma_I) &= \\ - (|v_R|^2 + |v_I|^2 + |w_R|^2 + |w_I|^2 + 4(|\sigma_I|^2 + |\tau|^2)) d\psi &- 4(\operatorname{Re}(\bar{\sigma}_R \sigma_I)) d\theta \\ - \operatorname{Re}(\bar{v}_R w_R + \bar{v}_I w_I)(d\phi + d\chi) & \end{aligned} \quad (\text{C.0.16})$$

The  $\begin{bmatrix} i & 0 \\ 0 & 0 \end{bmatrix}$  component gives

$$\begin{aligned} \bar{v}_R dv_I - \bar{v}_I dv_R + \bar{\sigma}_R d\sigma_I - \bar{\sigma}_I d\sigma_R &= -\operatorname{Re}(\bar{v}_R w_R + \bar{v}_I w_I) d\psi - \operatorname{Re}(\bar{v}_R w_I - \bar{v}_I w_R) d\theta \\ - (|v_R|^2 + |v_I|^2 + |\sigma_R|^2 + |\sigma_I|^2) d\phi &+ (|\sigma_R|^2 + |\sigma_I|^2) d\chi \end{aligned} \quad (\text{C.0.17})$$

and finally the  $\begin{bmatrix} 0 & 0 \\ 0 & i \end{bmatrix}$  component gives

$$\begin{aligned} \bar{w}_R dw_I - \bar{w}_I dw_R - \bar{\sigma}_R d\sigma_I + \bar{\sigma}_I d\sigma_R &= -\operatorname{Re}(\bar{v}_R w_R + \bar{v}_I w_I) d\psi - \operatorname{Re}(\bar{v}_R w_I - \bar{v}_I w_R) d\theta \\ - (|w_R|^2 + |w_I|^2 + |\sigma_R|^2 + |\sigma_I|^2) d\chi &+ (|\sigma_R|^2 + |\sigma_I|^2) d\phi \end{aligned} \quad (\text{C.0.18})$$

If we add (C.0.17) and (C.0.18) we get

$$\begin{aligned} \bar{v}_R dv_I - \bar{v}_I dv_R + \bar{w}_R dw_I - \bar{w}_I dw_R &= \\ - (|w_R|^2 + |w_I|^2) d\chi - (|v_R|^2 + |v_I|^2) d\phi &- 2\operatorname{Re}(\bar{v}_R w_R + \bar{v}_I w_I) d\psi - 2\operatorname{Re}(\bar{v}_R w_I - \bar{v}_I w_R) d\theta \end{aligned} \quad (\text{C.0.19})$$

If we take them away, we get

$$\begin{aligned} & \bar{v}_R dv_I - \bar{v}_I dv_R - \bar{w}_R dw_I + \bar{w}_I dw_R + 2(\bar{\sigma}_R d\sigma_I - \bar{\sigma}_I d\sigma_R) = \\ & \left( |w_R| + |w_I|^2 + 2(|\sigma_R|^2 + |\sigma_I|^2) \right) d\chi - \left( |v_R| + |v_I|^2 + 2(|\sigma_R|^2 + |\sigma_I|^2) \right) d\phi \quad (\text{C.0.20}) \end{aligned}$$

We can solve (C.0.15), (C.0.16), (C.0.19), (C.0.20) using Mathematica to get the result in the main text, (5.7.7)

# Appendix D

## The Three Instanton Scalar Field

The equation we want to solve is still

$$2\text{Tr}_2(\Lambda^\dagger \mathbf{q} \Lambda) + \text{Tr}_2([\Omega^\dagger, P]\Omega - \Omega^\dagger[\Omega, P]) - \text{Tr}_2(\{P, \Lambda^\dagger \Lambda\}) = 0 \quad (\text{D.0.1})$$

Note that in this appendix Re and Im refer to  $\text{Re}_{\mathbb{H}}$  and  $\text{Im}_{\mathbb{H}}$  unless otherwise stated.

We now work out what each of these terms are equal to. First of all, we have

$\text{Tr}_2(\Lambda^\dagger \mathbf{q} \Lambda)$  This turns out to be

$$2 \begin{bmatrix} 0 & -\text{Re}(\bar{v} \mathbf{q} u) & \text{Re}(\bar{u} \mathbf{q} w) \\ \text{Re}(\bar{v} \mathbf{q} u) & 0 & -\text{Re}(\bar{w} \mathbf{q} v) \\ -\text{Re}(\bar{u} \mathbf{q} w) & \text{Re}(\bar{w} \mathbf{q} v) & 0 \end{bmatrix} \quad (\text{D.0.2})$$

Then we also have  $\text{Tr}_2\{P, \Lambda^\dagger \Lambda\}$

$$\begin{bmatrix} 0 & b\text{Re}(\bar{w}v) + c\text{Re}(\bar{u}w) - 2a(|u|^2 + |v|^2) & 2b(|w|^2 + |u|^2) - a\text{Re}(\bar{v}w) - c\text{Re}(\bar{u}v) \\ 2a(|v|^2 + |u|^2) - c\text{Re}(\bar{u}w) - b\text{Re}(\bar{w}v) & 0 & a\text{Re}(\bar{u}w) + b\text{Re}(\bar{v}u) - 2c(|w|^2 + |v|^2) \\ a\text{Re}(\bar{v}w) + c\text{Re}(\bar{u}v) - 2b(|u|^2 + |w|^2) & 2c(|v|^2 + |w|^2) - b\text{Re}(\bar{v}u) - a\text{Re}(\bar{u}w) & 0 \end{bmatrix} \quad (\text{D.0.3})$$

Next, we calculate  $\text{Tr}_2([\Omega^\dagger, P]\Omega - \Omega^\dagger[\Omega, P])$  in sections, as  $\text{Tr}_2(2\Omega^\dagger P\Omega - \{P, \Omega^\dagger \Omega\})$ .

First, we have  $2\text{Tr}_2(\Omega^\dagger P\Omega)$

$$2a \begin{bmatrix} 0 & 2|\sigma_1|^2 - \text{Re}(\bar{\tau}_1 \tau_2) & \text{Re}(\bar{\sigma}_1 \sigma_2 - \bar{\tau}_1 \sigma_3) \\ \text{Re}(\bar{\tau}_2 \tau_1) - 2|\sigma_1|^2 & 0 & \text{Re}(\bar{\tau}_2 \sigma_2) - \text{Re}(\bar{\sigma}_1 \sigma_3) \\ \text{Re}(\bar{\sigma}_3 \tau_1) - \text{Re}(\bar{\sigma}_2 \sigma_1) & \text{Re}(\bar{\sigma}_3 \sigma_1) - \text{Re}(\bar{\sigma}_2 \tau_2) & 0 \end{bmatrix}$$

$$\begin{aligned}
& +2b \begin{bmatrix} 0 & \text{Re}(\bar{\tau}_1\sigma_3) - \text{Re}(\bar{\sigma}_2\sigma_1) & \text{Re}(\bar{\tau}_1\tau_3) - 2|\sigma_2|^2 \\ \text{Re}(\bar{\sigma}_1\sigma_2) - \text{Re}(\bar{\sigma}_3\tau_1) & 0 & \text{Re}(\bar{\sigma}_1\tau_3 - \bar{\sigma}_3\sigma_2) \\ 2|\sigma_2|^2 - \text{Re}(\bar{\tau}_3\tau_1) & \text{Re}(\bar{\sigma}_2\sigma_3) - \text{Re}(\bar{\tau}_3\sigma_1) & 0 \end{bmatrix} \\
& +2c \begin{bmatrix} 0 & \text{Re}(\bar{\sigma}_2\tau_2) - \text{Re}(\bar{\sigma}_1\sigma_3) & \text{Re}(\bar{\sigma}_2\sigma_3) - \text{Re}(\bar{\sigma}_1\tau_3) \\ \text{Re}(\bar{\sigma}_3\sigma_1) - \text{Re}(\bar{\tau}_2\sigma_2) & 0 & 2|\sigma_3|^2 - \text{Re}(\bar{\tau}_2\tau_3) \\ \text{Re}(\bar{\tau}_3\sigma_1 - \bar{\sigma}_3\sigma_2) & -2|\sigma_3|^2 + \text{Re}(\bar{\tau}_3\tau_2) & 0 \end{bmatrix} \quad (\text{D.0.4})
\end{aligned}$$

Next we look at  $\text{Tr}_2(\{P, \Omega^\dagger\Omega\})$

$$\begin{aligned}
& a \begin{bmatrix} 0 & -2(2|\sigma_1|^2 + |\sigma_2|^2 + |\sigma_3|^2 + |\tau_1|^2 + |\tau_2|^2) & -\text{Re}(\bar{\sigma}_1\sigma_2) - \text{Re}(\bar{\tau}_2\sigma_3) - \text{Re}(\bar{\sigma}_3\tau_3) \\ 2(2|\sigma_1|^2 + |\sigma_2|^2 + |\sigma_3|^2 + |\tau_1|^2 + |\tau_2|^2) & 0 & \text{Re}(\bar{\tau}_1\sigma_2) + \text{Re}(\bar{\sigma}_1\sigma_3) + \text{Re}(\bar{\sigma}_2\tau_3) \\ \text{Re}(\bar{\sigma}_1\sigma_2) + \text{Re}(\bar{\tau}_2\sigma_3) + \text{Re}(\bar{\sigma}_3\tau_3) & -\text{Re}(\bar{\tau}_1\sigma_2) - \text{Re}(\bar{\sigma}_1\sigma_3) - \text{Re}(\bar{\sigma}_2\tau_3) & 0 \end{bmatrix} \\
& +b \begin{bmatrix} 0 & \text{Re}(\bar{\sigma}_2\sigma_1) + \text{Re}(\bar{\sigma}_3\tau_2) + \text{Re}(\bar{\tau}_3\sigma_3) & 2(2|\sigma_2|^2 + |\sigma_1|^2 + |\sigma_3|^2 + |\tau_1|^2 + |\tau_3|^2) \\ -\text{Re}(\bar{\sigma}_2\sigma_1) - \text{Re}(\bar{\sigma}_3\tau_2) - \text{Re}(\bar{\tau}_3\sigma_3) & 0 & \text{Re}(\bar{\tau}_1\sigma_1) + \text{Re}(\bar{\sigma}_1\tau_2) + \text{Re}(\bar{\sigma}_2\sigma_3) \\ -2(2|\sigma_2|^2 + |\sigma_1|^2 + |\sigma_3|^2 + |\tau_1|^2 + |\tau_3|^2) & -\text{Re}(\bar{\tau}_1\sigma_1) - \text{Re}(\bar{\sigma}_1\tau_2) - \text{Re}(\bar{\sigma}_2\sigma_3) & 0 \end{bmatrix} \\
& +c \begin{bmatrix} 0 & \text{Re}(\bar{\tau}_1\sigma_2) + \text{Re}(\bar{\sigma}_1\sigma_3) + \text{Re}(\bar{\sigma}_2\tau_3) & -\text{Re}(\bar{\tau}_1\sigma_1) - \text{Re}(\bar{\sigma}_1\tau_2) - \text{Re}(\bar{\sigma}_2\sigma_3) \\ -\text{Re}(\bar{\tau}_1\sigma_2) - \text{Re}(\bar{\sigma}_1\sigma_3) - \text{Re}(\bar{\sigma}_2\tau_3) & 0 & -2(2|\sigma_3|^2 + |\sigma_1|^2 + |\sigma_2|^2 + |\tau_2|^2 + |\tau_3|^2) \\ \text{Re}(\bar{\tau}_1\sigma_1) + \text{Re}(\bar{\sigma}_1\tau_2) + \text{Re}(\bar{\sigma}_2\sigma_3) & 2(2|\sigma_3|^2 + |\sigma_1|^2 + |\sigma_2|^2 + |\tau_2|^2 + |\tau_3|^2) & 0 \end{bmatrix} \quad (\text{D.0.5})
\end{aligned}$$

Finally we put them together to get  $\text{Tr}_2([\Omega^\dagger, P]\Omega - \Omega^\dagger[\Omega, P])$  as

$$\begin{aligned}
& a \begin{bmatrix} 0 & 2(3|\sigma_1|^2 + \Sigma^2 + |\tau_1|^2 + |\tau_2|^2) - 2\text{Re}(\bar{\tau}_1\tau_2) & 3\text{Re}(\bar{\sigma}_1\sigma_2) + \text{Re}((\bar{\tau}_3 + \bar{\tau}_2 - 2\bar{\tau}_1)\sigma_3) \\ -2(2|\sigma_1|^2 + \Sigma^2 + |\tau_1|^2 + |\tau_2|^2) + 2\text{Re}(\bar{\tau}_1\tau_2) & 0 & \text{Re}((2\bar{\tau}_2 - \bar{\tau}_1 - \bar{\tau}_3)\sigma_2) - 3\text{Re}(\bar{\sigma}_1\sigma_3) \\ -3\text{Re}(\bar{\sigma}_1\sigma_2) - \text{Re}((\bar{\tau}_3 + \bar{\tau}_2 - 2\bar{\tau}_1)\sigma_3) & -\text{Re}((2\bar{\tau}_2 - \bar{\tau}_1 - \bar{\tau}_3)\sigma_2) + 3\text{Re}(\bar{\sigma}_1\sigma_3) & 0 \end{bmatrix} \\
& +b \begin{bmatrix} 0 & \text{Re}((2\bar{\tau}_1 - \bar{\tau}_2 - \bar{\tau}_3)\sigma_3) - 3\text{Re}(\bar{\sigma}_2\sigma_1) & 2\text{Re}(\bar{\tau}_1\tau_3) - 2(3|\sigma_2|^2 + \Sigma^2 + |\tau_1|^2 + |\tau_3|^2) \\ -\text{Re}((2\bar{\tau}_1 - \bar{\tau}_2 - \bar{\tau}_3)\sigma_3) + 3\text{Re}(\bar{\sigma}_2\sigma_1) & 0 & \text{Re}((2\bar{\tau}_3 - \bar{\tau}_2 - \bar{\tau}_1)\sigma_1) - 3\text{Re}(\bar{\sigma}_3\sigma_2) \\ -2\text{Re}(\bar{\tau}_1\tau_3) + 2(3|\sigma_2|^2 + \Sigma^2 + |\tau_1|^2 + |\tau_3|^2) & -\text{Re}((2\bar{\tau}_3 - \bar{\tau}_2 - \bar{\tau}_1)\sigma_1) + 3\text{Re}(\bar{\sigma}_3\sigma_2) & 0 \end{bmatrix} \\
& +c \begin{bmatrix} 0 & \text{Re}((2\bar{\tau}_2 - \bar{\tau}_3 - \bar{\tau}_1)\sigma_2) - 3\text{Re}(\bar{\sigma}_1\sigma_3) & 3\text{Re}(\bar{\sigma}_2\sigma_3) - \text{Re}((2\bar{\tau}_3 - \bar{\tau}_2 - \bar{\tau}_1)\sigma_1) \\ 3\text{Re}(\bar{\sigma}_3\sigma_1) - \text{Re}((2\bar{\tau}_2 - \bar{\tau}_3 - \bar{\tau}_1)\sigma_2) & 0 & 2(2|\sigma_3|^2 + \Sigma^2 + |\tau_2|^2 + |\tau_3|^2) - 2\text{Re}(\bar{\tau}_2\tau_3) \\ -3\text{Re}(\bar{\sigma}_2\sigma_3) + \text{Re}((2\bar{\tau}_3 - \bar{\tau}_2 - \bar{\tau}_1)\sigma_1) & -2(2|\sigma_3|^2 + \Sigma^2 + |\tau_2|^2 + |\tau_3|^2) + 2\text{Re}(\bar{\tau}_2\tau_3) & 0 \end{bmatrix} \quad (\text{D.0.6})
\end{aligned}$$

where

$$\Sigma = |\sigma_1|^2 + |\sigma_2|^2 + |\sigma_3|^2 \quad (\text{D.0.7})$$

We can now write down three equations, one for each component of (7.2.4). First,

the  $\begin{bmatrix} 0 & -1 & 0 \\ 1 & 0 & 0 \\ 0 & 0 & 0 \end{bmatrix}$  component, together with the identity  $\tau_1 + \tau_2 + \tau_3 = 0$ , gives

$$\begin{aligned} 4\text{Re}(\bar{v}\mathbf{q}u) &= 2a(|u|^2 + |v|^2 + 2|\sigma_1|^2 + \Sigma^2 + |\tau_1|^2 + |\tau_2|^2 - \text{Re}(\bar{\tau}_1\tau_2)) \\ &+ b(3\text{Re}(\bar{\tau}_1\sigma_3) - 3\text{Re}(\bar{\sigma}_2\sigma_1) - \text{Re}(\bar{w}v)) + c(3\text{Re}(\bar{\tau}_2\sigma_2) - 3\text{Re}(\bar{\sigma}_1\sigma_3) - \text{Re}(\bar{u}w)) \end{aligned} \quad (\text{D.0.8})$$

Next, we have the  $\begin{bmatrix} 0 & 0 & 1 \\ 0 & 0 & 0 \\ -1 & 0 & 0 \end{bmatrix}$  component, which results in

$$\begin{aligned} 4\text{Re}(\bar{u}\mathbf{q}w) &= -a(3\text{Re}(\bar{\sigma}_1\sigma_2) - 3\text{Re}(\bar{\tau}_1\sigma_3) + \text{Re}(\bar{v}w)) \\ &+ 2b(|w|^2 + |v|^2 + 3|\sigma_2|^2 + \Sigma^2 + |\tau_1|^2 + |\tau_3|^2 - \text{Re}(\bar{\tau}_1\tau_3)) \\ &- c(3\text{Re}(\bar{\sigma}_2\sigma_3) - 3\text{Re}(\bar{\tau}_3\sigma_1) + \text{Re}(\bar{u}v)) \end{aligned} \quad (\text{D.0.9})$$

Finally, we have the equation resulting from  $\begin{bmatrix} 0 & 0 & 0 \\ 0 & 0 & -1 \\ 0 & 1 & 0 \end{bmatrix}$

$$\begin{aligned} 4\text{Re}(\bar{w}\mathbf{q}v) &= a(3\text{Re}(\bar{\tau}_2\sigma_2) - 2\text{Re}(\bar{\sigma}_1\sigma_3) - \text{Re}(\bar{u}w)) \\ &+ b(3\text{Re}(\bar{\tau}_3\sigma_1) - 3\text{Re}(\bar{\sigma}_3\sigma_2) - \text{Re}(\bar{v}u)) \\ &+ 2c(|w|^2 + |v|^2 + 2|\sigma_3|^2 + \Sigma^2 + |\tau_2|^2 + |\tau_3|^2 - \text{Re}(\bar{\tau}_2\tau_3)) \end{aligned} \quad (\text{D.0.10})$$

We can then use Mathematica to solve for the solutions give in (7.2.5)



# Appendix E

## The Three Instanton Potential

In this appendix Re and Im refer to  $\text{Re}_{\mathbb{H}}$  and  $\text{Im}_{\mathbb{H}}$  unless otherwise stated. First, we look at

$$\hat{x}_i D_i \phi = \hat{x}_i \left( iU^\dagger e_i b f \Delta^\dagger \mathcal{A} U + iU^\dagger \mathcal{A} \Delta f \bar{e}_i b^\dagger U \right) \quad (\text{E.0.1})$$

in this  $|x| \mapsto \infty$  limit. We will make use of these results:

$$\Delta \mapsto \begin{bmatrix} u & v & w \\ -x & 0 & 0 \\ 0 & -x & 0 \\ 0 & 0 & -x \end{bmatrix} \quad f_{kl} \mapsto \frac{1}{|x|^2} \delta_{kl} \quad (\text{E.0.2})$$

Then we can write

$$\hat{x}_i D_i \phi \mapsto \frac{i}{|x|^2} \left( \hat{x} U^\dagger b \mathbb{1}_3 \begin{bmatrix} \bar{u} & -\bar{x} & 0 & 0 \\ \bar{v} & 0 & -\bar{x} & 0 \\ \bar{w} & 0 & 0 & -\bar{x} \end{bmatrix} \mathcal{A} U + \hat{x} U^\dagger \mathcal{A} \begin{bmatrix} u & v & w \\ -x & 0 & 0 \\ 0 & -x & 0 \\ 0 & 0 & -x \end{bmatrix} \mathbb{1}_3 b^\dagger U \right) \quad (\text{E.0.3})$$



Where  $\mathcal{A}$ , as above, is

$$\begin{bmatrix} \mathbf{q} & 0 & 0 & 0 \\ 0 & 0 & -a & b \\ 0 & a & 0 & -c \\ 0 & -b & c & 0 \end{bmatrix} \quad (\text{E.0.4})$$

and

$$b = \begin{bmatrix} 0 & 0 & 0 \\ 1 & 0 & 0 \\ 0 & 1 & 0 \\ 0 & 0 & 1 \end{bmatrix} \quad (\text{E.0.5})$$

This gives

$$\frac{i}{|x|^2} \left( \hat{x}U^\dagger \begin{bmatrix} 0 & 0 & 0 & 0 \\ \bar{u}\mathbf{q} & 0 & \bar{x}a & -\bar{x}b \\ \bar{v}\mathbf{q} & -\bar{x}a & 0 & \bar{x}c \\ \bar{w}\mathbf{q} & \bar{x}b & -\bar{x}c & 0 \end{bmatrix} U + \hat{x}U^\dagger \begin{bmatrix} 0 & \mathbf{q}u & \mathbf{q}v & \mathbf{q}w \\ 0 & 0 & ax & -bx \\ 0 & -ax & 0 & cx \\ 0 & bx & -cx & 0 \end{bmatrix} U \right) \quad (\text{E.0.6})$$

which contracts as

$$\begin{aligned} \hat{x}_i D_i \phi = \frac{i}{|x|^2} & \left( \hat{x}U_1^\dagger \mathbf{q}uU_2 + \hat{x}U_2^\dagger \bar{u}\mathbf{q}U_1 + \hat{x}U_3^\dagger \bar{v}\mathbf{q}U_1 + \hat{x}U_1^\dagger \mathbf{q}vU_3 + \hat{x}U_1^\dagger \mathbf{q}wU_4 + \hat{x}U_4^\dagger \bar{w}\mathbf{q}U_1 \right. \\ & \left. + 2a|x|(U_2^\dagger U_3 - U_3^\dagger U_2) + 2b|x|(U_4^\dagger U_2 - U_2^\dagger U_4) + 2c|x|(U_3^\dagger U_4 - U_4^\dagger U_3) \right) \end{aligned} \quad (\text{E.0.7})$$

Expanding the  $U_i$  we get

$$\hat{x}_i D_i \phi = \frac{2i}{|x|^3} \left( \mathbf{q}(|u|^2 + |v|^2 + |w|^2) + a(u\bar{v} - v\bar{u}) + b(w\bar{u} - u\bar{w}) + c(v\bar{w} - w\bar{v}) \right) \quad (\text{E.0.8})$$

We now combine this result with the fact that the scalar field  $\phi$  tends to  $iq$  at infinity, to get

$$V = \lim_{|x|^2 \rightarrow \infty} - \int d^3S \frac{2}{|x|^3} \text{Tr} \left( \mathbf{q}^2(|u|^2 + |v|^2 + |w|^2) + \mathbf{q} \left( a(u\bar{v} - u\bar{w}) + b(w\bar{u} - u\bar{w}) + c(v\bar{w} - w\bar{v}) \right) \right) \quad (\text{E.0.9})$$

---

Evaluating the integral, we have

$$\mathcal{V} = -8\pi^2 \text{Tr} \left( \mathbf{q}^2 (|u|^2 + |v|^2 + |w|^2) + \mathbf{q} \left( a(u\bar{v} - v\bar{u}) + b(w\bar{u} - u\bar{w}) + c(v\bar{w} - w\bar{v}) \right) \right) \quad (\text{E.0.10})$$

Finally, we can evaluate the trace to get the solution in (7.3.6)



# Appendix F

## The Three Instanton Metric

In this appendix Re and Im refer to  $\text{Re}_{\mathbb{H}}$  and  $\text{Im}_{\mathbb{H}}$  unless otherwise stated. First, we have  $a^\dagger da$ . This is

$$\begin{bmatrix} \bar{u}du + \bar{\tau}_1 d\tau_1 + \bar{\sigma}_1 d\sigma_1 + \bar{\sigma}_2 d\sigma_2 & \bar{u}dv + \bar{\tau}_1 d\sigma_1 + \bar{\sigma}_1 d\tau_2 + \bar{\sigma}_2 d\sigma_3 & \bar{u}dw + \bar{\tau}_1 d\sigma_2 + \bar{\sigma}_1 d\sigma_3 + \bar{\sigma}_2 d\tau_3 \\ \bar{v}du + \bar{\sigma}_1 d\tau_1 + \bar{\tau}_2 d\sigma_1 + \bar{\sigma}_3 d\sigma_2 & \bar{v}dv + \bar{\tau}_2 d\tau_2 + \bar{\sigma}_1 d\sigma_1 + \bar{\sigma}_3 d\sigma_3 & \bar{v}dw + \bar{\sigma}_1 d\sigma_2 + \bar{\tau}_2 d\sigma_3 + \bar{\sigma}_3 d\tau_3 \\ \bar{w}du + \bar{\sigma}_2 d\tau_1 + \bar{\sigma}_3 d\sigma_1 + \bar{\tau}_3 d\sigma_2 & \bar{w}dv + \bar{\sigma}_2 d\sigma_1 + \bar{\sigma}_3 d\tau_2 + \bar{\tau}_3 d\sigma_3 & \bar{w}dw + \bar{\tau}_3 d\tau_3 + \bar{\sigma}_3 d\sigma_3 + \bar{\sigma}_2 d\sigma_2 \end{bmatrix} \quad (\text{F.0.1})$$

Next we look at the term  $a^\dagger b(dR)b^\dagger a$ . As before, we split  $dR$  into the sum of its components, and so we have

$$\begin{aligned} & \begin{bmatrix} \text{Im}(\bar{\sigma}_1 \tau) & |\sigma_1|^2 - \bar{\tau}_1 \tau_2 & \bar{\sigma}_1 \sigma_2 - \bar{\tau}_1 \sigma_3 \\ \bar{\tau}_2 \tau_1 - |\sigma_1|^2 & \text{Im}(\bar{\tau}_2 \sigma_1) & \bar{\tau}_2 \sigma_2 - \bar{\sigma}_1 \sigma_3 \\ \bar{\sigma}_3 \tau_1 - \bar{\sigma}_2 \sigma_1 & \bar{\sigma}_3 \sigma_1 - \bar{\sigma}_2 \tau_2 & \text{Im}(\bar{\sigma}_3 \sigma_2) \end{bmatrix} d\phi + \begin{bmatrix} \text{Im}(\bar{\tau}_1 \sigma_2) & \bar{\tau}_1 \sigma_3 - \bar{\sigma}_2 \sigma_1 & \bar{\tau}_1 \tau_3 - |\sigma_2|^2 \\ \bar{\sigma}_1 \sigma_2 - \bar{\sigma}_3 \tau_1 & \text{Im}(\bar{\sigma}_1 \sigma_3) & \bar{\sigma}_1 \tau_3 - \bar{\sigma}_3 \sigma_2 \\ |\sigma_2|^2 - \bar{\tau}_3 \tau_1 & \bar{\sigma}_2 \sigma_3 - \bar{\tau}_3 \sigma_1 & \text{Im}(\bar{\sigma}_2 \tau_3) \end{bmatrix} d\theta \\ & + \begin{bmatrix} \text{Im}(\bar{\sigma}_2 \sigma_1) & \bar{\sigma}_2 \tau_2 - \bar{\sigma}_1 \sigma_3 & \bar{\sigma}_2 \sigma_3 - \bar{\sigma}_1 \tau_3 \\ \bar{\sigma}_3 \sigma_1 - \bar{\tau}_2 \sigma_2 & \text{Im}(\bar{\sigma}_3 \tau_2) & |\sigma_3|^2 - \bar{\tau}_2 \tau_3 \\ \bar{\tau}_3 \sigma_1 - \bar{\sigma}_3 \sigma_2 & \bar{\tau}_3 \tau_2 - |\sigma_3|^2 & \text{Im}(\bar{\tau}_3 \sigma_3) \end{bmatrix} d\psi \end{aligned} \quad (\text{F.0.2})$$

Finally,  $a^\dagger a(dR)$  is given by

$$\begin{bmatrix} |u|^2 + |\tau_1|^2 + |\sigma_1|^2 + |\sigma_2|^2 & \bar{u}v + \bar{\tau}_1 \sigma_1 + \bar{\sigma}_1 \tau_2 + \bar{\sigma}_2 \sigma_3 & \bar{u}w + \bar{\tau}_1 \sigma_2 + \bar{\sigma}_1 \sigma_3 + \bar{\sigma}_2 \tau_3 \\ \bar{v}u + \bar{\sigma}_1 \tau_1 + \bar{\tau}_2 \sigma_1 + \bar{\sigma}_3 \sigma_2 & |v|^2 + |\tau_2|^2 + |\sigma_1|^2 + |\sigma_3|^2 & \bar{v}w + \bar{\sigma}_1 \sigma_2 + \bar{\tau}_2 \sigma_3 + \bar{\sigma}_3 \tau_3 \\ \bar{w}u + \bar{\sigma}_2 \tau_1 + \bar{\sigma}_3 \sigma_1 + \bar{\tau}_3 \sigma_2 & \bar{w}v + \bar{\sigma}_2 \sigma_1 + \bar{\sigma}_3 \tau_2 + \bar{\tau}_3 \sigma_3 & |w|^2 + |\tau_3|^2 + |\sigma_2|^2 + |\sigma_3|^2 \end{bmatrix} dR \quad (\text{F.0.3})$$

Because of the ADHM equations, this matrix must be real and symmetric, so this expression must be equal to

$$\begin{bmatrix} |u|^2 + |\tau_1|^2 + |\sigma_1|^2 + |\sigma_2|^2 & \operatorname{Re}(\bar{u}v + \bar{\tau}_1\sigma_1 + \bar{\sigma}_1\tau_2 + \bar{\sigma}_2\sigma_3) & \operatorname{Re}(\bar{u}w + \bar{\tau}_1\sigma_2 + \bar{\sigma}_1\sigma_3 + \bar{\sigma}_2\tau_3) \\ \operatorname{Re}(\bar{u}v + \bar{\tau}_1\sigma_1 + \bar{\sigma}_1\tau_2 + \bar{\sigma}_2\sigma_3) & |v|^2 + |\tau_2|^2 + |\sigma_1|^2 + |\sigma_3|^2 & \operatorname{Re}(\bar{v}w + \bar{\sigma}_1\sigma_2 + \bar{\tau}_2\sigma_3 + \bar{\sigma}_3\tau_3) \\ \operatorname{Re}(\bar{u}w + \bar{\tau}_1\sigma_2 + \bar{\sigma}_1\sigma_3 + \bar{\sigma}_2\tau_3) & \operatorname{Re}(\bar{v}w + \bar{\sigma}_1\sigma_2 + \bar{\tau}_2\sigma_3 + \bar{\sigma}_3\tau_3) & |w|^2 + |\tau_3|^2 + |\sigma_2|^2 + |\sigma_3|^2 \end{bmatrix} dR \quad (\text{F.0.4})$$

Expanding in the components of  $dR$ , we get

$$\begin{aligned} & \begin{bmatrix} \operatorname{Re}(\bar{u}v + \bar{\tau}_1\sigma_1 + \bar{\sigma}_1\tau_2 + \bar{\sigma}_2\sigma_3) & -(|u|^2 + |\tau_1|^2 + |\sigma_1|^2 + |\sigma_2|^2) & 0 \\ |v|^2 + |\tau_2|^2 + |\sigma_1|^2 + |\sigma_3|^2 & -\operatorname{Re}(\bar{u}v + \bar{\tau}_1\sigma_1 + \bar{\sigma}_1\tau_2 + \bar{\sigma}_2\sigma_3) & 0 \\ \operatorname{Re}(\bar{v}w + \bar{\sigma}_1\sigma_2 + \bar{\tau}_2\sigma_3 + \bar{\sigma}_3\tau_3) & -\operatorname{Re}(\bar{u}w + \bar{\tau}_1\sigma_2 + \bar{\sigma}_1\sigma_3 + \bar{\sigma}_2\tau_3) & 0 \end{bmatrix} d\phi \\ + & \begin{bmatrix} -\operatorname{Re}(\bar{u}w + \bar{\tau}_1\sigma_2 + \bar{\sigma}_1\sigma_3 + \bar{\sigma}_2\tau_3) & 0 & |u|^2 + |\tau_1|^2 + |\sigma_1|^2 + |\sigma_2|^2 \\ -\operatorname{Re}(\bar{v}w + \bar{\sigma}_1\sigma_2 + \bar{\tau}_2\sigma_3 + \bar{\sigma}_3\tau_3) & 0 & \operatorname{Re}(\bar{u}v + \bar{\tau}_1\sigma_1 + \bar{\sigma}_1\tau_2 + \bar{\sigma}_2\sigma_3) \\ -(|w|^2 + |\tau_3|^2 + |\sigma_2|^2 + |\sigma_3|^2) & 0 & \operatorname{Re}(\bar{u}w + \bar{\tau}_1\sigma_2 + \bar{\sigma}_1\sigma_3 + \bar{\sigma}_2\tau_3) \end{bmatrix} d\theta \\ + & \begin{bmatrix} 0 & \operatorname{Re}(\bar{u}w + \bar{\tau}_1\sigma_2 + \bar{\sigma}_1\sigma_3 + \bar{\sigma}_2\tau_3) & -\operatorname{Re}(\bar{u}v + \bar{\tau}_1\sigma_1 + \bar{\sigma}_1\tau_2 + \bar{\sigma}_2\sigma_3) \\ 0 & \operatorname{Re}(\bar{u}w + \bar{\tau}_1\sigma_2 + \bar{\sigma}_1\sigma_3 + \bar{\sigma}_2\tau_3) & -(|v|^2 + |\tau_2|^2 + |\sigma_1|^2 + |\sigma_3|^2) \\ 0 & |w|^2 + |\tau_3|^2 + |\sigma_2|^2 + |\sigma_3|^2 & -\operatorname{Re}(\bar{v}w + \bar{\sigma}_1\sigma_2 + \bar{\tau}_2\sigma_3 + \bar{\sigma}_3\tau_3) \end{bmatrix} d\psi \quad (\text{F.0.5}) \end{aligned}$$

The next step is to take the difference of each term and its transpose. We start with  $a^\dagger da$ . This is

$$\begin{aligned} & \begin{bmatrix} 0 & \bar{u}dv - \bar{v}du + \bar{\tau}_1d\sigma_1 - \bar{\sigma}_1d\tau_1 + \bar{\sigma}_1d\tau_2 - \bar{\tau}_2d\sigma_1 + \bar{\sigma}_2d\sigma_3 - \bar{\sigma}_3d\sigma_2 & 0 \\ -(\bar{u}dv - \bar{v}du + \bar{\tau}_1d\sigma_1 - \bar{\sigma}_1d\tau_1 + \bar{\sigma}_1d\tau_2 - \bar{\tau}_2d\sigma_1 + \bar{\sigma}_2d\sigma_3 - \bar{\sigma}_3d\sigma_2) & 0 & 0 \\ 0 & 0 & 0 \end{bmatrix} \\ + & \begin{bmatrix} 0 & \bar{u}dw - \bar{w}du + \bar{\tau}_1d\sigma_2 - \bar{\sigma}_2d\tau_1 + \bar{\sigma}_1d\sigma_3 - \bar{\sigma}_3d\sigma_1 + \bar{\sigma}_2d\tau_3 - \bar{\tau}_3d\sigma_2 & 0 \\ 0 & 0 & 0 \\ -(\bar{u}dw - \bar{w}du + \bar{\tau}_1d\sigma_2 - \bar{\sigma}_2d\tau_1 + \bar{\sigma}_1d\sigma_3 - \bar{\sigma}_3d\sigma_1 + \bar{\sigma}_2d\tau_3 - \bar{\tau}_3d\sigma_2) & 0 & 0 \end{bmatrix} \\ + & \begin{bmatrix} 0 & 0 & 0 \\ 0 & 0 & \bar{v}dw - \bar{w}dv + \bar{\sigma}_1d\sigma_2 - \bar{\sigma}_2d\sigma_1 + \bar{\tau}_2d\sigma_3 - \bar{\sigma}_3d\tau_2 + \bar{\sigma}_3d\tau_3 - \bar{\tau}_3d\sigma_3 \\ 0 & -(\bar{v}dw - \bar{w}dv + \bar{\sigma}_1d\sigma_2 - \bar{\sigma}_2d\sigma_1 + \bar{\tau}_2d\sigma_3 - \bar{\sigma}_3d\tau_2 + \bar{\sigma}_3d\tau_3 - \bar{\tau}_3d\sigma_3) & 0 \end{bmatrix} \quad (\text{F.0.6}) \end{aligned}$$

Next we have  $a^\dagger b(dR)b^\dagger a$ , which gives

$$\begin{aligned}
& 2 \begin{bmatrix} 0 & |\sigma_1|^2 - \text{Re}(\bar{\tau}_1 \tau_2) & \text{Re}(\bar{\sigma}_1 \sigma_2 - \bar{\tau}_1 \sigma_3) \\ -(|\sigma_1|^2 - \text{Re}(\bar{\tau}_1 \tau_2)) & 0 & \text{Re}(\bar{\tau}_2 \sigma_2 - \bar{\sigma}_1 \sigma_3) \\ -\text{Re}(\bar{\sigma}_1 \sigma_2 - \bar{\tau}_1 \sigma_3) & -\text{Re}(\bar{\tau}_2 \sigma_2 - \bar{\sigma}_1 \sigma_3) & 0 \end{bmatrix} d\phi \\
& + 2 \begin{bmatrix} 0 & \text{Re}(\bar{\tau}_1 \sigma_3 - \bar{\sigma}_2 \sigma_1) & \text{Re}(\bar{\tau}_1 \tau_3) - |\sigma_2|^2 \\ -\text{Re}(\bar{\tau}_1 \sigma_3 - \bar{\sigma}_2 \sigma_1) & 0 & \text{Re}(\bar{\sigma}_1 \tau_3 - \bar{\sigma}_3 \sigma_2) \\ |\sigma_2|^2 - \text{Re}(\bar{\tau}_3 \tau_1) & -\text{Re}(\bar{\sigma}_1 \tau_3 - \bar{\sigma}_3 \sigma_2) & 0 \end{bmatrix} d\theta \\
& + \begin{bmatrix} 0 & \text{Re}(\bar{\sigma}_2 \tau_2 - \bar{\sigma}_1 \sigma_3) & \text{Re}(\bar{\sigma}_2 \sigma_3 - \bar{\sigma}_1 \tau_3) \\ -\text{Re}(\bar{\sigma}_2 \tau_2 - \bar{\sigma}_1 \sigma_3) & 0 & |\sigma_3|^2 - \text{Re}(\bar{\tau}_2 \tau_3) \\ -\text{Re}(\bar{\sigma}_2 \sigma_3 - \bar{\sigma}_1 \tau_3) & \text{Re}(\bar{\tau}_3 \tau_2) - |\sigma_3|^2 & 0 \end{bmatrix} d\psi \quad (\text{F.0.7})
\end{aligned}$$

The final one is the terms from  $a^\dagger a(dR)$ - remembering that  $dR$  is antisymmetric, this gives

$$\begin{aligned}
& \begin{bmatrix} 0 & -(|u|^2 + |v|^2 + |\tau_1|^2 + |\tau_2|^2 + |\sigma_1|^2 + \Sigma^2) & -\text{Re}(\bar{v}w + \bar{\sigma}_1 \sigma_2 + \bar{\tau}_2 \sigma_3 + \bar{\sigma}_3 \tau_3) \\ |u|^2 + |v|^2 + |\tau_1|^2 + |\tau_2|^2 + |\sigma_1|^2 + \Sigma^2 & 0 & \text{Re}(\bar{u}w + \bar{\tau}_1 \sigma_2 + \bar{\sigma}_1 \sigma_3 + \bar{\sigma}_2 \tau_3) \\ \text{Re}(\bar{v}w + \bar{\sigma}_1 \sigma_2 + \bar{\tau}_2 \sigma_3 + \bar{\sigma}_3 \tau_3) & -\text{Re}(\bar{u}w + \bar{\tau}_1 \sigma_2 + \bar{\sigma}_1 \sigma_3 + \bar{\sigma}_2 \tau_3) & 0 \end{bmatrix} d\phi \\
& + \begin{bmatrix} 0 & \text{Re}(\bar{v}w + \bar{\sigma}_1 \sigma_2 + \bar{\tau}_2 \sigma_3 + \bar{\sigma}_3 \tau_3) & |u|^2 + |w|^2 + |\tau_1|^2 + |\tau_3|^2 + 2|\sigma_2|^2 + \Sigma^2 \\ -\text{Re}(\bar{v}w + \bar{\sigma}_1 \sigma_2 + \bar{\tau}_2 \sigma_3 + \bar{\sigma}_3 \tau_3) & 0 & ) \\ -(|u|^2 + |w|^2 + |\tau_1|^2 + |\tau_3|^2 + 2|\sigma_2|^2 + \Sigma^2) & -\text{Re}(\bar{u}v + \bar{\tau}_1 \sigma_1 + \bar{\sigma}_1 \tau_2 + \bar{\sigma}_2 \sigma_3) & 0 \end{bmatrix} d\theta \\
& + \begin{bmatrix} 0 & \text{Re}(\bar{u}w + \bar{\tau}_1 \sigma_2 + \bar{\sigma}_1 \sigma_3 + \bar{\sigma}_2 \tau_3) & -\text{Re}(\bar{u}v + \bar{\tau}_1 \sigma_1 + \bar{\sigma}_1 \tau_2 + \bar{\sigma}_2 \sigma_3) \\ -\text{Re}(\bar{u}w + \bar{\tau}_1 \sigma_2 + \bar{\sigma}_1 \sigma_3 + \bar{\sigma}_2 \tau_3) & 0 & -(|v|^2 + |w|^2 + |\tau_2|^2 + |\tau_3|^2 + |\sigma_3|^2 + \Sigma^2) \\ \text{Re}(\bar{u}v + \bar{\tau}_1 \sigma_1 + \bar{\sigma}_1 \tau_2 + \bar{\sigma}_2 \sigma_3) & |v|^2 + |w|^2 + |\tau_2|^2 + |\tau_3|^2 + 2|\sigma_3|^2 + \Sigma^2 & 0 \end{bmatrix} d\psi \quad (\text{F.0.8})
\end{aligned}$$

Where  $\Sigma^2 = |\sigma_1|^2 + |\sigma_2|^2 + |\sigma_3|^2$ . Now we can solve (5.7.1), using

$$a^\dagger dC_r = a^\dagger da - a^\dagger b(dR)b^\dagger a + a^\dagger a(dR) \quad (\text{F.0.9})$$

, by expanding and rearranging it into the form

$$a^\dagger da - (a^\dagger da)^T = a^\dagger b(dR)b^\dagger a - (a^\dagger b(dR)b^\dagger a)^T - (a^\dagger a(dR) + (dR)a^\dagger a) \quad (\text{F.0.10})$$

This gives three equations, one for each of the basis elements of  $o(3)$ . First, the

$$\begin{bmatrix} 0 & 1 & 0 \\ -1 & 0 & 0 \\ 0 & 0 & 0 \end{bmatrix} \text{ component gives}$$

$$\begin{aligned} & \bar{u}dv - \bar{v}du + \bar{\tau}_1d\sigma_1 - \bar{\sigma}_1d\tau_1 + \bar{\sigma}_1d\tau_2 - \bar{\tau}_2d\sigma_1 + \bar{\sigma}_2d\sigma_3 - \bar{\sigma}_3d\sigma_2 = \\ & \left( |u|^2 + |v|^2 + |\tau_1|^2 + |\tau_2|^2 + 3|\sigma_1|^2 + \Sigma^2 - 2\text{Re}(\bar{\tau}_1\tau_2) \right) d\phi \\ & + \left( 2\text{Re}(\bar{\tau}_1\sigma_3 - \bar{\sigma}_2\sigma_1) - \text{Re}(\bar{v}w + \bar{\sigma}_1\sigma_2 + \bar{\tau}_2\sigma_3 + \bar{\sigma}_3\tau_3) \right) d\theta \\ & + \left( 2\text{Re}(\bar{\sigma}_2\tau_2 - \bar{\sigma}_1\sigma_3) - \text{Re}(\bar{u}w + \bar{\tau}_1\sigma_2 + \bar{\sigma}_1\sigma_3 + \bar{\sigma}_2\tau_3) \right) d\psi \end{aligned} \quad (\text{F.0.11})$$

Next, the  $\begin{bmatrix} 0 & 0 & -1 \\ 0 & 0 & 0 \\ 1 & 0 & 0 \end{bmatrix}$  component gives

$$\begin{aligned} & \bar{u}dw - \bar{w}du + \bar{\tau}_1d\sigma_2 - \bar{\sigma}_2d\tau_1 + \bar{\sigma}_1d\sigma_3 - \bar{\sigma}_3d\sigma_1 + \bar{\sigma}_2d\tau_3 - \bar{\tau}_3d\sigma_2 = \\ & \left( 2\text{Re}(\bar{\sigma}_1\sigma_2 - \bar{\tau}_1\sigma_3) + \text{Re}(\bar{v}w + \bar{\sigma}_1\sigma_2 + \bar{\tau}_2\sigma_3 + \bar{\sigma}_3\tau_3) \right) d\phi \\ & \left( 2\text{Re}(\bar{\tau}_1\tau_3) - (|u|^2 + |w|^2 + |\tau_1|^2 + |\tau_3|^2 + 3|\sigma_2|^2 + \Sigma^2) \right) d\theta \\ & + \left( 2\text{Re}(\bar{\sigma}_2\sigma_3 - \bar{\sigma}_1\tau_3) + \text{Re}(\bar{u}v + \bar{\tau}_1\sigma_1 + \bar{\sigma}_1\tau_2 + \bar{\sigma}_2\sigma_3) \right) d\psi \end{aligned} \quad (\text{F.0.12})$$

Finally, we have the  $\begin{bmatrix} 0 & 0 & 0 \\ 0 & 0 & -1 \\ 0 & 1 & 0 \end{bmatrix}$  component

$$\begin{aligned} & \bar{v}dw - \bar{w}dv + \bar{\sigma}_1d\sigma_2 - \bar{\sigma}_2d\sigma_1 + \bar{\tau}_2d\sigma_3 - \bar{\sigma}_3d\tau_2 + \bar{\sigma}_3d\tau_3 - \bar{\tau}_3d\sigma_3 = \\ & \left( 2\text{Re}(\bar{\tau}_2\sigma_2 - \bar{\sigma}_1\sigma_3) - \text{Re}(\bar{u}w + \bar{\tau}_1\sigma_2 + \bar{\sigma}_1\sigma_3 + \bar{\sigma}_2\tau_3) \right) d\phi \\ & \left( 2\text{Re}(\bar{\sigma}_1\tau_3 - \bar{\sigma}_3\sigma_2) - \text{Re}(\bar{u}v + \bar{\tau}_1\sigma_1 + \bar{\sigma}_1\tau_2 + \bar{\sigma}_2\sigma_3) \right) d\theta \\ & + \left( |v|^2 + |w|^2 + |\tau_2|^2 + |\tau_3|^2 + 3|\sigma_3|^2 + \Sigma^2 - \text{Re}(\bar{\tau}_2\tau_3) \right) d\psi \end{aligned} \quad (\text{F.0.13})$$

A bit of rearrangement gives

$$\bar{u}dv - \bar{v}du + \bar{\tau}_1d\sigma_1 - \bar{\sigma}_1d\tau_1 + \bar{\sigma}_1d\tau_2 - \bar{\tau}_2d\sigma_1 + \bar{\sigma}_2d\sigma_3 - \bar{\sigma}_3d\sigma_2 = \quad (\text{F.0.14})$$

$$\begin{aligned}
& \left( |u|^2 + |v|^2 + |\tau_1 - \tau_2|^2 + 3|\sigma_1|^2 + \Sigma^2 \right) d\phi \\
& + \left( 3\text{Re}(\bar{\tau}_1\sigma_3 - \bar{\sigma}_2\sigma_1) - \text{Re}(\bar{v}w) \right) d\theta + \left( 3\text{Re}(\bar{\sigma}_2\tau_2 - \bar{\sigma}_1\sigma_3) - \text{Re}(\bar{u}w) \right) d\psi \\
\bar{u}dw - \bar{w}du + \bar{\tau}_1d\sigma_2 - \bar{\sigma}_2d\tau_1 + \bar{\sigma}_1d\sigma_3 - \bar{\sigma}_3d\sigma_1 + \bar{\sigma}_2d\tau_3 - \bar{\tau}_3d\sigma_2 = & \quad (\text{F.0.15}) \\
& \left( 3\text{Re}(\bar{\sigma}_1\sigma_2 - \bar{\tau}_1\sigma_3) + \text{Re}(\bar{v}w) \right) d\phi - \left( |u|^2 + |w|^2 + |\tau_1 - \tau_3|^2 + 3|\sigma_2|^2 + \Sigma^2 \right) d\theta \\
& + \left( 3\text{Re}(\bar{\sigma}_2\sigma_3 - \bar{\sigma}_1\tau_3) + \text{Re}(\bar{u}v) \right) d\psi
\end{aligned}$$

$$\begin{aligned}
\bar{v}dw - \bar{w}dv + \bar{\sigma}_1d\sigma_2 - \bar{\sigma}_2d\sigma_1 + \bar{\tau}_2d\sigma_3 - \bar{\sigma}_3d\tau_2 + \bar{\sigma}_3d\tau_3 - \bar{\tau}_3d\sigma_3 = & \quad (\text{F.0.16}) \\
& \left( 3\text{Re}(\bar{\tau}_2\sigma_2 - \bar{\sigma}_1\sigma_3) - \text{Re}(\bar{u}w) \right) d\phi + \left( 3\text{Re}(\bar{\sigma}_1\tau_3 - \bar{\sigma}_3\sigma_2) - \text{Re}(\bar{u}v) \right) d\theta \\
& + \left( |v|^2 + |w|^2 + |\tau_2 - \tau_3|^2 + 3|\sigma_3|^2 + \Sigma^2 \right) d\psi
\end{aligned}$$

We can now use Mathematica to solve these to get the solution in the main text,  
(7.4.4)





# Bibliography

- [1] J. P. Allen and D. J. Smith. The low energy dynamics of charge two dyonic instantons. *JHEP*, 02:113, 2013. doi: 10.1007/JHEP02(2013)113.
- [2] M. F. Atiyah, N. J. Hitchin, V. G. Drinfeld, and Yu. I. Manin. Construction of instantons. *Phys. Lett.*, A65:185–187, 1978. doi: 10.1016/0375-9601(78)90141-X. [,133(1978)].
- [3] D. Bak and A. Gustavsson. One dyonic instanton in 5d maximal sym theory. *JHEP*, 07:021, 2013. doi: 10.1007/JHEP07(2013)021.
- [4] D. Bak and K.-M. Lee. Comments on the moduli dynamics of 1/4 bps dyons. *Phys. Lett.*, B468:76–80, 1999. doi: 10.1016/S0370-2693(99)01217-4.
- [5] D. Bak, C.-k. Lee, K.-M. Lee, and P. Yi. Low-energy dynamics for 1/4 bps dyons. *Phys. Rev.*, D61:025001, 2000. doi: 10.1103/PhysRevD.61.025001.
- [6] A. A. Belavin, A. M. Polyakov, A. S. Schwartz, and Yu. S. Tyupkin. Pseudo-particle solutions of the yang-mills equations. *Phys. Lett.*, B59:85–87, 1975. doi: 10.1016/0370-2693(75)90163-X. [,350(1975)].
- [7] A. V. Belitsky, S. Vandoren, and P. van Nieuwenhuizen. Yang-mills and d instantons. *Class. Quant. Grav.*, 17:3521–3570, 2000. doi: 10.1088/0264-9381/17/17/305.
- [8] E. B. Bogomolny. Stability of classical solutions. *Sov. J. Nucl. Phys.*, 24:449, 1976. [Yad. Fiz.24,861(1976)].

- [9] D. Bohm. *Wholeness and the Implicate Order*. Routledge, 1980.
- [10] Y. Brihaye and J. Nuyts. Instantons in  $su(4)$  gauge theories. *Phys. Lett.*, 66B: 346–348, 1977. doi: 10.1016/0370-2693(77)90011-9.
- [11] M.-Y. Choi, K. K. Kim, C. Lee, and K.-M. Lee. Higgs structures of dyonic instantons. *JHEP*, 04:097, 2008. doi: 10.1088/1126-6708/2008/04/097.
- [12] C.-S. Chu, V. V. Khoze, and G. Travaglini. Notes on noncommutative instantons. *Nucl. Phys.*, B621:101–130, 2002. doi: 10.1016/S0550-3213(01)00576-4.
- [13] A. Cockburn. *Aspects of Vortices and Hyperbolic Monopoles*. PhD thesis, University of Durham, 2015.
- [14] S. R. Coleman. The quantum sine-gordon equation as the massive thirring model. *Phys. Rev.*, D11:2088, 1975. doi: 10.1103/PhysRevD.11.2088. [,128(1974)].
- [15] S. R. Coleman. The uses of instantons. *Subnucl. Ser.*, 15:805, 1979. [,382(1978)].
- [16] A. Collinucci and A. Wijns. Topology of Fibre bundles and Global Aspects of Gauge Theories. In *2nd Modave Summer School in Theoretical Physics Modave, Belgium, August 6-12, 2006*, 2006.
- [17] D. H. Correa, G. S. Lozano, E. F. Moreno, and F. A. Schaposnik. Comments on the  $u(2)$  noncommutative instanton. *Phys. Lett.*, B515:206–212, 2001. doi: 10.1016/S0370-2693(01)00846-2.
- [18] E. Corrigan, P. Goddard, H. Osborn, and S. Templeton. Zeta function regularization and multi - instanton determinants. *Nucl. Phys.*, B159:469–496, 1979. doi: 10.1016/0550-3213(79)90346-8.
- [19] M. de Vroome.  *$N=2$  Supersymmetric Theories, Dyonic Charges and Instantons*. PhD thesis, Utrecht U., 2007.
- [20] G. H. Derrick. Comments on nonlinear wave equations as models for elementary particles. *J. Math. Phys.*, 5:1252–1254, 1964. doi: 10.1063/1.1704233.

- 
- [21] N. Dorey, V. V. Khoze, and M. P. Mattis. Multi - instanton calculus in  $n=2$  supersymmetric gauge theory. *Phys. Rev.*, D54:2921–2943, 1996. doi: 10.1103/PhysRevD.54.2921.
- [22] N. Dorey, T. J. Hollowood, V. V. Khoze, and M. P. Mattis. The calculus of many instantons. *Phys. Rept.*, 371:231–459, 2002. doi: 10.1016/S0370-1573(02)00301-0.
- [23] M. R. Douglas and N. A. Nekrasov. Noncommutative field theory. *Rev. Mod. Phys.*, 73:977–1029, 2001. doi: 10.1103/RevModPhys.73.977.
- [24] C. Furey. *Standard model physics from an algebra?* PhD thesis, Waterloo U., 2015.
- [25] R. Gopakumar, S. Minwalla, and A. Strominger. Noncommutative solitons. *JHEP*, 05:020, 2000. doi: 10.1088/1126-6708/2000/05/020.
- [26] S. Gull, A. Lasenby, and C. Doran. Imaginary numbers are not real—the geometric algebra of spacetime. *Foundations of Physics*, 23:1175–1201, 01 1993. doi: 10.1007/BF01883676.
- [27] J. Gutowski. Symmetry and particle physics. Lecture notes on ArXiv, 2007.
- [28] M. M. H. Garland. Why instantons are monopoles. *Commun. Math. Phys.*, (121):85–90, 1989.
- [29] M. Hamanaka. *Noncommutative solitons and D-branes*. PhD thesis, Tokyo U., 2003.
- [30] M. Hamanaka and T. Nakatsu. Adhm construction of noncommutative instantons. In *Proceedings, 20th International Colloquium on Integrable Systems and Quantum Symmetries (ISQS-20): Prague, Czech Republic, June 17-23, 2012*, 2013.

- [31] M. Hamanaka and T. Nakatsu. Noncommutative instantons revisited. *Journal of Physics: Conference Series*, 411:012016, jan 2013. doi: 10.1088/1742-6596/411/1/012016. URL <https://doi.org/10.1088/1742-6596/411/1/012016>.
- [32] K. Hashimoto, H. Hata, and S. Moriyama. Brane configuration from monopole solution in noncommutative superyang-mills theory. *JHEP*, 12:021, 1999. doi: 10.1088/1126-6708/1999/12/021.
- [33] A. Hatcher. *Algebra Topology*. CUP, 2009.
- [34] D. Hestenes. Zitterbewegung in quantum mechanics. *Foundations of Physics*, 40:1–54, 2010.
- [35] E. Hitzer. Introduction to clifford’s geometric algebra. *Journal of the Society of Instrument and Control Engineers*, 51(4):338–350, April 2012.
- [36] A. Iskauskas. *A Study of Noncommutative Instantons*. PhD thesis, Durham U., CPT, 2015-06-14. URL <http://etheses.dur.ac.uk/11106>.
- [37] A. Iskauskas and D. J. Smith. Moduli space dynamics of noncommutative  $u(2)$  instantons. *JHEP*, 06:036, 2015. doi: 10.1007/JHEP06(2015)036.
- [38] R. Jackiw. Introduction to the yang-mills quantum theory. *Rev. Mod. Phys.*, 52:661–673, 1980. doi: 10.1103/RevModPhys.52.661.
- [39] A. Kapustin, A. Kuznetsov, and D. Orlov. Noncommutative instantons and twistor transform. *Commun. Math. Phys.*, 221:385–432, 2001. doi: 10.1007/PL00005576.
- [40] H.-C. Kim, S. Kim, E. Koh, K. Lee, and S. Lee. On instantons as Kaluza-Klein modes of M5-branes. *JHEP*, 12:031, 2011. doi: 10.1007/JHEP12(2011)031.
- [41] S. Kim, K.-M. Lee, and S. Lee. Dyonic instantons in 5-dim yang-mills chern-simons theories. *JHEP*, 08:064, 2008. doi: 10.1088/1126-6708/2008/08/064.

- [42] J. Lambek. If hamilton had prevailed. In *Mathematical Conversations*. Springer, 2001.
- [43] N. D. Lambert and D. Tong. Dyonic instantons in five-dimensional gauge theories. *Phys. Lett.*, B462:89–94, 1999. doi: 10.1016/S0370-2693(99)00894-1.
- [44] O. Lechtenfeld. Noncommutative instantons and solitons. *Fortsch. Phys.*, 52:596–605, 2004. doi: 10.22323/1.011.0017,10.1002/prop.200410150. [PoS-jhw2003,017(2003)].
- [45] K.-M. Lee, D. Tong, and S. Yi. The moduli space of two  $u(1)$  instantons on noncommutative  $\mathbb{R}^4$  and  $\mathbb{R}^3 \times S^1$ . *Phys. Rev.*, D63:065017, 2001. doi: 10.1103/PhysRevD.63.065017.
- [46] R. W. M. F. Atiyah. Instantons and algebraic geometry. *55*, 55(2):117–124, 1977.
- [47] S. Mandelstam. Soliton Operators for the Quantized Sine-Gordon Equation. *Phys. Rev.*, D11:3026, 1975. doi: 10.1103/PhysRevD.11.3026. [,138(1975)].
- [48] N. S. Manton. A remark on the scattering of bps monopoles. *Phys. Lett.*, 110B: 54–56, 1982. doi: 10.1016/0370-2693(82)90950-9.
- [49] J. E. Moyal. Quantum mechanics as a statistical theory. *Proc. Cambridge Phil. Soc.*, 45:99–124, 1949. doi: 10.1017/S0305004100000487.
- [50] J. E. Moyal. Quantum mechanics as a statistical theory. *Mathematical Proceedings of the Cambridge Philosophical Society*, 45(1):99–124, 1949. doi: 10.1017/S0305004100000487.
- [51] A. K. M.R. Francis. The construction of spinors in geometric algebra. *Ann. Phys.*, 317(2):383–409, 2005.
- [52] P. S. N. Manton. *Topological Solitons*. CUP, 2004.

- [53] M. Nakahara. *Geometry, Topology and Physics*. Taylor and Francis, 2 edition, 2003.
- [54] N. Nekrasov and A. S. Schwarz. Instantons on noncommutative  $\mathbb{R}^4$  and (2,0) superconformal six-dimensional theory. *Commun. Math. Phys.*, 198:689–703, 1998. doi: 10.1007/s002200050490.
- [55] N. A. Nekrasov. Noncommutative instantons revisited. *Commun. Math. Phys.*, 241:143–160, 2003. doi: 10.1007/s00220-003-0911-8.
- [56] H. Osborn. Semiclassical functional integrals for selfdual gauge fields. *Annals Phys.*, 135:373, 1981. doi: 10.1016/0003-4916(81)90159-7.
- [57] K. Peeters and M. Zamaklar. Motion on moduli spaces with potentials. *JHEP*, 12:032, 2001. doi: 10.1088/1126-6708/2001/12/032.
- [58] J. Polchinski. *String Theory*. CUP, 1999.
- [59] R. W. R.S. Ward. *Twistor Geometry and Field Theory*. CUP, 1990.
- [60] A. Signer. Abc of susy. *J. Phys.*, G36:073002, 2009. doi: 10.1088/0954-3899/36/7/073002.
- [61] T. Skyrme. A unified field theory of mesons and baryons. *Nucl. Phys. A.*, 31: 556–569, 1962. doi: 10.1016/0029-5582(62)90775-7.
- [62] G. 't Hooft. Computation of the quantum effects due to a four-dimensional pseudoparticle. *Phys. Rev.*, D14:3432–3450, 1976. doi: 10.1103/PhysRevD.18.2199.3,10.1103/PhysRevD.14.3432. [,70(1976)].
- [63] D. Tong. Tasi lectures on solitons: Instantons, monopoles, vortices and kinks. In *Theoretical Advanced Study Institute in Elementary Particle Physics: Many Dimensions of String Theory (TASI 2005) Boulder, Colorado, June 5-July 1, 2005*, 2005.

- 
- [64] E. J. Weinberg and P. Yi. Magnetic monopole dynamics, supersymmetry, and duality. *Phys. Rept.*, 438:65–236, 2007. doi: 10.1016/j.physrep.2006.11.002.